

New Ligands for Gold: Bonding Mode and Structural Complex Characterisation

by

Christoph Erik Strasser

Dissertation presented for the degree of

PHILOSOPHIAE DOCTOR

at

Stellenbosch University

Department of Chemistry and Polymer Science

Faculty of Science

Supervisor: Prof. Helgard G. Raubenheimer

Co-Promotor: Dr. Stephanie Cronje

December 2008

Declaration

By submitting this dissertation electronically, I declare that the entirety of the work contained therein is my own, original work, that I am the owner of the copyright thereof (unless to the extent explicitly otherwise stated) and that I have not previously in its entirety or in part submitted it for obtaining any qualification.

Date: December 2008

Acknowledgements / Danksagungen

Ek wil graag dankie sê vir almal wie vir hierdie proefskrif bygedra en dit moontlik gemaak het:

Prof. Helgard G. Raubenheimer for his outstanding guidance through this thesis and Dr. Stephanie Cronje for her experience in synthetic chemistry that made these reactions work.

My laboratory colleagues: Bertie Barnard, Jacorien Coetzee, William Gabrielli, Tesfamariam Hagos, Ulrike Horvath, Leigh-Anne de Jongh, Anneke Krüger, Adelé le Roux, Stefan Nogai, Oliver Schuster, Xia Sheng and Elzet Stander-Grobler for an excellent atmosphere making work in the organometallic laboratory a joyful experience that will certainly be missed.

I am indebted to Dr. Jan Gertenbach, Dr. Stefan D. Nogai, and Dr. Oliver B. Schuster for training and guidance in operating the crystal diffractometer as well as help from Prof. Leonard J. Barbour, Dr. Liliana Dobrzańska, Tia Jacobs, Leigh Loots, Dr. Clive Oliver, Storm Potts and Dr. Klaus Wurst in solving problems encountered with the crystal structures contained in this dissertation.

Mrs. Elsa Malherbe and Ms. Jean M. McKenzie for recording most of the NMR spectra and help with NMR experiments.

Dr. Paul F. M. Verhoeven for his assistance in recording far-infrared spectra

Mr. Philip Allen, Mr. Tommy Daniels, Mr. Johnny Smit, Ms. Petra Snyman and Mr. Eric Ward for their always swift assistance in technical matters.

Besonderer Dank ergeht an meine Eltern und Grosseltern, die mich in meinem Chemiestudien immer nach Kräften finanziell unterstützt und diese Arbeit ermöglicht haben. Financial support from Stellenbosch University is also greatly acknowledged.

Abstract

Novel gold(I) trithiophosphite complexes were synthesised by utilising the ligands $P(SR)_3$ ($R = Me, Ph$) and 1,2-bis(1,3,2-dithiaphospholan-2-ylthio)ethane (2L). Reaction with $(tht)AuCl$ or $(tht)AuC_6F_5$ readily yielded the corresponding complexes $(RS)_3PAuX$ and ${}^2L(AuX)_2$ ($X = Cl, C_6F_5$) as well as $\{Au[P(SMe)_3]_2\}CF_3SO_3$. Structural characterisation by X-ray diffraction revealed linear complexes in part associating by $Au\cdots Au$ and/or $Au\cdots S$ contacts, two polymorphs of one compound associating by either $Au\cdots S$ interactions or π -stacking was also obtained. $(MeS)_3PAuCl$ and $(MeO)_3PAuCl$ were found to be isostructural in the solid state.

The complex chloro[tris(4-methylthiazol-2-yl)phosphane]gold, **A**, was used to probe the electronic influence tris(azol-2-yl)phosphanes exert upon gold(I) by substituting the chloride with various thiolates. In contrast to Ph_3PAuCl , only NCS^- and $PhC(O)S^-$ afforded stable compounds which could be attributed to a weaker donating capability of the tris-(azolyl)phosphane ligand class. The compounds **A** and chloro[tris(thiazol-2-yl)phosphane]-gold, **B**, were shown to crystallise in 4 new polymorphs and solvates bringing the total to an exceptional seven. Among the solid-state structures of **A** the rare instance of a polymorph and a thf solvate not exhibiting aurophilic interactions as opposed to the original structure were observed. Complex **B** was shown to crystallise in polymorphs where dimers are associated either by $Au\cdots Au$ or $Au\cdots Cl$ interactions but otherwise exhibit similar arrangements of the ligand, this set of polymorphs is unprecedented amongst gold complexes. An NMR experiment proved that tris(thiazolyl)phosphane complexes are subject to hydrolysis under alkaline conditions.

A trimeric gold(I) heterometallacycle, obtained by reacting $(tht)AuCl$ with 4,4-dimethyl-2-(2-thienyl)oxazoline deprotonated at C-5 of the thiophene ring, was structurally characterised. Intramolecular $Au\cdots S$ interactions were found to be present which precluded interaction of the gold atoms with other metal centres such as $Me_3CNCAuCl$ or $AgNO_3$. A second solvate obtained additionally exhibits $Au\cdots Au$ interactions. The scope of uncommon bis-imine coordination to Au^I was expanded by utilising 1,2-bis(1-imidazolylmethyl)-2,4,6-trimethylbenzene (2L) to synthesise the $[Au_2(\mu\text{-}{}^2L)_2]^{2+}$ cation. The triflate salt forms the first porous crystal structure of gold and the co-crystallised solvent could be partially removed by evacuation at elevated temperatures. Utilising a ditopic phosphite ligand instead of the commonly used ditopic phosphane ligands, a new cationic species of the type $[Au_2(\mu\text{-}{}^2L)_3]^{2+}$ was characterised in the solid state for the first time.

Finally, employing 2-phenylthiazole and 1-(thiazol-2-yl)piperidine which can be deprotonated at C-5 of the thiazole ring, Fischer-type pentacarbonyltungsten carbenate complexes were prepared and structurally characterised. Starting from these complexes, the analogous Fischer-type methoxycarbene as well as carbyne complexes could be obtained by alkylation and formal oxide abstraction, respectively. The latter products readily formed dinuclear adducts with AuCl.

A Fischer-type methoxycarbene could be transferred to Au^I affording the first such gold(I) complex exhibiting Au...Au interactions in the solid state as well as a rare agostic Au...H interaction which was examined by low-temperature ¹H NMR measurements. Transfer of the carbenate ligand derived from 1-(thiazol-2-yl)piperidine to Ph₃PAu⁺ afforded an auated thiazole product (by an unprecedented loss of CO) which may be represented as a pseudo-abnormal azolydene complex owing to W(CO)₅-coordination at a distant nitrogen. The carbenate originating from 2-phenylthiazole, on the other hand, afforded, by rare W(CO)₅-trapping and without CO-loss, a pseudo Fischer-type carbene complex.

Carbene transfer to gold was complemented by the first transfers of *r*NHC ligands from chromium and tungsten to gold(I) affording a novel class of complexes, all of which were structurally characterised. This work bridges the unnatural divide created between Fischer and *N*-heterocyclic carbene complexes.

Opsomming

Nuwe goud(I) tritiofosfietkomplekse met die ligande $P(SR)_3$ en 1,2-bis(1,3,2-ditiafosfolaan-2-ieltio)etaan (2L) is gesintetiseer. Reaksie met $(tht)AuCl$ of $(tht)AuC_6F_5$ lei gereedlik tot die vorming van ooreenkomstige komplekse $(RS)_3PAuX$ en $^2L(AuX)_2$ sowel as $\{Au[P(SMe)_3]_2\}-CF_3SO_3$. Strukturele karakterisering met X-straal diffraksie toon lineêre komplekse wat gedeeltelik deur $Au\cdots Au$ en/of $Au\cdots S$ kontakte assosieer. Twee polimorfe van een verbinding, wat deur $Au\cdots S$ interaksies of π -pakking assosieer, is beskryf. Ondersoek van die molekulêre strukture van $(MeS)_3PAuCl$ en $(MeO)_3PAuCl$ het getoon dat die verbindings isostruktureel is in die vaste toestand.

Die kompleks chloro[tris(4-metieltiasool-2-iel)fosfaan]goud, **A**, is gebruik in 'n ondersoek na die elektroniese invloed wat tris(asool-2-iel)fosfane op goud(I) uitoefen deur substitusie van die chloried met verskeie tiolate. In teenstelling met Ph_3PAuCl , het net NCS^- en $PhC(O)S^-$ stabiele verbindings gelever. Hierdie resultaat kan toegeskryf word aan die swakker donasievermoë van die tris(asool-2-iel)fosfaan ligandgroep. Verbinding **A** en chloro[tris(tiasool-2-iel)fosfaan]goud, **B**, kristalliseer in 4 nuwe polimorfe en solvate, in totaal sewe. Tussen die verskeie vastetoestand strukture van **A** is die ongewone gevalle van 'n polimorf en 'n thf solvaat, wat nie aurofiliese interaksies bevat nie in teenstelling met die situasie in die oorspronklike struktuur, waargeneem. Kompleks **B** kristalliseer in polimorfe wat óf in $Au\cdots Au$ óf in $Au\cdots Cl$ interaksies betrokke is maar andersyds dieselfde rangskikking as die ligand het. 'n KMR eksperiment het bewys dat hidrolise van tris(tiasoliel)fosfaankomplekse onder alkaliese toestande voorkom.

'n Trimeriese goud(I) heterometaalassiklus, verkry deur die reaksie van $(tht)AuCl$ met C-5-gedeprotoneerde 4,4-dimetiel-2-(tiëen-2-iel)oksasolien, is struktureel gekarakteriseer. Intramolekulêre $Au\cdots S$ interaksies is teenwoordig en het die reaksie van die heterometaalassiklus met ander metaalverbindings soos $Me_3CNCAuCl$ of $AgNO_3$ verhoed. Die omvang van bis-imien koördinasie aan Au^I is uitgebrei deur die gebruik van 1,2-bis(imidasool-1-ielmetiel)-2,4,6-trimetielbenseen (2L) om die $[Au_2(\mu-^2L)]^{2+}$ kation te sintetiseer. Die triflaat sout toon die eerste poreuse kristalstruktuur van goud en oplosmiddel kon onder vakuum by 'n hoë temperatuur deelsgewys verwyder word. 'n Ander kationiese spesie, $[Au_2(\mu-^2L)_3]^{2+}$, is vir die eerste keer in die vaste toestand gekarakteriseer deur gebruik te maak van 'n ditopiese fosfietligand in plaas van die algemene ditopiese fosfaanligande.

Ten laaste, het die gebruik van 2-fenieltiasool en 1-(tiasool-2-iel)piperidien, wat op C-5 van die tiasoolring gedeprotoneer kan word, die isolasie van Fischer-tipe pentakarboniel-wolframkarbeniaatkomplekse wat struktureel gekarakteriseer kon word verseker. Deur hierdie komplekse as uitgangstowwe te gebruik kon analoë Fischer-tipe metoksiekarbeen- sowel as karbynkomplekse verkry word deur alkilering en formele oksiedverwydering, onderskeidelik. Een Fischer-tipe metoksiekarbeenkompleks kon omgeskakel word in 'n Au^I kompleks, die eerste voorbeeld van só 'n goud(I) kompleks wat $Au \cdots Au$ interaksies in die vastetoestand het. Buitengewone agostiese $Au \cdots H$ interaksies is ondersoek met lae-temperatuur 1H KMR analise. Die oordrag van die karbeenligand afgelei van 1-(tiasool-2-iel)piperidien na Ph_3PAu^+ , het 'n goud-tiasoolproduk, wat voorgestel kan word as 'n pseudo abnormale asielideen kompleks as gevolg van die koördinasie van die $W(CO)_5$ fragment op 'n verwyderde stikstof atoom, tot gevolg deur die ongekende verlies van CO uit 'n gekoördineerde asielgroep. Die karbeenligand berei uit 2-fenieltiasool, het in teenstelling via 'n buitengewone skaars $W(CO)_5$ vasvangings sonder CO verlies, tot die vorming van 'n pseudo Fischer tipe karbeen kompleks gelei.

Karbeen oordragreaksies na goud is uitgebrei deur die eerste oordragte van $rNHC$ ligande van chroom en wolfram na Au^I om aanleiding te gee tot die vorming van 'n nuwe groep van komplekse wat almal met enkel-kristal X-straal diffraktometrie gekarakteriseer is. Hierdie werk oorbrug die onnatuurlike skeiding tussen Fischer en N-heterosikliese karbeenkomplekse.

Zusammenfassung

Neuartige Gold(I) Trithiophosphitkomplexe wurden von den Liganden $P(SR)_3$ ($R = Me, Ph$) und 1,2-Bis(1,3,2-dithiaphospholan-2-ylthio)ethan (2L) erhalten. $(tht)AuCl$ oder $(tht)AuC_6F_5$ reagieren bereitwillig mit diesen Liganden zu den jeweiligen Komplexen $(RS)_3PAuX$ und ${}^2L(AuX)_2$ ($X = Cl, C_6F_5$) sowie $\{Au[P(SMe)_3]_2\}CF_3SO_3$. Strukturelle Charakterisierung durch Einkristallröntgendiffraktometrie zeigte lineare Komplexe, die teilweise unter Ausbildung von $Au\cdots Au$ - oder $Au\cdots S$ -Kontakten assoziieren; zwei Polymorphe eines Komplexes, die jeweils unter Ausbildung von $Au\cdots S$ -Kontakten oder π -Stapel kristallisieren, konnten erhalten werden. $(MeS)_3PAuCl$ und $(MeO)_3PAuCl$ sind im Festzustand isostrukturell.

Der Komplex Chloro[tris(4-methylthiazol-2-yl)phosphan]gold, **A**, wurde herangezogen, um den elektronischen Einfluss von Tris(azolyl)phosphanen auf Gold(I) zu untersuchen; dazu wurde der Chloridligand durch verschiedene Thiolate substituiert. Im Gegensatz zu Ph_3PAuCl zeigte sich, dass nur NCS^- und $PhC(O)S^-$ stabile Verbindungen liefern; dies konnte auf eine verringerte Elektronendonorfähigkeit der Tris(azolyl)phosphane zurückgeführt werden. Die Komplexe **A** und Chloro[tris(thiazol-2-yl)phosphan]gold, **B**, konnten in vier neuen Polymorphen und Solvaten kristallisiert werden, insgesamt wurden damit sieben solche Strukturen bestimmt. Die Strukturen von **A** stellen den selten zu beobachtenden Fall dar, in dem eine Verbindung als neues thf-Solvat und Polymorph im Gegensatz zur ursprünglichen Struktur ohne $Au\cdots Au$ -Kontakte kristallisiert. Von Komplex **B** konnte ein neues Polymorph kristallisiert werden, das über $Au\cdots Cl$ -Kontakte verbrückte Dimere enthält. Ein schon bekanntes Polymorph kristallisiert mit einer ähnlichen Anordnung der Liganden, ist aber über $Au\cdots Au$ -Interaktionen stabilisiert. Diese Ausbildung von unterschiedlichen Kontakten in verschiedenen Polymorphen wurde zum ersten Mal beobachtet. Ein NMR-Experiment konnte zeigen, dass Komplexe von Tris(azolyl)phosphanen im alkalischen Medium hydrolyseempfindlich sind.

Ein trimerer Gold(I) Heterometallacyclus wurde durch die Reaktion von $(tht)AuCl$ mit 4,4-Dimethyl-2-(2-thienyl)oxazolin, das am C-5 des Thiophenrings deprotoniert wurde, erhalten und die Kristallstruktur bestimmt. Intramolekulare $Au\cdots S$ -Kontakte verhindern eine Reaktion des Heterometallacyclus mit anderen Metallzentren, zB $Me_3CNCAuCl$ oder $AgNO_3$. Ein weiteres thf-Solvat der Verbindung zeigt zusätzlich intermolekulare $Au\cdots Au$ -Interaktionen. Die wenigen Literaturbeispiele von bis-Imin-Koordination zu Gold(I) wurden durch die Synthese des $[Au_2(\mu\text{-}{}^2L)_2]^{2+}$ -Kations [${}^2L = 1,3\text{-Bis(imidazol-1-ylmethyl)-2,4,6\text{-trimethylbenzen}$]

erweitert. Das Triflatsalz zeigt im Festzustand die erste poröse Kristallstruktur eines Goldkomplexes. Cokristallisiertes Lösungsmittel konnte teilweise im Vakuum bei erhöhter Temperatur unter Erhaltung der Struktur entfernt werden. Eine weitere kationische Spezies des Typs $[\text{Au}_2(\mu\text{-}^2\text{L})_3]^{2+}$ wurde erstmalig mit einem zweizähligen Phosphitliganden statt der üblicherweise verwendeten Phosphanliganden im Festzustand charakterisiert.

Schliesslich wurden Pentacarbonylwolfram-Carbeniatkomplexe des Fischer-Typs dargestellt und strukturell charakterisiert. 2-Phenylthiazol und 1-(Thiazol-2-yl)piperidin wurden an C-5 des Thiazolrings deprotoniert und mit $\text{W}(\text{CO})_6$ und wässrigem $[\text{NMe}_4]\text{Cl}$ zu den Produkten umgesetzt. Ausgehend von diesen Verbindungen konnten die analogen Methoxycarbenkomplexe sowie Carbinkomplexe durch Alkylierung bzw. formale Oxidabspaltung erhalten werden. Die Carbinkomplexe bildeten binucleare Addukte mit AuCl .

Ein Methoxycarbenkomplex konnte auf Au^{I} übertragen werden und der erste solche Goldkomplex – der $\text{Au}\cdots\text{Au}$ -Kontakte im Festzustand sowie agostische $\text{Au}\cdots\text{H}$ -Interaktionen, die durch ^1H NMR-Spektroskopie bei niedriger Temperatur untersucht wurden, zeigt – konnte erhalten werden. Transfer eines Carbeniatliganden [gebildet aus 1-(Thiazol-2-yl)piperidin] auf Ph_3PAu^+ führte in einem Fall zu einem aurierten Thiazol (durch einen in der Literatur beispiellosen CO -Verlust), dieses kann durch den fernen Stickstoff als pseudo-abnormaler Azolyldenkomplex beschrieben werden. Der aus 2-Phenylthiazol gebildete Carbeniatligand ergab andererseits durch ein selten beobachtetes Abfangen eines $\text{W}(\text{CO})_5$ -Fragments ohne Verlust von CO einen Carbenkomplex des pseudo-Fischer-Typs.

Carbenübertragung auf Gold wurde weiters durch den ersten Transfer eines $r\text{NHC}$ -Liganden von Chrom und Wolfram zu Au^{I} ergänzt. Alle Komplexe dieser neuen Verbindungsklasse wurden strukturell charakterisiert. Diese Ergebnisse verbinden die unnatürliche Trennung von Carbenkomplexen des Fischer-Typs und *N*-heterocyclischen Carbenkomplexen.

Table of Contents

General remarks and abbreviations	16
Publications, posters and oral presentations	19
Chapter 1: General introduction	
1.1 Gold and relativistic effects	21
1.2 Usage of gold in medicine	23
1.3 Gold in catalysis	24
1.4 Polymorphism in gold complexes	27
1.5 General aims and dissertation outline	29
Chapter 2: Trithiophosphite complexes of gold(I)	
2.0 Abstract	34
2.1 Introduction	35
2.1.1 Aims	37
2.2 Results and discussion	38
2.2.1 Synthesis of the compounds	38
2.2.2 Thermal gravimetric analysis	41
2.2.3 Spectroscopic analyses	41
2.2.3.1 $^{31}\text{P}\{^1\text{H}\}$ NMR spectroscopy	41
2.2.3.2 ^1H and $^{13}\text{C}\{^1\text{H}\}$ NMR spectroscopy	43
2.2.3.3 ^{19}F NMR spectroscopy	44
2.2.3.4 Infrared spectroscopy	44
2.2.3.5 Mass spectrometry	45
2.2.4 Crystallography	46
2.3 Conclusions	56
2.4 Experimental	57
2.4.1 Crystallography	57
2.4.2 Instrumentation	59
2.4.3 General procedures and reagents	59
2.4.4 Synthesis of the compounds	60
2.4.4.1 – 1,2-Bis(1,3,2-dithiaphospholan-2-ylthio)ethane	60
2.4.4.2 Tetrakis(ethanenitrile)copper(1+) triflate	61
2.4.4.3 Chloro(trimethyltrithiophosphite)gold, 1	61
2.4.4.4 (Pentafluorophenyl)(trimethyltrithiophosphite)gold, 2	62

Table of Contents	11
2.4.4.5 Chloro(triphenyltrithiophosphite)gold, 3	62
2.4.4.6 (Pentafluorophenyl)(triphenyltrithiophosphite)gold, 4	62
2.4.4.7 Dichloro{ μ -[1,2-bis(1,3,2-dithiaphospholan-2-ylthio)ethane]} digold, 5	63
2.4.4.8 { μ -[1,2-Bis(1,3,2-dithiaphospholan-2-ylthio)ethane]}-bis(pentafluorophenyl)digold, 6	63
2.4.4.9 Bis(trimethyltrithiophosphite)gold(1+) triflate, 7	64
2.4.4.10 Chloro(trimethylphosphite)gold, 8	64
2.4.4.11 <i>catena</i> -(μ -Trifluoromethanesulfonato- $\kappa^2 O:O'$)-(μ -trimethyltrithiophosphite- $\kappa P:\kappa S$)copper, 9	64
Chapter 3: Tris(azolyl)phosphane complexes of gold(I)	
3.0 Abstract	66
3.1 Introduction	67
3.1.1 Aims	71
3.2 Results and discussion	72
3.2.1 Preparation of the ligands and complexes	72
3.2.2 Infrared spectroscopy	76
3.2.3 Mass spectrometry	76
3.2.4 NMR spectroscopy	77
3.2.4.1 ^{15}N NMR spectroscopy	79
3.2.4.2 Hydrolysis of 2c followed by $^{31}\text{P}\{^1\text{H}\}$ NMR spectroscopy	81
3.3 Crystallography	82
3.3.1 Polymorphs and solvates of 2b and 2c	82
3.3.2 Molecular structures of the ligands 1c , 1d and 1e	90
3.3.3 Molecular structures of 2a , 2d , 3a , 3a , 3b -0.5C ₆ H ₁₄ and 4 -0.83CDCl ₃	92
3.4 Conclusions	97
3.5 Experimental	98
3.5.1 Crystallography	98
3.5.2 Synthesis of the complexes	101
3.5.3.1 Tris(4,5-dimethylthiazol-5-yl)phosphane, 1d	102
3.5.3.2 Tris(4-methylthiazolyl)phosphane sulfide, 1e	102
3.5.3.3 Chloro[tris(4,5-dimethylthiazol-2-yl)phosphane]gold, 2d	103
3.5.3.4 (Thiocyanato- κS)[tris(4-methylthiazol-2-yl)-phosphane]gold, 3a	103
3.5.3.5 (Thiobenzoato)[tris(4-methylthiazol-2-yl)phosphane]gold, 3b	103

3.5.3.6 Bis(pentafluorophenyl)[μ -tris(1-methylimidazol-2-yl)phosphane- $\kappa^2 P:N$]digold, 4	104
3.5.3.7 Hydrolysis of 2c with aqueous NaOH	104
 Chapter 4: Heterometallacyclic complexes of gold(I)	
4.0 Abstract	106
4.1 Introduction	107
4.1.1 Heterometallacycles containing gold	107
4.1.1.1 $N^{\wedge}C^-$, $N^{\wedge}N$ - and related ligands	107
4.1.1.2 Ligands with phosphorus donor atoms	110
4.1.1.3 Heterometallacycles obtained from $C^{\wedge}C$ -ligands	112
4.1.1.4 Other ligands	113
4.1.2 Porous crystalline compounds	114
4.1.3 Digold(I) compounds bridged by three ditopic $P^{\wedge}P$ ligands – a special type of heterometallacyclic gold complex	115
4.1.4 Aims	117
4.2 Results and discussion	118
4.2.1 Synthesis and structural characterisation of a trimeric, 18-membered heterometallacycle with $N^{\wedge}C^-$ coordination: <i>cyclo</i> -tris{[μ -4,4-dimethyl-2-(thien-2-yl- κC^5)oxazoline- κN]gold}, 1	118
4.2.1.1 Synthesis and spectroscopic characterisation of complex 1	119
4.2.1.2 Crystallography	121
4.2.2 Synthesis of gold complexes of bitmb – the [Au ₂ (μ -bitmb) ₂] ²⁺ cation, 2	127
4.2.2.1 Spectroscopic characterisation	128
4.2.2.2 Crystallographic characterisation of the complexes	130
4.2.2.3 Removal of solvent from 2b ·2CH ₂ Cl ₂	135
4.2.3 Ag ^I and Au ^I -complexes of 4,4-dimethyl-2-(pyridin-4-yl)-oxazoline, 3 and 4	136
4.2.3.1 Spectroscopic characterisation	137
4.2.3.2 Crystallography	138
4.2.3.3 Au ^I complexes of 4,4-dimethyl-2-(pyridin-4-yl)-oxazoline, 4a and 4b	140
4.2.4 A novel tricyclic digold(I) complex: tris[μ - <i>N,N</i> -bis(1,3,2-dioxaphospholan-2-yl- κP)methanamine]digold(2+) triflate, 5	141
4.2.4.1 Spectroscopic characterisation	142

Table of Contents	13
4.2.4.2 Crystallography	143
4.2.5 The attempted syntheses of other $[\text{Au}_2(\mu\text{-}^2\text{L})_3]^{2+}$ compounds	145
4.2.5.1 The attempted synthesis of $[\text{Au}_2(\mu\text{-dppe})_3](\text{CF}_3\text{SO}_3)_2$	145
4.2.5.2 The attempted synthesis of $[\text{Au}_2(\mu\text{-tmdpd})_3](\text{CF}_3\text{SO}_3)_2$ – crystal structure of $[\text{Au}(\text{tmdpd})_2]\text{CF}_3\text{SO}_3$, 7 .	146
4.3 Conclusions	148
4.4 Experimental	150
4.4.1 Crystallography	150
4.4.2 Preparation of the compounds	150
4.4.2.1 Attempted reaction of 1 with silver nitrate	153
4.4.2.2 Attempted cocrystallisation of 1 with $\text{Me}_3\text{CNCAuCl}$	153
4.4.2.3 <i>Cyclo</i> -bis $\{\mu\text{-}1,3\text{-bis}[(\text{imidazol-}1\text{-yl-}\kappa\text{N})\text{methyl}]\text{-}2,4,6\text{-}$ trimethylbenzene $\}$ digold(2+) tetrafluoroborate, 2a	154
4.4.2.4 <i>Cyclo</i> -bis $\{\mu\text{-}1,3\text{-bis}[(\text{imidazol-}1\text{-yl-}\kappa\text{N})\text{methyl}]\text{-}2,4,6\text{-}$ trimethylbenzene $\}$ digold(2+) trifluoromethanesulfonate, 2b	154
4.4.2.5 <i>Catena</i> - $[\mu\text{-}4,4\text{-dimethyl-}2\text{-}(\text{pyridin-}4\text{-yl-}\kappa\text{N})\text{oxazoline-}\kappa\text{N}]\text{-}$ $[\mu\text{-nitrate-}\kappa^3\text{O}(\text{Ag}):O(\text{Ag}'):O'(\text{Ag})]\text{silver}$, 3	155
4.4.2.6 $[4,4\text{-dimethyl-}2\text{-pyridin-}4\text{-yl-}\kappa\text{N})\text{oxazoline-}\kappa\text{N}]\text{gold}(1+)\text{-}$ trifluoromethanesulfonate, 4a	155
4.4.2.7 $[4,4\text{-dimethyl-}2\text{-}(\text{pyridin-}4\text{-yl-}\kappa\text{N})\text{oxazoline-}\kappa\text{N}]\text{gold}(1+)\text{-}$ tetrafluoroborate, 4b	156
4.4.2.8 <i>N,N</i> -Bis(1,3,2-dioxaphospholan-2-yl)methanamine	156
4.4.2.9 Tris $[\mu\text{-}N,N\text{-bis}(1,3,2\text{-dioxaphospholan-}2\text{-yl-}\kappa\text{P})\text{methanamine}]\text{-}$ digold(2+) trifluoromethanesulfonate, 5	156
4.4.2.10 Synthesis of $[\text{Au}_2(\mu\text{-dppe})_2](\text{CF}_3\text{SO}_3)_2 \cdot 2\text{CH}_3\text{CN}$, 6	157
4.4.2.11 Synthesis of $[\text{Au}(\text{tmdpd})_2]\text{CF}_3\text{SO}_3$, 7	157
Chapter 5: Carbene and carbyne complexes with unconventional N-heterocyclic side chains: interaction with gold(I) fragments	
5.0 Abstract	158
5.1 Introduction	159
5.1.1 Carbenes	159
5.1.2 Carbynes	163
5.1.3 Carbene and carbyne transfer to gold fragments	165
5.1.4 Aims of this study	167
5.2 Results and discussion	167

Table of Contents	14
5.2.1 The attempted synthesis of 2-thiazolyl carbyne complexes	167
5.2.2 Syntheses of 5-thiazolyl carbyne and carbene complexes	169
5.2.2.1 Syntheses of (acyl)pentacarbonyltungstates(1-)	
4a, 4b and 5a, 5b	170
5.2.2.2 Syntheses of Fischer-type methoxy carbene complexes	
6a and 6b	171
5.2.2.3 Syntheses of the carbyne complexes 7a and 7b	172
5.2.3 Transfer to gold(I) centres	173
5.2.3.1 Transfer of heterocyclic carbene ligands to the gold fragments	
AuCl and Ph ₃ PAu ⁺ – isolation of 8b , 9a , and 10b	173
5.2.3.2 Interaction of carbyne complexes 7a and 7b with gold centres	178
5.2.3.3 Transfer of <i>r</i> NHC ligands to Au ^I	179
5.3 Spectroscopic characterisation	181
5.3.1 Infrared spectroscopy	182
5.3.2 Mass spectrometry	183
5.3.3 NMR spectroscopy	187
5.3.3.1 ¹ H NMR spectroscopy	187
5.3.3.2 ¹³ C{ ¹ H} NMR spectroscopy	192
5.3.3.3 ³¹ P{ ¹ H}NMR spectroscopy	194
5.3.3.4 Solid-state CPMAS ¹³ C NMR spectroscopy	195
5.4 Single crystal X-ray diffraction	197
5.4.1 Molecular structures of the carbeniate complexes 5a and 5b	197
5.4.2 Molecular structure of H ⁺ -bridged carbeniate 5c ·2CHCl ₃	202
5.4.3 Crystal and molecular structures of the Fischer-type methoxycarbene complexes 6a and 6b	204
5.4.4 Molecular structures of the carbyne complexes 7a and 7b	208
5.4.5 Crystal and molecular structure of a gold Fischer-type carbene complex, 8b	210
5.4.6 Molecular structure of the decarbonylated gold complex 9a ·0.5CH ₂ Cl ₂	212
5.4.7 Molecular structure of the carbene transfer product 10b ·C ₅ H ₁₂	215
5.4.8 Molecular structure of 11a ·0.5C ₄ H ₈ O	218
5.4.9 Molecular structures of <i>r</i> NHC complexes 12W , 13 and 14	219
5.4.10 Molecular structure of <i>r</i> NHC complex 16	222
5.5 Conclusions	223
5.6 Experimental	225
5.6.1 Crystal structure determinations	225

5.6.2 General procedures and reagents	229
5.6.3 Syntheses of the compounds	230
5.6.3.1 Lithium pentacarbonyl{[2-(1-piperidinyl)thiazol-5-yl]carbonyl}-tungstate(1-), 4a	230
5.6.3.2 Tetramethylammonium pentacarbonyl{[2-(1-piperidinyl)thiazol-5-yl]carbonyl}tungstate(1-), 5a	230
5.6.3.3 Pentacarbonyl{methoxy[2-(1-piperidinyl)thiazol-5-yl]methylidene}tungsten, 6a	231
5.6.3.4 <i>cis</i> -Dicarbonylchloro{[2-(1-piperidinyl)thiazol-5-yl]methylidyne}- <i>cis</i> -bis(pyridine)tungsten, 7a	232
5.6.3.5 Pentacarbonyl-2 κ^5 C-[μ -2-(1-piperidinyl)thiazol-5-yl-1 κ C ⁵ :2 κ N ³]- (triphenylphosphane-1 κ P)goldtungsten, 9a	233
5.6.3.6 <i>cis</i> -Dicarbonyl-2 κ^2 C-dichloro-1 κ ,2 κ -{ μ -[2-(1-piperidinyl)thiazol-5-yl]methylidyne-1 κ C ¹ :2 κ C ¹ }- <i>cis</i> -bis(pyridine-2 κ N)goldtungsten(<i>Au-W</i>), 11a	234
5.6.3.7 – 2-Phenylthiazole, 1b	234
5.6.3.8 Tetramethylammonium pentacarbonyl[(2-phenylthiazol-5-yl)carbonyl]tungstate(1-), 5b	235
5.6.3.9 Pentacarbonyl[methoxy(2-phenylthiazol-5-yl)methylidene]tungsten, 6b	235
5.6.3.10 <i>cis</i> -Dicarbonylchloro[(2-phenylthiazol-5-yl)methylidyne]- <i>cis</i> -bis(pyridine)tungsten, 7b	236
5.6.3.11 Chloro[methoxy(2-phenylthiazol-5-yl)methylidene]gold, 8b	236
5.6.3.12 Pentacarbonyl-2 κ^5 C-[μ -(2-phenylthiazol-5-yl)carbonyl-1 κ C:2 κ O]- (triphenylphosphane-1 κ P)goldtungsten, 10b	237
5.6.3.13 Reaction of 7b with (tht)AuC ₆ F ₅	238
5.6.3.14 Pentacarbonyl(1,2-dimethyl-5-phenyl-1 <i>H</i> -pyridin-4-ylidene)chromium, 12Cr	238
5.6.3.15 Pentacarbonyl(1,2-dimethyl-5-phenyl-1 <i>H</i> -pyridin-4-ylidene)tungsten, 12W	238
5.6.3.16 Chloro(1,2-dimethyl-5-phenyl-1 <i>H</i> -pyridin-4-ylidene)gold, 13	239
5.6.3.17 (1,2-Dimethyl-5-phenyl-1 <i>H</i> -pyridin-4-ylidene)-(triphenylphosphane)gold(1+) triflate, 14	239
5.6.3.18 Pentacarbonyl(1-methyl-1 <i>H</i> -pyridin-4-ylidene)chromium, 15	240
5.6.3.19 Chloro(1-methyl-1 <i>H</i> -pyridin-4-ylidene)gold	241

General remarks

Nomenclature

Nomenclature in this thesis has been kept as systematic as viable and trivial names have been largely avoided. The IUPAC recommendations of the Commission on Nomenclature of Inorganic Chemistry in A. Salzer: “Nomenclature of organometallic compounds of the transition elements (IUPAC Recommendations 1999)”, *Pure Appl. Chem.* **1999**, *71*, 1557–1585, have been incorporated. All alkanes and alkyl groups, unless noted otherwise, are unbranched. “Hexanes” refers to the commercial mixture of isomers.

When referring to specific atoms in a compound, the numbers resemble the scheme applied in nomenclature, *e.g.* the carbon atom between the nitrogen and sulfur atoms in a thiazole ring is C-2.

Crystallography

In place of the obsolete estimated standard deviation (e.s.d.) the measure of uncertainty of bond lengths and angles is referred to as the standard uncertainty (s.u.) (symbol *u*) which is now the preferred term. Values of s.u.s have always been rounded up to the nearest single digit. For readability, the unit Ångström (Å, 10⁻¹⁰ m) is used instead of the picometre. Differences in bond parameters have been deemed significant if the intervals of 3 s.u.s, counting from each value in the appropriate direction, do not overlap. Data collection and figure drawing parameters are summarised in Section 2.4.1, p. 57.

Associated with this thesis a crystallographic information (CIF) file containing all crystal structures reported will be deposited electronically and can be obtained *via* the J. S. Gericke Library, Stellenbosch University. If published, these CIF files can also be obtained *via* the Cambridge Crystallographic Data Centre, 12 Union Road, Cambridge CB2 1EZ, United Kingdom; data_request@ccdc.cam.ac.uk; *via* www.ccdc.cam.ac.uk/data_request/cif or supplementary material of the appropriate journal. The CIF entries of published structures that are deposited with the J. S. Gericke Library have been edited for consistent nomenclature but are otherwise identical to those with the CCDC.

Abbreviations used in this thesis

bipy	2,2'-bipyridine
bitmb	1,3-bis(imidazol-2-ylmethyl)-2,4,6-trimethylbenzene
br	broad (referring to peak shape)
Bu	butyl
Bz	benzoyl
Cp	η^5 -cyclopentadienyl
CP	cross-polarisation
dcm	dichloromethane
dec.	decomposition
dmpm	bis(dimethylphosphanyl)methane
dmsO	dimethylsulfoxide [(methylsulfinyl)methane]
dppe	1,2-bis(diphenylphosphanyl)ethane
dppm	bis(diphenylphosphanyl)methane
EI	electron impact
eq.	equivalent
ESI	electrospray ionisation
Et	ethyl
FAB	fast atom bombardment
Fc	ferrocenyl
IR	infrared; abbreviations used in conjunction with infrared spectroscopy:
	m medium strength
	s strong
	sh shoulder
	vs very strong
	w weak
L	generic ligand
M	generic metal
MAS	magic angle spinning
Me	methyl
MALDI	matrix-assisted laser desorption ionisation

MS	mass spectrometry
NMR	nuclear magnetic resonance; abbreviations used in conjunction with NMR:
CP	cross-polarisation
d	doublet
m	multiplet
MAS	magic angle spinning (54.7° against B_0)
q	quadruplet
s	singlet (if a coupling constant is given it was obtained from the satellite doublet signal)
t	triplet (generally of 1:2:1 intensity pattern, for coupling with ^{14}N a 1:1:1 pattern is observed)
Ph	phenyl
py	(<i>N</i> -coordinated) pyridine
R	any organic residue (if not specified)
s.u.	standard uncertainty, replaces the obsolete e.s.d. (estimated standard deviation)
Tf	trifluoromethylsulfonyl, trifyl
thf	tetrahydrofuran (oxacyclopentan)
tht	tetrahydrothiophene (sulfacyclopentan)
tmdpd	tetramethyldiphosphane disulfide [$\text{Me}_2\text{P}(\text{S})\text{P}(\text{S})\text{Me}_2$]
tmeda	<i>N,N,N',N'</i> -tetramethylethan-1,2-diamine
triflate	trifluoromethanesulfonate
X	generic halogen (if not specified)

Publications by the author

G. Laus, C. E. Strasser, M. Holzer, K. Wurst, G. Pürstinger, K.-H. Ongania, M. Rauch, G. Bonn and H. Schottenberger
“The (*E*)-2-Ferrocenylethenylcobaltocenium Cation. A Missing Link in Heteronuclear Bimetalloocene-Based Donor–Acceptor Conjugate Chemistry Exhibiting Irregular Solvatochromism”
Organometallics **2005**, *24*, 6085–6093.

G. Laus, C. E. Strasser, K. Wurst and H. Schottenberger
“Crystal structure of (*E*)-2-ruthenocenylethenylcobaltocenium hexafluorophosphate [(C₅H₅)Ru(C₁₂H₁₀)Co(C₅H₅)] [PF₆][−]”
Z. Kristallogr. – New Cryst. Struct. **2006**, *221*, 103–104.

C. E. Strasser, S. Cronje, H. Schmidbaur and H. G. Raubenheimer
“The preparation, properties and X-ray structures of gold(I) trithiophosphite complexes”
J. Organomet. Chem. **2006**, *691*, 4788–4796.

L. de Jongh, C. E. Strasser, S. Cronje and H. G. Raubenheimer
“Bis[μ -bis(diphenylphosphino)methane- $\kappa^2 P:P$]digold(I)(Au–Au) dinitrate perdeuteromethanol solvate”
Acta Crystallogr., Sect. E: Struct. Rep. Online **2007**, *63*, m2137–m2138.

X. Sheng, C. E. Strasser, H. G. Raubenheimer and R. C. Luckay
“Isopropylammonium (isopropylamino)oxoacetate monohydrate”
Acta Crystallogr., Sect. E: Struct. Rep. Online **2007**, *63*, o4361.

C. E. Strasser, S. Cronje and H. G. Raubenheimer
“The low-temperature phase of diethylammonium tetrachloridocuprate(II)”
Acta Crystallogr., Sect. E: Struct. Rep. Online **2007**, *63*, m2915–m2916.

C. E. Strasser, W. F. Gabrielli, C. Esterhuysen, O. B. Schuster, S. D. Nogai, S. Cronje and H. G. Raubenheimer
“Preparation of tris(azolyl)phosphine gold(I) complexes: digold(I) coordination and variation in solid state intermolecular interactions”
New J. Chem. **2008**, *32*, 138–150.

C. E. Strasser, W. F. Gabrielli, O. B. Schuster, S. D. Nogai, S. Cronje and H. G. Raubenheimer
“Crystal and molecular structures of tris(1-methylimidazol-2-yl)phosphine, tris(4-methylthiazol-2-yl)phosphine and its sulfide”
J. Chem. Crystallogr., submitted.

Poster presentations

3rd Cape Organometallic Symposium,
Breakwater Lodge, Waterfront, Cape Town, South Africa, October 21st, 2005.
“Ethene-bridged bi- and trimetallocenes having unusual solvatochromic behaviour in solution”
C. E. Strasser, G. Laus, M. Holzer, K. Wurst, G. Pürstinger, K.-H. Ongania, M. Rauch, H. Schottenberger and H. G. Raubenheimer.

Cape Organometallic Symposium – Organometallics and their Applications,
Breakwater Lodge, Waterfront, Cape Town, South Africa, August 9th–11th, 2006.
“Preparation and crystallographic study of the first gold(I) trithiophosphite complexes”
C. E. Strasser, S. Cronje, H. Schmidbaur and H. G. Raubenheimer.

9th FIGIPAS Meeting in Inorganic Chemistry,
Vienna University of Technology, Vienna, Austria, July 4th–7th, 2007.
“Variation in association and crystallisation of new gold(I) complexes”
C. E. Strasser, W. F. Gabrielli, S. Cronje and H. G. Raubenheimer.

Oral presentations

The following oral presentations incorporating parts of this dissertation have been held in English by the author at the respective venues:

SACI Young Chemist Mini Symposium,
University of Cape Town, Cape Town, South Africa, May 2006.
“Gold(I) trithiophosphite complexes – a synthetic and analytical study”

SACI Young Chemist Mini Symposium,
University of the Western Cape, Bellville, South Africa, May 2007.
“Unique Coordination Modes of Gold”

Cape Organometallic Symposium 08,
Breakwater Lodge, Waterfront, Cape Town, South Africa, October 24th, 2008.
“Interconnectivity between Fischer carbene ligands from group 6 metals to gold(I)”

Conference Attendance

Science at Synchrotrons,
iThemba LABS, Faure, South Africa, February 5th–10th, 2007.

1

General Introduction

1.1 Gold and relativistic effects

The heavier members of the periodic table of the elements, especially the transition metals following the lanthanides, are noticeably affected by relativistic effects. Those effects reach a pronounced maximum for gold. Its neighbours platinum and mercury are significantly less influenced by this phenomenon.¹

A consequence of relativistic effects is the similar energy of the 6s and 5d electrons caused by relativistic contraction of the former and expansion of the latter orbitals. Both levels are thus accessible for hybridisation and are actively involved in bonding. The colour of gold is also a result of relativistic effects, though definitive results are surprisingly elusive.¹ The coinage metals Cu, Ag and Au form group 11 in the periodic table and would be expected to show the oxidation state I in their compounds, which is indeed observed. While the “unorthodox” oxidation state II for copper is attributed to its compact, nodeless d-orbitals experiencing electron-electron repulsion,¹ gold can exhibit any oxidation state from –I to V, most commonly I and III in complexes, as a consequence of the chemically non-inert d electrons and the low-lying 6s orbital that can accommodate an additional electron.² Proof of the latter is manifested in the existence of the auride anion, Au[–], a unique feature amongst transition metals.³ This anion is capable of replacing Br[–] and I[–] in crystal lattices.⁴

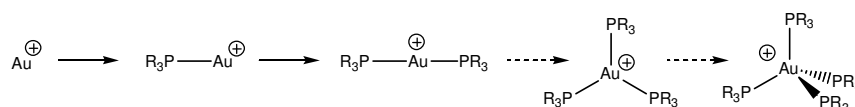
1 P. Pyykkö, *Angew. Chem., Int. Ed. Engl.* **2004**, *43*, 4412–4456 (*Angew. Chem.* **2004**, *116*, 4512–4557).

2 P. Pyykkö, *Angew. Chem., Int. Ed. Engl.* **2002**, *41*, 3573–3578 (*Angew. Chem.* **2002**, *114*, 3723–3728).

3 A. H. Sommer, *Nature* **1943**, *152*, 215.

4 (a) R. Wormuth and R. W. Schmutzler, *Thermochim. Acta* **1990**, *160*, 97–102; (b) C. Feldmann and M. Jansen, *Z. Anorg. Allg. Chem.* **1995**, *621*, 1907–1912.

Apart from peculiar oxidation states, the coordination geometry of gold is special in that the Au^{I} oxidation state, with which this thesis will deal exclusively, strongly prefers linear dicoordinate 14-valence electron complexes.⁵ In contrast to its lighter group members, it is reluctant to expand its coordination sphere to trigonal-planar or tetrahedral coordination which – in unchelated complexes – can only be achieved with the strongest donors such as phosphanes and is usually prone to dissociation in solution or decomposition in the solid state by release of ligand.⁶ Theoretical studies show that the energy released upon coordination of phosphanes to Au^{I} plunges sharply after two ligands have been accommodated (Scheme 1.1). The relativistically calculated Au–P bond energies for successive PH_3 coordination to Au^+ are 270 and 245 kJ mol^{-1} for the first two and only 60 and 75 kJ mol^{-1} for the last two PH_3 ligands.⁷



Scheme 1.1 Schematic representation of stepwise phosphane coordination to Au^{I} .

The trend not to readily coordinate to more than two ligands, however, does not discourage the gold atoms in Au^{I} complexes to associate in the solid state and in concentrated solutions, a phenomenon *Schmidbaur* has termed “aurophilicity”.⁸ These attractive closed-shell d^{10} – d^{10} interactions are also a consequence of relativistic effects and occur in the metal–metal separation range of 2.8 to *ca.* 3.5 Å. Their strength (up to 46 kJ mol^{-1}) is comparable to hydrogen bonds.¹ In some gold(I) complexes a $\text{Au}\cdots\text{Au}$ distance of less than 2.88 Å is observed⁹ which is the interatomic distance in gold metal, proof of a bonding interaction between these atoms. Two ligands bridging

5 P. Schwerdtfeger, P. D. W. Boyd, A. K. Burrell, W. T. Robinson and M. J. Taylor, *Inorg. Chem.* **1990**, 29, 3593–3607.

6 (a) H. Schmidbaur and R. Franke, *Chem. Ber.* **1972**, 105, 2985–2997;

(b) P. G. Jones, *Acta Crystallogr., Sect. B: Struct. Crystallogr. Cryst. Chem.* **1980**, 36, 3105–3107.

7 P. Schwerdtfeger, H. L. Hermann and H. Schmidbaur, *Inorg. Chem.* **2003**, 42, 1334–1342.

8 (a) F. Scherbaum, B. Huber, G. Müller and H. Schmidbaur,

Angew. Chem., Int. Ed. Engl. **1988**, 27, 1542–1544 (*Angew. Chem.* **1988**, 100, 1600–1602);

(b) F. Scherbaum, A. Grohmann, B. Huber, C. Krüger and H. Schmidbaur,

Angew. Chem., Int. Ed. Engl. **1988**, 27, 1544–1546 (*Angew. Chem.* **1988**, 100, 1602–1604).

9 See for example: (a) M. A. Bennett, S. K. Bhargava, K. D. Griffiths, G. B. Robertson,

W. A. Wickramasinghe and A. C. Willis, *Angew. Chem., Int. Ed. Engl.* **1987**, 26, 258–260

(*Angew. Chem.* **1987**, 99, 261–262); (b) F. Scherbaum, B. Huber, G. Müller and H. Schmidbaur,

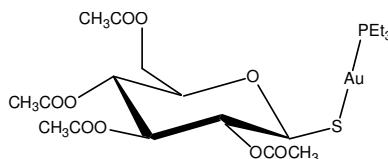
Angew. Chem., Int. Ed. Engl. **1988**, 27, 1542–1544 (*Angew. Chem.* **1988**, 100, 1600–1602);

(c) M. Desmet, H. G. Raubenheimer and G. J. Kruger, *Organometallics* **1997**, 16, 3324–3332.

the gold centres greatly facilitate the formation of such a close contact. The only example where an unbridged Au^I may engage in this kind of aggregation is a pentanuclear complex, but the assignment of oxidation states are ambiguous and the authors suggest that it may also be regarded as a Au^{III} centre.¹⁰

1.2 Usage of gold in medicine

Medicines containing gold have been administered since the early ages in Egypt and China as described in the scriptures of a contemporary alchemist.¹¹ In the late 19th century, Na[AuCl₄] was used in the treatment of syphilis where it might have had some advantage over the mercury compounds used at that time. Only when Koch discovered the antibacterial action of [Au(CN)₂]⁻ in 1890, chrysotherapy was re-investigated with an increasingly scientific approach. As this complex was in time proven to act against the tubercle bacillus [which was then believed to cause rheumatoid arthritis (RA)], gold compounds, notably Au^I thiolates, were used against this disease. In 1960 the efficacy of this therapy was finally proven and chrysotherapy remains one of the effective measures against RA even though the action of gold is not well understood. In 1985 the then new compound AuranofinTM (Scheme 1.2) was introduced, the first orally administrable gold drug¹² in contrast to the other injectable thiolates. New fields for medical applications of gold complexes are the treatment of cancer, malaria and HIV. For the former a relationship between the established Pt^{II} drugs and the isoelectronic Au^{III} compounds can be envisaged.¹³



Scheme 1.2 Structural formula of the drug AuranofinTM.

10 R. Usón, A. Laguna, M. Laguna, J. Jiménez and P. G. Jones, *Angew. Chem., Int. Ed. Engl.* **1991**, *30*, 198–199 (*Angew. Chem.* **1991**, *103*, 190–191).

11 (a) T. L. Davis and L.-C. Wu, *J. Chem. Educ.* **1936**, *13*, 103–105;

(b) Z. Huaizhi and N. Yuantao, *Gold Bull.* **2001**, *34*, 24–29.

12 G. J. Higby, *Gold Bull.* **1982**, *15*, 130–140.

13 (a) M. J. Abrams and B. A. Murrer, *Science* **1993**, *261*, 725–730; (b) C. F. Shaw III, *Chem. Rev.* **1999**, *99*, 2589–2600; (c) E. R. T. Tiekink, *Gold Bull.* **2003**, *36*, 117–124.

1.3 Gold in catalysis

For a long time gold was neglected in the field of catalysis. Due to its most noble status it was perceived to be unreactive. Only scattered reports of reactions catalysed by gold and its complexes have thus surfaced in the 20th century. This potential of gold was acknowledged only recently ensuing an explosive growth of the numbers of contributions published in this field.¹⁴

In the 1980s *Haruta* started developing the catalytic oxidation of CO to CO₂ by gold on oxide supports;¹⁵ a very important reaction in fuel cell design as CO poisons platinum electrodes and has to be removed from the gas feed. Another important heterogeneous reaction is the hydrochlorination of alkenes for which Au^{III} was predicted to be the superior catalyst, which was later verified.¹⁶

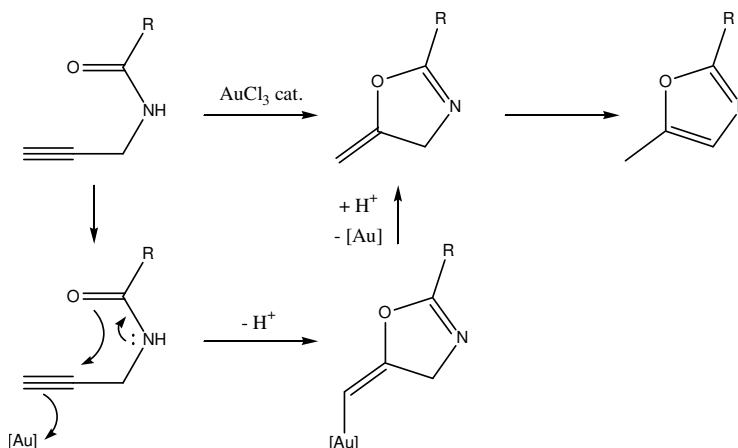
Homogeneous applications of gold catalysis now focus on the activation of alkynes and allenes, as well as activated alkenes to a lesser extent. The catalysts [AuCl₄]⁻ and AuCl₃ used initially have now mostly been replaced with phosphane-gold(1+) species with weakly coordinating counter-ions. A great advantage of these compounds is their inertness against oxidation by O₂ and against interference by moisture and most common functional groups. As a soft metal cation, Au^I does not interact strongly with these mostly hard donor atoms and the reactions can be performed without the need for adherence to special conditions.^{14d} The action of Au^I is thought to result from its alkyne-philicity (even though structurally characterised alkyne π complexes of this metal are rarities)¹⁷ paired with its preference of linear-dicoordinate geometry. This attack by Au^I renders one carbon atom of the alkyne electrophilic and thus susceptible to attack by various nucleophiles, always affording the Markovnikov product for

14 (a) A. S. K. Hashmi, *Angew. Chem., Int. Ed. Engl.* **2005**, *44*, 6990–6993 (*Angew. Chem.* **2005**, *117*, 7150–7154); (b) G. J. Hutchings, *Catal. Today* **2005**, *100*, 55–61; (c) A. S. K. Hashmi and G. J. Hutchings, *Angew. Chem., Int. Ed. Engl.* **2006**, *45*, 7896–7936 (*Angew. Chem.* **2006**, *118*, 6297–6300); (d) H. C. Shen, *Tetrahedron* **2008**, *64*, 3885–3903.

15 M. Haruta, T. Kobayashi, H. Sano, N. Yamada, *Chem. Lett.* **1987**, 405–408.

16 B. Nkosi, N. J. Coville and G. J. Hutchings, *Appl. Catal.* **1988**, *43*, 33–39.

17 See for example: (a) D. M. P. Mingos, J. Yau, S. Menzer and D. J. Williams, *Angew. Chem., Int. Ed. Engl.* **1995**, *34*, 1894–1895 (*Angew. Chem.* **1995**, *107*, 2045–2047); (b) K. Köhler, S. J. Silverio, I. Hyla-Kryspin, R. Gleiter, L. Zsolnai, A. Driess, G. Huttner and H. Lang, *Organometallics* **1997**, *16*, 4970–4979; (c) P. Schulte and U. Behrens, *Chem. Commun.* **1998**, 1633–1634.



Scheme 1.3 Example of a nucleophilic addition to an alkyne catalysed by AuCl_3 .¹⁸

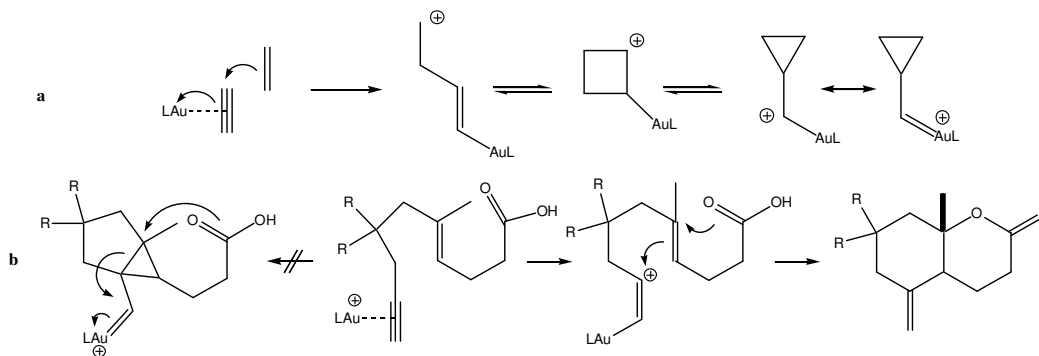
terminal alkynes. Typical reactions of alkynes proceed by attack of the gold at the alkyne, addition of an electrophile and hydrolysis of the organogold product (Scheme 1.3).^{14d}

If, however, an alkene adds to an alkyne activated by a gold catalyst, formally a carbocation results that may rearrange to a gold-substituted α -cyclopropyl cation. (Scheme 1.4). This species may also be drawn as a (cyclopropylmethylidene)gold(1+) complex. Based on evidence from reaction pathways *Fürstner* and *Morency*,¹⁹ however, postulate that the carbocation resonance form more closely relates to reality. In a report of *Hashmi* some additional data²⁰ is compiled that confirm the findings of the former authors. Different substitution of the attacked double bond always gives products derived from the more stable carbocation, while a carbene intermediate would sometimes mean that attack would be more efficient on the sterically more crowded cyclopropane site as shown in Scheme 1.4 (b): From sterical considerations, the carbene structure shown to the left should be expected to react with both cyclopropane carbons. However, efficient synthesis of the product on the right indicates that a carbocationic structure has the higher contribution. The last step is a proto-deauration yielding the exo-double bond.

18 M. D. Milton, Y. Inada, Y. Nishibayashi and S. Uemura, *Chem. Commun.* **2004**, 2712–2713.

19 A. Fürstner and L. Morency, *Angew. Chem., Int. Ed. Engl.* **2008**, *47*, 5030–5033 (*Angew. Chem.* **2008**, *120*, 5108–5111).

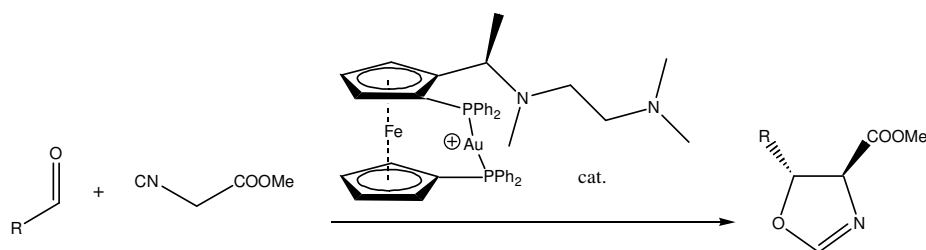
20 A. S. K. Hashmi, *Angew. Chem., Int. Ed. Engl.* **2008**, *47*, 6754–6756 (*Angew. Chem.* **2008**, *120*, 6856–6858).



Scheme 1.4 Activation of a triple bond by gold and addition of a double bond: (a) different possible structures of the intermediate resulting from the attack are shown, L = tertiary phosphane; (b) see discussion.

This evidence is in support of the view that gold carbene complexes, at least those of the Schrock-type invoked in gold catalysis, resemble gold-stabilised carbocations rather than carbenes and that π back-donation from the metal is negligible.²¹ This result is also reflected in the bond lengths of gold carbene complexes which feature in Chapter 5 and is discussed in more detail in the introduction of that Chapter.

Stereospecific catalysis by gold has also been investigated;²² an early report on a gold-catalysed stereoselective aldol condensation involved the reaction of $\text{CNCH}_2\text{COOMe}$ with aldehydes to form 4,5-disubstituted oxazolines shown in Scheme 1.5 which are extremely useful precursors for enantiomerically pure amino acids and -alcohols. As catalyst a substituted 1,1'-bis(diphenylphosphanyl)ferrocene gold complex that both comprises a substituent of point chirality and is axially chiral in itself was used.²³



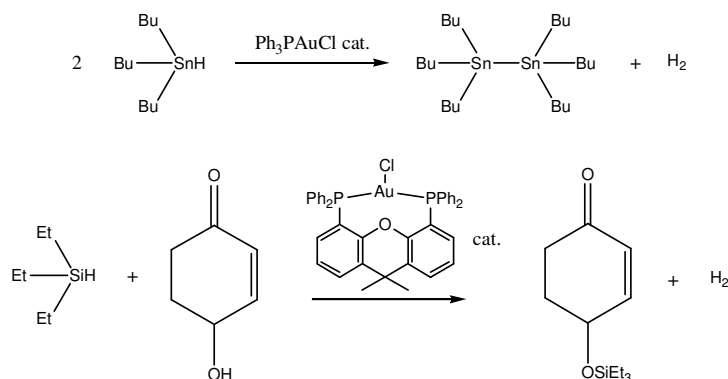
Scheme 1.5 Gold-catalysed enantioselective aldol condensation.

21 P. K. Hurlburt, J. J. Rack, J. S. Luck, S. F. Dec, J. D. Webb, O. P. Anderson and S. H. Strauss, *J. Am. Chem. Soc.* **1994**, *116*, 10003–10014.

22 N. Bongers and N. Krause, *Angew. Chem., Int. Ed. Engl.* **2008**, *47*, 2178–2181 (*Angew. Chem.* **2008**, *120*, 2208–2211).

23 Y. Ito, M. Sawamura and T. Hayashi, *J. Am. Chem. Soc.* **1986**, *108*, 6405–6406.

Other reactions of interest to organometallic chemistry have been shown to be catalysed by gold as well, *e.g.* the oxidative dimerisation of triorganostannanes to hexaorganodistannane and dihydrogen²⁴ as well as the oxidative silylation of hydroxyl groups by triethylsilane affording the triethylsilyl ester or ether and dihydrogen.²⁵ Aldehyde, alkyne, alkene and halide groups are unaffected by the latter reaction (Scheme 1.6). Gold(I) hydrides have been implicated in the catalytic cycle, but eluded detection.



Scheme 1.6 Oxidative coupling reactions catalysed by Au^I phosphane complexes.

1.4 Polymorphism in gold complexes

When a given compound crystallises it will most often afford crystals of fairly uniform appearance and a characteristic spatial arrangement of the molecules within the associated unit cell. Sometimes, the molecules are arranged differently in the lattice of two crystals formed and hence different unit cell dimensions are observed. The space group and/or crystal system may also be different but this is not a necessity. When such different forms of a compound in the solid state are observed that fulfil the conditions above, they are called polymorphs. True polymorphs must therefore have exactly the same molecular composition, *i.e.* the same cations, anions and neutral molecules are present in the same ratio in both crystalline forms. Usually polymorphs will give themselves away by crystals of different shape and/or colour. This

24 H. Ito, T. Yajima, J. Tateiwa and A. Hosomi, *Tetrahedron Lett.* **1999**, 40, 7807–7810.

25 H. Ito, K. Takagi, T. Miyahara and M. Sawamura, *Org. Lett.* **2005**, 7, 3001–3004.

definition, however, has certain intrinsic limitations and *e.g.* for conformational isomers other definitions exist;²⁶ for the scope of this dissertation the definition above is sufficient.

A different situation ensues when a compound crystallises with enclosed solvent that merely occupies a cavity formed by inefficient packing of the host. These co-crystallised solvent molecules can often be substituted for other molecules of similar size, *e.g.* by crystallisation from a different solvent.²⁷ Such crystals do not constitute true polymorphs as they do not comprise the same molecular species but are merely different solvates of the same compound; sometimes in the literature the term pseudo-polymorphism is used.

In the pharmaceutical industry polymorphism, the formation of solvates and co-crystals (similar to a solvate but the co-crystallised species is a solid at room temperature) are major factors that must be considered.^{26,28} On the one hand, these different crystalline forms – be it a polymorph, solvate or co-crystallisate – may exhibit different solubilities and hence bioavailabilities.²⁹ On the other hand, such a material may be considered a new invention and therefore not be protected by patents that may only apply to a specific crystalline form of the drug. The latter enables competitors to essentially market the same drug without associated research and development expenses.

Polymorphism is especially interesting when observed with gold compounds. Variations in aggregation by aurophilic contacts usually lead to different luminescent behaviour and several studies in this field have been published.³⁰ For Ph_3AsAuCl , examination of the luminescence spectra has led to the discovery of polymorphic

26 J. Bernstein, in *Polymorphism in Molecular Crystals (IUCr Monographs on Crystallography, 14)*, Clarendon Press, Oxford, **2002**.

27 S.-S. Yun, J.-K. Kim, J.-S. Jung, C. Park, J.-G. Kang, D. R. Smyth and E. R. T. Tiekink, *Cryst. Growth Des.* **2006**, *6*, 899–909.

28 R. Hilfiker, in *Polymorphism in the Pharmaceutical Industry*, Wiley, New York, **2006**.

29 J. K. Halebian, *J. Pharm. Sci.* **1975**, *64*, 1269–1288.

30 (a) R. L. White-Morris, M. M. Olmstead and A. L. Balch, *J. Am. Chem. Soc.* **2003**, *125*, 1033–1040; (b) W. Lu, N. Zhu and C.-M. Che, *J. Am. Chem. Soc.* **2003**, *125*, 16081–16088; (c) E. M. Gussenhoven, J. C. Fettinger, D. M. Pham, M. M. Malwitz and A. L. Balch, *J. Am. Chem. Soc.* **2005**, *127*, 10838–10839; (d) R. L. White-Morris, M. M. Olmstead, S. Attar and A. L. Balch, *Inorg. Chem.* **2005**, *44*, 5021–5029.

forms of this complex.³¹ Given that hydrogen bonds are of similar strength than aurophilic interactions,¹ such interactions have been utilised in the design of polymorphs.³²

1.5 General aims and dissertation outline

New ligands that have not found application in the field of gold chemistry are presented in this dissertation and their interaction with Au^I centres is investigated. Some of these ligands are rather simple and readily available, it is thus surprising that they have not found use in gold chemistry before. A summary of the aims regarding the investigations presented in the Chapters is presented below, detailed aims and summaries will be given in separate sections in the respective Chapters.

Trithiophosphites of the general formula P(SR)₃, related to normal phosphites by replacing oxygen with sulfur, have not received much attention as ligands in coordination chemistry. The chemistry of these potentially multidentate, but yet simple, ligands towards several gold(I) fragments was thus to be developed. Structural characterisation of the complexes synthesised would elucidate how the trithiophosphite ligands bond to Au^I, since coordination to soft phosphorus and sulfur atoms is available. Finally, extension of trithiophosphite coordination chemistry to Ag^I and Cu^I, in the latter case with hard counter ions, was envisaged.

In the instance of tris(azol-2-yl)phosphanes, the same points made above apply: These ligands are polydentate with a central soft phosphorus as well as soft sulfur and harder imine nitrogen centres in the heterocyclic residues. Yet, they have not been extensively explored in coordination chemistry, especially *P*-coordinated metal complexes are rare. It was anticipated that chloride substitution from the simple chloro[tris(azol-2-yl)phosphane]gold compounds by sulfur nucleophiles can be used as a method to synthesise new compounds and give insight into the stability of complexes of this

31 B. Weissbart, L. J. Larson, M. M. Olmstead, C. P. Nash and D. S. Tinti, *Inorg. Chem.* **1995**, *34*, 393–395.

32 D. R. Smyth, B. R. Vincent and E. R. T. Tiekink, *Cryst. Growth Des.* **2001**, *1*, 113–117.

new ligand class. As these simple gold chloride complexes were also shown to exhibit polymorphism,³³ another goal was to isolate new polymorphs of these compounds which would give insight into the factors governing the respective crystal lattices. A last aim of this chapter was to investigate the propensity of such tris(azol-2-yl)phosphanegold complexes to undergo hydrolysis.

The synthesis of (hetero)metallacycles incorporating gold(I) is a field of ever increasing importance. These compounds exhibit a multitude of useful properties; from the battle against cancer, HIV and malaria to crystal engineering in the search for novel materials that exhibit desirable and specifically tailored properties. The first aim associated with the synthesis of heterometallacycles was to complete the characterisation of a trimeric 18-membered heterometallacycle of the general formula $[\text{AuL}]_3$, especially the molecular structure needed to be secured by single crystal X-ray diffraction. Secondly, utilising a bis(imidazol-1-ylmethyl)benzene the scope of imidazole bis-imine coordination of Au^{I} was to be explored with the goal to obtain a porous crystal structure. Removal of co-crystallised solvent and analysis of the lattice changes was a further aim. A last target was the structural determination of a $[\text{Au}_2(\mu\text{-}^2\text{L})_3]^{2+}$ dication where two Au^{I} centres are coordinated in a trigonal-planar fashion by three bidentate ligands. As only few structures of such dications are known and all are phosphane complexes, the employment of different ligands for this task was envisioned.

Finally, another topic that has not been explored is carbene and carbyne complexes bearing heterocyclic residues at the carbon bonded to the metal. These complexes are valuable starting materials for reactions with gold(I) electrophiles which can proceed under transfer of the ligand to gold. Again, thiazolyl groups in the complex offer soft sulfur and harder imine nitrogen atoms as additional sites for metal coordination. Therefore, the chemistry of tungsten Fischer-type carbene and carbyne complexes with heterocyclic substituents was to be investigated. Firstly, suitable conditions had to be found to isolate tungsten carbyne complexes with thiazole groups attached to the

33 W. F. Gabrielli, *Ph.D. thesis*, Stellenbosch University, 2006.

carbyne carbon. Furthermore, the interaction of these compounds as well as the related Fischer-type carbene complexes with gold(I) reagents then had to be probed to again gain insight into the behaviour of Au^I when exposed to a variety of different donor centres. A focus would also be the verification of a proposed transient reaction product. Finally, the exploration of remote *N*-heterocyclic carbene transfer from group 6 metals to Au^I would complement the known classes of gold carbene complexes. The use of different analytical methods was expected to determine which canonical form of the *r*NHC ligand, the classic pyridinylidene carbene resonance structure with a Au–C double bond or the charge-separated metalated pyridinium cation form with a formal Au–C single bond, has the higher contribution.

In **Chapter 2**, the synthesis and characterisation of trithiophosphite complexes of gold(I) are reported. The compounds could be prepared by reacting the ligands with (tht)AuCl (tht = tetrahydrothiophene); they are fairly stable and differences as well as similarities to their normal phosphite analogues were observed. Most compounds could be characterised by single crystal X-ray diffraction and are linear dicoordinate complexes. Au[⋯]Au and Au[⋯]S contacts could be observed in the solid state structures of several complexes. A copper(I) trithiophosphite complex with triflate counter ions crystallised in a chain motif exhibiting rare Cu^I centres bridged by two triflate anions.

The preparation of novel tris(azol-2-yl)phosphane complexes of gold(I) is reported in **Chapter 3**. All compounds were characterised by single crystal X-ray diffraction, *P*-coordination of the ligands was always observed. Only the tris(imidazol-2-yl)phosphane ligand is capable of coordinating to another Au^I centre. Tris(thiazol-2-yl)phosphane-gold(I) complexes are less stable than their tris(aryl)phosphane analogues and decompose when a chloride ligand is substituted for alkyl- or arylthiolates. Four new polymorphs and solvates were found for the compounds chloro[tris(thiazol-2-yl)phosphane]gold and chloro[tris(4-methylthiazol-2-yl)phosphane]gold that exhibit strikingly different association phenomena in the solid state.

In **Chapter 4**, two different thf solvates of *cyclo*-tris{[4,4-dimethyl-2-(2-thienyl- κ C⁵)-oxazoline- κ N]gold} could be structurally characterised exhibiting different association in the solid state. The *cyclo*-bis{1,3-bis[(imidazol-2-yl- κ N)methyl]-2,4,6-trimethylbenzene}digold(2+) cation could be crystallised with tetrafluoroborate and triflate counter ions, the latter yielded a porous crystal structure in the solid state and the solvent could be partially removed. A novel [Au₂(μ -²L)₃]²⁺ cation was synthesised using *N,N*-bis(1,3,2-dioxaphospholan-2-yl)methanamine as the ditopic ligand (²L), the compound exhibits stronger Au \cdots Au interactions as well as Au–P bonds than similar compounds with ditopic phosphane ligands.

Finally, the synthesis of Fischer-type carbenate, carbene and carbyne complexes incorporating unusual 5-substituted thiazole precursors is reported in **Chapter 5**. The carbenate and carbene complexes react with selected Au^I electrophiles to yield gold(I) acyl- and carbene complexes. Most notably, the first Fischer-type carbene complex exhibiting aurophilic interactions in the solid state was found; one carbenate transfer reaction to Ph₃PAu⁺ proceeded with unprecedented loss of CO to yield a *pseudo*-abnormal gold(I) carbene complex. A different carbenate salt afforded a gold acyl complex that still retains the W(CO)₅ fragment coordinated to the acyl oxygen, thus forming a *pseudo*-carbene complex. This compound substantiates earlier proposals of the structure of this intermediate product on the way to gold acyl complexes. Transfer of *r*NHC ligands from group 6 pentacarbonylmetal fragments to Au^I proceeded similarly, stable *r*NHC gold complexes were obtained and all were characterised, amongst other methods, by single crystal X-ray diffraction.

... neue Verbindungen herzustellen und Strukturen zu erforschen, die noch nie ein Mensch zuvor gesehen hat.

alternative Zielsetzung, frei nach *Gene Roddenberry*

2

Trithiophosphite Complexes of Gold(I)¹

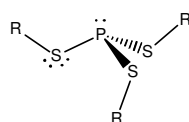
2.0 Abstract

The first trithiophosphite complexes of gold(I) were synthesised and fully characterised. Reaction of (tht)AuX (X = Cl or C₆F₅; tht = tetrahydrothiophene) with trithiophosphites P(SR)₃ (R = Me or Ph) and the bicyclic [$\overline{\text{SCH}_2\text{CH}_2\text{S}}\overline{\text{P}}\text{SCH}_2$]₂ (²L) afforded the corresponding molecular complexes (RS)₃PAuX [R = Me and X = Cl (**1**); R = Me and X = C₆F₅ (**2**); R = Ph and X = Cl (**3**); R = Ph and X = C₆F₅ (**4**)], and ²L(AuX)₂ [X = Cl (**5**) or X = C₆F₅ (**6**)]. Reacting (tht)AuCl consecutively with two mole equivalents of P(SMe)₃ and then with AgOTf, yielded the ionic compound {Au[P(SMe)₃]₂}OTf, **7**. Additionally, (MeS)₃PCuOTf, **9**, was synthesised to explore the effect of a harder metal on these ligands. The compounds were characterised by multinuclear NMR spectroscopy, IR measurements and mass spectrometry, and the crystal and molecular structures of **1**, **3**, **6**, **9**, two polymorphs of **2** as well as the known (MeO)₃PAuCl, **8**, were determined by X-ray diffraction. The halide complexes **1** and **8** are isostructural and exhibit infinite chains of “crossed-sword”-type aurophilic interactions with Au[⋯]Au contact distances of 3.2942(3) and 3.1635(4) Å, respectively. Additionally, in the structure of **1** Au[⋯]S contacts are present. Complex **6** exhibits a long Au[⋯]Au contact of 3.4671(9) Å. Au[⋯]S interactions between 3.3455(7) and 3.520(2) Å are present in the structures of **1** and one polymorph of **2**. Complex **9** represents a rare example of doubly triflate-bridged Cu^I.

¹ All gold complexes in this Chapter have been described in a publication: C. E. Strasser, S. Cronje, H. Schmidbaur and H. G. Raubenheimer: “The preparation, properties and X-ray structures of gold(I) trithiophosphite complexes”, *J. Organomet. Chem.* **2006**, *691*, 4788–4796. The compound numbers in this Chapter correspond to those used in the publication.

2.1 Introduction

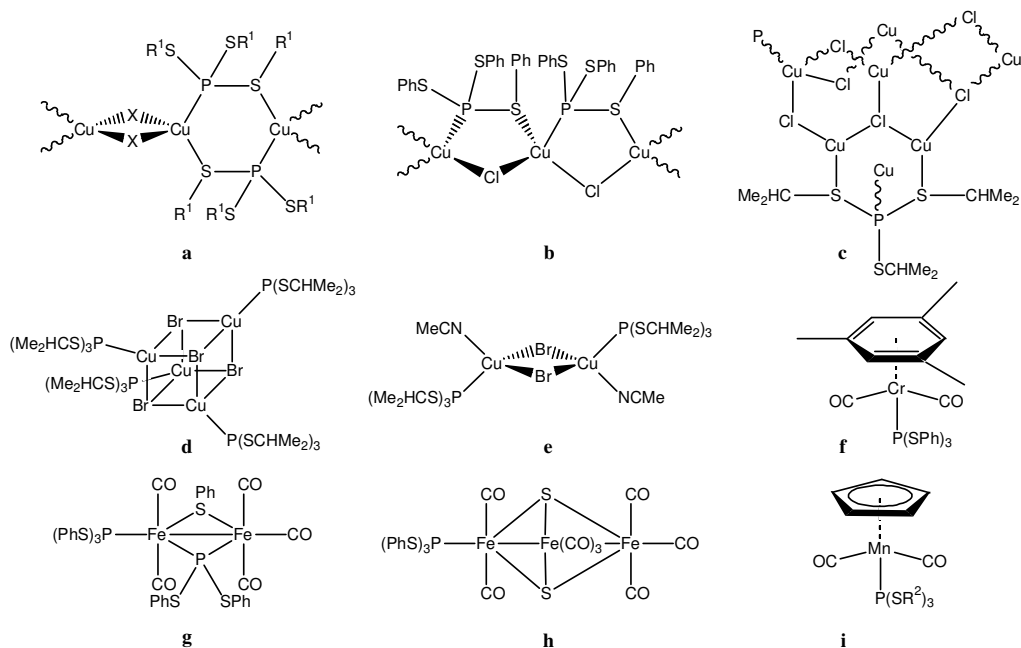
Even though trithiophosphites were reported for the first time in 1872 as the main product of heating ethanethiol with phosphorus trichloride in an attempt to synthesise dichloro(ethylthio)phosphane,² relatively little coordination chemistry with these ligands is known. This may in part be ascribed to the properties of trithiophosphites whose dreadful odour resembling organic sulfanes and phosphites as well as their toxicity render them unattractive substrates to study. Furthermore, the P–S bond of trithiophosphites is not only susceptible to hydrolysis, but also not very strong and cleavage may occur during reactions with metal cations. This property was used as an approach towards the synthesis of copper clusters where trithiophosphite complexes of Cu^I halides were slowly converted to Cu^I dialkyldisulfane complexes.³ Furthermore, the potentially multidentate (Scheme 2.1) nature of trithiophosphites may allow metal cations to form polymers.⁴ An article by *Kataeva et al.* summarises the known coordination chemistry of trithiophosphites.⁵



Scheme 2.1 Trithiophosphite coordination takes place first at the phosphorus centre; sulfur atoms may then be utilised.

A limited number of crystal structures, shown in Scheme 2.2, have been determined for a series of trithiophosphite (L) complexes of Cu^I halides and pseudohalides.^{4,6}

- 2 A. Michaelis, *Chem. Ber.* **1872**, 5, 6–9.
- 3 L. I. Kursheva, O. N. Kataeva, D. B. Krivolapov, E. S. Batyeva and O. G. Sinyashin, *Heteroat. Chem.* **2006**, 17, 542–546.
- 4 L. I. Kursheva, O. N. Kataeva, A. T. Gubaidullin, F. S. Khasyanzyanova, E. V. Vakhitov, D. B. Krivolapov and E. S. Batyeva, *Russ. J. Gen. Chem.* **2003**, 73, 1516–1521.
- 5 O. N. Kataeva, D. B. Krivolapov, A. T. Gubaidullin, I. A. Litvinov, L. I. Kursheva and S. A. Katsyuba, *J. Mol. Struct.* **2000**, 554, 127–140.
- 6 (a) O. N. Kataeva, I. A. Litvinov, V. A. Naumov, L. I. Kursheva and E. S. Batyeva, *Inorg. Chem.* **1995**, 34, 5171–5174;
(b) P. G. Jones, A. K. Fischer, L. Frolova and R. Schmutzler, *Acta Crystallogr., Sect. C: Cryst. Struct. Commun.* **1998**, 54, 1842–1844.



Scheme 2.2 Crystallographically characterised trithiophosphite complexes. (a) typical *catena*-structure obtained with Cu^I halides: R¹ = Et and X = Cl, Br or I; R¹ = C₃H₇ or Bu and X = Br; R¹ = C₃H₇ and X = SCN (*S*- and *N*-coordinating); (b) *catena*-[CuCl{P(SPh)₃}] showing asymmetrical bridges, (c)–(e); the sterically bulky P(SCHMe₂)₃ ligand gives rise to a cluster, (c), cubane, (d), the only trithiophosphite structure, (e), with a solvent coordinating to Cu^I; (f)–(i) other complexes, R² = Ph, CHMe₂.

These comprise two [MnCp(CO)₂L]-type compounds,⁷ a [Cr(η⁶-arene)(CO)₂L]⁸ and one each of a di- and trinuclear iron carbonyl complex.⁹

Other organometallic trithiophosphites, *e.g.* tris(ferrocenyl)trithiophosphite and tris(cymantrenyl)trithiophosphite [cymantrene = tricarbonyl(η⁵-cyclopentadienyl)manganese]¹⁰ and 1,1'-bis{[1,1'-ferrocenediylbis(thio)]phosphanyl}thio}ferrocene [structurally similar to 1,2-bis(1,3,2-dithiaphospholan-2-ylthio)ethane by replacing the

7 O. G. Sinyashin, I. Yu. Gorshunov, V. A. Milyukov, E. S. Batyeva, I. A. Litvinov, O. N. Kataeva, A. G. Ginzburg and V. I. Sokolov, *Izv. Akad. Nauk., Ser. Khim.* **1994**, 1116–1119.

8 V. A. Milyukov, A. V. Zverev, S. M. Podlesnov, D. B. Krivolapov, I. A. Litvinov, A. T. Gubaidullin, O. N. Kataeva, A. G. Ginzburg and O. G. Sinyashin, *Russ. J. Gen. Chem.* **2000**, *70*, 698–703.

9 (a) B. Wu, H. Su, X. Yan, X. Hu, Q. Liu, *Jiegou Huaxue* **1992**, *11*, 339–342;

(b) Q. Liu, B. Wu, X. Hu, S. Liu, X. Yan and J. Shi, *Huaxue Xuebao* **1992**, *50*, 778–782.

10 V. A. Milyukov, A. V. Zverev, S. M. Podlesnov, D. B. Krivolapov, I. A. Litvinov, A. T. Gubaidullin, O. N. Kataeva, A. G. Ginzburg and O. G. Sinyashin, *Eur. J. Inorg. Chem.* **2000**, 225–228.

ethylene groups by 1,1'-ferrocenediyl], that could themselves act as ligands have been described.¹¹

Addition compounds of AuCl₃ with trithiophosphites have been mentioned but have only been characterised *via* their melting points.¹² No other gold–trithiophosphite interactions have been investigated.

Organic tetrathiophosphates – in contrast to the related trithiophosphites – have virtually found no application in coordination chemistry. One example of an adventitious isolation of a [tris(1-methylethyl)tetrathiophosphate]copper(1+) complex was reported by the same Russian group that has developed Cu^I trithiophosphite chemistry.¹³ The only other example is that of diiodo(tridodecyltetrathiophosphate)-mercury, again only used to identify the tetrathiophosphate ligand by the melting point of a metal complex derivative.¹⁴

2.1.1 Aims

Trithiophosphite complexes of Cu^I are known and the chemistry is well established (*vide supra*), but the group of *Krivolapov* and *Litvinov* never reported complexes with other coinage metals. Therefore, the main aims of the investigation described in this Chapter were to synthesise new trithiophosphite complexes of Au and Ag, characterise the products by means of multinuclear NMR, far IR spectroscopy and mass spectrometry. Secondly, we planned to investigate the molecular structures of the new complexes by single crystal X-ray diffraction. As mentioned above, trithiophosphites are potentially multidentate ligands, able to form coordinative bonds with their phosphorus *and* sulfur atoms, thus elucidation of the coordination sphere around the metal centres in complexes with these ligands is of great interest. The tendency of Au^I to form discrete, 14-e⁻ linear dicoordinate complexes¹⁵ and the possibility of additional stabilisation by interaction with available sulfur atoms – leading ultimately

11 M. Herberhold, C. Dörnhöfer, A. Scholz and G.-X. Jin,

Phosphorus, Sulfur Silicon Relat. Elem. **1992**, *64*, 161–168.

12 A. Lippert and E. E. Reid, *J. Am. Chem. Soc.* **1938**, *60*, 2370–2371.

13 L. I. Kursheva, A. M. Il'in, E. S. Batyeva, O. N. Kataeva and A. T. Gubaidullin, *Russ. J. Gen. Chem.* **2001**, *71*, 484.

14 L. C. F. Blackman and M. J. S. Dewar, *J. Chem. Soc.* **1957**, 169–171.

15 P. Schwerdtfeger, H. L. Hermann and H. Schmidbaur, *Inorg. Chem.* **2003**, *42*, 1334–1342.

to 18- e^- tetrahedral complexes as is commonly observed in the case of Cu^I – should be considered. Furthermore, expanding the utilisation of trithiophosphites by including silver to simultaneously fill the gap between Cu and Au and assist in understanding the different forces present in complexes of these metals was envisioned. To complement these findings, the synthesis of trithiophosphite complexes with Cu^I and non- or weakly coordinating anions was another target.

It was foreseen that the results obtained for all these complexes could then be compared with the widely known trialkylphosphite analogues thus allowing assessment of the influence of the exchange of oxygen for sulfur on the properties of these compounds.

Lastly, the results obtained from trithiophosphite complexes of gold could be extended to include the possibility of complex formation with tetrathiophosphates; not only to extend the variety of ligands used in gold chemistry but in particular to gather more extensive information on a family of curiously neglected ligands in coordination chemistry.

2.2 Results and discussion

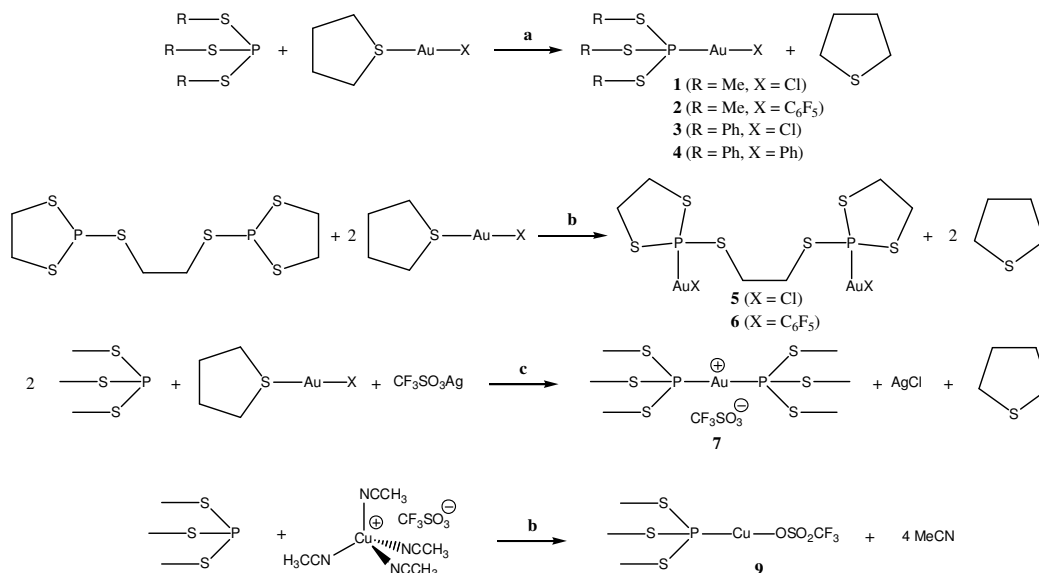
2.2.1 Synthesis of the compounds

The ligands were synthesised according to literature¹⁶ by reacting appropriate amounts of disulfanes with white phosphorus in MeCN, induced by a drop of saturated aqueous KOH. The bicyclic ligand, 1,2-bis(1,3,2-dithiaphospholan-2-ylthio)ethane was obtained by addition of ethane-1,2-dithiol to an Et_2O solution of pyridine and PCl_3 . Employment of NEt_3 was found to precipitate the triethylammonium thiolate salt and was unsuccessful. However, it was found out later that a better method is reacting neat ethane-1,2-dithiol with PCl_3 ;¹⁷ initially it was thought that liberated HCl would induce side reactions, however, this is not the case.

16 C. Wu, *J. Am. Chem. Soc.* **1965**, *87*, 2522.

17 L. C. Gomes de Lima, M. B. Gomes de Lima, R. M. Matos, M. do Rosário Menezes, D. S. Raslan, E. de Souza and A. L. A. B. de Souza, *Phosphorus, Sulfur Silicon Relat. Elem.* **2000**, *166*, 1–14.

The preparation of the complexes is outlined in Scheme 2.3. The syntheses of the neutral simple, monomolecular and dimolecular complexes, **1–6**, were readily achieved in high yields by substituting tetrahydrothiophene from either (tht)AuCl or



Scheme 2.3 Synthesis of the compounds **1–9**; conditions: (a) thf, r.t. for X = Cl and Et₂O, 0 °C for X = C₆F₅ (b) thf, r.t. (c) ethanenitrile/thf, r.t.

(tht)AuC₆F₅ with the respective trithiophosphite ligand. The substitutions were carried out in thf at room temperature for the chloro complexes or in Et₂O solution at 0 °C for the pentafluorophenyl compounds. Evaporation of all volatile matter afforded microcrystalline product mixtures that were, especially in the case of the pentafluorophenyl derivatives, contaminated with some metallic gold. Filtration through Celite yielded the complexes as colourless microcrystalline compounds after stripping of the solvent *in vacuo*. Preparation of the cationic compound, **7**, was effected by reacting two mole equivalents of P(SMe)₃ with (tht)AuCl and AgOTf in a mixture of ethanenitrile and thf. The known¹⁸ phosphite complex (MeO)₃PAuCl, **8**, was prepared analogously to **1**. Compound **9**, wherein *P*-, *S*-, and *O*-donors feature (*vide infra*) was prepared from [Cu(CH₃CN)₄]OTf in thf. This starting material itself was prepared by anion exchange in ethanenitrile. As CuCl is minutely soluble but NaCl virtually insoluble¹⁹ in ethanenitrile, the reaction proceeds readily towards the products.

18 (a) M. Levi-Malvano, *Atti Accad. Naz. Lincei. Cl. Sci. Fis., Mat. Nat. Rend.* **1910**, 17, 847–857;

(b) A. E. Arbuzov, V. M. Zoroastrova, *Izv. Akad. Nauk. SSSR, Ser. Khim.* **1952**, 809–817;

(c) H. Schmidbaur and R. Franke, *Chem. Ber.* **1972**, 105, 2985–2997.

19 T. Pavlopoulos and H. Strehlow, *Z. Phys. Chem.* **1954**, 202, 474–479.

Compounds **1–4** are stable for months without any signs of decomposition when stored at $-16\text{ }^{\circ}\text{C}$. Stability at room temperature, however, is lower and slow deterioration with deposition of metallic gold occurs within days. Complexes of the bicyclic ligand, **5** and **6**, as well as the homoleptic **7** are more sensitive and turn yellow within weeks upon storage in the freezer. This might be caused by P–S bond cleavage which was observed in the synthesis of iron carbonyl complexes of trithiophosphites.⁹ While **1** and **3** are soluble in polar, aprotic solvents, complexes **2** and **4** are also soluble in Et_2O ; all compounds are insoluble in aliphatic hydrocarbons. The solubility of the binuclear complexes is poor; **5** does not dissolve at all and **6** only dissolves in thf when freshly prepared but after prolonged storage becomes insoluble; this may be attributed to decomposition. The complexes exhibit a faint odour of the parent thiol and are decomposed slowly by moisture indicating the higher tendency of P–S bond cleavage over P–C bond cleavage encountered in Chapter 3 (see Section 3.2.4.2). Protic solvents like methanol effect fast decomposition indicating a destabilising effect of the coordinated gold on the ligand. This pathway has been used to convert coordinated trithiophosphites to phosphonates by hydrolysis of copper(I) halide complexes.²⁰

Attempts were made to synthesise silver complexes of trithiophosphites employing AgBr or AgOTf , but in all cases only insoluble coordination polymers were obtained that could not be structurally characterised. It is thought that Ag may form similar complicated complexes to the Cu complex (c) in Scheme 2.2 which are insoluble and difficult to characterise by any other means than by single crystal X-ray diffraction. The only compounds known that contain a silver centre *P*-bonded to a PS_3 group are complexes of P_4S_3 which is described in the reports as only weakly coordinating.²¹

The synthesis of gold tetrathiophosphate complexes was also investigated but these ligands were found to be of inferior donating ability compared to dialkylsulfanes and therefore could not substitute tht from the gold starting compounds $(\text{tht})\text{AuCl}$ and $(\text{tht})\text{AuC}_6\text{F}_5$. A reaction of Me_3PS_4 with $\text{Ph}_3\text{PAuNO}_3$ is thought to have furnished a

20 L. I. Kursheva, L. V. Frolova, M. V. Bykova and E. S. Batyeva, *Zh. Obshch. Khim.* **1996**, 66, 1458–1459.

21 (a) A. Adolf, M. Gonsior and I. Krossing, *J. Am. Chem. Soc.* **2002**, 124, 7111–7116;
(b) I. Raabe, S. Antonijevic and I. Krossing, *Chem. Eur. J.* **2007**, 13, 7510–7522.

complex based on the observation of an infrared absorption assigned to free NO_3^- , however no crystals were obtained and the compound emitted such a strong odour that further analyses were not possible. $\text{Na}[\text{AuCl}_4]$ reacts with Ph_3PS_4 to form a red oil which exhibits at least 8 signals in its $^{31}\text{P}\{^1\text{H}\}$ NMR spectrum, indicating fragmentation of the ligand by the gold centre; crystallisation was again unsuccessful.

2.2.2 Thermal gravimetric analysis

A crystalline sample of complex **1** (4.0 mg) was heated at a rate of $10\text{ }^\circ\text{C min}^{-1}$ to $400\text{ }^\circ\text{C}$. The sample mass was constant up to the melting point ($114\text{ }^\circ\text{C}$) when rapid loss (44.3%) of weight set in until $176\text{ }^\circ\text{C}$ was reached. Thereafter the mass remained fairly constant up to $400\text{ }^\circ\text{C}$ when a final loss of 45.7% occurred. A yellow solid remained in the pan. The observed weight loss (45.7%) falls within the theoretical loss to afford the possible decomposition products Au_2S (47.4%) and AuCl (42.6%).

2.2.3 Spectroscopic analyses

The signals of multinuclear NMR analysis of the reported compounds are summarised in Table 2.1. The fragment ions observed in the mass spectrometric analyses are reported in Table 2.2.

2.2.3.1 $^{31}\text{P}\{^1\text{H}\}$ NMR spectroscopy.

The coordination of the trithiophosphite ligands to the Au^{I} centre could be verified by comparison of the ^1H and ^{31}P NMR spectra of the free ligands and complexes. Coordination to the AuCl moiety does not greatly affect the ^{31}P NMR chemical shift, $\Delta\delta^{22}$ 2.3 to lower field for **1** and 2.2 to higher field for **3**. This result is in contrast to the large $\Delta\delta$ (38 to 48) to lower field observed for AuCl adducts of simple tertiary phosphanes²³ and with the ^{31}P NMR upfield change in chemical shift ($\Delta\delta$ 20) associated with normal phosphite coordination to AuCl .^{23a} Upon coordination to the AuC_6F_5 fragment, however, a pronounced downfield change in chemical shift $\Delta\delta$,

22 To avoid confusion, all $\Delta\delta$ values are quoted as absolute values, the direction of the shift must be obtained from context.

23 (a) M. J. Mays and P. A. Vergnano, *J. Chem. Soc., Dalton Trans.* **1979**, 1112–1115;

(b) G. H. Woehrle, L. O. Brown and J. E. Hutchison, *J. Am. Chem. Soc.* **2005**, *127*, 2172–2183.

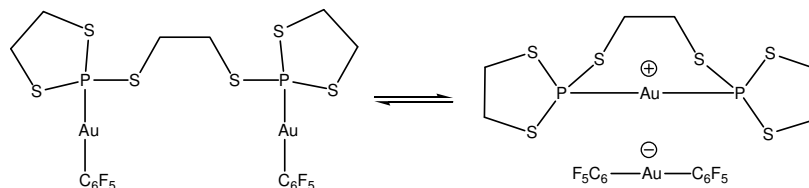
Table 2.1 NMR data of compounds **1–9**^a

Compound		(MeO) ₃ PAuCl 8	(MeS) ₃ PAuCl 1	(MeS) ₃ PAuCF ₅ 2	[(MeS) ₃ P] ₂ AuOTf 7	(MeS) ₃ PcuOTf 9	(PhS) ₃ PAuCl 3	(PhS) ₃ PAuCF ₅ 4	² L(AuCF ₅) ₂ 6
Nucleus	Solvent	CDCl ₃	CDCl ₃	CDCl ₃	CDCl ₃	CD ₃ CN	CD ₂ Cl ₂	CDCl ₃	C ₄ D ₈ O
¹ H (300 MHz)	CH ₃	3.74 (d, ³ J _{PH} 14.0, ¹ J _{CH} 150) ^b	2.43 (d, ² J _{PH} 17.6, ¹ J _{CH} 144) ^b	2.51 (d, ³ J _{PH} 16.4, ¹ J _{CH} 143) ^b	2.40 (d, ³ J _{PH} 14.7, ¹ J _{CH} 144) ^b	2.31 (d, ³ J _{PH} 12.1, ¹ J _{CH} 155) ^b			
	<i>o</i> -Ph						7.64 (m, 6 H)	7.60 (m, 6 H) ^c	
	<i>m</i> -Ph						7.46 (m, 6 H)	7.37 (m, 6 H) ^c	
	<i>p</i> -Ph						7.54 (m, 3 H)	7.43 (m, 3 H) ^c	
¹³ C{ ¹ H} (75 MHz) ^a	ring-CH ₂								3.65 (m, 8 H) ^c
	bridge-CH ₂								3.46 (m, 4H) ^c
¹³ C{ ¹ H} (75 MHz) ^a	CH ₃	53.1 (br s)	16.1 (s)	15.4 (s)	15.2 (d, ² J _{PC} 4.0)	14.2 (d, ² J _{PC} 10.1)			
	<i>i</i> -C ₆ H ₅						136.9 (d, ² J _{PC} 5.0)	136.6 (d, ² J _{PC} 3.7)	
	<i>o</i> -C ₆ H ₅						131.5 (d, ³ J _{PC} 3.6)	130.7 (d, ³ J _{PC} 3.3)	
	<i>m</i> -C ₆ H ₅						130.6 (d, ⁴ J _{PC} 2.8)	130.0 (d, ⁴ J _{PC} 2.8)	
	<i>p</i> -C ₆ H ₅						129.0 (br s)	128.5 (br s)	
	<i>o</i> -C ₆ F ₅			149.3 (d-m, ¹ J _{FC} 229)				148.6 (d-m, ¹ J _{FC} 230)	<i>d</i>
	<i>m</i> -C ₆ F ₅			140.0 (d-m, ¹ J _{FC} 248)				139.4 (d-m, ¹ J _{FC} 248)	<i>d</i>
	<i>p</i> -C ₆ F ₅			137.6 (d-m, ¹ J _{FC} 253)				137.0 (d-m, ¹ J _{FC} 253)	<i>d</i>
	ring-CH ₂								41.3 (s) ^e
	bridge-CH ₂								36.6 (br s) ^e
¹⁹ F (376 MHz)	<i>o</i> -C ₆ F ₅			-116.7 (m, 2 F)				-115.9 (m, 2 F)	-115.4 (m, 4 F)
	<i>m</i> -C ₆ F ₅			-162.2 (m, 2 F)				-162.7 (m, 2 F)	-163.7 (m, 4 F)
	<i>p</i> -C ₆ F ₅			-157.4 (m, 1 F)				-158.2 (t, ³ J _{FF} 20.0, 1 F)	-159.6 (t, ³ J _{FF} 19.6, 2 F)
³¹ P{ ¹ H} (121 MHz)	P(SR) ₃	121.0 (s)	123.4 (s)	144.3 (s)	128.1 (s)	108.64 (br s)	142.1 (s)	161.3 (s)	134 (br s)

^a *i*-C₆F₅ and CF₃SO₃⁻ carbons were not observed due to low intensity and signal splitting ^b ¹J_{CH} coupling constants obtained from ¹³C satellites

^c at 400 MHz ^d not observed due to low solubility of the compound ^e at 101 MHz

averaging 20 for the trithiophosphite ligands, was observed. All ^{31}P NMR signals appear as sharp singlets except for the binuclear complex **6** which shows a broad signal. Homoleptic rearrangement is common in LAuC_6F_5 complexes, has been observed with other ligands²⁴ and is reported in this dissertation (Chapter 5, p. 178). A homoleptic rearrangement of complex **6** would afford a cyclic, cationic bis(trithiophosphite) complex that has not been isolated (Scheme 2.4).



Scheme 2.4 Possible homoleptic rearrangement of complex **6** that would cause the ^{31}P NMR signal to be broadened.

2.2.3.2 ^1H and $^{13}\text{C}\{^1\text{H}\}$ NMR spectroscopy.

The proton NMR spectra for **1**, **2** and **7** show a very small downfield shift of the methyl signal by 0.2–0.3 ppm. The $^1J_{\text{CH}}$ coupling constants obtained from the ^{13}C satellites also remain essentially unchanged at an average value of 143 Hz upon coordination of $\text{P}(\text{SMe})_3$ in the gold complexes. In the copper compound **9** a substantial increase in the coupling constant to 155 Hz was observed which could be attributed to additional *S*-coordination of $\text{P}(\text{SMe})_3$ operative in solution. The aromatic protons in **3** and **4** are minutely shifted to lower field (*ca.* $\Delta\delta$ 0.1–0.2 vs. free ligand) but, nevertheless, allowing the discrimination between *meta*- and *para*-signals that overlap in the spectrum of the free ligand.

In the ^{13}C NMR spectra of **2** and **4** the *ipso*-carbon atoms of the pentafluorophenyl groups and the CF_3SO_3 -carbon in **7** were not observed due to too low intensity. Binuclear **6** was not soluble enough to detect any carbon resonances of the C_6F_5 groups. Unexpectedly, the J_{PC} coupling constants of all ligands decrease upon coordination, again showing dissimilarity to the simple phosphanes^{23b} and the results reported in Chapter 3 (p. 77). Though the protons of the trimethyltrithiophosphite complexes **1**, **2** and **7** all indicate coupling with the ^{31}P nucleus, a substantial $^2J_{\text{PC}}$ in

24 (a) K. Coetzee, *M.Sc. thesis*, Stellenbosch University, **2005**; (b) W. F. Gabrielli, *Ph.D. thesis*, Stellenbosch University, **2006**; (c) L. de Jongh, *M.Sc. thesis*, Stellenbosch University, **2008**.

the ^{13}C NMR spectra is only observed for the free ligand ($^2J_{\text{PC}}$ 18 Hz). The gold complexes with the exception of **7** ($^2J_{\text{PC}}$ 4 Hz) only exhibit a sometimes broadened singlet for the methyl carbon atoms, similar to the methyl resonance of **8**. This could be due to fast ligand exchange in the complexes as was observed for phosphane and phosphite complexes.^{18c} The copper complex **9** again shows a $^2J_{\text{PC}}$ coupling constant of 10 Hz which may be a result of additional *S*-coordination by the ligand.

For the $\text{P}(\text{SPh})_3$ ligand the ^{13}C NMR signals are split into doublets up to the *meta* carbon atoms. The *para* carbons appear as broad singlets and the values of the J_{PC} coupling constants especially for the ipso carbons ($^2J_{\text{PC}}$ 5–6 Hz), are lower than for the free ligand (13 Hz). With the cyclic ligand, 1,2-bis(1,3,2-dithiaphospholan-2-ylthio)ethane, the sharp doublet of doublets of the two bridging carbon atoms at higher field strength in the free ligand spectrum¹⁷ is again reduced to a broad singlet in **6**.

2.2.3.3 ^{19}F NMR spectroscopy.

The pentafluorophenyl groups of **2**, **4** and **6** were examined by ^{19}F NMR spectroscopy and the usual pattern of chemical shifts and multiplicities for the AuC_6F_5 moiety was observed.²⁵ The *ortho*-fluorine atoms in the C_6F_5 group resonate at *ca.* δ –116 while the *meta*- and *para*-signals are observed around δ –163 and –158, respectively. The latter signal is usually present as a triplet caused by a $^3J_{\text{FF}}$ coupling of *ca.* 20 Hz with the pair of *meta*-fluorine atoms; the other signals are multiplets. A $^5J_{\text{FF}}$ coupling of the *para*-fluorine to the *ortho* pair is small and usually not observed, the exception being **2** in which the *para*-signal is further split into a multiplet.

2.2.3.4 Infrared spectroscopy.

Routine IR spectra essentially show the absorptions of the ligand groups for complexes **1**, **3** and **5**. Compounds **2**, **4** and **7** in addition exhibit the characteristic $\nu(\text{C}-\text{F})$ vibrations of the C_6F_5 - or CF_3SO_3 -groups (*cf.* Scheme 2.3 above for the structures of the compounds).

25 F. Mohr, E. Cerrada and M. Laguna, *Organometallics* **2006**, 25, 644–648.

Far-IR spectra in the frequency range 600–200 cm^{-1} of compounds **1**, **3** and **5** were recorded in polyethylene discs in attempts to locate Au–Cl vibrations. Compound **1** exhibits a sharp $\nu(\text{Au}-^{35}\text{Cl})$ band at 315 cm^{-1} with a $\nu(\text{Au}-^{37}\text{Cl})$ satellite at 308 cm^{-1} consistent with theory; $\nu(\text{Au}-\text{Cl})$ for the phosphite complex **8** has been reported at 326 cm^{-1} .²⁶ Combined with the crystallographic findings (*vide infra*) these results suggest that the Au \cdots S contacts in **1** could weaken the Au–Cl bonds compared to those in the known phosphite complex, **8**.

The spectrum of **3** shows two vibrations at 339 and 318 cm^{-1} , but only the band at higher wavenumber has a shoulder indicative of an unresolved $\nu(\text{Au}-^{37}\text{Cl})$ vibration. The Au–Cl stretching band for $(\text{PhO})_3\text{PAuCl}$ was reported at 340 cm^{-1} ,²⁶ suggesting that both ligands induce a similar electronic effect since no close intermolecular contacts are observed in the molecular structures of these compounds (*vide infra*).

Compound **5** shows a broad $\nu(\text{Au}-\text{Cl})$ band at larger wavenumber, 323 cm^{-1} , suggesting that Au \cdots Au interactions are present as would be expected from the insolubility of the compound and the effect of intermolecular Au \cdots S contacts in **1**.

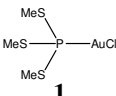
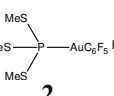
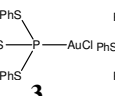
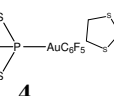
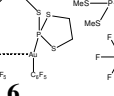
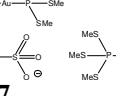
2.2.3.5 Mass spectrometry.

The FAB mass spectra of compounds **2**, **4** and **6** show the loss of a pentafluorophenyl unit but the molecular ion was only observed for **2** and **4**. For compounds **1** and **3** FAB-MS measurements failed to give interpretable patterns – at least $[\text{M} - \text{Cl}]^+$ peaks similar to those of *r*NHC complexes discussed in Chapter 5 would have been expected – and thus ESI-MS in thf/ethanenitrile solution was employed. Fragmentation of the trithiophosphite ligand was observed leading to strong signals for clusters of the type $[(\text{RS})_3\text{PAu}\cdot(\text{AuSR})_n]^+$ ($n = 1$ or 2) along with other ions. However, due to the insolubility of **5** no mass spectrum could be obtained with any of above ionisation methods.

Notably, **1** does lose the trithiophosphite ligand on heating but then rather fragments by Au–Cl bond cleavage under ionising conditions. Observed m/z values and corresponding ions are shown in Table 2.2.

26 D. R. Williamson and M. C. Baird, *J. Inorg. Nucl. Chem.* **1972**, *34*, 3393–3400.

Table 2.2 MS data of **1–9**^a

Compound							
Formula	C ₃ H ₉ Au– ClP(SMe) ₃	C ₉ H ₉ Au– F ₅ PS ₃	C ₁₈ H ₁₅ Au– ClP(SPh) ₃	C ₂₄ H ₁₅ Au– F ₅ PS ₃	C ₁₈ H ₁₂ Au ₂ – F ₁₀ P ₂ S ₆	C ₇ H ₁₈ Au– F ₃ O ₃ P ₂ S ₇	C ₄ H ₉ Cu– F ₃ O ₃ PS ₄
Exact mass	403.90	535.92	589.94	721.97	1065.79	689.84	383.84
Method	ESI	FAB	ESI	FAB	FAB	ESI	FAB
M ⁺		536 (9)		722 (15)			
(RS) ₃ PAu ⁺	369 (30) ^b						
[Au{P(SR) ₃ }] ⁺	541 (15) ^b		913 (30) ^d		535 (1) ^h	541 (90) ^b	
[M – C ₆ F ₅] ⁺		369 (18)		555 (20)	899 (1)		
[(RS) ₃ PAu·AuSR] ⁺	613 (62) ^b		861 (100) ^d				
[(RS) ₃ PAu·2AuSR] ⁺			1167 (30) ^d				
Other ions	567 (40)	522 (10) ^c	1123 (30) 817 (70)	613 (5) ^e 446 (8) ^f 249 (58) ^g	595 (1) 164 (15) 162 (24)	785 (7) ⁱ 583 (12)	385 (10) ^j 401 (15)

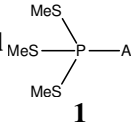
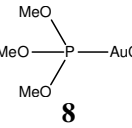
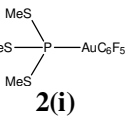
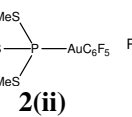
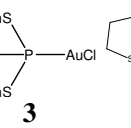
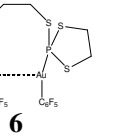
^a All *m/z* based on ³⁵Cl and ⁶³Cu isotopes ^b R = Me ^c [M – C₆F₅ + C₇H₇NO₃]⁺
^d R = Ph ^e [M – SPh]⁺ ^f [M – C₆F₅ – SPh]⁺ ^g [P(SPh)₂]⁺
^h ²LAu⁺ ⁱ [{(MeS)₃P }₂Au·AuSMe]⁺ ^j [M + H]⁺

2.2.4 Crystallography

Compounds **1**, **2**, **3**, **6**, **8** and **9** (*cf.* Scheme 2.3 above) furnished crystals suitable for X-ray diffraction. For compound **2** two polymorphs, both in the space group $P\bar{1}$, were determined. Polymorphism in gold complexes was subsequently again observed in a number of other compounds reported in the next Chapters, it therefore may be a quite common phenomenon. Important bond lengths and angles of complexes **1–8** are given in Table 2.3.

First, a modification with two independent molecules in the asymmetric unit [referred to in the following discussion as polymorph **2(i)** with molecules **2(i)-1** and **2(i)-2**] was crystallised by diffusing pentane vapour into an Et₂O solution of **2**; later, crystals of the more symmetric polymorph, **2(ii)**, with only one molecule in the asymmetric unit were obtained by layering a thf solution of **2** with pentane. Complex **1**, the isostructural **8** as well as **6** exhibit Au⁺–Au interactions.

Table 2.3 Bond lengths/Å and angles/° of compounds **1–6**.

Compound						
	1	8	2(i)	2(ii)	3	6
Au–P	2.2352(8)	2.211(2)	2.266(2)	2.270(2)	2.218(2)	2.271(2)
Au–Cl	2.3100(8)	2.311(2)			2.282(2)	
Au–C			2.043(5)	2.041(5)		2.06(1)
Au···Au		3.1635(4)				3.4671(9)
Au···S				3.520(2)		
P–S	2.077(2)	1.579(4) ^a	2.073(2)	2.081(2)	2.094(2)	2.081(3)
(1, 2, 3)	2.090(1)	1.578(4) ^a	2.080(2)	2.068(2)	2.090(2)	2.067(4)
	2.074(1)	1.582(3) ^a	2.074(2)	2.081(2)	2.084(2)	2.086(4)
			2.082(2)			
			2.076(2)			
			2.070(2)			
P–Au–Cl	178.55(3)	175.90(4)			176.99(6)	
P–Au–C			178.9(2)	178.6(2)		171.7(3)
			174.2(2)			
Au–P–S	118.59(4)	117.0(2) ^a	116.16(8)	117.37(7)	115.13(8)	118.8(2)
(1, 2, 3)	119.37(4)	106.7(2) ^a	112.87(8)	107.06(7)	114.64(9)	114.7(2)
	106.57(4)	119.0(2) ^a	107.47(8)	118.34(7)	108.53(8)	113.6(2)
			121.42(8)			
			116.83(8)			
			108.08(8)			

^a P–O distances and Au–P–O angles

In general, it was noted that even though it is potentially possible for trithiophosphite ligands to adopt local C_3 symmetry in the crystal (see discussion of **3** below), in agreement with Au^I complexes of tertiary phosphanes *e.g.* Et₃PAuCl²⁷ or Ph₃PAuCl,²⁸ it was not observed. Two of the SMe or SPh moieties in the trithiophosphite complexes are bent more or less towards the gold while the S–C axis of the third group points away from the metal centre. This observation is also echoed by the Au–P–S angles which are in the order of 116–118° for the former and 108° for the latter moieties.

The crystal structures of **1** and **8** (Figure 2.1), in the orthorhombic space group *Pbca* are isostructural and exhibit infinite, slightly bent chains along the *a*-axis owing to

27 E. R. T. Tiekink, *Acta Crystallogr., Sect. C: Cryst. Struct. Commun.* **1989**, *45*, 1233–1234.

28 N. C. Baenziger, W. E. Bennett and D. M. Soboroff, *Acta Crystallogr., Sect. B: Struct. Crystallogr. Cryst. Chem.* **1976**, *32*, 962–963.

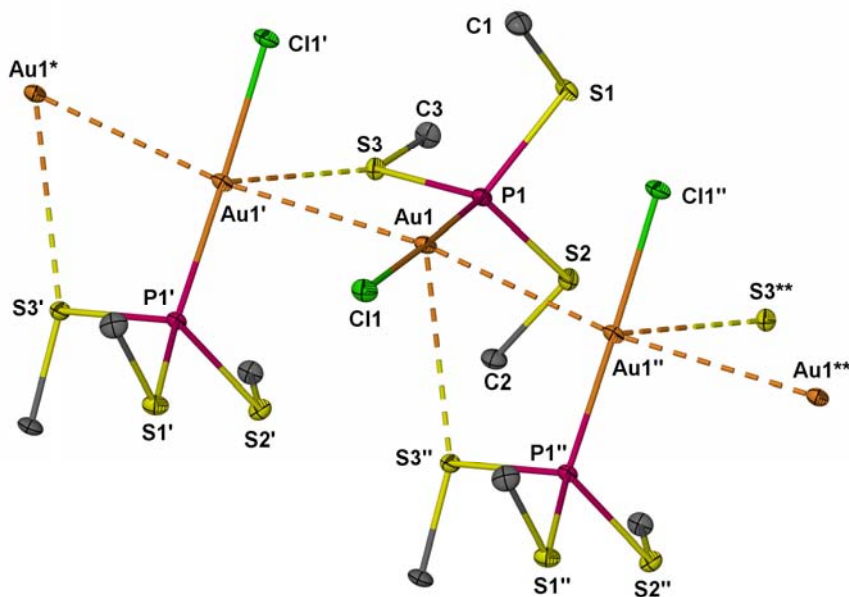


Figure 2.1 Molecular structure of **1**: symmetry codes $' = x - 1/2, y, 1/2 - z$; $'' = 1/2 + x, y, 1/2 - z$; the asterisked atoms are related by one translation in a . Compound **8** is completely isostructural but naturally lacks the Au \cdots S contacts.

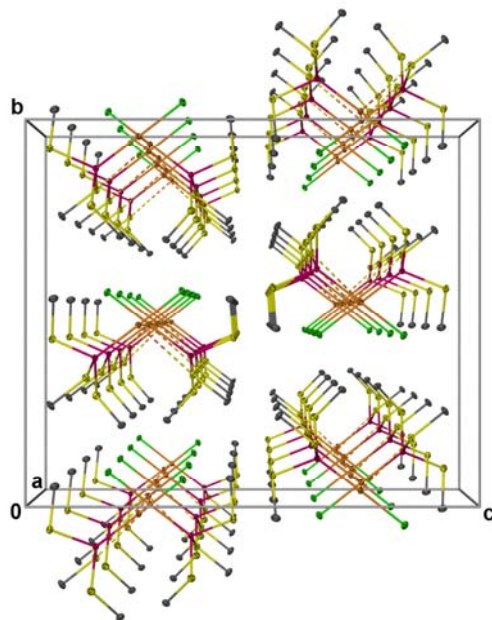


Figure 2.2 Molecular arrangement of **1** viewed along the chains of aurophilic interactions parallel to the a axis; the packing of compound **8** is identical.

Au \cdots Au interactions. Au1 \cdots Au1 \cdots Au1'' angles are 170.783(8) $^\circ$ for **1** and 166.17(2) $^\circ$ for **8** ($' = x - 1/2, y, 1/2 - z$; $'' = 1/2 + x, y, 1/2 - z$), with the P–Au–Cl axes oriented in the “crossed-sword” motif (Figure 2.2). The Cl1–Au1 \cdots Au1'–Cl1' torsion angles are

103.88(4)° and 100.96(6)°, for **1** and **8**, respectively. It is clear from Au–P bond lengths [2.2352(8) and 2.211(2) Å for **1** and **8**, respectively] that the trimethylphosphite ligand is both more strongly bonded to the Au^I centre and causes stronger aurophilic interactions between the molecules. The differences in bond lengths are more pronounced than for the triphenyltrithiophosphite and triphenylphosphite ligands (*vide infra*).

One sulfur atom of **1** is also involved in an intermolecular sub-van der Waals contact [Au1···S3' 3.3455(7) Å; ' = ½ + x, y, ½ – z] “supporting” the Au chain and may in part be responsible for weakening the Au–P bond and affording longer aurophilic interactions in **1** [3.2942(3) Å compared to 3.1635(4) Å in **8**]. Au···S contacts have previously been found to play a role in the packing of other gold(I) complexes in this dissertation (see the following Chapters) and in literature.²⁹ The compounds Me₃PAuCl³⁰ [Au···Au distances 3.271(1), 3.386(1) and 3.356(1) Å] and Et₃PAuCl²⁷ [shortest Au···Au distance 3.615(2) Å] which have tertiary phosphane ligands of similar or less steric requirement than P(SMe)₃ or P(OMe)₃, crystallise in space groups of lower symmetry suggesting that the sulfur and oxygen lone pairs could be involved in directing the crystallisation of compounds **1** and **8**.

Triphenyltrithiophosphite crystallises in the trigonal space group $R\bar{3}$ and the molecules exhibit local C_3 symmetry at the phosphorus atom.³¹ Upon coordination to AuCl, the P–S bonds, uniformly 2.1168(7) Å in the free ligand,^{31c} undergo significant shortening to 2.094(2) (P1–S1), 2.090(2) (P1–S2) and 2.084(2) Å (P1–S3) for the three independent PhS groups in **3** (Figure 2.3). The P–S–C angles, 99.99(5) Å in the free ligand, are not greatly affected by coordination and remain at 99.1(2)° (P1–S1–C11) to 103.8(2)° (P1–S3–C31). In contrast to the isostructural **1** and **8**, monoclinic **3** (space group $P2_1/c$) is not isostructural with triclinic chloro(triphenylphosphite)gold

29 M. Preisenberger, A. Schier and H. Schmidbaur, *J. Chem. Soc., Dalton Trans.* **1999**, 1645–1650.

30 K. Angermaier, E. Zeller and H. Schmidbaur, *J. Organomet. Chem.* **1994**, 472, 371–376.

31 (a) V. A. Alfonsov, I. A. Litvinov, O. N. Kataeva, D. A. Pudovik and S. A. Katsyuba, *Zh. Obshch. Khim.* **1995**, 65, 1129–1133; two other crystal structure determinations were reported by (b) N. Burford, B. W. Royan and P. S. White, *Acta Crystallogr., Sect. C: Cryst. Struct. Commun.* **1990**, 46, 274–276; and (c) M. Nieger, E. Niecke and U. Fischer, *Private communication to the Cambridge Crystallographic Data Centre*, No. 115547, **1999**.

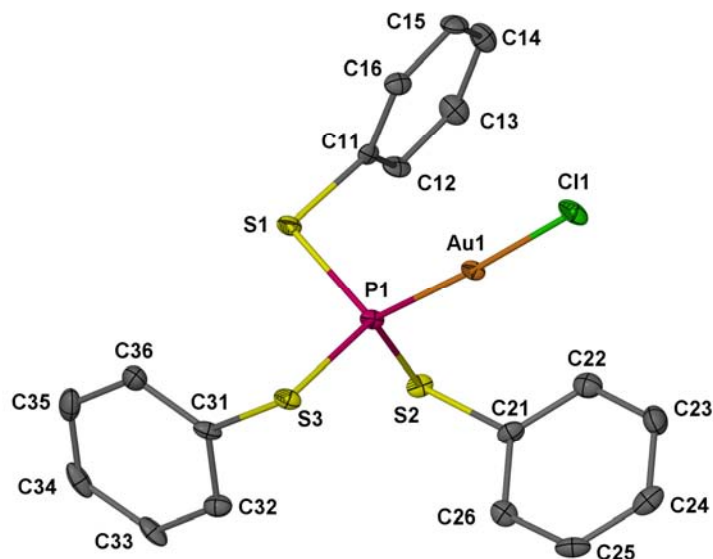


Figure 2.3 Molecular structure of **3**.

(space group $P\bar{1}$).³² This may be due to the absence of Au \cdots Au and Au \cdots S interactions in these structures; thus classical forces prevail in the crystals and lead to different structures. The Au–Cl and Au–P distances and the P–Au–Cl angles in **3** and (PhO)₃PAuCl are comparable at 2.282(2), 2.218(2) Å and 176.99(6)° for **3** and 2.273(5), 2.192(5) Å and 178.5(2)° for the oxo-analogue, respectively.

In contrast to **1**, polymorphs **2(i)** and **2(ii)** [both in the triclinic space group $P\bar{1}$, $Z = 4$ for **(i)** and $Z = 2$ for **(ii)**] shown in Figures 2.4 and 2.5 do not exhibit aurophilic interactions, which may be due to the prevalence of other association phenomena discussed below as steric repulsion is not likely to contribute. Instead, **2(i)** exhibits infinite AA'BB' stacks of pentafluorophenyl groups (distances between the phenyl centroids AA' = BB' 3.668, A'B 3.534, and B'A 3.541 Å) for both crystallographically independent molecules running in the direction of the spatial vector defined by the cell axes as shown in Figure 2.6. The pentafluorophenyl groups of **2(ii)**, on the other hand, exhibit no $\pi\cdots\pi$ interaction, but Au \cdots S contacts between molecules related by an inversion centre are observed which are in the range of the sum of the van der Waals radii [Au1 \cdots S3' 3.520(2) Å; ' = -x, 1 - y, 1 - z].

32 P. B. Hitchcock and P. L. Pye, *J. Chem. Soc., Dalton Trans.* **1977**, 1457–1460.

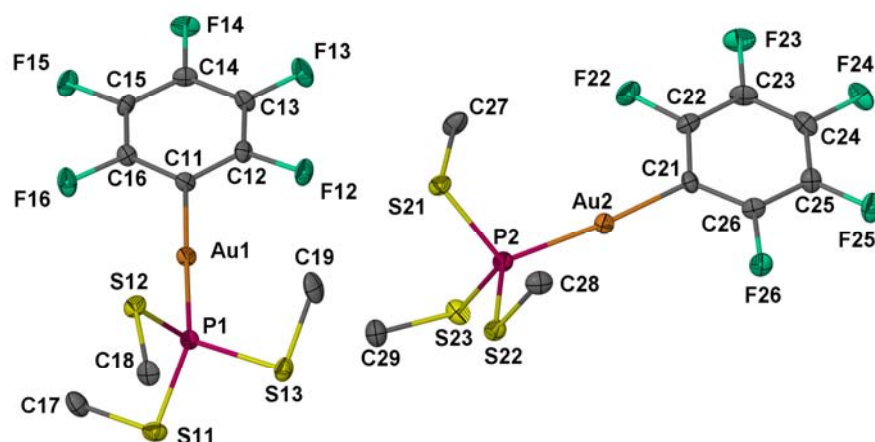


Figure 2.4 Molecular structure of **2(i)**.

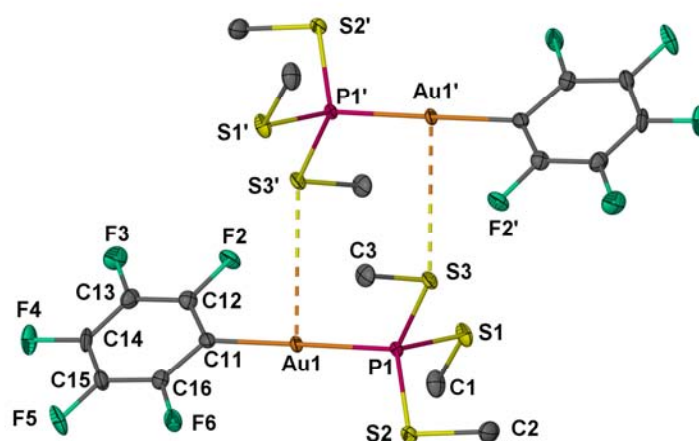


Figure 2.5 Molecular structure of **2(ii)**; primed atoms are related by a centre of inversion located between the Au atoms.

Even though the packing of the molecules in both polymorphs is governed by different modes of interaction, the normalised cell volumes ($V_n = V/Z$) differ by less than 1%. Molecule **2(i)-2** exhibits significantly distorted geometry at the gold centre $174.2(2)^\circ$ compared to **2(i)-1** whose angle [$178.9(2)^\circ$] is close to the expected 180° , as it is for **2(ii)**. The plane of the C_6F_5 ring in **2(i)-1** is nearly eclipsed with the P1–S13 bond while the C_6F_5 ring in **2(i)-2** adopts a staggered conformation also found in polymorph **(ii)**.

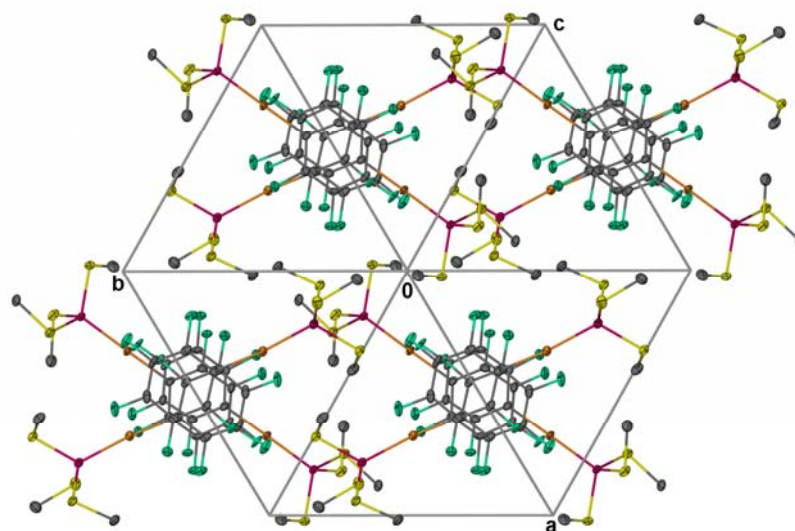


Figure 2.6 Packing diagram of **2(i)** viewed along the spatial vector of the unit cell.

The bond lengths in both polymorphs are the same within experimental error, the Au–P distances in both polymorphs of **2** [2.266(2), 2.272(2) in **2(i)** and 2.270(2) Å in **2(ii)**] are longer than the Au–P distance in **1** [2.2352(8) Å], resembling the situation in Ph_3PAuCl [Au–P 2.235(3) Å]²⁸ and $\text{Ph}_3\text{PAuC}_6\text{F}_5$ [Au–P 2.27(1) Å].³³

The crystal structure of 1,2-bis(1,3,2-dithiaphospholan-2-ylthio)ethane (the ligand in **6**) has been reported.³⁴ It crystallises in the space group $P2_1/c$ with two molecules in the unit cell. Only half of the molecule is unique and an inversion centre is located at the bridging C–C bond. Two P–S distances [2.120(3) and 2.126(3) Å] and the exocyclic P–S–C angle [98.7(3)°] are comparable to the values in $\text{P}(\text{SPh})_3$. In the five-membered ring the P–S–C angles [96.9(3)° and 101.8(3)°] are slightly distorted.

In the molecular structure of the binuclear complex **6** shown in Figure 2.7, the conformation of the ligand has changed: instead of the arrangement with an inversion centre, a structure with a C_2 axis through the C1–C1' and Au1...Au1' bonds is observed which allows intramolecular aurophilic bonding with an Au...Au distance of 3.4671(9) Å and leading to a *pseudo*-cyclic complex. The P1–Au1...Au1'–P1' torsion angle is 110.2(2)°. Again, coordination causes the P–S bonds to shorten to 2.067(4),

³³ R. W. Baker and P. J. Pauling, *J. Chem. Soc., Dalton Trans.* **1972**, 2264–2266.

³⁴ M. G. Newton, H. C. Brown, C. J. Finder, J. B. Robert, J. Martin and D. Tranqui, *J. Chem. Soc., Chem. Commun.* **1974**, 455–456.

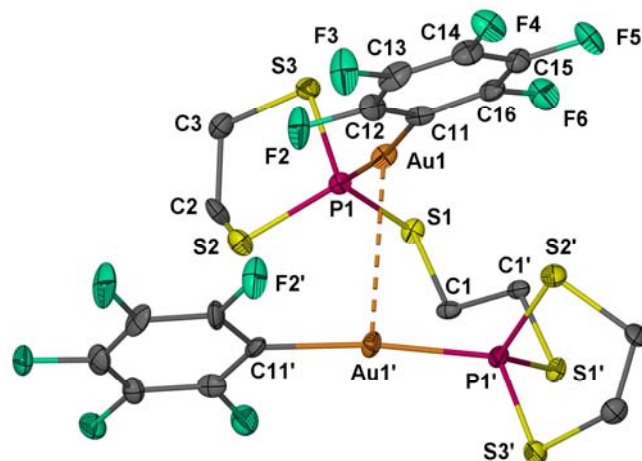
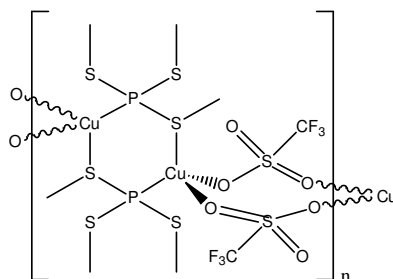


Figure 2.7 Molecular structure of **6**. Primed atoms are related by a two-fold rotation; a C_2 axis bisects the Au–Au' and C1–C1' bonds.

2.081(3) and 2.086(4) Å. The Au–P–S angles do not follow the trend of the other compounds with two angles at *ca.* 117° and one at 108° but have intermediate values [118.8(2)°, 114.7(2)° and 113.6(2)°], probably caused by restraints associated with the five-membered ring. The P1–Au1–C11 angle of 171.7(3)° deviates from linearity, a result of the attractive intramolecular interaction between the gold atoms. Such deviations have been observed in other structures.³⁵

The molecular structure of the copper complex prepared for comparison, **9**, is shown in Figure 2.8. Bond lengths and angles are given in Table 2.4. The structure consists of chains of tetrahedrally coordinated Cu^I centres that are bridged by two $P(SMe)_3$ ligands in a $\kappa^2P:S$ fashion forming 6-membered rings in the chair conformation. Two triflate molecules each employ two oxygen atoms to bridge two copper atoms, yielding 8-membered rings (Scheme 2.5). Both motives alternate along each chain running parallel to the *a* axis in the crystal. This result came as a surprise as triflate is usually regarded as a non- or weakly-coordinating ligand and crystallisation occurred from thf. The structure can be compared to that of other (trialkyltrithiophosphite)-copper(I) halides which usually crystallise in this alternating bridging motif if the alkyl substituents are not too bulky [see Scheme 2.2 (a)].^{5,6c}

³⁵ U. E. I. Horvath, S. Cronje, J. M. McKenzie, L. J. Barbour and H. G. Raubenheimer, *Z. Naturforsch., B: Chem. Sci.* **2004**, *59*, 1605–1617.



Scheme 2.5 Connectivity of the chains formed by compound **9** in the solid state.

The Cu–P [2.1895(7) Å] and Cu–S [2.2943(8) Å] bonds in **9** are shortened considerably compared to other copper trithiophosphite complexes with averaged Cu–P and Cu–S distances of 2.22 and 2.39 Å,^{4,5,6} respectively (the notable exceptions are the Cu–P bonds in structure of [CuBr{P(SC₃H₇)₃}]^{6c} which a comparable length and in the structure of [CuBr{P(SBu)₃}]^{6c} associated with large s.u. values). This is most likely due the poor donating nature of the triflate bridges, hence copper demands more electron density from the softer donor atoms. Two Cu–S bonds in the structure of P(SCHMe₂)₃ coordinated to a (CuCl)₄ cluster [Scheme 2.2 (c)] are also significantly shorter [2.207(7) and 2.185(8) Å] than in **9**.⁴ This result might originate from a similar effect of electron demand from the CuCl moieties within the cluster. The effect of the Cu–S bond to the trithiophosphite ligand in **9** is still noticeable in the adjacent P–S bond which is expectedly elongated [2.1192(9) Å]

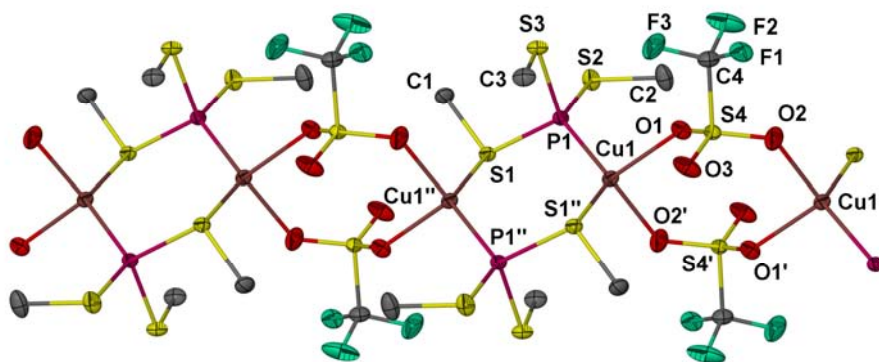
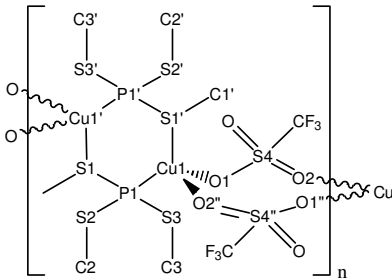


Figure 2.8 Part of the infinite coordination polymer formed by **9** (symmetry codes: ' = 1 – x, 1 – y, 1 – z; '' = –x, 1 – y, 1 – z); unlabeled atoms are related by one unit cell translation along the *a* axis.

Table 2.4 Bond lengths/Å and angles/° of compound **9**.


Cu–P	2.1895(7)	P1–Cu1–S1′	121.88(3)
Cu–S′	2.2943(8)	P1–Cu1–O1	104.59(6)
Cu–O (1, 2)	2.147(2), 2.065(2)	P1–Cu1–O2″	123.32(7)
		S1′–Cu1–O1	105.35(5)
		S1′–Cu1–O2″	102.03(7)
		O1–Cu1–O2″	95.18(8)
P1–S1(Cu)	2.1192(9)	P1–S1–C1	104.48(9)
P1–S (2, 3)	2.0941(9), 2.089(1)	P1–S–C (2, 3)	98.7(1), 101.75(9)
(Cu)S1–C1	1.816(3)	S1–P1–S2	100.09(4)
S–C (2, 3)	1.815(3), 1.814(3)	S2–P1–S3	99.29(4)
		S3–P1–S1	107.89(4)

Symmetry codes: ′ –x, 1 – y, 1 – z; ″ 1 – x, 1 – y, 1 – z.

compared to 2.0941(9) and 2.089(1) Å in the uncoordinated groups] due to the presence of adjacent positive charges; the appropriate S–C bond is not significantly different from the other two.

The fact that two triflate anions bridge two Cu^I centres is a very rare observation, only two other structures (tetrahedral with *P:P'*- or *N:N'*-coordination at the other two sites) are exclusively bridged by triflate.³⁶ One additional structure is known for Cu^{II}.³⁷ This result is in stark contrast to the wealth of structurally characterised Ag^I complexes that exhibit this motif. Compared to the Cu–O distances in **9** [2.147(2) and 2.065(2) Å], the analogous distances in the *N:N'*-bonded structure are longer at 2.336(6) and 2.350(7) Å; the *P:P'*-bonded structure has one slightly longer and a comparable bond [2.111(4) and 2.189(4) Å] while the O–Cu–O angles are 88.9(2)° and 98.0(2)°, respectively.

36 (a) R. T. Stibrany, H. J. Schugar and J. A. Potenza, *Private communication to the Cambridge Crystallographic Data Centre*, No. 603057, **2006**; (b) R. T. Stibrany and J. A. Potenza, *Private communication to the Cambridge Crystallographic Data Centre*, No. 639034, **2007**.

37 E. D. Blue, T. B. Gunnoe, J. L. Petersen and P. D. Boyle, *J. Organomet. Chem.* **2006**, *691*, 5988–5993.

The O1–Cu–O2' ($\angle = 1 - x, 1 - y, 1 - z$), P–Cu–O2' and P–Cu–S'' ($\angle = -x, 1 - y, 1 - z$) angles in **9** [$95.18(8)^\circ$, $123.32(7)^\circ$ and $121.88(3)^\circ$] are significantly distorted from the tetrahedral ideal of 109.5° .

Bis(triphenylphosphane)copper(1+) trifluoromethanesulfonate has been shown to crystallise as the salt $[\text{Cu}(\text{CH}_3\text{CN})_2(\text{PPh}_3)_2]\text{CF}_3\text{SO}_3$ from ethanenitrile, which spontaneously recrystallises as the neutral complex $[\text{Cu}(\text{CF}_3\text{SO}_3)(\text{PPh}_3)_2(\text{thf})]$ when it is dissolved in thf. The latter compound exhibits Cu–O(thf) and Cu–O(triflate) bond lengths of 2.125(2) and 2.168(2) Å, respectively, showing that thf is indeed capable of forming a bond with Cu^{I} that is shorter than the triflate Cu–O bond despite the additional Coulomb attraction in the latter instance.³⁸

2.3 Conclusions

The first gold(I) trithiophosphite complexes were isolated, characterised and the crystal and molecular structures of an array of different complexes could be determined. The complexes of the monodentate ligands are fairly stable when kept at low temperatures, the bidentate ligand employed furnishes more sensitive compounds. Protic solvents effect decomposition due to hydrolysis. The structural analysis revealed that contrary to most Cu^{I} complexes of trithiophosphites, wherein one sulfur atom is used as a coordination site as well, Au^{I} does not expand its coordination number beyond the classic linear coordination and therefore does not engage in coordinate bonds from sulfur atoms. $\text{Au}^{\text{I}}\cdots\text{S}$ contacts could, however, be observed in some compounds influencing their solid state structures.

Related silver(I) trithiophosphite complexes could not be crystallised, a result partly ascribed to the tendency of Ag^{I} to aggregate into clusters. Synthesis of such complexes could maybe succeed employing other silver centres that are already coordinatively nearly saturated and do not contain labile ligands.

An example of a trithiophosphite complex of Cu^I that also contains a weakly coordinating anion was also isolated, surprisingly exhibiting a chain motif and not incorporating any solvent.

Finally, tetrathiophosphates proved to be unable to form complexes with Au^I probably being too weak donors.

2.4 Experimental

2.4.1 Crystallography

All crystal structures in this dissertation were determined at $T = 100$ K with a Bruker SMART Apex diffractometer³⁹ using graphite-monochromated Mo-K α radiation ($\lambda = 0.71073$ Å). Intensities were measured using the ω -scan mode and were corrected for Lorentz and polarisation effects. The structures were solved with direct methods or the heavy atom(s) were located by a Patterson synthesis and refined by full-matrix least-squares on F^2 using the SHELXL-97 set of programmes within the X-SEED environment.⁴⁰ All non-hydrogen atoms were refined with anisotropic displacement parameters and all hydrogen atoms were placed in calculated positions except where noted otherwise. Figures were created using X-SEED and all thermal displacement ellipsoids drawn at the 50% probability level. Thickness of normal bonds was set to 0.1 Å while for sub-van der Waals interactions and hydrogen bonds fragmented bonds of 0.08 Å diameter are used throughout. The colours of the respective elements are consistent in all Figures. Data and parameters associated with crystal structures presented in this Chapter are summarised in Table 2.5.

39 (a) R. H. Blessing, *Acta Crystallogr., Sect. A: Fundam. Crystallogr.* **1995**, *51*, 33–38;

(b) SADABS Absorption correction software (v. 2.05), *Bruker AXS Inc., Madison WI*, **2002**;

(c) SMART Data collection software (v. 5.629), *Bruker AXS Inc., Madison WI*, **2003**;

(d) SAINT Data reduction software (v. 6.45), *Bruker AXS Inc., Madison WI*, **2003**.

40 (a) G. M. Sheldrick, *SHELX97, Programmes for crystal structure solution and refinement*,

University of Göttingen, Germany, **1997**; (b) L. J. Barbour, *J. Supramol. Chem.* **2001**, *1*, 189–191;

(c) J. L. Atwood and L. J. Barbour, *Cryst. Growth Des.* **2003**, *3*, 3–8.

Table 2.5 Crystallographic parameters of **1–3, 6, 8** and **9**.

Compound	(MeS) ₃ PAuCl 1	(MeO) ₃ PAuCl 8	(MeS) ₃ PAuClF ₅ 2(i)	(MeS) ₃ PAuClF ₅ 2(ii)	(PhS) ₃ PAuCl 3	² L(AuClF ₅) ₂ ^b 6	(MeS) ₃ PCuOTf 9
Empirical formula	C ₃ H ₉ AuClPS ₃	C ₃ H ₉ AuClO ₃ P	C ₉ H ₉ AuF ₅ PS ₃	C ₉ H ₉ AuF ₅ PS ₃	C ₁₈ H ₁₅ AuClPS ₃	C ₁₈ H ₁₂ Au ₂ F ₁₀ P ₂ S ₆	C ₄ H ₉ CuF ₃ O ₃ PS ₄
<i>M_r</i>	404.69	356.49	536.30	536.30	590.90	1066.5	384.89
Crystal habit	Needle	Needle	Block	Block	Block	Block	Block
Crystal dimensions/mm	0.2 × 0.1 × 0.05	0.5 × 0.1 × 0.1	0.05 × 0.04 × 0.03	0.1 × 0.1 × 0.005	0.2 × 0.2 × 0.15	0.1 × 0.08 × 0.04	0.1 × 0.08 × 0.04
Crystal system	Orthorhombic	Orthorhombic	Triclinic	Triclinic	Monoclinic	Monoclinic	Monoclinic
Space group	<i>Pbca</i> (No. 61)	<i>Pbca</i> (No. 61)	<i>P</i> $\bar{1}$ (No. 2)	<i>P</i> $\bar{1}$ (No. 2)	<i>P2</i> ₁ / <i>c</i> (No. 14)	<i>I2</i> / <i>a</i> (No. 15)	<i>P2</i> ₁ / <i>c</i> (No. 14)
<i>a</i> /Å	6.5671(6)	6.2810(8)	11.739(2)	7.705(2)	15.156(2)	9.0659(15)	8.835(2)
<i>b</i> /Å	15.651(2)	14.507(2)	11.757(2)	10.060(2)	13.119(2)	17.155(3)	18.306(3)
<i>c</i> /Å	18.314(2)	17.324(2)	12.672(2)	11.014(2)	10.147(2)	17.061(3)	8.173(2)
α /°	90	90	103.971(2)	65.077(2)	90	90	90
β /°	90	90	105.090(2)	82.579(3)	100.834(2)	94.020(4)	102.674(3)
γ /°	90	90	110.925(2)	69.830(3)	90	90	90
<i>V</i> /Å ³	1882.3(3)	1578.6(3)	1464.9(3)	726.6(2)	1981.7(5)	2646.8(8)	1289.6(4)
<i>Z</i> , <i>D_c</i> /Mg m ⁻³	8, 2.856	8, 3.000	4, 2.432	2, 2.451	4, 1.980	4, 2.676	4, 1.982
μ (MoK α)/mm ⁻¹	16.670	19.119	10.614	10.699	7.953	11.749	2.488
No. of reflections, unique	10206, 2007	8198, 1604	8780, 6057	7786, 2963	11766, 4510	7592, 2726	7349, 2612
<i>R</i> _{int}	0.0259	0.0268	0.0201	0.0282	0.0443	0.0510	0.0208
<i>hkl</i> index range	± 8, -19 to 16, -21 to 23	± 7, -14 to 18, -18 to 21	± 14, ± 14, -15 to 16	± 9, ± 12, ± 13	± 19, -17 to 16, -12 to ± 11, -21 to 20, -21 to 13	± 11, -14 to 22, -9 to 14	± 11, -14 to 22, -9 to 10
θ range/°	2.22–26.75	2.35–26.36	1.79–26.79	2.04–26.41	2.07–28.28	1.69–26.43	2.23–26.35
Data, restraints, parameters	1924, 0, 85	1514, 0, 85	5267, 0, 349	2770, 0, 175	3815, 0, 217	2308, 0, 172	2425, 0, 148
<i>F</i> (000)	1488	1296	1000	500	1128	1976	768
<i>R</i> ₁ , <i>wR</i> ₂ [<i>I</i> > 2 σ (<i>I</i>)] ^a	0.0163, 0.0395	0.0218, 0.0446	0.0341, 0.0813	0.0279, 0.0632	0.0462, 0.0856	0.0531, 0.1002	0.0303, 0.0734
<i>R</i> ₁ , <i>wR</i> ₂ (all data) ^a	0.0173, 0.0399	0.0239, 0.0453	0.0407, 0.0845	0.0310, 0.0644	0.0588, 0.0890	0.0666, 0.1047	0.0326, 0.0746
Goodness-of-fit	1.101	1.188	1.029	1.079	1.130	1.139	1.044
Max. and min. transmission	0.436, 0.151	0.821, 0.285	0.727, 0.482	0.586, 0.382	0.305, 0.174	0.625, 0.397	0.907, 0.789
Largest differential peak and hole/eÅ ⁻³	1.613, -1.059	1.347, -1.590	2.505, -1.403	2.037, -1.088	2.222, -2.641	2.748, -2.048	0.865, -0.419
CCDC ref. No.	609872	609877	609873	609874	609875	609876	

^a $w = 1/[\sigma^2(F_o^2) + (aP)^2 + bP]$ where $P = (F_o^2 + 2F_c^2)/3$ ^b **L** = 1,2-bis(1,3,2-dithiaphospholan-2-ylthio)ethane

2.4.2 Instrumentation

^1H , ^{13}C , ^{15}N , ^{19}F and ^{31}P NMR spectra (δ in ppm) were recorded on Varian VXR 300, Varian VNMRS 300, Varian Unity Inova 400 or Varian Unity Inova 600 instruments at the indicated frequency. ^1H and ^{13}C NMR spectra were referenced relative to residual solvent peaks; ^{15}N , ^{19}F and ^{31}P NMR spectra were referenced externally to neat MeNO_2 , neat CFCl_3 or 85% H_3PO_4 , respectively. IR spectra were recorded at 4 cm^{-1} resolution on a Nicolet Avatar 300 FT-IR instrument equipped with a Smart Performer ZnSe disk ATR accessory. The spectra were corrected for ATR effects using Omnic software supplied with the spectrometer. Far-IR spectra were recorded in polyethylene discs at 4 or 2 cm^{-1} resolution on a Nicolet Nexus FT-IR spectrometer using a solid substrate beam splitter and a DTGS polyethylene detector. EI mass spectra were recorded on an AMD 604 instrument at 70 eV. ESI mass spectra were recorded on a Waters API Quattro Micro instrument at 15–50 V cone voltage. FAB mass spectra were recorded in (nitrophenyl)methanol matrices on a VG 70 SEQ mass spectrometer by the University of the Witwatersrand. Thermal gravimetric analyses were conducted on a TA instruments TGA Q500 device. Melting points were determined on a Stuart Scientific SMP3 instrument or on a Fischer Scientific (Pittsburgh PA, St. Louis MO) and Eimer & Amend (New York NY) hot stage apparatus and are uncorrected. Elemental analyses were performed by the University of Cape Town or the University of the Witwatersrand.

2.4.3 General procedures and reagents

Cooling baths at $-78\text{ }^\circ\text{C}$ were prepared with a propan-1-ol/dry ice slush. All work was conducted under an atmosphere of dry argon using standard Schlenk- and vacuum-line techniques. All solvents were distilled under a dry dinitrogen atmosphere,⁴¹ CH_2Cl_2 and MeCN were distilled from CaH_2 ; pentane, hexane, hexanes and methylbenzene were distilled from sodium; Et_2O and thf were dried with sodium wire and sodium benzophenone ketyl radical. Anhydrous propanone was distilled from 3 \AA molecular sieves. Methanol and ethanol were dried by distillation from the respective magnesium alkoxides. Ethane-1,2-diol, CHCl_3 and NEt_3 were distilled and stored over

⁴¹ R. J. Errington, in *Advanced Practical Inorganic and Metalorganic Chemistry*, Chapman & Hall, London, 1997, p. 92.

3 Å molecular sieves. Pyridine was distilled, stored over 3 Å molecular sieves and re-distilled prior to use. Butyllithium and methyllithium were standardised in the appropriate solvent prior to use following the procedure of *Winkle*.⁴² Supplied chemicals were used without further purification except when noted otherwise.

Bromopentafluorobenzene, butyllithium in hexanes, phosphorus trichloride, silver(I) triflate and pyridine were obtained from Aldrich Chemical Co.; Celite (diatomaceous earth), crude copper(I) chloride, dimethyldisulfane, diphenyldisulfane, ethane-1,2-dithiol, sodium triflate and trimethylphosphite were obtained from Fluka AG; tetrahydrothiophene from ACROS and anhydrous magnesium sulfate and sodium sulfate from Saarchem.

2.4.4 Synthesis of the compounds

The trithiophosphite ligands P(SMe)₃ and P(SPh)₃ were prepared in a modification of the simple literature procedure,¹⁶ propanone was replaced with ethanenitrile. (tht)AuCl⁴³ and (tht)AuC₆F₅^{43b} were prepared according to the literature procedure. CuCl was prepared according to the procedure of *Vaidya*⁴⁴ by heating impure greenish CuCl with propane-1,2,3-triol furnishing a colourless powder.

A gift of Ph₃PAuCl by *Jacorien Coetsee* is greatly acknowledged.

2.4.4.1 – 1,2-bis(1,3,2-dithiaphospholan-2-ylthio)ethane.

An Et₂O solution (40 ml) of ethane-1,2-dithiol (2.25 g, 24 mmol) was added dropwise to a stirred solution of freshly distilled PCl₃ (2.05 g, 15 mmol) and pyridine (4.07 g, 52 mmol) in Et₂O (60 ml) at 0 °C. After 2 h pyridine hydrochloride was removed by filtration and washed with CH₂Cl₂ (60 ml). The solvents were removed *in vacuo* and the remaining colourless solid extracted with methylbenzene (100 ml) and again

42 M. R. Winkle, J. M. Lansinger and R. C. Ronald, *J. Chem. Soc., Chem. Commun.* **1980**, 87–88.

43 (a) A. Haas, J. Helmbrecht and U. Niemann, in *Handbuch der Präparativen Anorganischen Chemie*, ed. G. Brauer, Stuttgart, Enke **1978**, p. 1014;

(b) R. Uson, A. Laguna and M. Laguna, *Inorg. Synth.* **1989**, 26, 85–91.

44 B. K. Vaidya, *Nature* **1929**, 123, 414.

filtered. The solvent was removed *in vacuo* affording a colourless microcrystalline solid (0.789 g, 31%).

M.p. 123 °C

The compound is soluble in CH₂Cl₂ and thf, slightly soluble in methylbenzene and insoluble in Et₂O or alkanes.

2.4.4.2 *Tetrakis(ethanenitrile)copper(I+) trifluoromethanesulfonate.*

A solution of NaOTf (1.21 g, 7.03 mmol, 1 eq.) in 20 ml ethanenitrile was degassed by repeatedly applying a vacuum and filling the Schlenk tube with argon. Solid white CuCl (701 mg, 7.08 mmol, 1 eq.) was added, the reaction mixture was heated to 80 °C to initiate the reaction and then left stirring overnight at room temperature. The suspension was filtered through Celite pre-treated with Et₂O and the colourless solution thus obtained was concentrated to *ca.* 7 ml. Addition of methylbenzene (20 ml) caused precipitation of the colourless crystalline product and the vessel was cooled to –30 °C for another 30 min to effect further crystallisation. Removal of the yellowish mother liquor furnished 2.57 g (97%) of the title compound.

2.4.4.3 *Chloro(trimethyltrithiophosphite)gold, I.*

Ligand P(SMe)₃ (0.146 g, 0.85 mmol) was dissolved in thf (15 ml) and (tht)AuCl (0.272 g, 0.85 mmol) was added. The resulting homogeneous slightly yellowish solution was stirred for 1 h. All volatiles were removed *in vacuo* during which the compound started to precipitate from the solution. The obtained solid was again dissolved in thf (15 ml), filtered through Celite and stripped of solvent affording the target compound as a colourless microcrystalline solid in quantitative yield (0.342 g). Crystals suitable for an X-ray diffraction measurement were grown by layering a trichloromethane-*d* solution with pentane. Found: C, 8.7; H, 2.3. C₃H₉AuCIPS₃ requires C, 8.90; H, 2.24%. ν/cm^{-1} 2920 s (CH₃), 1415 vs (CH₃), 694 s, 566 vs, 512 vs, 503 vs, 315 s (Au³⁵Cl) and 308 m (Au³⁷Cl).

M.p. 114 °C (dec.)

The compound is soluble in CH₂Cl₂, trichloromethane and thf, it is insoluble in Et₂O and alkanes and decomposes in protic solvents.

2.4.4.4 (Pentafluorophenyl)(trimethyltrithiophosphite)gold, **2**.

A solution of P(SMe)₃ (0.107 g, 0.62 mmol) in Et₂O (30 ml) was cooled to 0 °C and transferred *via* a Teflon cannula to a second Schlenk tube charged with (tht)AuC₆F₅ (0.273 g, 0.60 mmol). The mixture was stirred for 45 min at 0 °C followed by filtration of the purplish solution through Celite previously washed with Et₂O. After removal of the volatiles *in vacuo* a crude purple product was obtained. The filtration procedure was repeated to afford a colourless microcrystalline solid (0.283 g, 87%). Crystals of polymorph **A** suitable for an X-ray diffraction measurement were grown by diffusing pentane vapour into an Et₂O solution. Polymorph **B** crystallised from a thf solution layered with pentane. Found: C, 20.1; H, 1.7. C₉H₉AuF₅PS₃ requires C, 20.2; H, 1.7%. ν/cm^{-1} 2917 s (CH₃), 1634 m, 1501 s, 1454 vs, 1419 vs (CH₃), 1061 s, 952 vs, 790 s and 693 m.

M.p. 92 °C (dec.)

The compound is soluble in all common organic solvents except alkanes, it decomposes in protic solvents.

2.4.4.5 Chloro(triphenyltrithiophosphite)gold, **3**.

The complex was prepared in an analogous manner to **1** employing P(SPh)₃ (0.346 g, 0.97 mmol) and (tht)AuCl (0.315 g, 0.98 mmol) affording a viscous colourless oil which slowly crystallised over several days at -16 °C yielding a colourless solid (0.539 g, 95%). A crystal suitable for an X-ray structure determination was grown from a thf solution layered with Et₂O at -16 °C. Found: C, 36.4; H, 2.7. C₁₈H₁₅AuClPS₃ requires C, 36.6; H, 2.6%. ν/cm^{-1} 3044 m (CH), 1572 m, 1470 vs, 1436 vs, 1082 s, 1023 s, 745 vs, 687 vs, 461 vs, 339 s (AuCl), 318 s, 262 m and 235 m.

M.p. 63 °C (dec. without melting)

The compound is soluble in CH₂Cl₂, CHCl₃ and thf, but insoluble in Et₂O or alkanes.

2.4.4.6 (Pentafluorophenyl)(triphenyltrithiophosphite)gold, **4**.

The compound was prepared in an analogous manner to **2** employing P(SPh)₃ (0.145 g, 0.40 mmol) and (tht)AuC₆F₅ (0.189 g, 0.42 mmol). After evaporation of all volatiles a colourless crystalline solid was obtained (0.283 g, 97%). Found: C, 40.0;

H, 2.1. $C_{24}H_{15}AuF_5PS_3$ requires C, 39.9; H, 2.1%. ν/cm^{-1} 3054 m (CH), 1638 m, 1609 m, 1503 s, 1456 vs, 1438 vs, 1355 s, 1060 s, 952 vs, 741 s and 683 s.

M.p. 86 °C (dec.)

The compound is soluble in all common organic solvents except alkanes. Protic solvents effect decomposition.

2.4.4.7 Dichloro{ μ -[1,2-bis(1,3,2-dithiaphospholan-2-ylthio)ethane]}digold, **5**.

A solution of (tht)AuCl (0.218 g, 0.68 mmol) and 1,2-bis(1,3,2-dithiaphospholan-2-ylthio)ethane (0.115 g, 0.34 mmol) in thf (15 ml) was stirred at r.t. A precipitate was observed and after 1.5 h the volatiles were removed *in vacuo* affording a yellowish solid (0.263 g, 96%). Only limited analytical data could be obtained due to the insolubility of the material. Found: C, 8.9; H, 1.5%. $C_6H_{12}Au_2Cl_2P_2S_6$ requires C, 9.0; H, 1.5%. ν/cm^{-1} 2958 s (CH₂), 2922 s (CH₂), 1416/1411 vs (CH₂), 1288 m, 1202 vs, 938 s, 837 vs, 728 m, 673 s, 433 m, 371 m and 323 s (AuCl).

M.p. 95 °C (dec. without melting)

The compound is insoluble.

2.4.4.8 { μ -[1,2-Bis(1,3,2-dithiaphospholan-2-ylthio)ethane]}-bis(pentafluorophenyl)digold, **6**.

A solution of 1,2-bis(1,3,2-dithiaphospholan-2-ylthio)ethane (0.077 g, 0.23 mmol) in thf (10 ml) was cooled to 0 °C and (tht)AuC₆F₅ (0.210 g, 0.46 mmol) was added. After stirring the homogeneous solution for 30 min the volatiles were removed *in vacuo* during which the product started to precipitate. The dry solid was again dissolved in thf (30 ml), filtered through Celite and stripped of solvent to afford a colourless crystalline product (0.216 g, 87%). Crystals suitable for X-ray diffraction were obtained by layering a thf solution with pentane. Found: C, 20.4; H, 1.2. $C_{18}H_{12}Au_2F_{10}P_2S_6$ requires C, 20.3; H, 1.1%. ν/cm^{-1} 2924 w (CH₂), 1638/1632 m, 1502 vs, 1452 vs, 1357 s, 1199 m, 1061 s, 952 s and 789 s.

M.p. 158 °C (dec. without melting)

The compound is only soluble in thf when freshly prepared. It ages within days turning yellow and becomes insoluble.

2.4.4.9 *Bis(trimethyltrithiophosphite)gold(1+) trifluoromethanesulfonate, 7.*

Ligand P(SMe)₃ (0.139 g, 0.81 mmol) was dissolved in ethanenitrile (10 ml) and (tht)AuCl (0.130 g, 0.41 mmol) was added which yielded a yellow precipitate. After 1 h, thf (10 ml) was added which dissolved the precipitate affording a hazy yellowish solution. A solution of AgOTf (0.102 g, 0.40 mmol) in ethanenitrile (5 ml) was added causing immediate precipitation of AgCl. The suspension was stirred for another hour and then filtered through Celite. The filter was washed with thf (20 ml) and the filtrate evaporated *in vacuo* affording a yellow oil which slowly crystallised at -16 °C. Treatment of the crude product with Et₂O (40 ml), inverse filtration and drying *in vacuo* afforded a hygroscopic yellow solid (0.153 g, 56%) which is very sensitive to moisture. Found: C, 12.5; H, 2.9. C₇H₁₈AuF₃O₃P₂S₇ requires C, 12.2; H, 2.6%. ν/cm^{-1} 2916 m (CH₃), 2847 m (CH₃), 1422/1418 s (CH₃), 1253 s (CF₃SO₃⁻), 1219 vs (CF₃SO₃⁻), 1155 s, 1140 s, 1026 s and 955 m.

M.p. 60 °C (dec. with evolution of gas)

The compound is soluble in ethanenitrile and CH₂Cl₂, it is insoluble in Et₂O and alkanes.

2.4.4.10 *Chloro(trimethylphosphite)gold, 8.*

In an analogous manner to the preparation of **1** the reaction of trimethylphosphite (0.041 g, 0.33 mmol) and (tht)AuCl (0.108 g, 0.34 mmol) afforded a crystalline powder after evaporation of all volatiles. It was re-dissolved in thf (7 ml), the solution layered with pentane and stored at -16 °C whereupon the target compound crystallised as colourless needles (0.104 g, 90%). A suitable crystal was mounted for X-ray diffraction.

M.p. 101 °C

2.4.4.11 *catena-(μ-Trifluoromethanesulfonato-κ²O:O′)(μ-trimethyltrithiophosphite-κP:κS)copper, 9.*

Ligand P(SMe)₃ (202 mg, 1.2 mmol) was dissolved in thf (20 ml) and [Cu(CH₃CN)₄]OTf (440 mg, 1.2 mmol, 1 eq.) was added furnishing a homogeneous solution. After stirring for 15 min., a slight turbidity was observed and after 1.5 h all volatiles were removed *in vacuo* affording a yellowish oil. Trituration with Et₂O

(*ca.* 20 ml) and twice with *ca.* 20 ml methylbenzene caused the oil to solidify giving a colourless powder in quantitative yield. A crystal suitable for X-ray diffraction was grown from thf layered with pentane. Found C, 12.6; H, 2.2. $C_4H_9CuF_3O_3PS_4$ requires C, 12.5; H, 2.4%. ν/cm^{-1} 2999 w (CH₃), 2924 m (CH₃), 1605 w, 1421 m (CH₃), 1284 s (CF₃SO₃⁻), 1220 vs (CF₃SO₃⁻), 1169 vs (CF₃SO₃⁻), 1049 w, 1019 vs, 962 s, 764 w, 734 w, 668 m, 626 s and 577 w.

M.p. 140 °C (dec. to a rust-brown powder without melting)

The material is soluble in ethanenitrile and thf, it is insoluble in Et₂O and alkanes.

3 Tris(azol-2-yl)phosphane Complexes of Gold(I)¹

3.0 Abstract

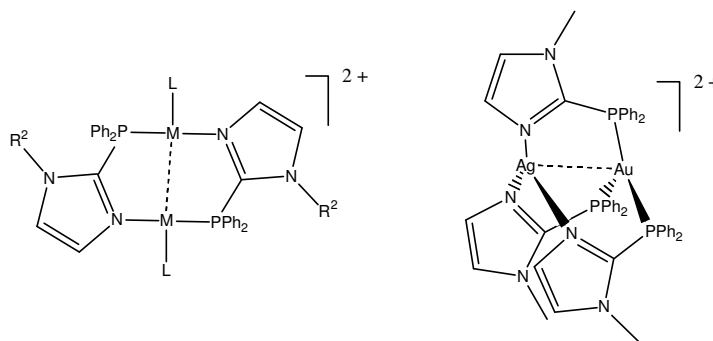
Various tris(azol-2-yl)phosphanes PR_3 ($\text{R} = 1\text{-methylimidazol-2-yl}$, thiazol-2-yl , $4\text{-methylthiazol-2-yl}$ or $4,5\text{-dimethylthiazol-2-yl}$), **1a–d**, were utilised to prepare complexes of the type R_3PAuCl , **2a–d**. The donor strength of the nitrogen atoms in the ligands was assessed with natural-abundance $^{15}\text{N}\{^1\text{H}\}$ NMR spectroscopy of **1a–c**. The chloride of **2c** could be successfully substituted by the anions NCS^- and PhC(O)S^- affording products **3a**, and **3b**, respectively. Sulfurisation of ligand **1c** furnished the phosphane sulfide **1e**. Crystal and molecular structures were determined of compounds **1c–e**, **2a–d**, **3a**, **3b** and **4**. Intriguingly, **2b** and **2c** crystallise in a total of seven polymorphs and solvates exhibiting different modes of intermolecular association. Compound **2b** crystallises in three polymorphs; two known polymorphs and the new solvate **2b** $\cdot 0.5\text{CH}_2\text{Cl}_2$ exhibit aurophilic interaction while the new third polymorph is stabilised by short $\text{Au}\cdots\text{Cl}$ interactions of $3.2660(9)$ Å. The newly discovered additional polymorph of **2c**, as well as the solvate **2c** $\cdot \text{C}_4\text{H}_8\text{O}$, lack any $\text{Au}\cdots\text{Au}$ contacts. Product **2b** is the first simple gold compound known to exhibit both $\text{Au}\cdots\text{Au}$ and $\text{Au}\cdots\text{Cl}$ contacts in different polymorphs. Compound **1e** is an inferior ligand for Au^{I} and reaction with $(\text{tht})\text{AuCl}$ ($\text{tht} = \text{tetrahydrothiophene}$) and $(\text{tht})\text{AuC}_6\text{F}_5$ sets up an equilibrium situation between **1e** and tht competing for coordination to gold.

1 All gold complexes presented in this Chapter as well as ligand **1d** have been described in a publication: C. E. Strasser, W. F. Gabrielli, C. Esterhuysen, O. B. Schuster, S. D. Nogai, S. Cronje and H. G. Raubenheimer: "Preparation of tris(azolyl)phosphine gold(I) complexes: digold(I) coordination and variation in solid state intermolecular interactions", *New J. Chem.* **2008**, *32*, 138–150.

In addition, the crystal and molecular structures of ligands **1a**, **1c** and **1e** have been submitted for publication: Christoph E. Strasser, William F. Gabrielli, Oliver B. Schuster, Stefan D. Nogai, Stephanie Cronje and Helgard G. Raubenheimer: "Crystal and molecular structures of tris(1-methylimidazol-2-yl)phosphine, tris(4-methylthiazol-2-yl)phosphine and its sulfide", *J. Chem. Crystallogr.* **2008**, submitted for publication.

3.1 Introduction

Alkyl- and arylphosphanes count amongst the most useful ligands in coordination chemistry. However, complexes of phosphanes with one or more azolyl residues have received much less attention. The available literature deals mainly with complexes of (1-alkylimidazol-2-yl)diphenylphosphanes where cationic, bridged, binuclear coinage metal complexes with *P:N*-coordination are a popular motif.² A mixed Ag^I/Au^I complex has been reported in which the gold centre is selectively coordinated to the phosphorus atoms and the silver centre solely by the imidazole nitrogen atoms (Scheme 3.1).³



Scheme 3.1 Complexes of 1-alkylimidazol-2-ylphosphanes; M = Ag, Au and L = MeCN in the Ag complex, the Au complex does not entail ancillary ligands.

Metal complexes of tris(imidazolyl)phosphane ligands have mainly been used in molecular models for carbonic anhydrase (Scheme 3.2).⁴ This enzyme is vital in living organisms as it accelerates the simple reaction of CO₂ hydration and ionisation⁵ (Equation 3.1) by a factor of 10⁷. The enzyme contains a Zn centre coordinated by three histidine residues; tris(imidazolyl)phosphanes are convenient scaffolds for studying this simple but important reaction on the scale of a comparatively small

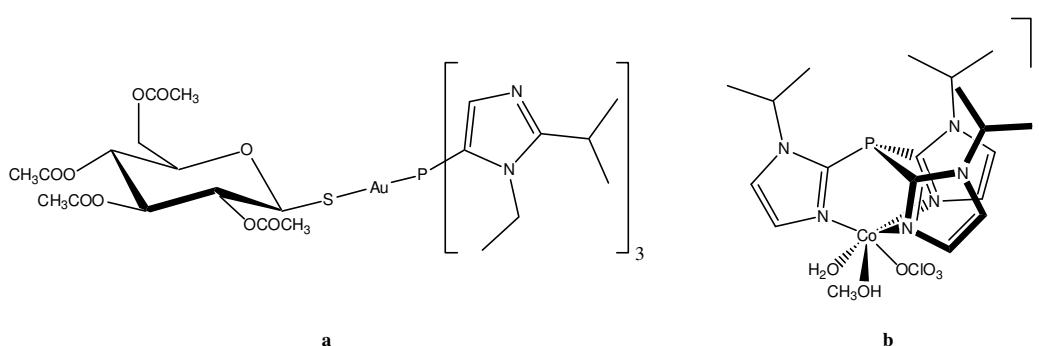


- 2 (a) A. Burini, B. R. Pietroni, R. Galassi, G. Valle and S. Calogero, *Inorg. Chim. Acta* **1995**, 229, 299–305; (b) F. Bachechi, A. Burini, M. Fontani, R. Galassi, A. Macchioni, B. R. Pietroni, P. Zanello and C. Zuccaccia, *Inorg. Chim. Acta* **2001**, 323, 45–54.
- 3 V. J. Catalano and S. J. Horner, *Inorg. Chem.* **2003**, 42, 8430–8438.
- 4 (a) C. Kimblin, B. M. Bridgewater, D. G. Churchill and G. Parkin, *J. Chem. Soc., Dalton Trans.* **2000**, 2191–2194; (b) T. B. Koerner and R. S. Brown, *Can. J. Chem.* **2002**, 80, 183–191; (c) P. C. Kunz, G. J. Reiß, W. Frank and W. Kläui, *Eur. J. Inorg. Chem.* **2003**, 3945–3951.
- 5 R. G. Khalifah, *J. Biol. Chem.* **1971**, 246, 2561–2573.

complex that allows for facile handling and accumulation of spectroscopic information.⁶

In these instances only the imine nitrogen atoms are utilised as coordination centres resembling the κ^3N,N',N'' -coordination mode found in similar complexes of the hydridotris(pyrazol-2-yl)borate (scorpionate) ligands, with the phosphorus serving mainly as a probe for convenient ^{31}P NMR analysis.

Employment of tris(imidazolyl)phosphanes as *P*-coordinating ligands has only been reported twice encompassing one complex each of Au^{I} (Scheme 3.2) and Pt^{II} .⁷ The former is the only *P*-coordinated tris(azolyl)phosphane complex so far characterised by X-ray diffraction.



Scheme 3.2 (a) Structure of the Auranofin[™] analogue and only *P*-coordinated structure of a tris(imidazolyl)phosphane reported to date;^{7b} (b) typical κ^3N,N',N'' scorpionate-coordination of a tris(imidazolyl)phosphane as a model for the catalytic site of carbonic anhydrase.^{4a}

Examples of phosphane complexes with thiazolyl moieties are even less common and for the Au^{I} centre only diphenyl(thiazol-2-yl)phosphane⁸ and, recently, (perfluorobenzothiazol-2-yl)diphenylphosphane have been utilised. As both benzothiazole and gold have advantageous properties in this regard, complexes of the latter ligand were employed in a phosphorescence study.⁹

6 W. Kläui, C. Piefer, G. Rheinwald and H. Lang, *Eur. J. Inorg. Chem.* **2000**, 1549–1555.

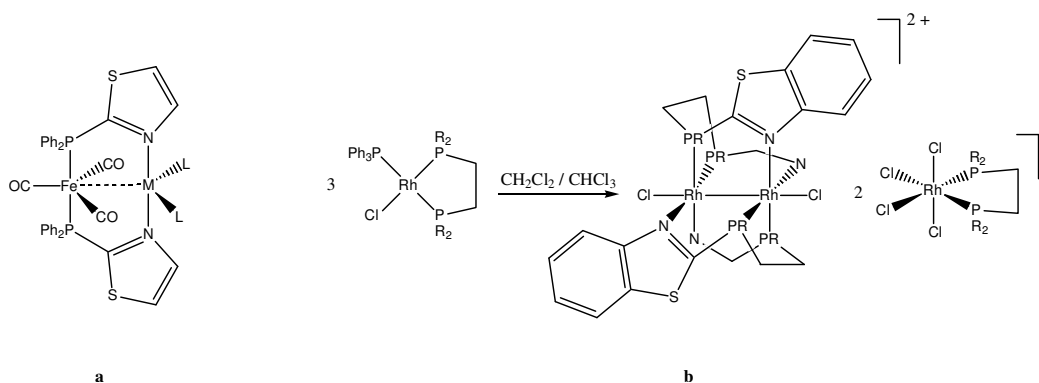
7 (a) S. S. Moore and G. M. Whitesides, *J. Org. Chem.* **1982**, 47, 1489–1493;

(b) R. A. Bell, C. J. L. Lock, C. Scholten and J. F. Valliant, *Inorg. Chim. Acta* **1998**, 274, 137–142.

8 A. Antiñolo, F. Carrillo-Hermosilla, E. Diez-Barra, J. Fernández-Baeza, A. Lara-Sánchez, A. Otero and J. Tejada, *J. Organomet. Chem.* **1998**, 570, 97–105.

9 E. J. Fernández, A. Laguna, J. M. López-de-Luzuriaga, M. Monge, M. Montiel, M. E. Olmos and M. Rodríguez-Castillo, *Dalton Trans.* **2006**, 3672–3677.

Other examples that were found to exhibit *N*-coordination of one (benzo)thiazole moiety in addition to phosphane coordination, include complexes of Rh^{I} and Rh^{II} ,¹⁰ as well as the combinations $\text{Fe}^0/\text{Cd}^{\text{II}}$ and $\text{Fe}^0/\text{Hg}^{\text{II}}$ ¹¹ which have been characterised by X-ray crystal structure determinations (Scheme 3.3). The ligand bis[bis(benzothiazol-2-yl)phosphanyl]ethane chelates a Rh^{I} centre by *P:P'*-coordination. The complex is, however, unstable and yields a unique mixed $\text{Rh}^{\text{II}}/\text{Rh}^{\text{III}}$ complex salt when left in chlorinated solvents.^{10b} Intriguingly, in the binuclear $\text{Fe}^0/\text{Cd}^{\text{II}}$ and $\text{Fe}^0/\text{Hg}^{\text{II}}$ complexes, Fe^0 is *P*-coordinated while $\text{Hg}^{\text{II}}/\text{Cd}^{\text{II}}$ are *N*-coordinated which may be a result of the fact that the group 12 metals were introduced last and ligand rearrangement is inhibited.



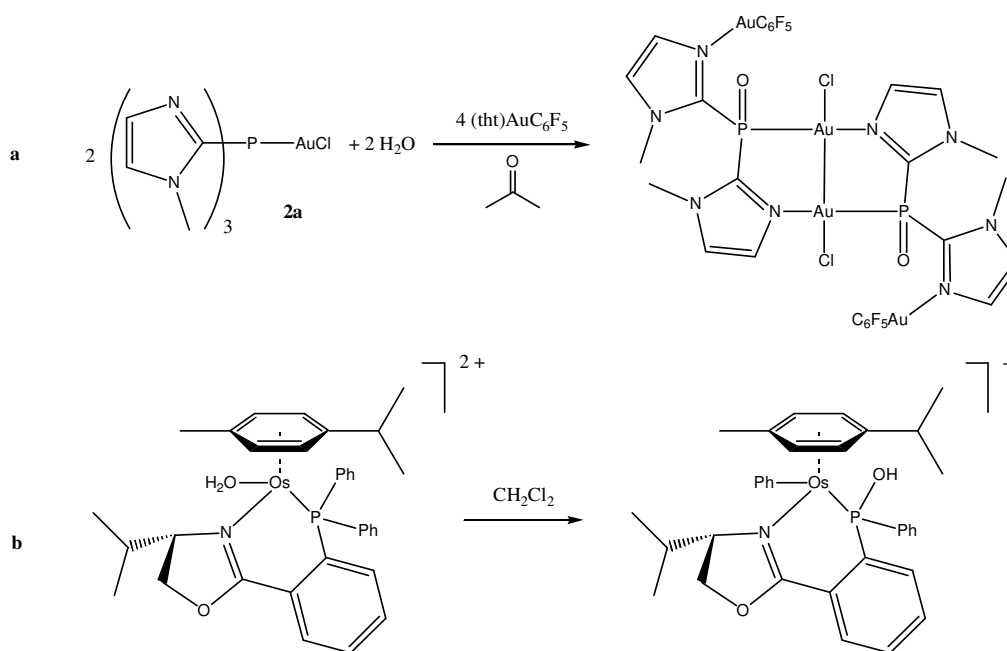
Scheme 3.3 (a) Binuclear $\text{Fe}^0/\text{M}^{\text{II}}$ ($\text{M} = \text{Hg}$, $\text{L} = \text{SCN}$ or $\text{M} = \text{Cd}$, $\text{L} = \text{I}$) complexes synthesised from tricarbonylbis[diphenyl(thiazol-2-yl)phosphane]iron and ML_2 ; (b) A *P:P'*-coordinated Rh^{I} complex ($\text{R} = \text{benzothiazol-2-yl}$) undergoes oxidation in chlorinated solvents to yield a binuclear cationic Rh^{II} complex and a Rh^{III} anion; two benzothiazole groups in the cation are not fully shown.

Tris(thiazol-2-yl)phosphane, in turn, has only found applications in two reports of Rh^{I} and Pt^{II} complexes.^{7a,12} The latter complex was the first example to demonstrate the tris(thiazolyl)phosphane ligand class. No crystal and molecular structures of complexes with this ligand have been determined.

- 10 (a) M. F. M. Al-Dulaymmi, P. B. Hitchcock and R. L. Richards, *J. Organomet. Chem.* **1988**, 338, C31–C34; (b) M. F. M. Al-Dulaymmi, A. Hills, P. B. Hitchcock, D. L. Hughes and R. L. Richards, *J. Chem. Soc., Dalton Trans.* **1992**, 241–248; (c) M. F. M. Al-Dulaymmi, D. L. Hughes and R. L. Richards, *J. Organomet. Chem.* **1992**, 424, 79–86.
 11 S.-M. Kuang, Z.-Z. Zhang, F. Xue and T. C. W. Mak, *J. Organomet. Chem.* **1999**, 575, 51–56.
 12 A. Neveling, G. R. Julius, S. Cronje, C. Esterhuysen and H. G. Raubenheimer, *Dalton Trans.* **2005**, 181–192.

Ligands **1a–c** were examined by natural abundance $^{15}\text{N}\{^1\text{H}\}$ NMR spectroscopy in addition to the spectra of the complexes **2a–c** already described¹³ since no reference data is available for this class of ligands.

Hydrolysis of a tris(imidazol-2-yl)phosphane ligand by adventitious water was previously reported by *Gabrielli*.¹³ In this instance, hydrolytic cleavage of one 1-methylimidazole group was accompanied by oxidation of the *P*-coordinated gold centre to form a binuclear Au^{II} complex as shown in Scheme 3.4 (a). Other examples of phosphane hydrolysis occurring in the coordinated form have only been observed before for Os^{II} complexes in an intramolecular manner where a simultaneous migration of one phenyl group has been proposed [Scheme 3.4 (b)].¹⁴



Scheme 3.4 (a) Hydrolysis of compound **2a** and subsequent oxidation by (tht)AuC₆F₅ leads to a tetranuclear Au^I/Au^{II} complex; (b) Intramolecular hydrolysis of a phosphane ligand by a coordinated water molecule in an Os^{II} complex.

13 W. F. Gabrielli, *Ph.D. thesis*, Stellenbosch University, 2006.

14 D. Carmona, C. Vega, N. García, F. J. Lahoz, S. Elipe, L. A. Oro, M. P. Lamata, F. Viguri and R. Borao, *Organometallics* 2006, 25, 1592–1606.

Sulfurisation products of heterocyclic azolyphosphanes have also attracted little attention. Only a Ukrainian group is pursuing the synthesis of heterocyclic phosphanes and their oxidation products.¹⁵ However, coordination complexes of tris(azolyl)phosphane sulfides are unprecedented.

3.1.1 Aims

Following initial results obtained by *Gabrielli*,¹³ the chemistry of tris(azol-2-yl)phosphanes, which have not received much attention as ligands, had to be further explored. The first objective was to determine the electronic influence of a selected tris(thiazol-2-yl)phosphane on the Au^I centre to which it is coordinated. Towards this end, substitution of the chloride ligand with soft sulfur nucleophiles and examination of the stability of the products was anticipated to yield qualitative insight into how much electron density this ligand is able to supply. This data then enables comparison of the novel tris(azol-2-yl)phosphane-gold(I) complexes with their well established triarylphosphane congeners.

Related to the aim mentioned above and with reference to a previous isolation of a Au^{II} complex where a tris(1-methylimidazol-2-yl)phosphane underwent hydrolysis of one 1-methylimidazole group,¹³ the hydrolytic stability of tris(thiazol-2-yl)phosphane-gold(I) complexes needed further investigation. The aim was to establish a new pathway for the synthesis of R₂P(O)AuL complexes by controlled hydrolysis of such complexes.

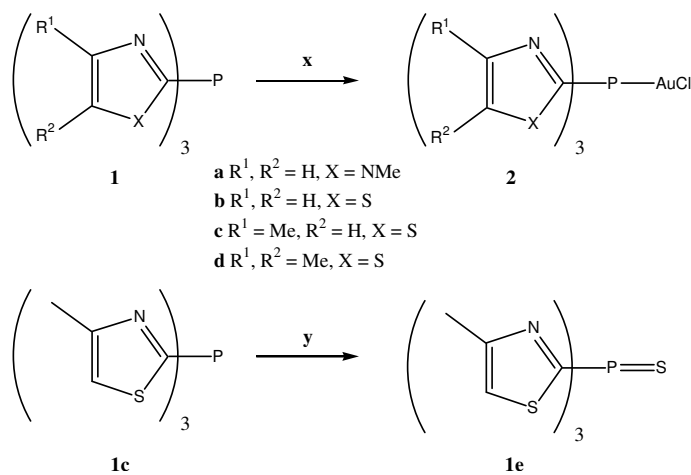
Focusing on early results indicating a tendency of chloro[tris(azol-2-yl)phosphane]-gold complexes to form polymorphs, it was also planned to investigate this behaviour in more detail in order to gain insight into the determining factors that affect the crystal packing in these complexes.

15 (a) A. A. Tolmachev, S. P. Ivonin, A. A. Anishenco and A. M. Pinchuk, *Heteroat. Chem.* **1998**, *9*, 461–470; (b) A. A. Tolmachev, A. A. Yurchenko, A. S. Merkulov, M. G. Semenova, E. V. Zarudnitskii, V. V. Ivanov and A. M. Pinchuk, *Heteroat. Chem.* **1999**, *10*, 585–597; (c) A. M. Pinchuk, S. A. Kovalyova, S. P. Ivonin, A. S. Merkulov, T. N. Kudrya, A. A. Chaikovskaya and A. A. Tolmachev, *Heteroat. Chem.* **2001**, *12*, 641–651; (d) A. A. Chaikovskaya, Yu. V. Dmitriv, S. P. Ivonin, A. M. Pinchuk and A. A. Tolmachev, *Heteroat. Chem.* **2005**, *16*, 599–604.

3.2 Results and discussion

3.2.1 Preparation of the ligands and complexes

The ligands **1b** and **1c** were prepared according to the literature protocol by reacting three mole equivalents of 2-lithioazole with PCl_3 at $-60\text{ }^\circ\text{C}$.^{7a} Compound **1d** required a lower reaction temperature of $-78\text{ }^\circ\text{C}$. At higher temperatures oxidative coupling of the lithium reagent by PCl_3 becomes a competing reaction and 4,4',5,5'-tetramethyl-2,2'-bithiazolyl can be isolated.¹⁶ Also at low temperatures the lithiated thiazole form is prevalent while at higher temperatures the ring-opened lithium (*Z*)-2-isocyanobut-2-en-3-thiolate is the main species present.¹⁷ Compound **1e** was prepared by sulfuration of **1c** by stirring a thf solution with excess sulfur for 8 days. Subsequently, synthesis of the gold complexes **2a–d** was effected by substitution of tht in $(\text{tht})\text{AuCl}$ in dichloromethane solution (Scheme 3.5).



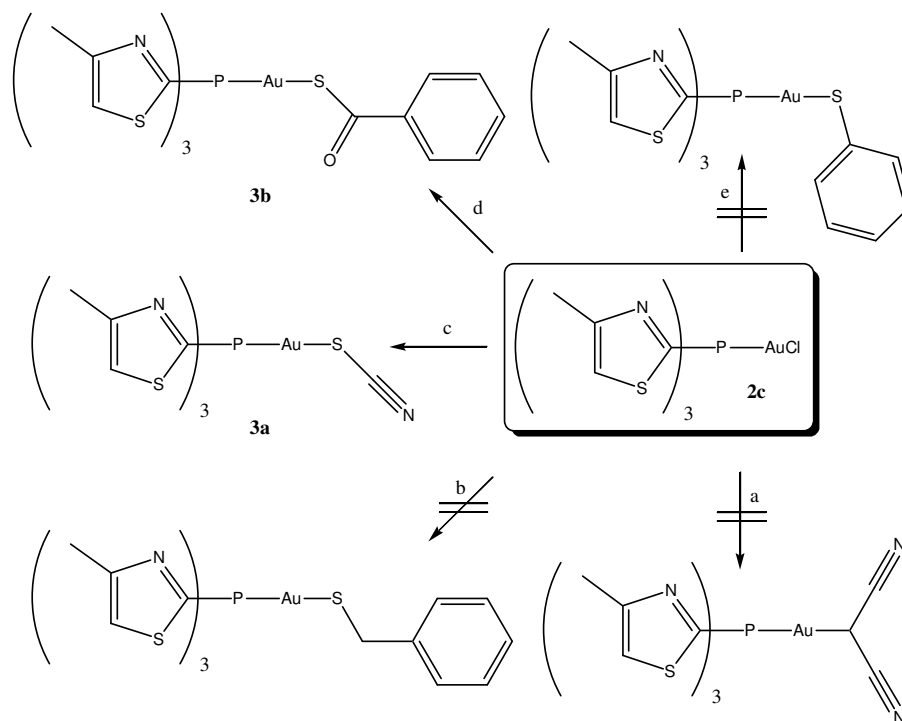
Scheme 3.5 Synthesis of complexes, **2a–d**, from ligands, **1a–d**, and synthesis of the sulfurisation product **1e** from **1c**. Reaction conditions: (x) $(\text{tht})\text{AuCl}$, CH_2Cl_2 , r.t.; (y) S_8 , thf, 8d, $45\text{ }^\circ\text{C}$.

The resulting compounds are generally soluble in polar aprotic solvents such as thf and dichloromethane but the tris(imidazolyl)phosphane complex **2a** is somewhat less soluble in these solvents although well soluble in methanol. The products are thermally stable and can be stored at room temperature for prolonged periods of time without noticeable decomposition. Attempts to substitute the chloride in the

16 Y. Uchida, Y. Takaya and S. Oae, *Heterocycles* **1990**, *30*, 347–351.

17 C. Hilf, F. Bosold, K. Harms, M. Marsch and G. Boche, *Chem. Ber./Recueil* **1997**, *130*, 1213–1221.

tris(4-methylthiazol-2-yl)phosphane complex **2c** by using aqueous NaNCS in a biphasic reaction¹⁸ or by treatment with LiSR [R = CH₂Ph, Ph or C(O)Ph] in anhydrous thf, produced only the two complexes **3a** and **3b** that contain electron-withdrawing residues attached to the sulfur (Scheme 3.6). With phenylmethanethiolate and benzenethiolate precipitation of (AuSR)_n and liberation of the free phosphane was observed. Decomposition with the former reagent was instantaneous while employing the latter thiolate a precipitate was only observed after several minutes. The electronic nature of chloro[tris(thiazol-2-yl)phosphane]gold complexes thus differs greatly from Ph₃PAuCl (Ph₃PAuSPh can be readily prepared)¹⁹ and is comparable to that of chloro{tris[3,5-bis(trifluoromethyl)phenyl]phosphane}gold. Employment of the latter complex and substitution of the chloride with benzenethiolate, gave the product in only 6% yield due to fast decomposition in solution.²⁰ Reaction of **2c** with NaCH(CN)₂ in anhydrous thf yielded a mixture; a reaction occurred according to



Scheme 3.6 Syntheses of the compounds **3a** and **3b** as well as attempted related syntheses:

(a) NaCH(CN)₂, thf (b) PhCH₂SLi, thf (c) NaNCS, K₂SO₄, CH₂Cl₂/H₂O

(d) PhC(O)SLi, thf (e) PhSLi, thf.

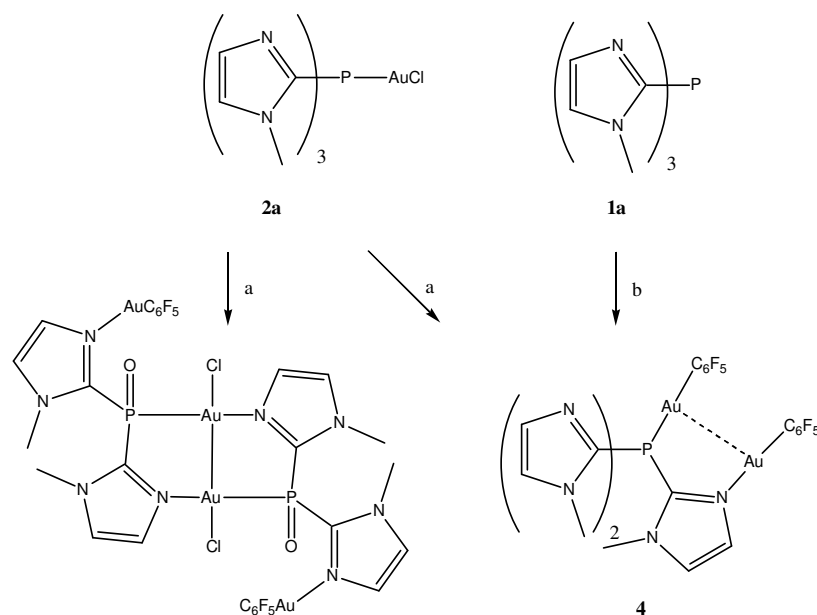
18 D. Schneider, S. Nogai, A. Schier and H. Schmidbaur, *Inorg. Chim. Acta* **2003**, 352, 179–187.

19 M. Nakamoto, W. Hiller, and H. Schmidbaur, *Chem. Ber.* **1993**, 126, 605–610.

20 K. Nunokawa, S. Onaka, T. Tatematsu, M. Ito and J. Sakai, *Inorg. Chim. Acta* **2001**, 322, 56–64.

the changes in the $^{31}\text{P}\{^1\text{H}\}$ NMR spectrum but, again, attempts to isolate a pure product failed. This could be the result of partial bis-auration of the activated methylene carbon that occurs relatively easily.²¹

Compounds **3a** and **3b** are somewhat less stable than **2a–d** at room temperature and slow decomposition with deposition of metallic gold occurs. Subsequently, the possibility of the imine nitrogen atoms acting as additional coordination centres towards gold(I) was explored. In reactions between the new phosphane complexes and $(\text{tht})\text{AuC}_6\text{F}_5$ a clear discrimination was found in that only **2a**, which contains a tris(imidazolyl)phosphane ligand, coordinated to another gold centre. Previous results indicated that addition of an excess of $(\text{tht})\text{AuC}_6\text{F}_5$ to **2a** afforded a mixture of products of which two – one a hydrolysis product containing a Au_2^{4+} core and the other, compound **4** (Scheme 3.7) – could be isolated.¹³



Scheme 3.7 Synthesis of compound **4** by the initial attempt to coordinate all imine nitrogen centres of **2a**¹³ via the conditions (a) and rational synthesis of **4** via conditions (b); reagents and conditions: (a) 3 $(\text{tht})\text{AuC}_6\text{F}_5$, propanone; (b) 2 $(\text{tht})\text{AuC}_6\text{F}_5$, thf.

Following these results, complex **4** was independently synthesised by reacting tris(imidazolyl)phosphane **1a** with two mole quantities of $(\text{tht})\text{AuC}_6\text{F}_5$ to obtain an analytically pure compound. In the solid form, both the propanone solvate crystals

and the solvent-free powder are stable at $-16\text{ }^{\circ}\text{C}$ but decompose slowly when dissolved and stored at room temperature. An investigation of the hydrolytic behaviour of the oxides and alkylphosphonium salts of tris(2-furyl)- and tris(thien-2-yl)-phosphane have shown that these compounds to effect the formation of the corresponding phosphonic acids $\text{R}_2\text{P}(\text{O})\text{OH}$.²²

As hydrolysis was not observed during the preparation of **3a**, the hydrolysis of tris(thiazol-2-yl)phosphanes was further investigated. For this purpose an NMR probing experiment (*vide infra*) was used with **2c** as the starting material.

As initial *P*-coordination of the ligands was always observed it is apparent that the coordination chemistry of Au^{I} to tris(imidazolyl)phosphanes is markedly different when compared to that of the isoelectronic Hg^{II} . A cationic tris[1-(1-methylethyl)-4-(1,1-dimethylethyl)imidazol-2-yl]phosphane complex of Hg^{II} has been shown to exhibit $\kappa^3\text{N},\text{N}',\text{N}''$ -coordination by the imidazole nitrogen atoms but no coordination to the phosphorus takes place.²³ Consequently, it appears that with tris(imidazolyl)phosphanes phosphorus is the superior donor atom for Au^{I} and Pt^{II} but not for other metals examined so far. On the other hand, in the few examples that have been investigated, tris(thiazol-2-yl)phosphanes have only been found to coordinate through the phosphorus atom and no involvement of the nitrogen atoms was detected.^{7a,12} It is anticipated that in future work coordination of tris(thiazol-2-yl)phosphanes to hard metal centres could lead to interesting coordination bonding patterns and compounds.

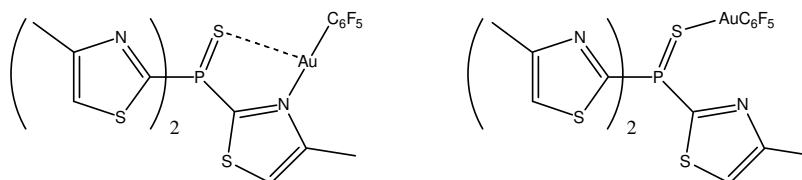
An attempt was made to utilise **1e** in preparing gold complexes, but this compound proved to be an inferior donor and tht was not substituted quantitatively from the Au^{I} starting materials. However, some reaction of **1e** with $(\text{tht})\text{AuC}_6\text{F}_5$ was corroborated by FAB MS analysis. Signals at m/z 721 and 722 were observed possibly corresponding to **2e** and its H^+ adduct, albeit no crystal structure could be obtained which would have been particularly interesting in this case as *S*- and *N*-coordination

22 (a) D. W. Allen, B. G. Hutley and M. T. J. Mellor, *J. Chem. Soc., Perkin Trans. 2* **1972**, 63–67;

(b) D. W. Allen, B. G. Hutley and M. T. J. Mellor,
J. Chem. Soc., Perkin Trans. 2 **1977**, 1705–1708.

23 C. Kimblin, V. J. Murphy, T. Hascall, B. M. Bridgewater, J. B. Bonanno and G. Parkin,
Inorg. Chem. **2000**, 39, 967–974.

(the latter, likely with a lateral *S*-contact, see Scheme 3.8) should be in mutual competition.



Scheme 3.8 Possible *N*- or *S*-coordinated structures for product **2e**.

3.2.2 Infrared spectroscopy

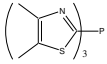
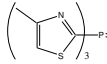
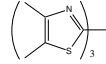
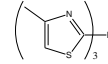
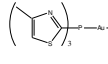
Most of the new compounds do not produce strong diagnostic peaks in their IR spectra, the notable exceptions are the gold thiocyanate **3a** and thiobenzoate **3b**. The $\nu(\text{C-N})$ in the thiocyanate group of **3a** is observed at 2122, 2114 (vs) and 2075 (w) cm^{-1} . The vibration frequencies are slightly lower than in Ph_3PAuSCN (2130 and 2075 cm^{-1})¹⁸ which shows aggregation by $\text{Au}\cdots\text{S}$ contacts in the solid state as opposed to the dimers of **3a** that are linked by aurophilic interactions (*vide infra*). Complex **3b** shows a very strong strong split $\nu(\text{C-O})$ signal at 1622 and 1616 cm^{-1} for the thiobenzoate. The carbonyl frequency for $\text{Ph}_3\text{PAuSC(O)Ph}$ ²⁴ was found at 1611 cm^{-1} which would be the result of the greater σ -donating ability of PPh_3 compared to **1c**. A $\nu(\text{P-S})$ vibration could not be identified upon analysis of the solid-state IR spectra of **1c** and **1e**.

3.2.3 Mass spectrometry

The ligands were examined by EI ionisation and the gold complexes by FAB ionisation, m/z values of fragments are reported in Table 3.1. Typical fragmentation patterns in EI include the loss of thiazole groups. In the FAB spectra the $[\text{M} + \text{H}]^+$ peak and the loss of the anionic ligand was always observed. It is not clear whether oxidation of **1e** and **1d** giving rise to $[\text{Fragment} + \text{O}]^+$ peaks occurred during sample preparation or during ionisation in the mass spectrometer.

²⁴ B. R. Vincent, D. J. Clarke, D. R. Smyth, D. de Vos and E. R. T. Tiekink, *Metal-Based Drugs* **2001**, 8, 79–84.

Table 3.1 Mass spectrometric data of **1d–3b**.^a

Compound					
	1d	1e	2d	3a	3b
Formula	C ₁₅ H ₁₈ N ₃ PS ₃	C ₁₂ H ₁₂ N ₃ PS ₄	C ₁₅ H ₁₈ AuClN ₃ PS ₃	C ₁₃ H ₁₂ AuN ₄ PS ₄	C ₁₉ H ₁₇ AuN ₅ OPS ₄
Exact mass	367.04	356.97	598.97	579.93	658.97
Method	EI	EI	FAB	FAB	FAB
[M + H] ⁺			600 (16)	581 (5)	660 (7)
M ⁺	367 (30)	357 (20)			
R ₃ PAu ⁺			564 (27)	522 (7)	522 (4)
[M – C ₄ H ₄ NS] ⁺	255 (100) ^b	259 (7)			
Others	383 (15) ^c 224 (25) ^d	341 (8) ^e 325 (7) ^f 243 (8) ^g 227 (100) ^h		675 (1) ⁱ	

^a Base peak in FAB spectra at *m/z* 154 [(3-nitrophenyl)methanol + H]⁺ ^b [M – C₅H₆NS]⁺
^c [M + O]⁺ ^d [C₅H₆NS]₂⁺ ^e [M – S + O]⁺ ^f [M – S]⁺ ^g [M – S – C₄H₄NS + O]⁺
^h [M – S – C₄H₄NS]⁺ ⁱ [M – SCN + C₇H₇NO₃]⁺

3.2.4 NMR spectroscopy

All ligands have been investigated by multinuclear NMR spectroscopy including natural-abundance ¹⁵N{¹H} NMR for the ligands **1a–c**. Data for ¹H, ¹³C{¹H} and ³¹P{¹H} NMR spectroscopy are summarised in Table 3.2, ¹⁵N{¹H} NMR data are reported in Table 3.3. The tris(thiazol-2-yl)phosphane ligands and complexes all furnish the expected ¹H, ¹³C and ³¹P NMR spectra. In the ¹H NMR spectrum the methyl resonances of tris(4,5-dimethylthiazol-2-yl)phosphane, **1d**, are isochronous, their different nature was only revealed in the ¹³C NMR spectrum where they are well separated. In the gold(I) chloride complex **2d** the two inequivalent methyl resonances in the ¹H NMR spectrum are just resolved.

In the tris(thiazol-2-yl)phosphane ligands coupling of the different hydrogens to each other and sometimes to the phosphorus was resolved. *J*_{HH} and *J*_{PH} are enhanced by coordination to the Au^I centre. Similar observations have been made with other heterocyclic phosphanes.^{6,25} Enhancement of the *J*_{PC} couplings of the ligand were also noted, especially for the *ipso*-carbon atom; this is in agreement with similar trends in

25 (a) T. N. Sorrell, W. E. Allen and P. S. White, *Inorg. Chem.* **1995**, *34*, 952–960;

(b) M. Enders, O. Fritz and H. Pritzkow, *Z. Anorg. Allg. Chem.* **2004**, *630*, 1501–1506.

Table 3.2 NMR data of compounds **1d–3b**.

Compound						
	1d	1e	2d	3a	3b^b	
Nucleus	Solvent	CD ₂ Cl ₂	CD ₂ Cl ₂	CD ₂ Cl ₂	CD ₂ Cl ₂	
¹ H (300 MHz)	Me	2.35 (s, 4/5-Me)	2.52 (s, 9 H) ^a	2.42 (s, 9 H, 4-Me) 2.40 (s, 9 H, 5-Me)	2.54 (s, 9 H)	2.56 (s, 9 H) ^c
	H-5 thiazole		7.40 (dq, ⁴ J _{PH} = 2.77, ⁴ J _{HH} = 0.88)	7.48 (s, 3 H)	7.43 (d, ⁴ J _{PH} 1.05, 3 H) ^c	
	<i>o</i> -Ph				8.05 (m, 2 H) ^c	
	<i>m</i> -Ph				7.37 (m, 2 H) ^c	
	<i>p</i> -Ph				7.48 (m, 1 H) ^c	
¹³ C{ ¹ H} (75.4 MHz)	Me	14.7 (s, 4-Me) 11.4 (s, 5-Me)	17.0 (s)	14.9 (s, 4-Me) 11.6 (s, 5-Me)	17.0 (m)	17.2 (s) ^d
	C-2 thiazole	152.7 (d, ¹ J _{PC} 12.9)	162.2 (d, ¹ J _{PC} 131.9)	151.7 (d, ¹ J _{PC} 99.0)	155.6 (d, ¹ J _{PC} 94.9)	156.5 (d, ¹ J _{PC} 85.5) ^d
	C-4 thiazole	161.3 (d, ³ J _{PC} 9.7)	158.5 (d, ³ J _{PC} = 24.5)	155.4 (d, ³ J _{PC} 21.0)	159.0 (d, ³ J _{PC} 22.3)	158.5 (d, ³ J _{PC} 20.5) ^d
	C-5 thiazole	133.7 (s)	122.9 (d, ³ J _{PC} = 3)	137.6 (s)	123.6 (s)	122.8 (s) ^d
	other signals			117.1 (m, SCN)		^c
	<i>i</i> -C ₆ H ₅					141.5 (s) ^d
	<i>o/m</i> -C ₆ H ₅					128.5 (s); 128.2 (s) ^d
	<i>p</i> -C ₆ H ₅					132.3 (s) ^d
³¹ P{ ¹ H} (121 MHz)	P	-33.2 (s)	12.7 (s)	-0.2 (s)	5.7 (s)	4.0 (br s) ^e

^a Coupling with H-4 of the thiazole ring was not resolved ^b Thiobenzoate carbonyl resonance in ¹³C{¹H} spectrum was not observed due to low intensity
^c At 400 MHz ^d At 101 MHz ^e At 162 MHz

simple arylphosphanes but the effect is more pronounced in the heterocyclic ligands. The *ipso*- $^1J_{PC}$ for **2d**, **3a** and **3b** are in the range of 85.5–99.0 Hz compared to 62.4 Hz in Ph_3PAuCl .²⁶ The ^{31}P NMR spectra of these complexes show a substantial downfield chemical shift difference ($\Delta\delta$ ca. 35)²⁷ compared to the free ligands which is generally observed on complexation of tertiary phosphanes to Au^{I} . Possible η^1 - κN -coordination of Au^{I} should give only a slight upfield shift as chelating $\kappa^3\text{N,N',N''}$ -scorpionate coordination results in strong shielding of the ^{31}P nucleus ($\Delta\delta$ 50) for a variety of metals.^{25b,28} Still, the phosphorus atom is the softer coordination site and thus preferred to the imine nitrogen lone pairs by the soft Au^{I} centre. However, tetrahedral coordination of Au^{I} has been observed with the hydridotris(pyrazol-1-yl)-borate ligand class²⁹ and a scorpionate-type coordination of tris(azol-2-yl)phosphanes to Au^{I} cannot *a priori* be ruled out.

While there is little difference in the ^{31}P chemical shift between the ligand pairs **1b** and **1c** as well as **2b** and **2c** indicating little influence of the additional methyl group, introducing a second methyl group effects significant shifts to higher field for **1d** and **2d**.

3.2.4.1 ^{15}N NMR spectroscopy.

The reluctance of the azole nitrogen atoms in tris(azol-2-yl)phosphanes to coordinate to Au^{I} which was observed for the tris(thiazol-2-yl)phosphanes¹³ and which is in contrast with previous results for azoles,³⁰ was a motivation to determine the ^{15}N chemical shifts of **2a–c** by natural abundance ^1H detected $^1\text{H},^{15}\text{N}$ gHMQC spectra to estimate their donor strength.¹³ However, spectra of the free ligands were not recorded and it seemed worthwhile to also determine their spectral parameters to estimate the change in donating ability ligands **1a–c** experience with *P*-coordination of Au^{I} . The ^{15}N NMR spectrum of 4-methylthiazole was determined for comparison by direct detection of the ^{15}N nucleus as a gHMQC experiment failed to yield a signal even at

26 G. H. Woehrle, L. O. Brown and J. E. Hutchison, *J. Am. Chem. Soc.* **2005**, *127*, 2172–2183.

27 Again, all $\Delta\delta$ are given in absolute values; the direction of change must be obtained from context.

28 G. A. Gray and T. A. Albright, *J. Am. Chem. Soc.* **1976**, *98*, 3857–3861.

29 (a) H. V. R. Dias and W. Jin, *Inorg. Chem.* **1996**, *35*, 3687–3694; (b) G. Gioia Lobbia, J. V. Hanna, M. Pellei, C. Pettinari, C. Santini, B. W. Skelton and A. H. White, *Dalton Trans.* **2004**, 951–958.

30 S. Cronje, H. G. Raubenheimer, H. S. C. Spies, C. Esterhuysen, H. Schmidbaur, A. Schier and G. J. Kruger, *Dalton Trans.* **2003**, 2859–2866.

Table 3.3 ^{15}N -NMR chemical shifts and coupling constants at 61 MHz for free heterocycles and compounds **1a–1c**. Compounds **2a–2c** are included for comparison.

Compound	Solvent	δ (ppm), J /Hz
1-Methylimidazole ³¹	(CD ₃) ₂ SO	-119.1 (N-3); -219.2 (N-1)
	CDCl ₃	-124.1 (N-3); -221.7 (N-1)
Thiazole	Neat ³²	-57.2
	CDCl ₃ ³¹	-62.0
4-Methylthiazole	80% v/v in CDCl ₃	-52.9 ^a
1a	(CD ₃) ₂ SO	-97.5, ² J_{PN} 50 ± 5 (N-3); -208.1 (N-1)
1b	CD ₂ Cl ₂	-41.3
1c	CD ₂ Cl ₂	-35.4
2a ¹³	(CD ₃) ₂ SO	-90.6, ² J_{PN} 89.3 (N-3); -206.3 (N-1)
2b ¹³	CD ₂ Cl ₂	-33.9, ² J_{PN} 27.8
2c ¹³	CD ₂ Cl ₂	-29.5, ² J_{PN} 89.4

^a Direct detection

low temperature probably due to proton exchange. The nitrogen nuclei become less shielded in the order free azole \gg tris(azol-2-yl)phosphane > chloro[tris(azol-2-yl)phosphane]gold. As expected, nitrogen atoms in the thiazole rings were less shielded than N-3 in the imidazole rings. As no *N*-coordination could be achieved with tris(thiazol-2-yl)phosphanes, it was estimated that tht coordinated to Au^I is only substituted by the azole nitrogen if the ^{15}N chemical shift occurs upfield from *ca.* δ -60.

Since the J_{PC} and J_{PH} coupling constants become larger upon coordination of the ligand, the question arose whether this trend would also be reflected for J_{PN} coupling constants. While complexes **2a–c** all show P–N coupling,¹³ this coupling was only clearly resolved in free ligand **1a**. It seems that the coupling is again enhanced by coordination of the phosphorus, yet further examples would be necessary to confirm the trend. The limited literature available on P–N coupling constants mainly deals with $^1J_{\text{PN}}$ values of phosphoramidite and phosphanous amide derivatives and their oxidation products with oxygen, sulfur or selenium. In these instances, either minor changes or a substantial decrease in the coupling constants is associated with the increase in coordination from tri- to tetracoordinate phosphorus.^{28,33}

31 B. C. Chen, W. von Philipsborn and K. Nagarajan, *Helv. Chim. Acta* **1983**, *66*, 1537–1555.32 J. P. Warren and J. D. Roberts, *J. Phys. Chem.* **1974**, *78*, 2507–2511.33 (a) B. Wrackmeyer, G. Kehr and H. Zhou, *Fresenius' J. Anal. Chem.* **1997**, *357*, 489–493; *J. Mol. Struct.* **1997**, *442*, 121–123; (c) J. Peralta-Cruz, V. I. Bakhmutov and A. Ariza-Castolo, *Magn. Reson. Chem.* **2001**, *39*, 187–193.

3.2.4.2 Hydrolysis of **2c** followed by $^{31}\text{P}\{^1\text{H}\}$ NMR spectroscopy.

A solution of **2c** in $(\text{CD}_3)_2\text{SO}$ was prepared and the ^{31}P NMR spectrum recorded to confirm the known resonance of the complex. Then 1.2 mole equivalents of aqueous NaOH were added. The solution became hot instantly and a colourless precipitate formed. Measurement of $^{31}\text{P}\{^1\text{H}\}$ NMR spectra every 6 min. (Figure 3.1) proved the practically instantaneous consumption of **2c** and the observation of two products and some free **1c**. Workup of the reaction mixture indicated the formation of new products (see Experimental section) but none of them could be isolated in pure form and characterised.

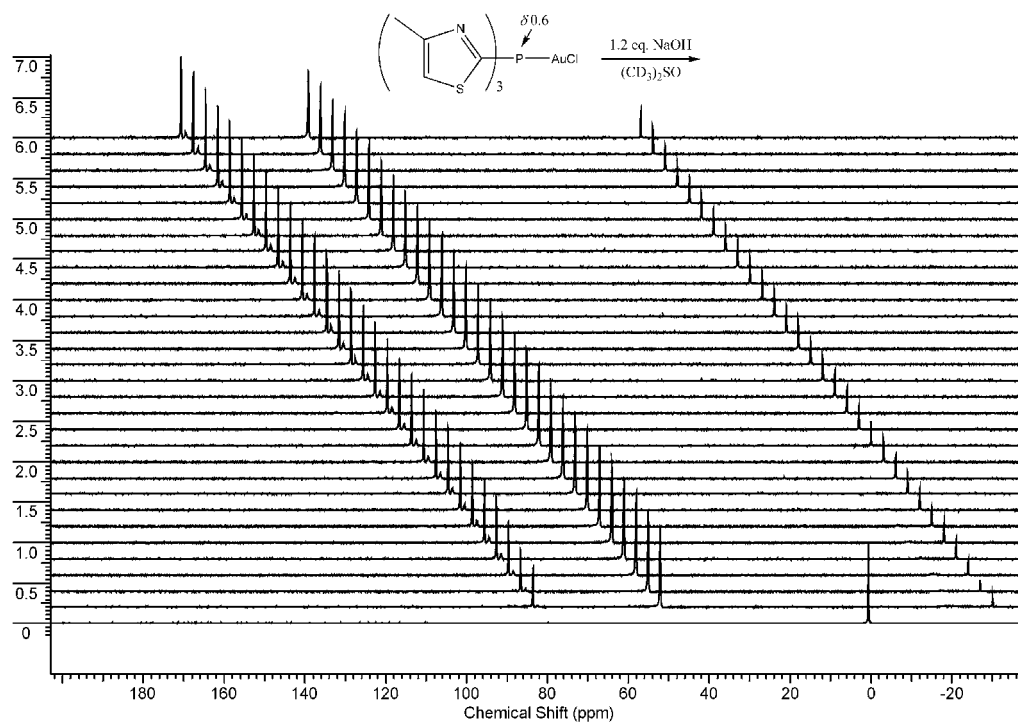


Figure 3.1 Offset of $^{31}\text{P}\{^1\text{H}\}$ NMR spectra for the hydrolysis reaction of **2c** with 1.2 mol eq. NaOH in $(\text{CD}_3)_2\text{SO}$. The resonance belonging to **2c** at $\delta 0.6$ in the spectrum recorded just before the addition of NaOH (lowest spectrum), disappears completely and gives rise to two major hydrolysis products at $\delta 49.1$ and 80.6 . The peak at $\delta -33.1$ corresponds to free phosphane from decomposition reactions (one fid was accumulated each 6 minutes over 3 hours). The y axis corresponds to arbitrary units of intensity, the chemical shift scale corresponds with the initial spectrum, others are offset by 3 ppm each for visibility.

3.3 Crystallography

Most polymorphs of **2b** and **2c** as well as **3a** exhibit aurophilic interactions while no Au...Au contacts are observed in the structures of **2a**, **2d** and **3b**·0.5C₆H₁₂. This may, amongst other factors, be due to the steric demand of the phosphane ligands or the thiobenzoate group, respectively. The molecular structure of **4**·0.83CDCl₃ exhibits short aurophilic interactions facilitated by a bridging ligand. Selected bond lengths and angles are summarised in Tables 3.4 and 3.5.

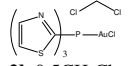
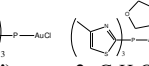
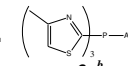
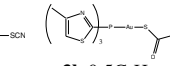
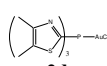
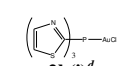
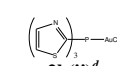
Polymorphism has already been described in the Chapter 2, Section 2.2.4 in one example. In the discussion below a whole array of polymorphs and solvates are encountered. While compounds **2b** and **2c** may be especially susceptible to polymorphism, the comparatively scarce literature data could be explained by the fact that crystallisations of complexes are not usually followed up further after the first crystal structure has been obtained. As is evident by the results presented below, it is often worth the effort to have a second look at a specific crystallisation; most often, additional polymorphs or solvates will give themselves away by their different crystal shapes.

At first, the polymorphs and solvates of compounds **2b** and **2c** are discussed together, followed by the crystal and molecular structures of the other compounds.

3.3.1 Polymorphs and solvates of **2b** and **2c**

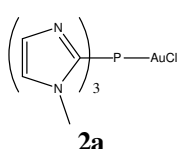
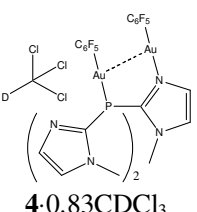
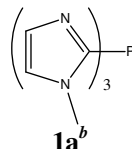
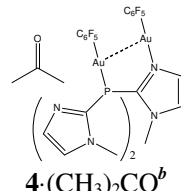
Different polymorphs are indicated by addition of **(i)**, **(ii)** *etc.* after the compound number while solvates are shown in the usual way. Of the compound chloro[tris(thiazol-2-yl)phosphane]gold, **2b**, two polymorphs **2b(i)** and **2b(ii)** as well as one structure of chloro[tris(4-methylthiazol-2-yl)phosphane]gold, **2c(i)**, were reported by *Gabrielli*.¹³ Both polymorphs **2b(i)** and **2b(ii)** comprise dimers of **2b** linked by aurophilic interactions with distances of 3.4563(2) and 3.3459(3) Å, respectively. In **2c(i)**, molecules related by a C₂ axis form dimers which associate by a short aurophilic contact of 3.0394(4) Å.

Table 3.4 Bond lengths/Å and angles/° of tris(thiazol-2-yl)phosphane compounds **1c–3b**·0.5C₆H₁₄.

Compound																
	1c	1e	2b(iii)	2b·0.5C₆H₁₄	2c(ii)	2c·C₄H₈O	3a^b	3b·0.5C₆H₁₄	1d	2d	2b(i)^d	2b(ii)^d	2c(i)^d			
Au–P			2.2096(8)	2.214(2)	2.212(2)	2.214(2)	2.211(1)	2.211(1)	2.237(5)	2.228(6)	2.250(2)	2.218(1)	2.2184(9)	2.217(1)	2.2260(9)	2.2169(8)
Au–Cl			2.2921(8)	2.285(2)	2.275(2)	2.283(1)	2.277(1)	2.271(1)	2.241(5)	2.253(6)	2.298(2) ^c	2.281(1)	2.2774(9)	2.276(1)	2.2900(9)	2.2901(8)
P–C(1,2,3)	1.820(2)	1.810(5)	1.805(3)	1.772(9)	1.799(8)	1.796(5)	1.795(5)	1.804(5)	1.801(6)	1.826(2)	1.813(5)	1.804(4)	1.801(4)	1.819(4)	1.810(3)	
	1.820(2)	1.811(3)	1.810(3)	1.805(9)	1.82(1)	1.803(5)	1.808(5)	1.807(5)	1.793(6)	1.831(2)	1.800(6)	1.800(4)	1.807(4)	1.812(4)	1.803(3)	
	1.820(2)	1.811(3)	1.810(3)	1.813(9)	1.811(9)	1.809(5)	1.809(5)	1.801(5)	1.818(6)	1.823(2)	1.786(6)	1.807(4)	1.808(4)	1.798(4)	1.797(3)	
Au···Au				3.2044(5)			3.007(2)	3.064(2)				3.4563(2)	3.3459(3)	3.0394(4)		
Cl–S			3.472(2)	3.334(3)		3.534(2)						3.373(2)	3.389(2)			
Other bonds	1.939(2)	3.2660(9)	(P=S)	(Au–Cl)				1.205(9) (C=O)								
								1.755(7) (CO–S)								
P–Au–Cl			176.36(3)	168.97(9)	174.00(9)	178.49(4)	178.92(6)	177.0(2) ^c	175.3(2) ^c	174.53(6) ^c	179.34(5)	174.06(4)	174.30(3)	167.83(3)		
						176.59(4)		175.3(2) ^c	172.4(2) ^c			178.03(4)				
Au–P–C			115.5(2)	121.7(3)	113.0(3)	112.4(2)	110.2(2)	114.0(2)	116.9(2)	115.1(2)	119.1(2)	115.4(2)	110.9(2)	108.4(1)		
(1,2,3)			111.5(2)	109.1(3)	112.0(3)	117.8(2)	116.6(2)	113.9(2)	113.0(2)	114.1(2)	113.6(2)	114.6(2)	119.3(2)	121.4(2)		
			116.9(2)	111.5(3)	118.1(3)	112.5(2)	114.1(2)	113.1(2)	112.6(2)	112.3(2)	110.5(2)	112.1(2)	113.3(2)	113.7(2)		
C–P–C	100.56(7)	105.1(2)	103.4(2)	103.5(4)	102.0(4)	104.1(2)	105.7(2)	105.9(2)	104.0(3)	99.45(7)	103.1(2)	103.9(2)	103.8(2)	103.5(2)	101.5(2)	
(1,2,3)	100.56(7)	105.3(2)	103.6(2)	103.0(4)	104.4(4)	102.6(2)	103.5(2)	104.3(2)	105.2(3)	99.83(7)	104.9(3)	104.0(2)	104.3(2)	106.5(2)	105.3(2)	
	100.56(7)	105.1(2)	104.5(2)	106.3(4)	105.8(4)	106.3(2)	106.0(2)	104.6(2)	103.9(3)	101.59(7)	106.4(2)	104.4(2)	105.5(2)	101.6(2)	104.7(2)	
Cl–Au···Au–Cl			180 ^a	161.21(9)			94.8(2) ^c	97.9(2) ^c			162.5(4)	180 ^a	74.65(4)			

^a Imposed by centre of inversion located between Au atoms ^b Only data associated with anisotropic atoms is given^c Au–S distance, Cl–Au–S angle and S–Au···Au–S torsion angle ^d Data taken from ref.¹³ for comparison.

Table 3.5 Bond lengths/Å and angles/° of compounds **2a** and **4**·0.83CDCl₃.

Compound				
	2a	4·0.83CDCl₃	1a^b	4·(CH₃)₂CO^b
Au–P	2.218(2)	2.265(2) 2.275(2) 2.266(2)		2.264(2)
Au–Cl	2.276(2)			
Au–N		2.060(5) 2.062(5) 2.060(5)		2.076(7)
(P)Au–C		2.047(6) 2.046(6) 2.045(6)		2.028(8)
(N)Au–C		2.004(6) 2.003(6) 2.008(6)		2.018(8)
Au···Au		3.0240(4) 3.0170(4) 2.9903(4)		2.9619(5)
P–C	1.800(5)	1.808(6) 1.793(6) 1.804(6)	1.829(2)	1.808(8)
(1, 2, 3)	1.806(6)	1.797(6) 1.794(6) 1.797(6)	1.817(2)	1.78(1)
	1.798(6)	1.805(6) 1.799(6) 1.791(6)	1.820(2)	1.811(8)
Other bonds		3.181(9) (C1–··–N13) ^a		
P–Au–C	178.59(5)	172.2(2) 174.5(2) 170.1(2)		175.9(2)
N–Au–C		178.5(2) 173.0(2) 179.0(2)		178.4(3)
Au–P–C	110.5(2)	112.0(2) 110.8(2) 109.9(2)		110.3(3)
(1, 2, 3)	116.3(2)	119.0(2) 115.5(2) 112.4(2)		120.9(3)
	115.1(2)	113.5(2) 117.8(2) 123.7(2)		113.9(3)
C–P–C	103.9(2)	103.7(3) 106.4(3) 107.0(3)	104.45(7)	102.3(4)
(1, 2, 3)	104.7(3)	101.1(3) 101.6(3) 102.5(3)	99.85(7)	102.4(4)
	105.2(3)	106.1(3) 103.4(3) 99.8(3)	98.66(7)	105.4(4)
P–Au···Au–N		23.5(2) 27.1(2) 20.1(2)		20.9(2)

^a Hydrogen-bonded CDCl₃ (C1–D1···N13) ^b Data from ref.¹³ for comparison

An additional polymorph and a hemi-dichloromethane solvate were obtained from complex **2b**. Furthermore, another polymorph of **2c** and a thf solvate were found in crystallisations of compound **2c**, but only the known **2c(i)** exhibits a rather short aurophilic interaction.¹³ The other crystal structures exclusively contain discrete molecules. Polymorphism in gold compounds focusing on luminescence has been studied previously and was summarised in a review.³⁴ In an attempt to utilise the comparatively weak aurophilic interactions¹³ of **2b** [exhibited in the polymorphs **2b(i)** and **2b(ii)**] with the strong interaction¹³ but greater steric hindrance of **2c** [as in **2c(i)**] to crystallise a dimer consisting of both molecules,³⁵ 15 mg of each compound was

³⁴ A. L. Balch, *Gold Bull.* **2004**, *37*, 45–50.

³⁵ Obtaining co-crystals of different Au^I complexes and studying their structural properties was an early aim of this thesis. However, no such co-crystallite was ever obtained despite a few serendipitous discoveries by other students within the research group. For examples of co-crystallites, see ref.¹³ and T. K. Hagos, *M.Sc. thesis*, Stellenbosch University, **2006**.

dissolved in the minimum amount of CH_2Cl_2 , the solution was layered with pentane and kept at $-16\text{ }^\circ\text{C}$. Needles of a new habit were indeed observed in the Schlenk tube. The compound, however, was $\mathbf{2b}\cdot 0.5\text{CH}_2\text{Cl}_2$ shown in Figure 3.2. It consists of two crystallographically independent molecules associated by an aurophilic interaction [$\text{Au}\cdots\text{Au}$ 3.2044(5) Å] and a close contact of 3.334(3) Å between Cl2 and S61' ($' = \frac{1}{2} + x, \frac{1}{2} - y, \frac{1}{2} + z$). While in every complex of ligands **1b** and **1c** at least one sulfur atom of the thiazole rings points towards the Au^{I} centre with typical distances of 3.57–3.89 Å in what could amount to a weak $\text{Au}\cdots\text{S}$ interaction, $\mathbf{2b}\cdot 0.5\text{CH}_2\text{Cl}_2$ is the only structure where nitrogen atoms (N21 and N61) are positioned in such a manner. The P–Au–Cl angles are appreciably more distorted by the aurophilic interaction [$168.97(9)^\circ$ and $174.00(9)^\circ$] than in the other structures.

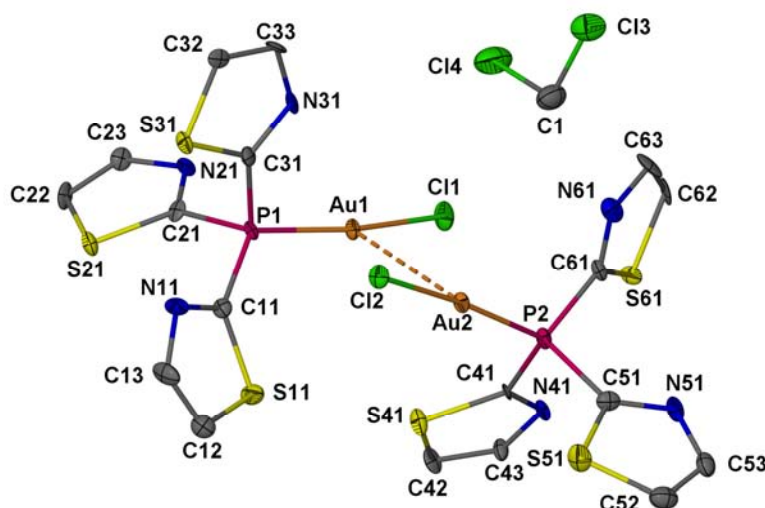


Figure 3.2 Molecular structure of $\mathbf{2b}\cdot 0.5\text{CH}_2\text{Cl}_2$.

Intriguingly, blocks of the already known triclinic **2b(ii)** were found alongside the needles of $\mathbf{2b}\cdot 0.5\text{CH}_2\text{Cl}_2$ in the same crystallisation vessel. Later, a crystal of the third polymorph, **2b(iii)**, in the space group $P\bar{1}$ was found, again originating from the same vessel as $\mathbf{2b}\cdot 0.5\text{CH}_2\text{Cl}_2$. In the crystals of **2b(iii)** (Figure 3.3) no sign of $\text{Au}\cdots\text{Au}$ interactions like in all other structures of **2b**¹³ are observed. The structure is instead stabilised by relatively short and rather unusual intermolecular $\text{Au}\cdots\text{Cl}$ contacts of 3.2660(9) Å between molecules ordered into dimers (symmetry operator $1 - x, 2 - y, -z$). This mode of stabilisation is observed for a few other gold(I) complexes of

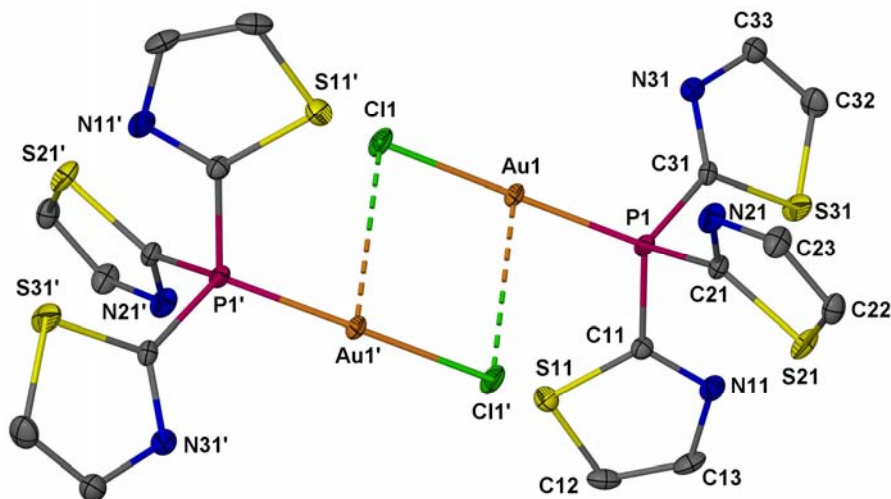


Figure 3.3 Molecular structure of **2b(iii)**; primed atoms are related by a centre of inversion located between the Au atoms.

tertiary phosphanes with heterocyclic substituents such as chloro[tris(2-furyl)phosphane]gold,³⁶ chloro[tris(thien-2-yl)arsane]gold³⁷ and fluorinated derivatives of Ph_3PAuCl .³⁸ In the present structure **2b(iii)**, furthermore a weak contact between C11 and S21' ($' = 1 + x, 1 + y, z$) of 3.472(1) Å is observed. Compound **2b** is believed to be the first example of a complex exhibiting both kinds of aggregation in different polymorphs, with **2b(iii)** showing one of the closest intermolecular Au \cdots Cl contact distances known for a neutral Au^I compound.

The rather similar structures of **2b(ii)**¹³ and **2b(iii)** (they are generally related by moving one molecule of the dimer along the P–Au–Cl vector; minor differences in the conformation of the thiazole rings are also present) allow a direct comparison of the effects of the different associations. Especially the Au–P bond in **2b(iii)** [2.2096(8) Å] is significantly shortened by the intermolecular Au \cdots Cl interaction [compared to the distance of 2.2260(9) Å in **2b(ii)**] while the Au–Cl bonds are of comparable length [2.2900(9) and 2.2921(8) Å for **2b(ii)** and **2b(iii)**, respectively]. While association *via* halogen bridges is common for Cu^I and Ag^I, *ab initio* calculations suggest that Au^I

36 S. Y. Ho and E. R. T. Tiekink, *Z. Kristallogr. – New Cryst. Struct.* **2002**, 217, 591–592.

37 U. Monkowius, S. Nogai and H. Schmidbaur, *Z. Naturforsch., B: Chem. Sci.* **2003**, 58, 751–758.

38 (a) H. W. Chen and E. R. T. Tiekink, *Acta Crystallogr., Sect. E: Struct. Rep. Online* **2003**, 59, m50–m51; (b) P. Tasker, D. Coventry, S. Parsons and D. Messenger, *Private communication to the Cambridge Crystallographic Data Centre*, No. 276800, **2005**.

prefers aurophilic interaction to other means of aggregation.³⁹ However, replacement of the model ligand PH₃ by tris-heterocyclic phosphanes might influence this affinity towards the chloride-bridged type.

Several compounds are known where solvate formation is accompanied by changes in the type or strength of aurophilic interactions.⁴⁰ Yet, only one example is known of a compound that crystallises unsolvated with and solvated without aurophilic interactions.⁴¹ These authors crystallised the [Au{C(NHMe)(OMe)}₂]⁺ cation with the anion of 2,3-dichloro-5-cyano-6-hydroxy-*p*-benzoquinone. The molecular structure of the solvent-free salt consists of dimers of the cation held together by an aurophilic interaction of 3.1955(3) Å, while crystals of the trichloromethane solvate consist of single cations sandwiched between two anions. Hydrogen bonds are present in both structures.⁴²

Two crystal structures that contain compound **2c** were determined in addition to the already known **2c(i)**, which was obtained by crystallisation of the compound from dichloromethane/Et₂O.¹³ The second crystal structure, **2c**·C₄H₈O, shown in Figure 3.4, was obtained by crystallisation of **2c** from thf/pentane. It crystallises in the chiral orthorhombic space group *P*2₁2₁2₁ and consists of discrete molecules arranged around channels running parallel to the *b* axis that incorporate the thf guests. The P–Au–Cl angle approaches linearity [178.92(6)°] as is expected for an undisturbed coordination sphere around a Au^I centre. Cooperative interaction of **2c** with the thf molecule is therefore sufficiently strong to override the attraction between the Au centres. A contact between Cl1 and S21' [*r*' = *x*, *y* – 1, *z*; 3.534(2) Å], roughly equal to the sum of the van der Waals radii, is also observed. It is longer and weaker than similar associations in the crystal structures **2b(i)** and **2b(ii)**.¹³ Without the influence of the aurophilic interaction, the Au–P [2.211(1) Å] and particularly the Au–Cl [2.271(1) Å]

39 (a) P. Schwerdtfeger, H. L. Hermann and H. Schmidbaur, *Inorg. Chem.* **2003**, *42*, 1334–1342;

(b) E. O'Grady and N. Kaltsoyannis, *Phys. Chem. Chem. Phys.* **2004**, *6*, 680–687.

40 (a) Z. Assefa, B. G. McBurnett, R. J. Staples, J. P. Fackler, Jr., B. Assmann, K. Angermaier and H. Schmidbaur, *Inorg. Chem.* **1995**, *34*, 75–83;

(b) Z. Assefa, M. A. Omary, B. G. McBurnett, A. A. Mohamed, H. H. Patterson, R. J. Staples and J. P. Fackler, Jr., *Inorg. Chem.* **2002**, *41*, 6274–6280.

41 F. Jiang, M. M. Olmstead and A. L. Balch, *J. Chem. Soc., Dalton Trans.* **2000**, 4098–4103.

42 A. Codina, E. J. Fernández, P. G. Jones, A. Laguna, J. M. López-de-Luzuriaga, M. Monge, M. E. Olmos, J. Pérez and M. A. Rodríguez, *J. Am. Chem. Soc.* **2002**, *124*, 6781–6786.

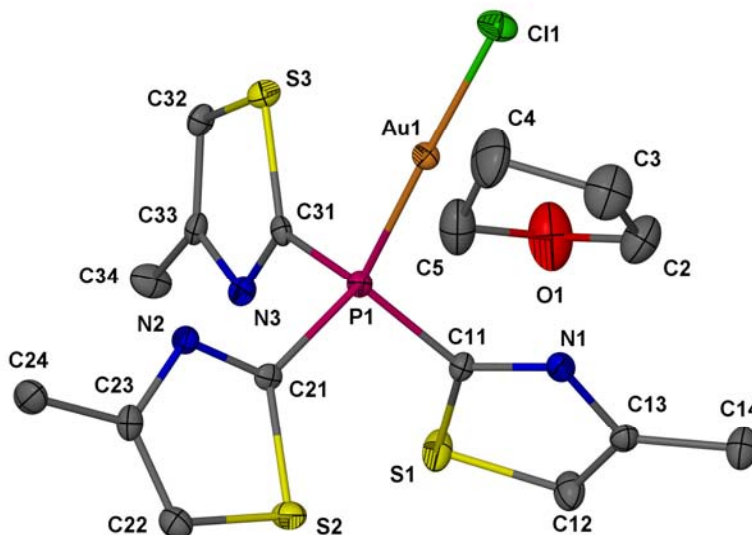


Figure 3.4 Molecular structure of **2c**·C₄H₈O.

bond in **2c**·C₄H₈O are significantly strengthened as is reflected in shorter bond lengths compared to those found in **2c(i)** [2.2169(8) and 2.2901(8) Å,¹³ respectively].

A second polymorph, **2c(ii)**, was found alongside crystals of **2c(i)** in another crystallisation from dichloromethane/hexane and was later also isolated amongst **2c**·C₄H₈O in a repeated crystallisation from thf/pentane. Monoclinic **2c(ii)** crystallises in the space group *P2₁/c* with two crystallographically independent molecules that exhibit similar arrangement of the thiazole moieties (Figure 3.5). In the crystal, the molecules form crystallographically independent alternating layers parallel to the *ac* plane as is shown in Figure 3.6. It came as somewhat of a surprise that the molecular structure of this polymorph did not exhibit any aurophilic interactions or sub-van der Waals contacts except the usual thiazole ring aligned with the Au–Cl axis affording a distance of 3.430 Å between Au2 and S41. There are only two other examples of compounds crystallising in polymorphs with and without aurophilic interactions, chloro[tris(4-methylphenyl)phosphane]gold⁴³ and [(AuCl)₂(μ-dppm)] [dppm = bis-(diphenylphosphanyl)methane].⁴⁴ The lengths of the Au–Cl and Au–P bonds in **2c(ii)**

43 (a) P. D. Cookson and E. R. T. Tiekink, *Acta Crystallogr., Sect. C: Cryst. Struct. Commun.* **1994**, *50*, 1896–1898; (b) R. C. Bott, P. C. Healy and G. Smith, *Aust. J. Chem.* **2004**, *57*, 213–218.

44 (a) H. Schmidbaur, A. Wohlleben, F. Wagner, O. Orama, and G. Huttner, *Chem. Ber.* **1977**, *110*, 1748–1754;

(b) P. C. Healy, *Acta Crystallogr., Sect. E: Struct. Rep. Online* **2003**, *59*, m1112–m1114.

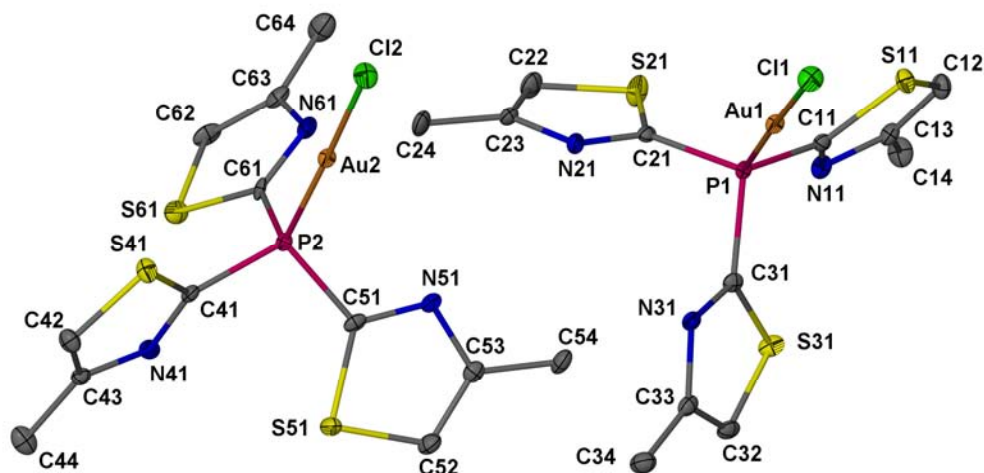


Figure 3.5 Molecular structure of **2c(ii)**

[on average 2.213(2) and 2.280(3) Å, respectively] are intermediate between those in **2c(i)**¹³ and the thf solvate [the Au–P bonds in **2c(ii)** and **2c**·C₄H₈O are similar].

Crystallisation from dichloromethane is believed to yield polymorph **2c(i)** as the major product, but crystals of **2c(ii)** may in fact be quite similar in energy. The structures of **2b(ii)** and **2b(iii)** as well as **2c(i)** and **2c(ii)** constitute concomitant polymorphs⁴⁵ by virtue of their simultaneous isolation from the same crystallisation

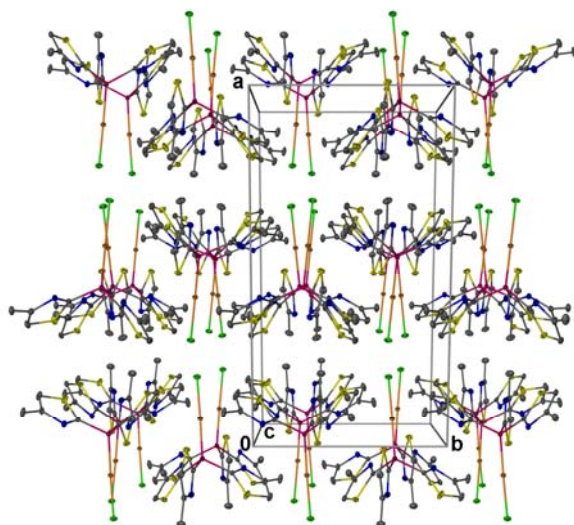


Figure 3.6 Packing diagram of **2c(ii)** viewed along the *c* axis. Each layer (parallel to the *bc* plane and stacked in an AB pattern) is exclusively formed by one of the two unique molecules.

45 J. Bernstein, R. J. Davey and J.-O. Henck, *Angew. Chem., Int. Ed. Engl.* **1999**, *38*, 3440–3461 (*Angew. Chem.* **1999**, *111*, 3646–3669).

vessels. This raises the question to what extent concentration, temperature and solvent choice influence the crystallisation process, and hence variations in intermolecular interaction of these compounds.

3.3.2 Molecular structures of the ligands *1c*, *1d* and *1e*

Compound **1c** shown in Figure 3.7 is the only tris(azol-2-yl)phosphane amongst **1a**,¹³ **1c** and **1d** that indeed crystallises exhibiting a threefold axis of rotation that passes through the phosphorus atom enabled by the polar trigonal space group $R3c$. Intriguingly, compounds **1a** and **1e** also crystallise in polar space groups. A similar symmetry among heterocyclic phosphanes has only been observed for tris(benzothiazol-2-yl)phosphane,⁴⁶ but here the planes of the benzothiazole groups are almost normal to the phosphorus' lone pair, thus rather resembling a cone surface than the propeller conformation of **1c**. The thiazolyl nitrogen atoms in **1c** are roughly pointing towards the phosphorus, an arrangement that is possibly dictated by lattice constraints incurred by the methyl groups.

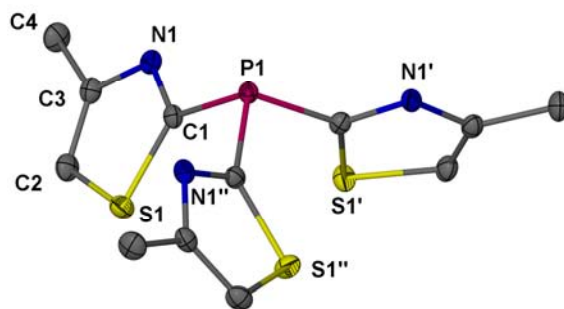


Figure 3.7 Molecular structure of **1c**

Compound **1e** crystallises in the polar orthorhombic space group $Cmc2_1$ where two thiazolyl substituents are asymmetric and the third is generated by the proper mirror plane defined by P1, S1 and C11. The molecular structure shown in Figure 3.8 exhibits thiazole rings parallel to the P1–S1 vector with the thiazolyl sulfur atoms engaging in S \cdots S contacts of 3.450(2) (S1 \cdots S11) and 3.448(2) Å (S1 \cdots S21 and S1 \cdots S21'; ' = -x, y, z) and thus resembles a conformation found in complexes of the scorpionate type. The P–S bond distance [1.939(2) Å] is shorter than in

46 T. Stey, M. Pfeiffer, J. Henn, S. K. Pandey and D. Stalke, *Chem. Eur. J.* **2007**, *13*, 3636–3642.

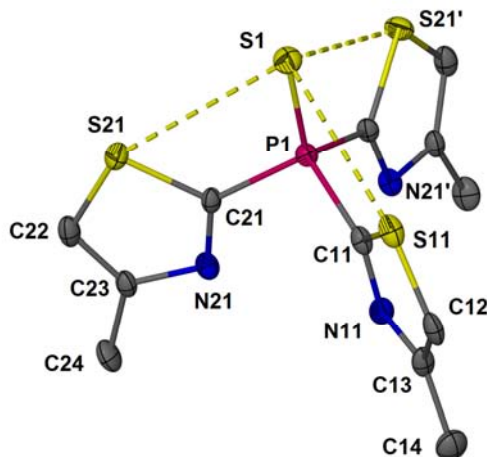


Figure 3.8 Molecular structure of **1e**. Primed atoms (symmetry code $-x, y, z$) are generated by a mirror plane passing through S1, P1 and C11.

triphenylphosphane sulfide (1.9554(7) Å in the monoclinic and 1.9545(9) Å in the triclinic polymorph).⁴⁷ The P–C bond distances in **1e** are comparable to those found in **1c** [on average 1.811(5) and 1.820(2) Å for **1e** and **1c**, respectively], the P–C bond shortening caused by Au^I coordination in complexes of **1c** is thus not reflected in **1e** – which can be rationalised as **1c** coordinating to a sulfur atom.

Ligand **1d** crystallises in the centrosymmetric monoclinic space group $P2_1/n$ and is therefore an exception amongst the other ligands **1a**,¹³ **1c** and **1e** which crystallise in polar space groups. All atoms in the molecule of **1d** shown in Figure 3.9 are crystallographically unique, all thiazole groups are unambiguously located in their respective positions and no indication of positional disorder by flipping of a thiazole ring by 180° is observed.

Compared to the average values in the triclinic^{47b} and monoclinic⁴⁸ polymorphs of triphenylphosphane, the P–C bonds and C–P–C angles in **1c** and **1d** exhibit comparable values. Even though the phenyl group is more symmetric than any thiazole group, PPh₃ never aligns with threefold rotational symmetry in any polymorph; the triclinic structure even comprises four independent molecules.

47 (a) C. Foces-Foces and A. L. Llamas-Saiz, *Acta Crystallogr., Sect. C: Cryst. Struct. Commun.* **1998**, *54*, IUC9800013 [sic]; (b) B. Ziemer, A. Rabis and H.-U. Steinberger, *Acta Crystallogr., Sect. C: Cryst. Struct. Commun.* **2000**, *56*, e58–e59.

48 B. J. Dunne and A. G. Orpen, *Acta Crystallogr., Sect. C: Cryst. Struct. Commun.* **1991**, *47*, 345–347.

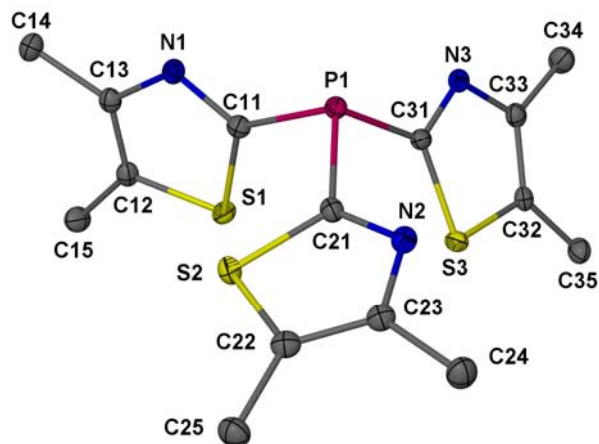


Figure 3.9 Molecular structure of **1d**.

3.3.3 Molecular structures of **2a**, **2d**, **3a**, **3b**·0.5C₆H₁₄ and 4·0.83CDCl₃

The molecular structure of **2a** displayed in Figure 3.10 consists of discrete molecules. Tris(2-methylphenyl)phosphane has a similar steric requirement compared to ligand **1a** and also inhibits Au[⋯]Au contacts even in bridged binuclear complexes.⁴⁹ Polyaurated onium species are the only structures where such contacts are present.⁵⁰

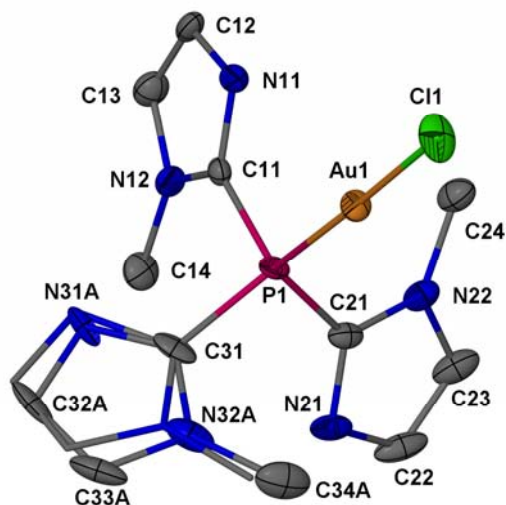


Figure 3.10 Molecular structure of **2a**. The other orientation of the imidazole ring is only shown in a stick representation.

49 M. Preisenberger, A. Schier and H. Schmidbaur, *Z. Naturforsch., B: Chem. Sci.* **1998**, *53*, 781–787.

50 (a) A. Kolb, P. Bissinger and H. Schmidbaur, *Z. Anorg. Allg. Chem.* **1993**, *619*, 1580–1588;

(b) Y. Yang, V. Ramamoorthy and P. R. Sharp, *Inorg. Chem.* **1993**, *32*, 1946–1950.

The individual orientations of the imidazole rings conform to the structures of **1a** and **4**·(CH₃)₂CO¹³ and is also observed in all unique molecules of **4**·0.83CDCl₃. One of the imidazole rings in **2a** is disordered and occupies two positions within the plane of the ring.

The molecular structure of **2d** shown in Figure 3.11 exhibits a thiazole ring that occupies two different positions that are flipped by 180°. The lack of discrimination between the *SN*- and *NS*-orientations can most likely be attributed to the two methyl substituents in the thiazole ring, given that no such disorder was found in any structures of ligand **1b** where the thiazole rings are unsubstituted. In the unsubstituted rings, the lone pair of the thiazolyl nitrogen atoms may thus have some directing influence on the conformation of the ring as disorder was again observed in complexes of the sterically similar tris(thien-2-yl)phosphane³⁷ which naturally lacks the imine nitrogen atoms. Such an influence of the nitrogen lone pair may thus be overridden by the methyl groups in the structure of **2d**. The absolute structure of **2d** in the polar space group *Pna*2₁ could not be established due to this disorder yielding an ambiguous Flack *x* parameter. The steric bulk of the ligand is just enough to render aurophilic interactions unfavourable and complex **2d** crystallises as discrete molecules. The Au–Cl [2.281(1) Å] and Au–P [2.218(1) Å] bond lengths are roughly comparable to the values in **2c(ii)** but longer than in **2c**·C₄H₈O.

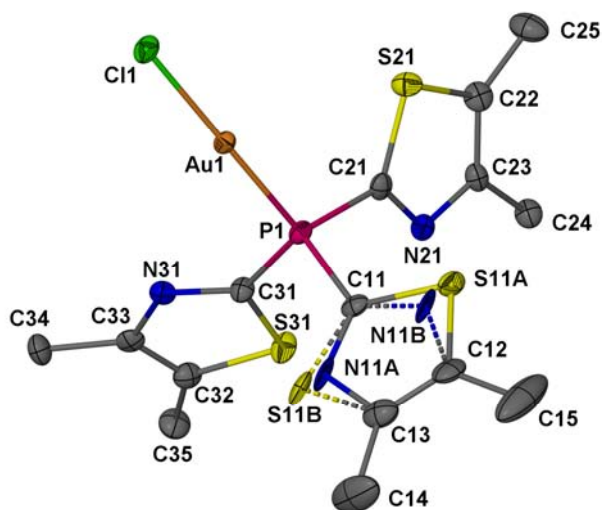


Figure 3.11 Molecular structure of **2d**.

Aurophilic interactions are however present in the molecular structure of **3a** which is unusual as it contains four independent molecules in the asymmetric unit (shown in Figure 3.12), arranged in pairs bonded by aurophilic interactions. The dimers themselves are ordered around *pseudo*- C_2 axes roughly similar to the structure of **2c(i)**¹³ and a *pseudo*-centre of inversion is located between these pairs; this symmetry, however, is not reflected in the crystal space group as is apparent from among other factors, the systematic absences in the diffraction pattern and the well defined Au \cdots Au distances of 3.007(2) Å (Au1 \cdots Au2) and 3.064(2) Å (Au3 \cdots Au4) that are significantly different and would necessarily have to be equal if the dimers were related by crystallographic symmetry. The quality of the dataset collected is hampered by the very small third dimension of the crystal, the low data to parameter ratio thus does not allow anisotropic treatment of all atoms. The absolute structure could also not be determined due to an ambiguous Flack x parameter. An array of other solvents used for crystallisation of **3a** all furnished the same thin plates and no polymorph or solvate was found. The molecular structure determination underlined the general inclination of ligand **1c** to form compounds that exhibit aurophilic interactions. In **3a** the smallest Au \cdots Au distances of all existing complexes of thiazol-2-ylphosphanes were found.

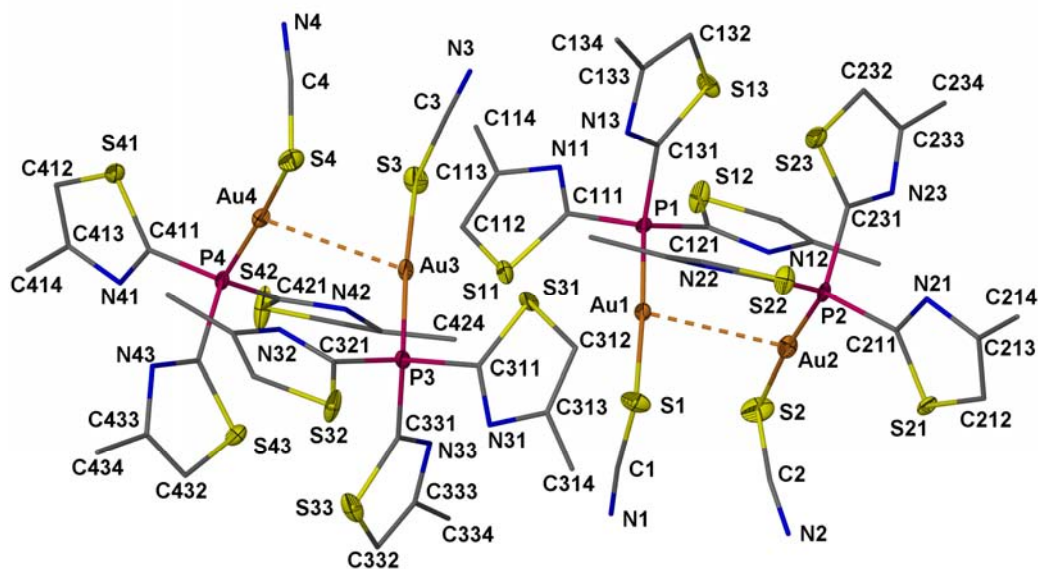


Figure 3.12 Molecular structure of **3a**. Only anisotropically refined atoms are shown as ellipsoids, atoms refined isotropically are represented in stick form.

The disorder observed for one imidazole ring in the structure of **2a** may also be present in the structure of **3b**·0.5C₆H₁₄ (Figure 3.13) where the direction of the thermal displacement ellipsoids suggest a minute mobility of the C11 thiazole ring within its plane, but this “wagging” could not be resolved. Complex **3b**·0.5C₆H₁₄ crystallises in discrete molecules without any Au···Au interactions which may be a result of the more bulky thiobenzoate group compared to the chloride or thiocyanate ligands of other structures of ligand **1c**. The porous structure consists of alternating

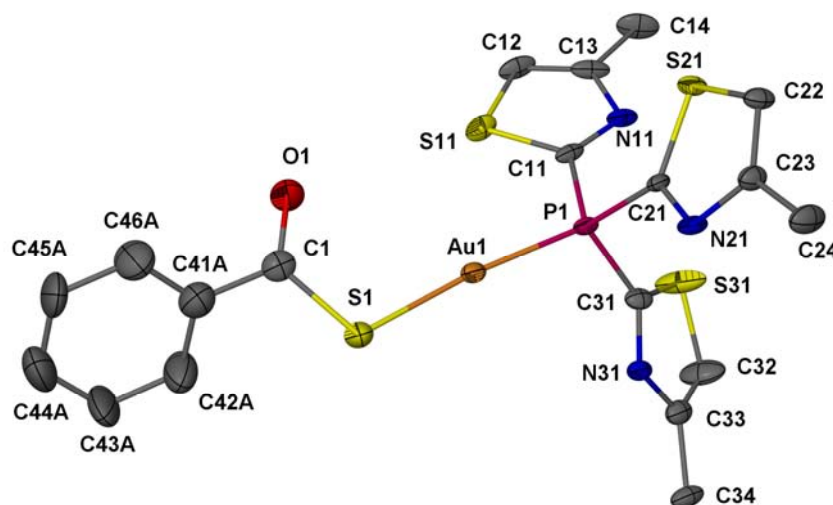


Figure 3.13 Molecular structure of **3b**·0.5C₆H₁₄; disordered hexane solvent and a second orientation of the benzene ring are not shown for clarity.

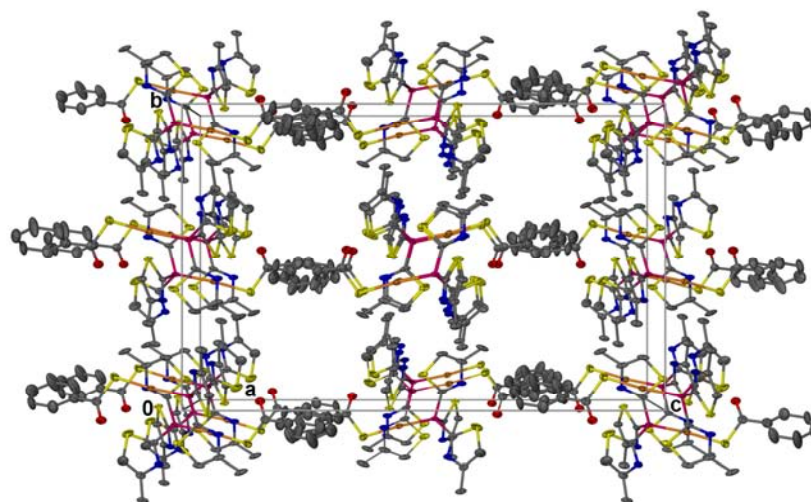


Figure 3.14 Packing diagram of **3b**·0.5C₆H₁₄ viewed along the *a* axis showing the channels occupied by the solvent and the alternating ligand/gold and thiobenzoate domains parallel to the *ab* plane; only one conformer of the benzene ring and no hexane solvent is shown.

layers of the phosphanegold and solvent/thiobenzoate domains along the *c* axis as depicted in Figure 3.14, whereas the hexane molecules are ordered into channels running along the *a* axis. The phenyl ring of the thiobenzoate is disordered into two positions, probably influenced by the highly disordered co-crystallised solvent which could not be modeled and – as judged from the size of the channels and amount of disorder – could approach a state found in the liquid.

The molecular structure of compound **4** had already been determined from crystals obtained from propanone/pentane which afforded the propanone solvate $4 \cdot (\text{CH}_3)_2\text{CO}$.¹³

Crystals of $4 \cdot 0.83\text{CDCl}_3$ were isolated from a trichloromethane-*d* solution (wherein **4** is initially well soluble) prepared for NMR spectroscopic study. The sample, however, gave only spectra of low quality evidently caused by spontaneous crystallisation during acquisition, as was seen on completion of the experiment. The structure of $4 \cdot 0.83\text{CDCl}_3$ shown in Figure 3.15 is remarkable in that it consists of three crystallographically independent molecules all showing a comparable arrangement as in the propanone solvate.¹³ A notable exception is the N31–Au4 bond vector which is bent out of the plane of the imidazole ring by *ca.* 19°. The molecules group around channels occupied by trichloromethane-*d*. One solvent molecule is disordered caused by a centre of inversion located between two of its chlorine atoms, thus giving rise to

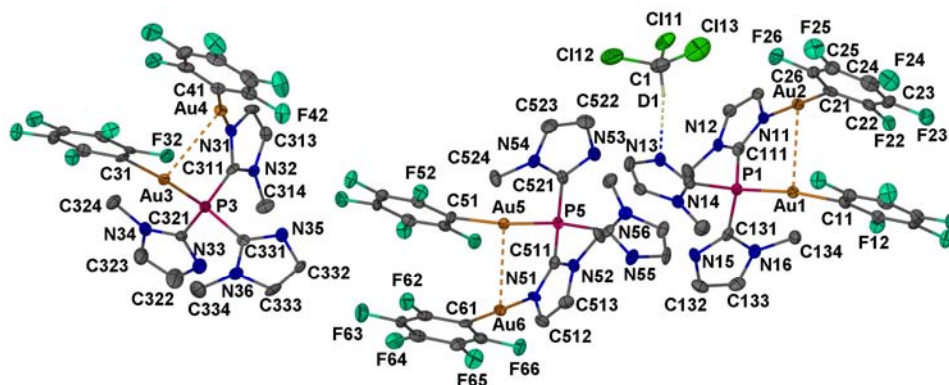


Figure 3.15 Molecular structure of $4 \cdot 0.83\text{CDCl}_3$; only one trichloromethane-*d* engaging in a hydrogen bond is shown; to avoid overlap the three unique molecules depicted belong to different unit cells.

the unusual 5:6 stoichiometry. A hydrogen bond is observed from D1 to N13 with C1–N13' 3.181(9) Å and C1–D1··N13' 156.01° ($\rho = 2 - x, 1 - y, 1 - z$). Compared to the known $4 \cdot (\text{CH}_3)_2\text{CO}$, all Au··Au distances are significantly extended [3.0240(4), 3.0170(4) and 2.9903(4) Å in the CDCl_3 solvate and 2.9619(5) Å in the propanone solvate] but other bond lengths are all comparable.

3.4 Conclusions

The tris(thiazol-2-yl)phosphanes **1b–d** have been prepared in a modification of the literature procedure, for 4,5-dimethylthiazole the reported temperature was too high and oxidative coupling of the 2-lithiated material was observed which was overcome by carefully maintaining a temperature of -78 °C throughout lithiation and reaction with PCl_3 . Gold(I) complexes of these ligands could be prepared by facile substitution of tetrahydrothiophene from (tht)AuCl or (tht)AuC₆F₅. Usually only the phosphorus atom coordinates to gold when tris(thiazol-2-yl)phosphanes are employed, however, tris(1-methylimidazol-2-yl)phosphane also employs one imine nitrogen atom in coordination to gold, forming the first C₆F₅AuN(imidazole)-type of compound.

Sulfurisation of tris(4-methylthiazol-2-yl)phosphane proceeded very slowly compared to the reaction times usually observed for tris(aryl)phosphanes and took 8 days to reach completion even with a large excess of sulfur. Low nucleophilicity was then also observed in the inability of this ligand to form stable Au^I complexes. Utilisation of different, harder metal centres with this multidentate ligand could yield interesting results.

¹⁵N{¹H} NMR spectroscopy revealed that the resonance of the imine nitrogen of tris(azol-2-yl)phosphanes appears at much lower field than in the free azoles. The downfield shift upon coordination of the ligands to Au^I is less pronounced.

Chloride substitution reactions of chloro[tris(4-methylthiazol-2-yl)phosphane]gold showed that a labilising effect of tris(thiazol-2-yl)phosphanes towards polymerisation to [Au(SR)]_n species can be observed compared to triphenylphosphane. Chloride could only be substituted by anions bearing electron-withdrawing groups at the sulfur

such as thiocyanate and thiobenzoate while alkylthiolate and, to a lesser extent, arylthiolate expelled the heterocyclic phosphane and condensed into polymeric $[\text{Au}(\text{SR})]_n$ species.

Earlier clues indicating facile hydrolysis of tris(azol-2-yl)phosphane complexes were confirmed in an NMR experiment, although the hydrolysis products proved elusive and none of them could be crystallised.

In particular – and this was the main focus of this Chapter – the structural solid state chemistry of tris(azol-2-yl)phosphane complexes of gold proved to be very rich in that a unique and large array of different polymorphs and solvates could be isolated. The results showed that the energy of the aurophilic bonding present in these structures may sometimes be overcome by normal van der Waals forces or packing effects to yield lattices containing unassociated molecules. Chloro[tris(4-methylthiazol-2-yl)phosphane]gold is only one of now three known compounds to crystallise in polymorphs with and without aurophilic interactions and the thf solvate is only the second gold compound in which aurophilic interactions are not observed in the solvate, but in the unsolvated structure. Furthermore, an unusual, and in this context unique, polymorph of chloro[tris(thiazol-2-yl)phosphane]gold exhibiting $\text{Au}\cdots\text{Cl}$ interactions was discovered that complements another structure which only exhibits $\text{Au}\cdots\text{Au}$ interactions in almost the same relative arrangement. The only major difference in the molecular structures of the two polymorphs is the position of the molecules along their respective Cl–Au–P vectors.

3.5 Experimental

3.5.1 Crystallography

Data associated with the crystal structures are summarised in Tables 3.7 and 3.8. For details on the measuring conditions and data processing see Chapter 2, p. 57. While solving the structure of **2d**, the thiazole ring containing C11 was found to be disordered in two positions related by a 180° rotation and populated 3:1, satisfactory

Table 3.6 Crystallographic parameters of **1c–e**, **2a** and the different structures of **2b**.

Compound	1c	1e	1d	2a	2b(iii)	2b·0.5CH ₂ Cl ₂
Empirical formula	C ₁₂ H ₁₂ N ₃ PS ₃	C ₁₂ H ₁₂ N ₃ PS ₄	C ₁₅ H ₁₈ N ₃ PS ₃	C ₁₂ H ₁₅ AuCIN ₆ P	C ₉ H ₆ AuCIN ₃ PS ₃	C ₉ H ₆ AuCIN ₃ PS ₃ ·CH ₂ Cl ₂
<i>M_r</i>	325.41	357.48	367.49	506.68	515.73	558.22
Crystal habit	Needle	Block	Prism	Prism	Block	Needle
Crystal dimensions/mm	0.30 × 0.05 × 0.05	0.50 × 0.30 × 0.20	0.10 × 0.03 × 0.03	0.31 × 0.10 × 0.07	0.33 × 0.15 × 0.14	0.34 × 0.08 × 0.05
Crystal system	Trigonal	Orthorhombic	Monoclinic	Monoclinic	Triclinic	Monoclinic
Space group	<i>R</i> 3 <i>c</i> (No. 161)	<i>Cmc</i> 2 ₁ (No. 36)	<i>P</i> 2 ₁ / <i>n</i> (No. 14)	<i>P</i> 2 ₁ / <i>n</i> (No. 14)	<i>P</i> $\bar{1}$ (No. 2)	<i>P</i> 2 ₁ / <i>n</i> (No. 14)
<i>a</i> /Å	15.238(1)	13.466(3)	12.760(2)	7.765(2)	8.611(2)	7.9518(9)
<i>b</i> /Å	15.238(1)	9.308(2)	9.7885(9)	18.867(5)	8.701(2)	20.261(2)
<i>c</i> /Å	10.588(2)	12.207(3)	13.923(2)	11.069(3)	9.512(2)	19.413(2)
α /°	90	90	90	90	90.821(3)	90
β /°	90	90	101.800(2)	90.540(4)	97.446(3)	96.018(2)
γ /°	120	90	90	90	106.515(3)	90
<i>V</i> /Å ³	2129.2(3)	1530.0(6)	1702.3(3)	1621.6(7)	676.5(2)	3110.6(6)
<i>Z</i> , <i>D_c</i> /Mg m ⁻³	6, 1.523	4, 1.552	4, 1.434	4, 2.075	2, 2.532	8, 2.384
μ (MoK α)/mm ⁻¹	0.623	0.717	0.528	9.337	11.634	10.296
No. of reflections, unique	4087, 949	4346, 1355	9941, 3606	8961, 3253	7937, 3162	17633, 6344
<i>R</i> _{int}	0.0153	0.0390	0.0206	0.0269	0.0281	0.0675
<i>hkl</i> index range	-19 to 18, -14 to 19, -13 to 12	-16 to 15, \pm 11, -15 to 9	-16 to 14, \pm 12, -15 to 17	\pm 9, -22 to 23, -13 to 8	\pm 11, \pm 11, \pm 12	\pm 9, -25 to 17, -22 to 24
θ range/°	2.67–27.08	2.66–26.36	2.43–26.73	2.13–26.44	2.16–28.28	2.01–26.44
Data, restraints, parameters	948, 1, 59	1273, 1, 105	3327, 0, 205	2740, 8, 215	3073, 0, 163	4748, 0, 352
Flack <i>x</i> parameter	0.07(8)	0.1(2)				
<i>F</i> (000)	1008	736	768	960	480	2088
<i>R</i> ₁ , <i>wR</i> ₂ [<i>I</i> > 2 σ (<i>I</i>)] ^a	0.0193, 0.0526	0.0387, 0.0844	0.0296, 0.0766	0.0308, 0.0657	0.0187, 0.0349	0.0481, 0.0833
<i>R</i> ₁ , <i>wR</i> ₂ (all data) ^a	0.0194, 0.0526	0.0423, 0.0865	0.0320, 0.0783	0.0412, 0.0699	0.0195, 0.0442	0.0739, 0.0909
Goodness-of-fit	1.115	1.068	1.076	1.042	1.054	0.991
Max. and min. transmission	0.970, 0.835	0.870, 0.661	0.987, 0.858	0.522, 0.335	0.196, 0.091	0.596, 0.117
Largest differential peak and hole/eÅ ⁻³	0.238, -0.175	0.470, -0.257	0.505, -0.194	2.173, -0.895	1.293, -1.119	1.663, -2.172
CCDC ref. no.	676984	676985	659052	659053	659056	659057

^a $w = 1/[\sigma^2(F_o^2) + (aP)^2 + bP]$ where $P = (F_o^2 + 2F_c^2)/3$

Table 3.7 Crystallographic parameters of the different structures of **2c** as well as **2d**, **3a**, **3b**·0.5C₆H₁₄ and **4**·0.83CDCl₃.

Compound	2c(ii)	2c ·C ₄ H ₈ O	2d	3a	3b ·0.5C ₆ H ₁₄	4 ·0.83CDCl ₃
Empirical formula	C ₁₂ H ₁₂ AuClN ₃ PS ₃	C ₁₂ H ₁₂ AuClN ₃ PS ₃ ·C ₄ H ₈ O	C ₁₅ H ₁₈ AuClN ₃ PS ₃	C ₁₃ H ₁₂ AuN ₄ PS ₄	C ₁₉ H ₁₇ AuN ₃ OPS ₄ ·0.5C ₆ H ₁₄	C ₂₄ H ₁₅ Au ₂ F ₁₀ N ₆ P _{0.83} CDCl ₃
<i>M_r</i>	557.81	629.94	599.91	580.44	702.62	1103
Crystal habit	Needle	Prism	Block	Block	Block	Prism
Crystal dimensions/mm	0.96 × 0.28 × 0.21	0.04 × 0.03 × 0.01	0.05 × 0.03 × 0.01	0.10 × 0.05 × 0.005	0.03 × 0.01 × 0.01	0.24 × 0.13 × 0.11
Crystal system	Monoclinic	Orthorhombic	Orthorhombic	Orthorhombic	Orthorhombic	Triclinic
Space group	<i>P2₁/c</i> (No. 14)	<i>P2₁2₁2₁</i> (No. 19)	<i>Pna2₁</i> (No. 33)	<i>Pca2₁</i> (No. 29)	<i>Pbca</i> (No. 61)	<i>P</i> $\bar{1}$ (No. 2)
<i>a</i> /Å	19.822(2)	9.0405(9)	12.954(2)	19.091(3)	10.6209(8)	12.325(2)
<i>b</i> /Å	10.333(1)	9.653(1)	11.294(2)	19.891(3)	17.664(2)	19.123(2)
<i>c</i> /Å	17.544(2)	24.273(3)	13.366(2)	19.781(3)	27.839(2)	20.242(2)
α /°	90	90	90	90	90	101.251(2)
β /°	109.950(1)	90	90	90	90	98.052(2)
γ /°	90	90	90	90	90	100.106(2)
<i>V</i> /Å ³	3377.7(6)	2118.3(4)	1955.6(4)	7511(2)	5222.7(7)	4530.7(8)
<i>Z</i> , <i>D_c</i> /Mg m ⁻³	8, 2.194	4, 1.975	4, 2.038	16, 2.053	8, 1.787	6, 2.425
μ (MoK α)/mm ⁻¹	9.329	7.454	8.064	8.366	6.035	10.069
No. of reflections, unique	35125, 6921	12563, 4472	11189, 3661	33095, 11670	29548, 5534	47479, 18211
<i>R_{int}</i>	0.0409	0.0326	0.0261	0.0759	0.0393	0.0334
<i>hkl</i> index range	± 24, ± 12, ± 21	-11 to 7, -12 to 10, ± 30	-16 to 15, -10 to 14, -16 to 14	± 21, -13 to 22, ± 22	-10 to 13, -20 to 22, -34 to 35	± 15, ± 23, ± 25
θ range/°	1.09–26.46	1.68–26.73	2.36–26.81	1.02–24.00	2.31–26.73	1.69–26.47
Data, restraints, parameters	6630, 0, 385	4210, 0, 238	3469, 9, 236	9310, 1, 502	4937, 12, 266	14419, 0, 1270
Flack <i>x</i> parameter		0.015(5)	0.519(7)	0.55(1)		
<i>F</i> (000)	2112	1216	1152	4416	2744	3074
<i>R</i> ₁ , <i>wR</i> ₂ [<i>I</i> > 2 σ (<i>I</i>)] ^a	0.0263, 0.0620	0.0245, 0.0489	0.0237, 0.0581	0.0635, 0.1485	0.0470, 0.1051	0.0288, 0.0622
<i>R</i> ₁ , <i>wR</i> ₂ (all data) ^a	0.0277, 0.0626	0.0268, 0.0495	0.0255, 0.0591	0.0905, 0.1584	0.0531, 0.1075	0.0450, 0.0761
Goodness-of-fit	1.170	0.906	1.046	1.049	1.207	1.083
Max. and min. transmission	0.142, 0.036	0.925, 0.655	0.922, 0.653	0.984, 0.534	0.937, 0.750	0.331, 0.240
Largest differential peak and hole/eÅ ⁻³	2.029, -1.001	1.429, -0.499	2.831, -0.680	8.375, -1.975	3.370, -1.154	1.525, -1.451
CCDC ref. no.	659059	659060	659061		659062	659064

^a $w = 1/[\sigma^2(F_o^2) + (aP)^2 + bP]$ where $P = (F_o^2 + 2F_c^2)/3$

modeling of the rings could only be achieved by splitting S11 and N11, thus giving average positions of the two orientations for the carbons in the thiazole ring, and constraining the rings to be flat. The anisotropic displacement parameters of S11 and N11, respectively, were constrained to be equal. It is also possible to solve the crystal structure in the space group *Pnma* but this imposes the same disorder on the other thiazole rings which have a defined orientation in space group *Pna2₁*. After establishing the connectivity of **3b**, additional diffuse electron density which belongs to the co-crystallised hexane solvent was located on the difference map, but could not be modeled. It was removed using the Squeeze routine in the Platon set of programmes.⁵¹ The phenyl ring of the thiobenzoate was also found to be disordered populating two different orientations in a 3:2 ratio which were constrained as flat regular hexagons and only the major orientation was refined anisotropically constraining C42A and C43A to have similar anisotropic displacement parameters.

3.5.2 Synthesis of the complexes

For a summary of general procedures and instrumentation *cf.* Chapter 2, p. 59.

Lithium phenylmethanethiolate, lithium benzenethiolate and lithium thiobenzoate were prepared by treatment of the respective free thiol with butyllithium solution in thf or Et₂O solution and were isolated as solids. NaCH(CN)₂ was prepared from propanedinitrile and sodium methoxide in methanol. Tris(thiazol-2-yl)phosphane, tris(4-methylthiazol-2-yl)phosphane,^{7a} (tht)AuCl⁵² and (tht)AuC₆F₅^{52b} were prepared according to described procedures.

The gift of tris(1-methylimidazol-2-yl)phosphane by *Dr. William Gabrielli* is greatly acknowledged.

Bromopentafluorobenzene, butyllithium in hexanes, 4,5-dimethylthiazole, 4-methylthiazole, phosphorus trichloride, and thiobenzoic acid were obtained from Aldrich. Benzenethiol, Celite (diatomaceous earth), propanedinitrile and thiazole were

51 A. L. Spek, *J. Appl. Crystallogr.* **2003**, *36*, 7–13.

52 (a) A. Haas, J. Helmbrecht and U. Niemann, in *Handbuch der Präparativen Anorganischen Chemie*, ed. G. Brauer, Stuttgart, Enke, **1978**, p. 1014;

(b) R. Uson, A. Laguna and M. Laguna, *Inorg. Synth.* **1989**, *26*, 85–91.

obtained from Fluka. Ammonium chloride and potassium sulfate were supplied by BDH; sulfur by Saarchem; tetrahydrothiophene by ACROS and phenylmethanethiol as well as sodium thiocyanate by Merck. Thin layer chromatography plates were supplied by Macherey-Nagel GmbH & Co. KG.

3.5.3.1 *Tris(4,5-dimethylthiazol-2-yl)phosphane, 1d.*

In a procedure similar to that reported by Moore and Whitesides^{7a} an ethereal solution of 4,5-dimethylthiazole (1.60 ml, 15.1 mmol) was added to an ethereal solution of BuLi (10.0 ml 1.51 M in hexanes, 15.1 mmol) cooled to $-78\text{ }^{\circ}\text{C}$ via a dropping funnel. Addition of PCl_3 (0.40 ml, 4.6 mmol) dissolved in Et_2O , workup with saturated aqueous NH_4Cl and extraction with CH_2Cl_2 afforded a yellow powder which was triturated with hexane (*ca.* 50 ml) to remove excess dimethylthiazole. Precipitation of the product with hexane from a dichloromethane solution and storage of the suspension overnight yielded well defined crystals amongst the amorphous precipitate (0.30 g, 18%); Found: C, 49.2; H, 4.7; N, 11.3. $\text{C}_{15}\text{H}_{18}\text{N}_3\text{PS}_3$ requires C, 49.0; H, 4.9; N, 11.4%.

M.p. $99\text{ }^{\circ}\text{C}$

The compound is soluble in CH_2Cl_2 , thf, methanol, slightly soluble in Et_2O but insoluble in alkanes.

3.5.3.2 *Tris(4-methylthiazol-2-yl)phosphane sulfide, 1e.*

In a Schlenk tube **1c** (177 mg, 0.54 mmol) and sulfur (154 mg, 0.60 mmol, 8.8 eq.) were dissolved in 15 ml thf and heated to $45\text{ }^{\circ}\text{C}$. Reaction progress was monitored daily by tlc (silica gel, hexane/ Et_2O 1:1; R_f : **1c** 0.25, **1e** 0.18). After 8 days all starting material had reacted and the solvent was removed *in vacuo*. The residue was re-suspended in 30 ml methanol and the suspension was filtered through Celite. Evaporation of the solvent gave a crude product which was recrystallised from CH_2Cl_2 /pentane to afford yellow needles (174 mg, 82%). A crystal suitable for X-ray diffraction was obtained from Et_2O /pentane.

M.p. $141\text{ }^{\circ}\text{C}$

The compound is soluble in CH_2Cl_2 , thf and methanol, it is slightly soluble in Et_2O but insoluble in alkanes.

3.5.3.3 Chloro[tris(4,5-dimethylthiazol-2-yl)phosphane]gold, **2d**.

Solid (tht)AuCl (0.30 g, 0.94 mmol) was added to a solution of **1d** (0.35 g, 0.95 mmol) in dichloromethane (20 ml). After 1 h the clear solution was filtered through Celite, the filter was washed with dichloromethane (20 ml) and the filtrate reduced to dryness. The residue was dissolved in dichloromethane, layered with hexane and stored at $-16\text{ }^{\circ}\text{C}$ for 2 days. The mother liquor was removed and the greenish solid was again dissolved in dichloromethane, the solution was filtered over Celite and the filtrate reduced to dryness yielding yellowish crystals suitable for X-ray diffraction (0.39 g, 67%); Found: C, 30.2; H, 2.8; N, 6.8. $\text{C}_{15}\text{H}_{18}\text{AuClN}_3\text{PS}_3$ requires C, 30.0; H, 3.0; N, 7.0%.

M.p. $86\text{ }^{\circ}\text{C}$ (dec.)

The compound is soluble in CH_2Cl_2 and thf, but insoluble in Et_2O or alkanes.

3.5.3.4 (Thiocyanato- κS)[tris(4-methylthiazol-2-yl)phosphane]gold, **3a**.

A solution of **2c** (247 mg, 0.44 mmol) in CH_2Cl_2 (10 ml) was added *via* a Teflon cannula to a degassed aqueous solution of NaNCS (55 mg, 0.68 mmol, 8 ml) containing 58 mg K_2SO_4 and the biphasic mixture was stirred vigorously for 3.5 h. The phases were separated with the help of a separating funnel and the aqueous phase was extracted with CH_2Cl_2 (3×3 ml). The combined organic phases were dried with Na_2SO_4 , filtered and the filter washed with dichloromethane (3×5 ml). Removal of the solvent *in vacuo* gave a colourless solid (0.24 g, 92%). Found: C, 26.7; H, 2.0; N, 9.4. $\text{C}_{13}\text{H}_{12}\text{AuN}_4\text{PS}_4$ requires C, 26.9; H, 2.1; N, 9.65%. ν/cm^{-1} 3067 s, 2961 w, 2918 w, 2130 s, 2122 vs, 2114 vs, 2075 w, 1497 m, 1437 m, 1387 s, 1360 s, 1287 m, 1261 w, 1055 m, 953 s, 859 s, 765 s and 709 m.

M.p. $105\text{ }^{\circ}\text{C}$ (dec.)

The compound is soluble in CH_2Cl_2 , thf, slightly soluble in Et_2O and insoluble in alkanes.

3.5.3.5 (Thiobenzoato)[tris(4-methylthiazol-2-yl)phosphane]gold, **3b**.

Lithium thiobenzoate (71 mg, 0.49 mmol) was dissolved in thf (25 ml). The mixture was stirred for 1.5 h after the addition of **2c** (245 mg, 0.44 mmol). After removal of the solvent the foamy residue was triturated with pentane and dissolved in CH_2Cl_2

(15 ml), filtered through Celite and the filter washed with again with CH₂Cl₂. The solution was concentrated *in vacuo*, layered with pentane and stored at -16 °C yielding a yellowish microcrystalline solid (0.25 g, 86%). Crystals of **3b**·0.5C₆H₁₄ suitable for X-ray diffraction were grown from a small sample dissolved in CH₂Cl₂ and layered with hexane. Found: C, 34.4; H, 2.6; N, 6.6. C₁₉H₁₇AuN₃OPS₄ requires C, 34.6; H, 2.6; N, 6.4%. ν/cm^{-1} 3070 s, 2953 m, 2918 m, 2856 m, 1622/1616 s, 1594 w, 1577 m, 1495 s, 1439 s, 1388 s, 1362 s, 1288 m, 1199 vs, 1167 s, 1063 m, 1045 m, 953 s, 906 vs, 860 m, 773 s, 757 s, 714 s and 688 vs.

M.p. 72 °C

The compound is soluble in CH₂Cl₂ and thf, slightly soluble in Et₂O but insoluble in alkanes.

3.5.3.6 *Bis(pentafluorophenyl)[μ -tris(1-methylimidazol-2-yl)phosphane- κ^2 -P:N]-digold, 4.*

The compounds (tht)AuC₆F₅ (261 mg, 0.58 mmol) and **1a** (79 mg, 0.29 mmol) were dissolved in thf (15 ml) and the purplish suspension was stirred for 30 min. All volatiles were removed *in vacuo* and the remaining solids were extracted with thf (25 ml) and filtered through Celite under an inert atmosphere. Some decomposition occurred during evaporation, thus the solid was re-dissolved in dichloromethane and filtered through Celite. The crude product was recrystallised from propanone layered with pentane and dried *in vacuo*. Yield 0.17 g (29%) of a colourless powder. Found: C, 28.9; H, 1.4; N, 8.2. C₂₄H₁₅Au₂F₁₀N₆P requires C, 28.8; H, 1.5; N, 8.4%.

M.p. 174 °C

The compound is soluble in thf, propanone and CH₂Cl₂. It is also soluble in trichloromethane-*d* forming a supersaturated solution stable for some time. Solubility in Et₂O is poor and alkanes do not dissolve the compound.

3.5.3.7 *Hydrolysis of 2c with aqueous NaOH.*

Complex **2c** (50 mg, 90 μ mol) was dissolved in (CD₃)₂SO. After initial acquisition of a ³¹P{¹H} NMR spectrum, NaOH (50 μ l, 2.12 M, 1.2 eq.) was added. Data collection was complete after 3 h and the sample was partitioned in CH₂Cl₂/H₂O after addition of a few drops of 50% MeCOOH. The organic phase was washed with water twice

and evaporated to dryness. The remaining solid was triturated with Et₂O to remove traces of dms-*d*₆. An excess of [NMe₄]Cl (15 mg, 0.14 mmol) was added to the combined aqueous phase from the partitioning above and it was subsequently extracted with CH₂Cl₂ (3×) and the organic phase was stripped of solvent. Both products tested positively for presence of gold, yet crystallisations from CH₂Cl₂/pentane (original organic phase) or CH₂Cl₂/Et₂O (original aqueous phase) only afforded amorphous precipitates.

4

Heterometallacyclic Complexes of Gold(I)

4.0 Abstract

Heterometallacyclic complexes of Au^I were prepared by using various classes of ditopic ligands. Deprotonation at C-5 of the thiophene ring in 4,4-dimethyl-2-(thien-2-yl)oxazoline and reaction with (tht)AuCl (tht = tetrahydrothiophene) afforded 18-membered rings of the 3:3 complex, **1**, exhibiting intramolecular Au^I⋯S contacts, and in another polymorph additional intermolecular Au^I⋯Au interactions, in the solid state. The heterometallacycle cannot incorporate another Au^I complex to form a rotaxane as the Au^I⋯S interactions prevent the thiazole rings to flip out of the plane.

By employing 1,3-bis(imidazol-1-ylmethyl)-2,4,6-trimethylbenzene (bitmb) the [Au₂(μ-bitmb)₂]²⁺ cation (a 24-membered heterometallacycle) was obtained with counter ions [BF₄]⁻, **2a**, and CF₃SO₃⁻, **2b**. The compounds are the first gold heterometallacycles comprising *N*-coordinated imidazole and crystallise in a “box”-shape hosting solvent molecules in the cavity created. The crystal structure of **2b**·2CH₂Cl₂ exhibits channels in the solid state structure and the solvent could partially be removed in a vacuum at 90 °C.

Employment of 4,4-dimethyl-2-(pyridin-4-yl)oxazoline as a ligand towards Ag^I and Au^I did not yield similar compounds to **1** as was intended. With AgNO₃ a solid-state structure of the 1:1 complex, **3**, exhibiting infinite chains was obtained. Reaction with Au^I gave compounds **4a** (the CF₃SO₃⁻ salt) and **4b** (the [BF₄]⁻ salt) whose structures could not be elucidated.

A range of ditopic ligands (2L), *N,N*-bis(1,3,2-dioxaphospholan-2-yl)methanamine, 1,2-bis(diphenylphosphanyl)ethane (dppe) and tetramethyldiphosphane disulfide were employed in attempts to obtain further examples of rare $[Au_2(\mu\text{-}^2L)_3]^{2+}$ -type cations. Only the first ligand afforded the solid-state structure of such a 3:2 complex, $5 \cdot 0.5CH_3CN$, while dppe gave a 2:2-complex, **6**, and tetramethyldiphosphane disulfide a 2:1-complex, **7**. The molecular structure of the latter complex exhibits a roughly tetrahedral arrangement of the sulfur donor atoms but the gold atom is situated towards the two sulfur atoms to which it forms true coordinative bonds rather than having equal bond lengths to all sulfur atoms.

4.1 Introduction

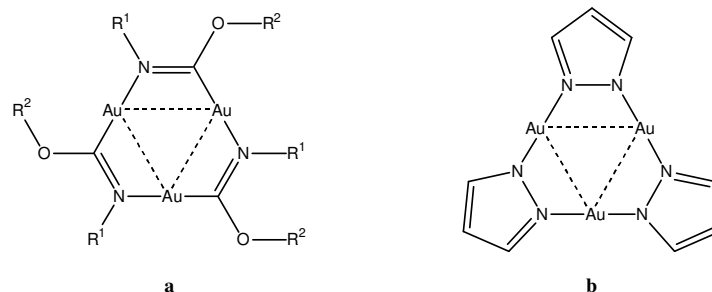
This chapter deals with heterometallacyclic rings wherein Au^I is homoleptically coordinated to ditopic ligands with the general formula $[Au_m(L^{\wedge}N)_n]$.¹ A broad range of bonding modes of such ditopic ligands can be defined and many of them have been explored. Ligands such as RS^- , R_2P^- and R_2N^- that can afford heterometallacycles *via* a single bridging atom, have been excluded from the discussion.

4.1.1 Heterometallacycles containing gold

4.1.1.1 $N^{\wedge}C^-$, $N^{\wedge}N^-$ and related ligands.

Many examples are known of metallacycles exhibiting homoleptic $N^{\wedge}C^-$ and $N^{\wedge}N^-$ coordination which includes the usually trimeric Au^I carbene² and pyrazolate complexes³ (Scheme 4.1). As all these compounds comprise three gold atoms in close proximity, they are exploited for crystal engineering by virtue of their different association by aurophilic contacts and/or π - π stacking. They have been shown to react

-
- 1 The notation " $L^{\wedge}N$ " in this Chapter shall represent a ditopic ligand coordinating through atoms L and N, thus forming a cyclic compound.
 - 2 In literature, these complexes are sometimes called 'carbeniates'. As the nitrogen atom is "aurylated" by the gold centre, the term 'carbene' is used here. See also Schemes 4.1(a) and 4.2(a).
 - 3 Representative examples include: (a) F. Bonati, G. Minghetti and G. Banditelli, *J. Chem. Soc., Chem. Commun.* **1974**, 88–89; (b) R. G. Raptis, H. H. Murray III and J. P. Fackler, Jr., *J. Chem. Soc., Chem. Commun.* **1987**, 737–739; (c) J. Barberá, A. Elduque, R. Giménez, L. A. Oro and J. L. Serrano, *Angew. Chem., Int. Ed. Engl.* **1996**, 35, 2832–2835 (*Angew. Chem.* **1996**, 108, 3048–3051); (d) G. Yang and R. G. Raptis, *Inorg. Chem.* **2003**, 42, 261–263; (e) P. Ovejero, M. J. Mayoral, M. Cano and M. C. Lagunas, *J. Organomet. Chem.* **2007**, 692, 1690–1697.



Scheme 4.1 (a) A typical trimeric cyclic gold carbene complex exhibiting intramolecular aurophilic interactions, intermolecular interactions are often observed as well, and (b) a trimeric Au^I pyrazolate; the heterocycles/carbene ligands may be substituted according to the desired property in the product.

with Ag⁺ and Tl⁺ cations to form sandwiches held together by metallophilic interactions.⁴ π -Acids such as perfluorinated aromatic compounds⁵ and Hg^{II} complexes of fluorinated arenes yield interstitial compounds that crystallise in assemblies showing π -stacking or metallophilic interactions.⁶

The phenomenon of solvoluminescence, *i.e.* the emission of light on dissolution in a suitable solvent after irradiation of the solid, has also been discovered with the cyclic carbene compound class.⁷ Associated with their strong tendency to form columns with Au \cdots Au interactions, research has also focused on the design of liquid crystals from trimeric carbenes and pyrazolates by introducing appropriate substituents.^{3c,e} Certain carbenes and pyrazolates also form other ring sizes than the usual 9-membered ring of the 3:3 complex; engineering the sterical demand of the ligands employed yielded an unusual 18-membered ring system in [Au₆(μ -3,5-diphenylpyrazolate)₆] (Scheme 4.2) rather than the expected trimer. Aurophilic interactions play a role as the six gold centres form two tetrahedra with a common edge, the two Au atoms of this common edge form a metallophilic contact.^{3b} The same directive effect was observed in a tetrameric carbene-imidate where a pyridine group coordinates to gold instead of the

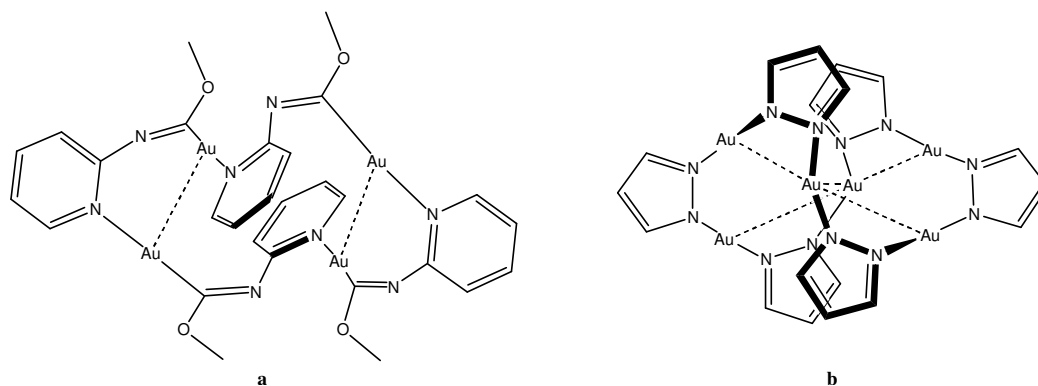
4 A. Burini, R. Bravi, J. P. Fackler, Jr., R. Galassi, T. A. Grant, M. A. Omary, B. R. Pietroni and R. J. Staples, *Inorg. Chem.* **2000**, *39*, 3158–3165.

5 M. A. Rawashdeh-Omary, M. A. Omary and J. P. Fackler, Jr., *J. Am. Chem. Soc.* **2001**, *123*, 9689–9691.

6 A. Burini, J. P. Fackler, Jr., R. Galassi, T. A. Grant, M. A. Omary, M. A. Rawashdeh-Omary, B. R. Pietroni and R. J. Staples, *J. Am. Chem. Soc.* **2000**, *122*, 11264–11265.

7 J. C. Vickery, M. M. Olmstead, E. Y. Fung and A. L. Balch, *Angew. Chem., Int. Ed. Engl.* **1997**, *36*, 1179–1181 (*Angew. Chem.* **1997**, *109*, 1227–1229).

imine-nitrogen of the ligand and each two adjacent gold centres engage in an aurophilic contact (Scheme 4.2).⁸



Scheme 4.2 (a) A tetrameric carbene-imidate complex with a pyridine substituent affording a tetrameric instead of a trimeric structure; (b) the hexameric gold 3,5-diphenylpyrazolate, phenyl substituents are omitted for clarity.

Other examples of ring formation with $N^{\wedge}C^{-}$ donors, albeit using Au^{III} , include the spontaneous metalation of 2-(pyridin-2-yl)-6-(thien-2-yl)pyridine by $[AuCl_4]^{-}$ to give a $[(AuCl_2)_2(\mu^{-2}L)_2]$ compound shown to be metalated at C-5 of the thiophene ring and the central pyridine ring left uncoordinated. This result is in contrast to similar complexes with isoelectronic Pt^{II} and Pd^{II} which selectively metalate C-3 of the thiophene ring to give monomeric $[MCIL]$ ($M = Pd, Pt$) complexes in which the central pyridine is also employed in coordination to the metal.⁹

Dimeric and trimeric metallacycles of Au^I with a selectively deprotonated $N^{\wedge}C^{-}$ thienyloxazoline ligand have been reported by *Desmet et al.*¹⁰

Amine $N^{\wedge}N$ -coordination of gold, although known, is uncommon. Complexes of the well-known ligands dien [*N*-(2-aminoethyl)ethane-1,2-diamine]¹¹ or cyclam (1,4,8,11-tetraazacyclotetradecane)¹² typically yield $[Au_2(\mu\text{-dien})_2]^{2+}$ or $[Au_2(\mu\text{-cyclam})_2]^{2+}$

8 C. Bartolomé, M. Carrasco-Rando, S. Coco, C. Cordovilla, P. Espinet and J. M. Martín-Alvarez, *Organometallics* **2006**, 25, 2700–2703.

9 (a) E. C. Constable, R. P. G. Henney and T. A. Leese, *J. Organomet. Chem.* **1989**, 361, 277–282;

(b) E. C. Constable, R. P. G. Henney, P. R. Raithby and L. R. Sousa,

Angew. Chem., Int. Ed. Engl. **1991**, 30, 1363–1364 (*Angew. Chem.* **1991**, 103, 1401–1403).

10 (a) M. Desmet, *Ph.D. thesis*, Rand Afrikaans University, **1996**;

(b) M. Desmet, H. G. Raubenheimer and G. J. Kruger, *Organometallics* **1997**, 16, 3324–3332.

11 J. Yau, D. M. P. Mingos, S. Menzer and D. J. Williams,

J. Chem. Soc., Dalton Trans. **1995**, 2575–2576.

12 J. Yau, D. M. P. Mingos and H. R. Powell, *Polyhedron* **1996**, 15, 367–369.

wherein Au^I is coordinated in a linear fashion despite the presence of additional free nitrogen centres.

Combined NHC¹³ and amine/imine C[^]N,¹⁴ ligands have also received attention mainly focused on structural chemistry in conjunction with aurophilic interactions and the development of macromolecular arrays by utilising polydentate ligands comprising these donor atoms.

Homoleptic cationic cyclic bis-imine N[^]N-complexes of Au^I surprisingly have not been synthesised, but bis-imidazoles have been combined with diphosphanes to furnish [Au₂(μ-P[^]N)₂]²⁺ heterometallacycles. These complexes have been synthesised in the search for Au complexes that may be used as drugs against cancer and HIV.¹⁵ Examples of imidazolyl(diphenyl)phosphanes, also exhibiting P[^]N(imine) coordination in the products that have been prepared for envisioned medical applications, are known as well.¹⁶ P[^]N(amine) coordination has been observed in the 2:2 complex of Au^I with (2-aminophenyl)diphenylphosphane in a study of the luminescence properties of group 11 metals.¹⁷

4.1.1.2 Ligands with phosphorus donor atoms.

The most common cationic (or overall neutral, if there is the possibility of deprotonating the ligand at a non-coordinating site, *e.g.* as in P–NH–P backbones) metallacycles of Au^I comprise diphosphanes with the classic P[^]P coordination. These compounds have found application in many fields, the most important being crown ether derivatives¹⁸ and cryptates for the determination of other cations by characteristic luminescence,¹⁹ research of structural properties such as chiral helical

13 For a definition of *N*-heterocyclic carbenes (NHCs) see Chapter 5, Section 5.1.1, p. 161.

14 (a) B. Liu, W. Chen and S. Jin, *Organometallics* **2007**, *26*, 3660–3667;

(b) M. K. Samantaray, K. Pang, M. M. Shaikh and P. Ghosh, *Inorg. Chem.* **2008**, *47*, 4153–4156.

15 F. Bachechi, A. Burini, R. Galassi, B. R. Pietroni and M. Severini, *J. Organomet. Chem.* **1999**, *575*, 269–277.

16 A. Burini, B. R. Pietroni, R. Galassi, G. Valle and S. Calogero, *Inorg. Chim. Acta* **1995**, *229*, 299–305.

17 O. Crespo, E. J. Fernández, M. Gil, M. C. Gimeno, P. G. Jones, A. Laguna, J. M. López-de-Luzuriaga and M. E. Olmos, *J. Chem. Soc., Dalton Trans.* **2002**, 1319–1326.

18 A. M. Gibson and G. Reid, *J. Chem. Soc., Dalton Trans.* **1996**, 1267–1274.

19 (a) V. J. Catalano, H. M. Kar and B. L. Bennett, *Inorg. Chem.* **2000**, *39*, 121–127;

(b) V. J. Catalano, M. A. Malwitz and B. C. Noll, *Chem. Commun.* **2001**, 581–582.

structures in the solid state,²⁰ dynamic behaviour of such metallacycles²¹ or catalytic and medical uses.²²

Reports from the group of *Puddephatt* deal with heterometallacycles that can be exploited to form [2]-catenanes.²³ These are usually designed by utilising bidentate phosphane and bidentate alkyne ligands. The conditions of formation of such interlocked rings depend on the final size of the heterometallacycle and the nature of the group linking the two (2-propynyloxy)arene moieties commonly used as building blocks. It has been found that linker functionalities which can participate in delocalisation of the electrons in the aromatic rings will not produce catenanes due to resulting unfavourable interactions with other arene groups.^{23a,b} The compounds are useful in the elucidation of luminescence often observed concomitant with aurophilic contacts²⁴ and are precursors of self-organised polymeric gold-containing structures.²⁵

Homoleptic $P^{\wedge}C^{-}$ type compounds were obtained by reacting 2-monolithiated triphenylphosphane with a Au^I complex. The resulting heterometallacycle was useful in preparing Au^{II} and Au^{III} compounds.²⁶ Neutral cyclic compounds with $P^{\wedge}S^{-}$ coordination were isolated with 2-(diethylphosphanyl)ethane-1-thiol to explore their antiarthritic properties, but were inferior to AuranofinTM in which the monomeric gold centre is coordinated by a phosphane and thiolate as well.²⁷

20 A. Deák, T. Megyes, G. Tárkányi, P. Király, L. Biczók, G. Pálinkás and P. J. Stang, *J. Am. Chem. Soc.* **2006**, *128*, 12668–12670.

21 J. H. K. Yip and J. Prabhavathy, *Angew. Chem., Int. Ed. Engl.* **2001**, *40*, 2159–2162 (*Angew. Chem.* **2001**, *113*, 2217–2220).

22 M. C. Gimeno, A. Laguna, C. Sarroca and P. G. Jones, *Inorg. Chem.* **1993**, *32*, 5926–5932.

23 (a) W. J. Hunks, J. Lapierre, H. A. Jenkins and R. J. Puddephatt, *J. Chem. Soc., Dalton Trans.* **2002**, 2885–2889; (b) F. Mohr, D. J. Eisler, C. P. McArdle, K. Atieh, M. C. Jennings and R. J. Puddephatt, *J. Organomet. Chem.* **2003**, *670*, 27–36; (c) N. C. Habermehl, M. C. Jennings, C. P. McArdle, F. Mohr and R. J. Puddephatt, *Organometallics* **2005**, *24*, 5004–5014.

24 (a) M.-C. Brandys, M. C. Jennings and R. J. Puddephatt, *J. Chem. Soc., Dalton Trans.* **2000**, 4601–4606; (b) W. J. Hunks, M. C. Jennings and R. J. Puddephatt, *Z. Naturforsch., B: Chem. Sci.* **2004**, *59*, 1488–1496.

25 T. J. Burchell, D. J. Eisler, M. C. Jennings and R. J. Puddephatt, *Chem. Commun.* **2003**, 2228–2229.

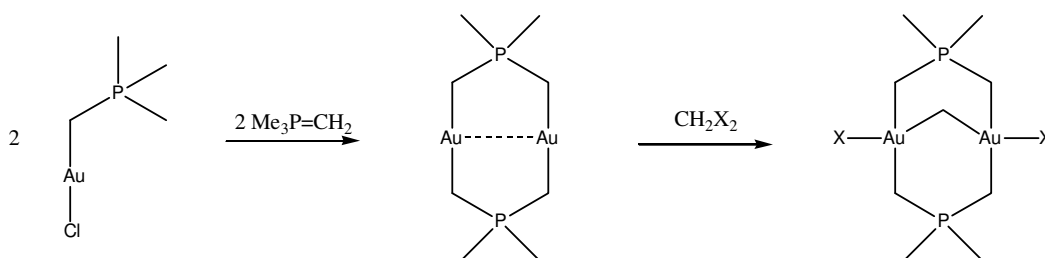
26 M. A. Bennett, S. K. Bhargava, K. D. Griffiths, G. B. Robertson, W. A. Wickramasinghe and A. C. Willis, *Angew. Chem., Int. Ed. Engl.* **1987**, *26*, 258–260 (*Angew. Chem.* **1987**, *99*, 261–262).

27 J. Weinstock, B. M. Sutton, G. Y. Kuo, D. T. Walz and M. J. DiMartino, *J. Med. Chem.* **1974**, *17*, 139–140.

Further examples include bis(phosphane sulfide) ($S^{\wedge}S$)²⁸ and phosphane/phosphane selenide ($P^{\wedge}Se$) coordinated metallacycles²⁹ which have been synthesised particularly to explore the scope of Au chemistry with soft ditopic ligands, research group 11 metallophilic interactions or gain further insight into rare gold–selenium bonds, respectively.

4.1.1.3 Heterometallacycles from $C^{\wedge}C$ -ligands.

Schmidbaur and coworkers have reported phosphorus-ylide complexes of gold which can be converted to $C^{\wedge}C^{-}$ coordinated heterometallacycles when stirred with excess ylide.³⁰ Due to the adjacent phosphonium group, the Au–C bonds are very stable and the compounds are not decomposed by air or moisture. Various reactions of this heterometallacyclus have been studied. It readily adds one or two equivalents of halogen to afford Au^{II} and Au^{III} complexes, respectively, the former with an intramolecular Au–Au bond. Another unique feature of this heterometallacyclus is its ability to add CH_2X_2 and form the bicyclic scaffold shown in Scheme 4.3.



Scheme 4.3 Synthesis of heterometallacycles with ylide coordination of Au^I; X = Cl, Br or I.

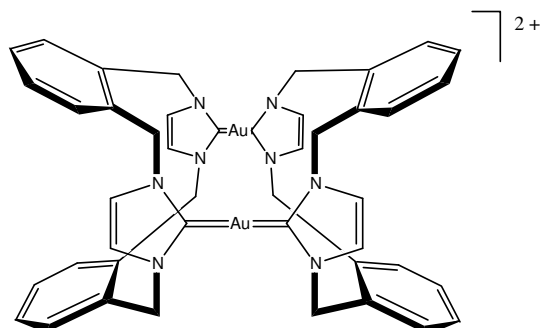
Recent examples of cationic metallacycles include complexes of cyclic biscarbenes of the type $[Au_2(\mu-C^{\wedge}C)_2]^{2+}$ (two ditopic NHC ligands linked by two Au centres, Scheme 4.4). Such complexes have been obtained instead of the targeted intramolecularly chelated $[Au(C^{\wedge}C)]^+$ coordination compound. Even linear biscarbene ligands yield

28 M. C. Gimeno, A. Laguna, M. Laguna and F. Sanmartín, *Organometallics* **1993**, *12*, 3984–3991.

29 H. Schmidbaur, J. Ebner von Eschenbach, O. Kumberger and G. Müller, *Chem. Ber.* **1990**, *123*, 2261–2265.

30 (a) H. Schmidbaur and R. Franke, *Angew. Chem., Int. Ed. Engl.* **1973**, *12*, 416–417 (*Angew. Chem.* **1973**, *85*, 449–450); (b) P. Jandik, U. Schubert and H. Schmidbaur, *Angew. Chem., Int. Ed. Engl.* **1982**, *21*, 73 (*Angew. Chem.* **1982**, *94*, 74–75).

$[\text{Au}_2(\mu\text{-C}^{\wedge}\text{C})_2]^{2+}$ complexes. Owing to their lipophilic character, such compounds are selectively transported into the mitochondria of carcinoma cells.³¹

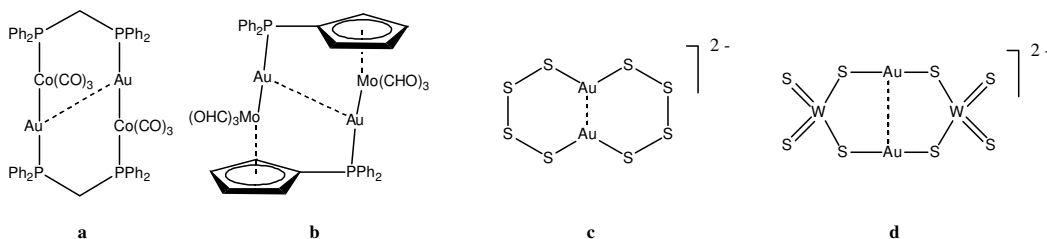


Scheme 4.4 An example of a heterometallacycle comprising bis-NHC coordination of Au^{I} .

4.1.1.4 Other ligands.

Some cyclic compounds that do not fit into the classification used above, are shown in Scheme 4.5. Some of them contain more than one metal centre.³²

Finally, the two examples (c) and (d) in Scheme 4.5 illustrate rare species of anionic cyclic compounds of gold.³³



Scheme 4.5 Metallacycles with gold–transition metal bonds (a), (b); and anionic cyclic compounds that contain gold (c), (d).

31 (a) P. J. Barnard, M. V. Baker, S. J. Berners-Price, B. W. Skelton and A. H. White, *Dalton Trans.* **2004**, 1038–1047; (b) X. Hu, I. Castro-Rodriguez, K. Olsen and K. Meyer, *Organometallics* **2004**, *23*, 755–764; (c) J.-W. Wang, H.-B. Song, Q.-S. Li, F.-B. Xu and Z.-Z. Zhang, *Inorg. Chim. Acta* **2005**, *358*, 3653–3658.

32 (a) A. Pons, O. Rossell, M. Seco and A. Perales, *Organometallics* **1995**, *14*, 555–557; (b) B. Brumas-Soula, F. Dahan and R. Poilblanc, *New J. Chem.* **1998**, 1067–1074.

33 (a) A. Müller, H. Dornfeld, G. Henkel, B. Krebs and M. P. A. Vieggers, *Angew. Chem., Int. Ed. Engl.* **1978**, *17*, 52 (*Angew. Chem.* **1978**, *90*, 57–58); (b) A. Müller, M. Römer, H. Bögge, E. Krickemeyer and K. Schmitz, *Inorg. Chim. Acta* **1984**, *85*, L39–L41.

4.1.2 Porous crystalline compounds

Solvent co-crystallisation is usually undesirable when examining a crystal by X-ray diffraction and often gives rise to complicated problems during refinement due to disorder caused by excessive mobility. The disorder can be so pronounced that the solvent molecule does not occupy discrete positions anymore but behaves similar to a liquid filling cavities or pores in the crystal. If the co-crystallised solvent is removed, *e.g.* by heating and/or by applying a vacuum, a crystal structure normally collapses to yield an amorphous solid ('efflorescence'). This can be nicely demonstrated with blue crystals of $\text{CuSO}_4 \cdot 5\text{H}_2\text{O}$ which, on gentle heating, afford a white amorphous powder of anhydrous copper(II)sulfate. As the water molecules evaporate, the structure lacks supporting hydrogen bonds and collapses.

Cyclic complexes, on the other hand, are able to crystallise in "box"- or "doughnut"-shapes and, given the right size, can incorporate solvent in the cavities created if the molecules are unable to form an efficient packing that utilises these cavities. If the solvent also occupies suitable interconnected sites, a porous crystal structure results. Owing to a pre-formed scaffold less likely to collapse, loss of solvent can possibly be tolerated and crystallinity be preserved. The possibility of additional stabilisation introduced by aurophilic bonding³⁴ could further assist in supporting the solid-state structure when solvent has been removed.

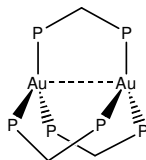
Heterometallacyclic compounds with ditopic bis[(benz)imidazol-1-ylmethyl]benzene ligands have been reported by *Dobrzańska et al.* The products are porous crystal structures that contain metals such as Ag^{I} as the central atom.³⁵ The question arose whether such compounds can also be obtained employing the heavier group member, Au. Crystal structures of porous materials containing this metal have not yet been reported.

34 H. Schmidbaur, S. Cronje, B. Djordjevic and O. Schuster, *Chem. Phys.* **2005**, *311*, 151–161 and references cited therein.

35 (a) L. Dobrzańska, G. O. Lloyd, H. G. Raubenheimer and L. J. Barbour, *J. Am. Chem. Soc.* **2005**, *127*, 13134–13135; (b) L. Dobrzańska, G. O. Lloyd, H. G. Raubenheimer and L. J. Barbour, *J. Am. Chem. Soc.* **2006**, *128*, 698–699; (c) L. Dobrzańska, G. O. Lloyd and L. J. Barbour, *New J. Chem.* **2007**, 669–676.

4.1.3 Digold(I) compounds bridged by three ditopic $P^{\wedge}P$ ligands – a special type of heterometallacyclic gold complex

Unexpectedly, bicyclic $[\text{Au}_2(\mu\text{-}^2\text{L})_3]^{2+}$ -type complexes (^2L being a bidentate ligand, Scheme 4.6) are still a laboratory curiosity and have received little attention, while structurally characterised mononuclear trigonal-planar Au^{I} complexes are more common.^{17,36}



Scheme 4.6 The general structure of a $[\text{Au}_2(\mu\text{-}^2\text{L})_3]^{2+}$ complex shown for a ditopic bis(phosphanyl)-methane ligand; substituents at the phosphorus atoms are not shown.

So far, only compounds where the bidentate ligand is a bisphosphane are known. The first crystallographically characterised compound, tris[μ -bis(dimethylphosphanyl)-methane]digold(2+) tetrafluoroborate, was reported in 1986.³⁷ The existence of such compounds in solution was further corroborated by ^{31}P NMR spectroscopy³⁸ and electrospray mass spectrometry.³⁹ However, MS cannot distinguish between $[\text{Au}_2(\mu\text{-}^2\text{L})_3]^{2+}$ and $[\text{}^2\text{LAu}(\mu\text{-}^2\text{L})\text{Au}^2\text{L}]^{2+}$ species. The latter was found in the solid state when the sterical demand of ^2L is too great^{22,40} or the spacing between the ligating phosphorus atoms too extensive.⁴¹

Among the molecular structures reported (Scheme 4.7) are derivatives with the ligand motif $\text{R}_2\text{PCH}_2\text{PR}_2$ (R = methyl³⁷ or phenyl⁴²). The former compound was examined as a catalyst in the C–C coupling of alkyl halides.⁴³ Complexes with a functional spacer

36 See for example: (a) P. G. Jones, *Acta Crystallogr., Sect. B: Struct. Crystallogr. Cryst. Chem.* **1980**, 36, 3105–3107; (b) F. Olbrich and R. J. Lagow, *Z. Anorg. Allg. Chem.* **1995**, 621, 1929–1932;

37 W. Bensch, M. Prelati, W. Ludwig, *J. Chem. Soc., Chem. Commun.* **1986**, 1762–1763.

38 S. Al-Baker, W. E. Hill and C. A. McAuliffe, *J. Chem. Soc., Dalton Trans.* **1985**, 2655–2659.

39 R. Colton, K. L. Harrison, Y. A. Mah and J. C. Traeger, *Inorg. Chim. Acta* **1995**, 231, 65–71.

40 T. M. McCleskey, L. M. Henling, K. A. Flanagan and H. B. Gray, *Acta Crystallogr., Sect. C: Cryst. Struct. Commun.* **1993**, 49, 1467–1469.

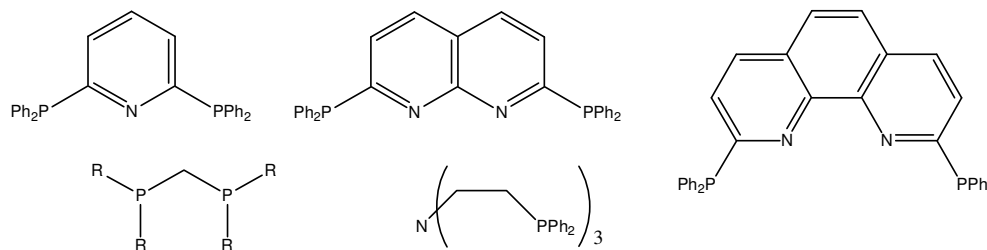
41 M.-C. Brandys and R. J. Puddephatt, *J. Am. Chem. Soc.* **2001**, 123, 4839–4840.

42 U. E. I. Horvath, unpublished results.

43 (a) H.-R. C. Jaw, M. M. Savas, R. D. Rogers and W. R. Mason, *Inorg. Chem.* **1989**, 28, 1028–1037;

(b) D. Li, C.-M. Che, H.-L. Kwong and V. W.-W. Yam, *J. Chem. Soc., Dalton Trans.* **1992**,

3325–3329; (c) K. H. Leung, D. L. Phillips, Z. Mao, C.-M. Che, V. M. Miskowski and C.-K. Chan, *Inorg. Chem.* **2002**, 41, 2054–2059.



Scheme 4.7 Ligands employed for the syntheses of $[\text{Au}_2(\mu\text{-}^2\text{L})_3]^{2+}$ complexes that have been crystallographically characterised. *P*-coordination of Au^{I} was observed in all cases. R = Me or Ph.

between the phosphorus atoms, 2,6-bis(diphenylphosphanyl)pyridine,⁴⁴ 2,7-bis(diphenylphosphanyl)-1,8-naphthyridine^{19a,45} and 2,9-bis(diphenylphosphanyl)-1,10-phenanthroline^{19b,46} were all utilised in the preparation of metallocryptands as mentioned in Section 4.1.1. For the metallocryptand complexes of naphthyridine and phenanthroline incorporation of a monovalent metal cation coordinating to the nitrogen atoms in the azine rings seems to be crucial in isolating crystals of the compound as the authors of one report failed to obtain such compounds in absence of M^+ . Crystals obtained were cryptates generated from the adventitious presence of the ubiquitous Na^+ .^{19a} An unusual example was a 2:2 binuclear complex of Au^{I} with tritopic tris[2-(diphenylphosphanyl)ethyl]amine where trigonal coordination at each gold centre is effected by two arms of one and one arm of another ligand; no amine coordination occurred.⁴⁷

The complexes have usually been obtained by reacting $(\text{tht})\text{AuCl}$ with 1.5 equivalents of ligand, followed by exchange of the halogen for a non-coordinating anion with $\text{Na}[\text{BF}_4]$, $\text{Na}[\text{BPh}_4]$ or LiClO_4 in aqueous or organic solution. Intramolecular aurophilic interactions were only observed in those complexes with only one atom placed between the two phosphorus centres. As a result of the employment of diphenylphosphanyl groups with a large steric demand in most complexes, intermolecular $\text{Au}\cdots\text{Au}$ interactions were absent.

44 S.-J. Shieh, D. Li, S.-M. Peng and C.-M. Che, *J. Chem. Soc., Dalton Trans.* **1993**, 195–196.

45 R.-H. Uang, C.-K. Chan, S.-M. Peng and C.-M. Che, *J. Chem. Soc., Chem. Commun.* **1994**, 2561–2562.

46 V. J. Catalano, B. L. Bennett, H. M. Kar and B. C. Noll, *J. Am. Chem. Soc.* **1999**, *121*, 10235–10236.

47 Md. N. I. Khan, R. J. Staples, C. King, J. P. Fackler, Jr. and R. E. P. Winpenny, *Inorg. Chem.* **1993**, *32*, 5800–5807.

Binuclear tetracoordinate Au^I complexes with three bridging ligands of the type [(AuX)₂(μ-²L)₃] have been reported for ²L = bis(diphenylphosphanyl)ethyne (X = Cl) – synthesised in conjunction with a study on luminescent gold complexes⁴⁸ – and for ²L = 1,4-bis(diphenylphosphanyl)pyridazine, (X = I).⁴⁹ The latter compound only adopts this type of configuration in the presence of iodide; with non-coordinating [PF₆]⁻ counter anions the structure consists of two-dimensional sheets of trigonal Au^I centres bridged by 1,4-bis(diphenylphosphanyl)pyridazine. The intended cryptation of additional metal centres by the pyridazine rings has not succeeded. The only complex reported that contains phosphonite ligands {²L = [(CF₃CH₂O)₂P]₂CH₂ and X = Cl} was used in a study on the photoactivation of M–X bonds.⁵⁰ The gold centres are distorted towards tetrahedral geometry by the terminal chloride ligands, therefore only a very weak aurophilic contact of 3.5295(7) Å is observed.

4.1.4 Aims

The most important aims and secondary objectives for the investigations described in the present Chapter can be summarised as follows:

- (a) To re-prepare a trimeric thienyloxazolinegold(I) heterometallacycle and complete the previously unsuccessful structural characterisation as well as verify its proposed connectivity and bonding structure. Elucidation of the fact why the trimer forms selectively and no polymeric material is obtained during preparation was anticipated. Furthermore, in the light of the results in Chapter 3, attention would also focus on the presence of polymorphs in crystallisations; the suitability of this complex to incorporate additional metal centres should also be probed as such reactions were observed for structurally related trimeric cyclic carbene complexes;
- to further explore the scope of gold(I) heterometallacycles, for this goal the employment of related ligands was planned.

48 M. Bardají, M. T. de la Cruz, P. G. Jones, A. Laguna, J. Martínez and M. D. Villacampa, *Inorg. Chim. Acta* **2005**, 358, 1365–1372.

49 V. J. Catalano, M. A. Malwitz, S. J. Horner and J. Vasquez, *Inorg. Chem.* **2003**, 42, 2141–2148.

50 J. L. Dempsey, A. J. Esswein, D. R. Manke J. Rosenthal, J. D. Soper and D. G. Nocera, *Inorg. Chem.* **2005**, 44, 6879–6892.

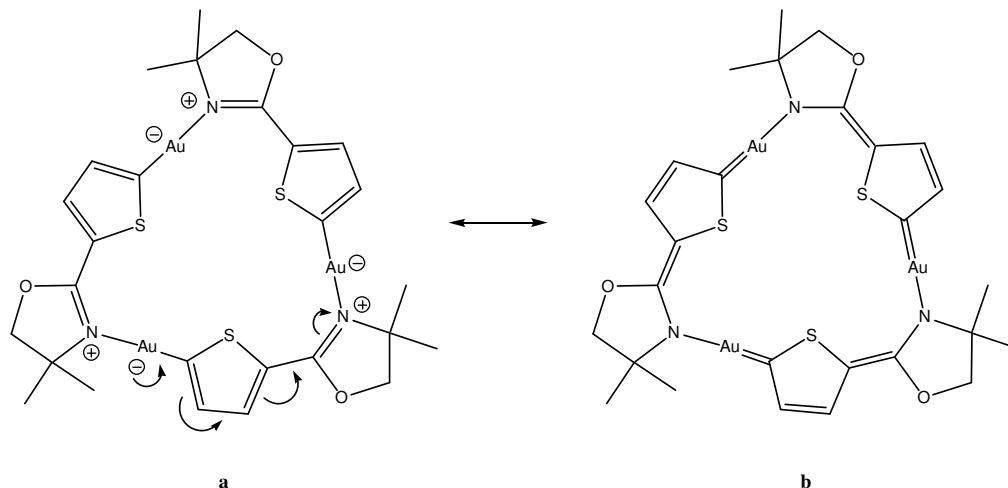
- (b) By utilising a bis(imidazolylmethyl)benzene for the synthesis of the first heterometallacycles of Au^I with *N*[^]*N* bis-imine coordination the preparation methods and stability of the products should come under the spotlight; characterisation of the complexes synthesised then requires finding suitable conditions that yield a porous crystal structure; the study of a porous crystal structure further entails removal of the solvent by suitable means and determination of the impact of this loss onto the lattice.
- (c) The final goal of this Chapter was to synthesise and characterise new [Au₂(μ-²L)₃]²⁺-type complexes where ²L is not a simple phosphane ligand to complement the small number of related phosphane complexes already known.

4.2 Results and discussion

4.2.1 Synthesis and structural characterisation of a trimeric, 18-membered heterometallacycle with *N*[^]*C*⁻ coordination: *cyclo-tris*{[μ-4,4-dimethyl-2-(thien-2-yl-κC⁵)oxazoline-κN]gold}, *I*

The compound, shown in Scheme 4.8, has been isolated before by *Desmet et al.* but was incompletely characterised.¹⁰ Only the connectivities within the compound could be established from unsatisfactory crystal data; space group problems prevented a more thorough investigation. The compound is related to other cyclic carbenes [*cf.* Scheme 4.1 (*a*)] and two important resonance structures can be drawn as is shown in Scheme 4.8 The compound is related to a remote carbene complex⁵¹ since the active nitrogen atom (bonded to Au^I) is distant from the carbene carbon atom, stabilisation through the α-sulfur atom will be less pronounced.

⁵¹ Compare the complexes in: H. G. Raubenheimer, M. Desmet, P. Olivier and G. J. Kruger, *J. Chem. Soc., Dalton Trans.* **1996**, 4431–4438.



Scheme 4.8 Connectivity of carbene compound **1** [(ionic representation (*a*)] and its neutral resonance structure, (*b*); formal electron pair movements are only shown for one thienyl-oxazoline unit in (*a*).

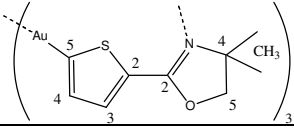
4.2.1.1 Synthesis and spectroscopic characterisation of complex **1**.

The ligand 4,4-dimethyl-2-(thien-2-yl)oxazoline can be deprotonated either at C-3 or C-5 of the thiophene ring, depending on whether butyllithium or the sterically hindered lithium bis(methylethyl)amide is employed.⁵² Upon deprotonation at C-5 and reaction with (tht)AuCl the ligand cleanly formed a colourless cyclic trimer, **1**, in high yield.

NMR data are reported in Table 4.1, assignments are in accordance with related literature values.⁵³ The ¹³C chemical shift at δ 165.3 of the thiophene ring at C-5 (free ligand: δ 126.5; $\Delta\delta$ 38.8) suggests only a small contribution from resonance structure (*b*) of Scheme 4.8. The resonance of the aurated C-3 of the typical remote carbene complex, *N*-protonated [4,4-dimethyl-2-(thien-2-yl- κ C³)oxazoline](triphenylphosphane)gold occurs at much lower field strength at δ 190.9¹⁰ ($\Delta\delta$ 61.4). Further proof of the predominance of the imine-coordinated thienylgold structure of **1** was obtained from the crystal structure determination described below.

52 A. J. Carpenter and D. J. Chadwick, *J. Chem. Soc., Perkin Trans. 1* **1985**, 173–181.

53 S. Selvaratnam, K. M. Lo and V. G. K. Das, *J. Organomet. Chem.* **1994**, 464, 143–148.

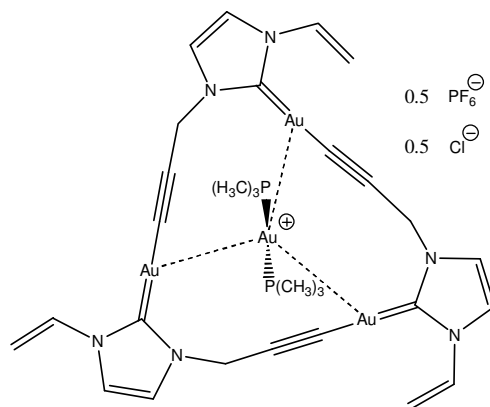
Table 4.1 NMR data of compound **1** recorded in CDCl₃^a


Nucleus		
¹ H (300 MHz)	H-4 thiophene (C11H)	7.90 (d, ³ J _{HH} 3.65, 3 H)
	H-3 thiophene (C12H)	7.04 (d, ³ J _{HH} 3.65, 3 H)
	CH ₂ oxazoline (C15H ₂)	4.30 (s, 6 H)
	CH ₃ oxazoline (C27H ₃ , C28H ₃)	1.56 (s, 18 H)
¹³ C{ ¹ H} (75.4 MHz)	C-5 thiophene (C10)	165.3 ^b
	C-4 thiophene (C11)	125.9
	C-3 thiophene (C12)	134.6 ^c
	C-2 thiophene (C13)	136.0 ^c
	C-2 oxazoline (C14)	164.4 ^b
	C-4 oxazoline (C15)	79.7
	C-5 oxazoline (C16)	67.8
	CH ₃ oxazoline (C17, C18)	28.9

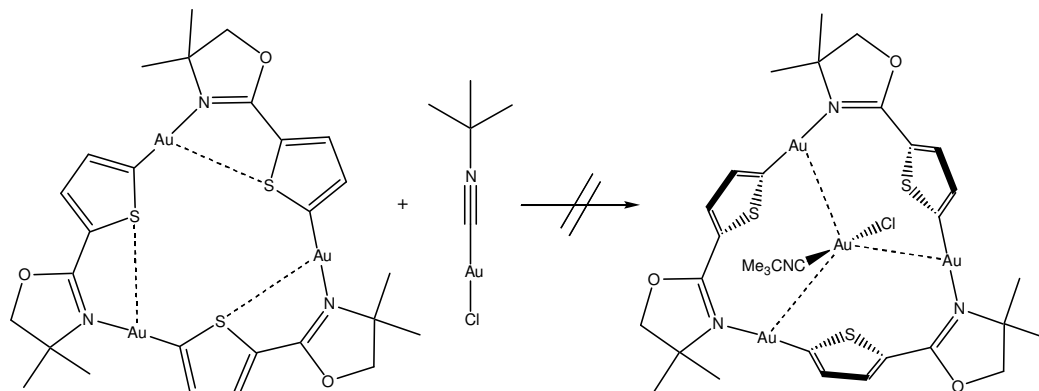
^a The atom numbering in brackets corresponds to the atom labels in Figures 4.1 and 4.3
^{bb,cc} These assignments are uncertain due to very similar shifts

ESI-mass spectrometric analysis of **1** did not exhibit m/z values corresponding to a molecular ion. The base peak at m/z 559 was assigned to [AuL₂]⁺.

Encouraged by the recent isolation of an unprecedented gold rotaxane in our laboratory comprising an 18-membered ring trapping a [Au(PMe₃)₂]⁺ group in the centre by aurophilic interactions (Scheme 4.9),⁴² the possible incorporation of metal cations into the heterometallacyclic ring system of **1** was investigated.

**Scheme 4.9** Cationic rotaxane complex comprising an 18-membered ring.

As the distance between the Au atoms in the structures of **1** is such that it would allow accommodation of another gold atom in the centre of the cycle forming three aurophilic interactions of *ca.* 3.65 Å, such a reaction was attempted as well. However, **1** does not react with chloro(2-isocyano-2-methylpropane)gold (Scheme 4.10) which was selected as a reagent due to its linear shape precluding any steric disturbances in the reaction.



Scheme 4.10 Possible reaction of **1** with Me₃CNCAuCl.

Solely crystals identified as **1**·0.75C₄H₈O were recovered when the reaction mixture was crystallised. The failure to react could possibly be ascribed to the stabilising Au⁺··S contacts within the macrocycle (*vide infra*), as a consequence the thiophene rings are held in place and do not twist 90° out of the cycle's plane to allow entrance of another Au^I centre and formation of a rotaxane. Alternatively, breaking of one Au–N bond and re-closure of the heterometallacycle would also allow the guest molecule to be accommodated, again the favourable Au⁺··S interactions most likely preclude this pathway. The three Au⁺··S contacts averaging distances of 3.29 Å in both molecular structures of **1** could be stronger than three aurophilic contacts at 3.65 Å.

4.2.1.2 Crystallography.

The crystallisation of compound **1** from thf/pentane afforded monoclinic yellowish crystals of **1**·0.75C₄H₈O (space group *C2/c*). Based on the similar normalised volume (874 Å³ in **1**·0.75C₄H₈O vs. 862 Å³ in the previous attempt) it is possible that the previous attempt to determine the crystal and molecular structure^{10a} also furnished this 6:8 thf solvate; albeit the data was solved for a wrong, triclinic lattice and space group

$P\bar{1}$ which could only establish the connectivities of the molecule. Selected bond lengths and angles of the structures of **1** are presented in Table 4.2.

The crystal and molecular structure of $1 \cdot 0.75\text{C}_4\text{H}_8\text{O}$ consists of neutral, isolated molecules shown in Figure 4.1. The C_2 axis of the $C2/c$ space group is necessarily separated from the molecule affording 8 molecules per unit cell. A possible threefold rotation symmetry in a trigonal or hexagonal lattice is not realised and the whole heterometallacycle is asymmetric and appears somewhat curved rather than being flat. The molecules of $1 \cdot 0.75\text{C}_4\text{H}_8\text{O}$ are ordered so that columns of thienyloxazoline groups form along the b axis, but closer association (*e.g.* π -stacking) is rendered impossible by the methyl substituents at the oxazoline, see Figure 4.2.

The thf molecules located in channels could not be modeled owing to their high disorder and their electron density was removed using the Squeeze routine in the Platon set of programmes.⁵⁴ A rough estimate of the number of thf molecules per unit cell was obtained from this process; to gain further evidence and unambiguously determine the identity of the co-solvent (as thf and pentane comprise 40 and 42 electrons, respectively, identification by electron density is impossible) several crystals were harvested and an ^1H NMR spectrum recorded. From the integrals of the

Table 4.2 Bond lengths/Å and angles/° of the solvates of compound **1**.

Solvate	$1 \cdot 0.75\text{C}_4\text{H}_8\text{O}$	$1 \cdot 2\text{C}_4\text{H}_8\text{O}$		$1 \cdot 0.75\text{C}_4\text{H}_8\text{O}$	$1 \cdot 2\text{C}_4\text{H}_8\text{O}$
Au1–C10	1.985(5)	1.982(6)	N1–C14	1.286(6)	1.280(8)
Au2–C20	1.990(5)	1.981(6)	N2–C24	1.272(6)	1.286(8)
Au3–C30	1.981(5)	1.989(6)	N3–C34	1.270(6)	1.276(8)
Au1–N2	2.059(4)	2.049(5)	Au1 \cdots Au1'		3.4988(6)
Au2–N3	2.058(4)	2.048(5)	Au3 \cdots Au3''		3.5172(7)
Au3–N1	2.051(4)	2.056(5)			
Au1 \cdots S2	3.270(3)	3.249(2)	C10–Au1–N2	175.1(2)	174.5(2)
Au2 \cdots S3	3.275(2)	3.358(2)	C20–Au2–N3	175.4(2)	174.2(2)
Au3 \cdots S1	3.277(2)	3.338(2)	C30–Au3–N1	172.1(2)	174.5(2)
	Angles of the thiophene ring planes with the Au1 Au2 Au3 plane			24.0(2)	21.0(2)
				8.6(2)	23.5(3)
				6.8(2)	17.6(3)

Symmetry codes: ' = $-x, 1 - y, 2 - z$; '' = $-x, 1 - y, 1 - z$.

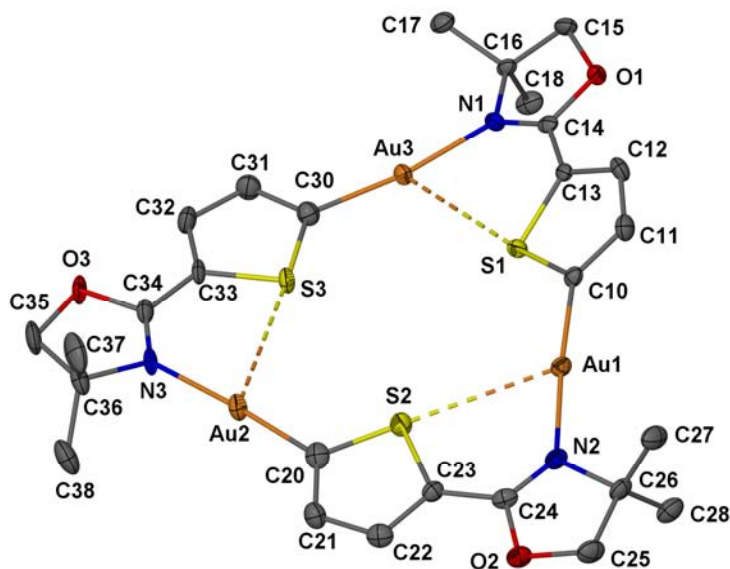


Figure 4.1 Molecular structure of $1 \cdot 0.75\text{C}_4\text{H}_8\text{O}$, disordered thf is not shown.

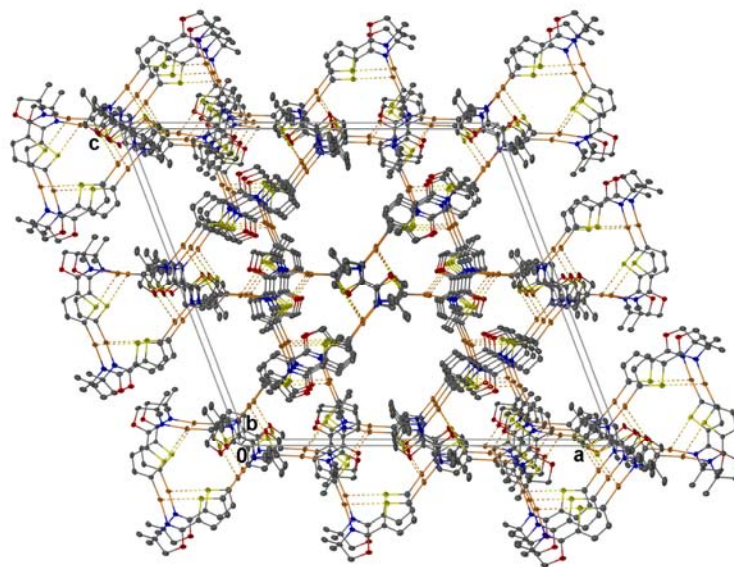


Figure 4.2 Packing diagram of $1 \cdot 0.75\text{C}_4\text{H}_8\text{O}$ showing stacks of the thienyloxazoline moieties; the channels in between are occupied by thf solvent (not shown).

solvent signals, now clearly identified as thf by their chemical shift and multiplicity, relative to the methyl peaks of **1** the crystal stoichiometry was unambiguously shown to be $1 \cdot 0.75\text{C}_4\text{H}_8\text{O}$, which is also completely in agreement with the residual electron density removed per unit cell.

From the molecular structure of $1 \cdot 0.75\text{C}_4\text{H}_8\text{O}$ it is immediately apparent why the ligands form cyclic trimers with gold, the geometry is predestined for three short $\text{Au}\cdots\text{S}$ contacts ranging from 3.270(3) to 3.277(2) Å. Such interactions are commonly observed with compounds containing gold and thiazole or thiophene rings,⁵⁵ further examples involving thiazole groups are discussed in Chapters 3 and 5. During synthesis these contacts are thought to direct the mutual orientation of the two heterocycles in the ligand to an (*E*)-configuration finally closing the ring rather than form polymeric chains, as was observed with other related compounds (*cf.* Section 4.2.3.2).

The Au–C distances in $1 \cdot 0.75\text{C}_4\text{H}_8\text{O}$ measure 1.985(5) Å on average which is comparable to the related dimeric heterometallacycle where C-3 of the thiophene ring is metalated [Au–C distances 2.01(1) and 2.04(1) Å]¹⁰ and significantly shorter than in the C-2 aurred deprotonated thienylgold(I) complex $\text{Ph}_3\text{PAuC}_4\text{H}_3\text{S}$ [Au–C distance 2.038(3) Å].⁵⁶ The Au–N bond lengths in $1 \cdot 0.75\text{C}_4\text{H}_8\text{O}$ average at 2.056(4) Å, again comparable to the C-3 aurred dimeric heterometallacycle [Au–N distances 2.065(8) and 2.081(8) Å], but are significantly longer than in a polyaurated cluster where one Au^{I} is coordinated by two imine nitrogen atoms of 2,4,4-trimethyloxazoline [1.99(1) Å].⁵⁷ However, this latter gold centre is cationic and additional effects from polyauration may also influence the bond length.

Later, in an attempt to co-crystallise **1** with chloro(2-isocyano-2-methylpropane)gold, colourless plates of triclinic $1 \cdot 2\text{C}_4\text{H}_8\text{O}$ in space group $P\bar{1}$, shown in Figure 4.3, were isolated. The structure contains two thf solvent molecules in the asymmetric unit and thus strictly is not a polymorph of the original $1 \cdot 0.75\text{C}_4\text{H}_8\text{O}$. Apart from the different stoichiometry of the co-crystallised solvent, the main difference between the two structures is the presence of weak $\text{Au}\cdots\text{Au}$ interactions to neighbouring molecules in $1 \cdot 2\text{C}_4\text{H}_8\text{O}$ with $\text{Au}\cdots\text{Au}$ distances of 3.4988(6) and 3.5172(7) Å. These aurophilic bonds to symmetry-generated atoms link individual cycles to infinite chains running

55 See for example: (a) S. Y. Ho and E. R. T. Tiekink, *Z. Kristallogr. – New Cryst. Struct.* **2003**, *218*, 73–74; (b) U. Monkowius, S. Nogai and H. Schmidbaur, *Z. Naturforsch., B: Chem. Sci.* **2003**, *58*, 751–758; (c) E. J. Fernández, A. Laguna, J. M. López-de-Luzuriaga, M. Monge, M. Montiel, M. E. Olmos and M. Rodríguez-Castillo, *Dalton Trans.* **2006**, 3672–3677.

56 K. A. Porter, A. Schier and H. Schmidbaur, *Organometallics* **2003**, *22*, 4922–4927.

57 F. Scherbaum, B. Huber, G. Müller and H. Schmidbaur, *Angew. Chem., Int. Ed. Engl.* **1988**, *27*, 1542–1544 (*Angew. Chem.* **1988**, *100*, 1600–1602).

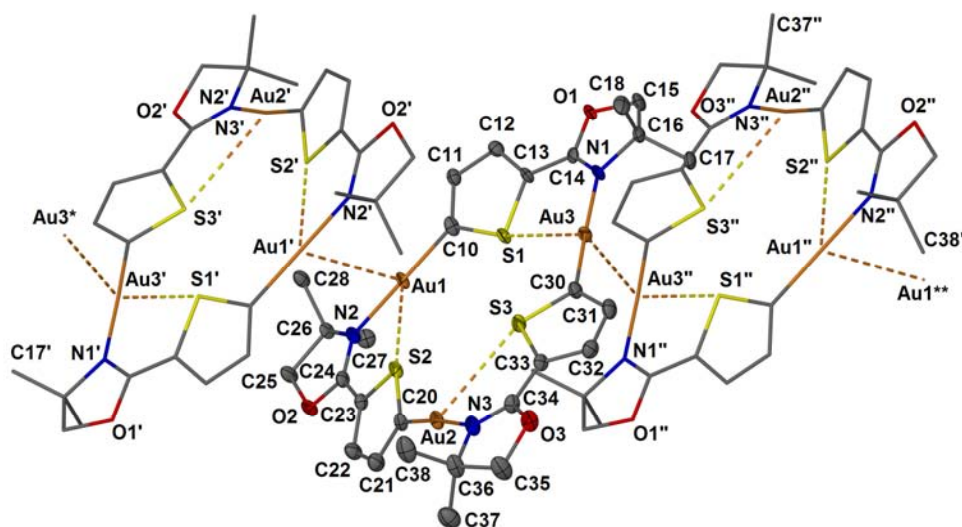


Figure 4.3 Molecular structure of $1 \cdot 2C_4H_8O$, two neighbouring cycles linked to **1** by aurophilic interactions are represented as stick-models; symmetry codes ' = $-x, 1 - y, 2 - z$; '' = $-x, 1 - y, 1 - z$; * = $-x, y, 1 + z$; ** = $x, y, z - 1$; co-crystallised thf is not shown.

parallel to the c axis (Figure 4.4). This motif has been observed in the much simpler trimeric carbene complex $[Au\{\mu-[C(NCH_2Ph)(OMe)]\}]_3$, albeit with on average longer intermolecular $Au \cdots Au$ distances, the shortest being 3.698 \AA .⁵⁸

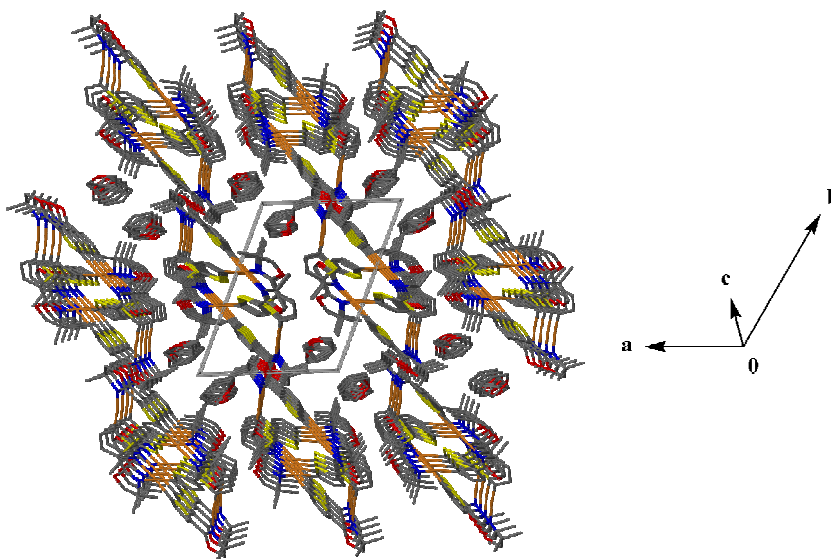


Figure 4.4 Packing diagram of $1 \cdot 2C_4H_8O$ viewed along the c axis, atoms are shown in stick representation, no $Au \cdots Au$ or $Au \cdots S$ contacts are indicated; the molecules are linked by aurophilic interactions into chains running parallel to the c axis, surrounded by channels that contain molecules of thf.

⁵⁸ A. L. Balch, M. M. Olmstead and J. C. Vickery, *Inorg. Chem.* **1999**, *38*, 3494–3499.

A higher degree of twisting of the thiophene rings out of the plane defined by the gold centres [average 20.7°] is also noted, which may be as a result of the additional stabilisation by aurophilic interactions thus weakening the Au \cdots S contacts. Two of these Au \cdots S contacts in **1**·2C₄H₈O consequently are notably longer [3.338(2) and 3.358(2) Å; one Au \cdots S contact of 3.249(2) Å is similar to **1**·0.75C₄H₈O] than in the other solvate. In the structure of **1**·0.75C₄H₈O only one thiophene ring exhibits a twist angle of $24.0(2)^\circ$ while the other two align closely with the Au₃-plane with twist angles of $8.6(2)^\circ$ and $6.8(2)^\circ$. The Au–C and Au–N bonds [average values 1.984(6) and 2.051(5) Å] in **1**·2C₄H₈O are virtually identical to those in the 6:8 thf solvate.

The question to what extent both molecular structures of **1** exhibit carbene character can be answered by comparing distinctive bond lengths within the thienyloxazoline backbone; Au–C bond lengths, on the other hand, are not useful as they are usually insensitive to the nature of the bond and/or ligand.⁵⁹ As indicated in Scheme 4.8, the resonance form (*b*) that contains a metal-carbon double bond also requires double bonds between the thiophene and oxazoline rings (labeled C13–C14 in Figure 4.1) as well as a double bond between C-3 and C-4 (C11–C12) of the thiophene unit; in addition the C-2–N bond (C14–N1) in the oxazoline fragment should be longer than a double bond.

The average bond lengths of these bonds in the two solvates of **1** are 1.443(6), 1.404(9) and 1.278(7) Å, respectively. The first bond linking both heterocycles in the ligand moiety is clearly longer than the average length of a conjugated C–C double bond (1.345 Å) and the C-3–C-4 (C11–C12) bond of the thiophene ring (which should be shortened if the resonance structure incorporating the Au–C double bond was prevalent) is comparable to the average in thiophenes (1.424 Å). Finally, the latter separation is in accordance with the typical value for a C sp^2 –N sp^2 double bond (1.279 Å).⁶⁰ The bond lengths found in both solvates of **1** also closely resemble those found in organotin derivatives of 4,4-dimethyl-2-(thien-2-yl)oxazoline which should

59 A. G. Orpen, L. Brammer, F. H. Allen, O. Kennard, D. G. Watson and R. Taylor, *J. Chem. Soc., Dalton Trans.* **1989**, S1–S83.

60 F. H. Allen, O. Kennard, D. G. Watson, L. Brammer, A. G. Orpen and R. Taylor, *J. Chem. Soc., Perkin Trans. 2* **1987**, S1–S19.

not exhibit any carbene character.^{53,61} Together with the ^{13}C NMR data (*vide supra*), it is concluded that the imine-coordinated thienylgold resonance structure [Scheme 4.8 (a)] is the main contribution to the actual bonding situation in **1**.

Taking both solvates of **1** presented above into account, it is again evident that having another look at crystallisations can be worthwhile and indeed often more than one structure of a given compound could be isolated when more than one crystallisation was set up. In this case, the second solvate was obtained from a failed reaction attempt and the presence of other chemical species might have had an influence in the crystallisation process of **1**. Differences and similarities between the structures obtained can lead to a greater understanding of the factors that influence a compound to crystallise in the way it is found in a specific polymorph or solvate.

4.2.2 Synthesis of gold complexes of bitmb – the $[\text{Au}_2(\mu\text{-bitmb})_2]^{2+}$ cation, **2**

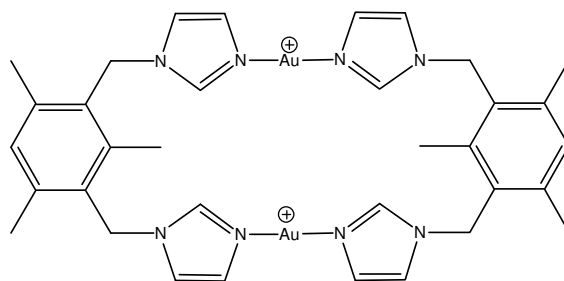
Homoleptic heterometallacycles incorporating Au^{I} coordinated by imine nitrogen atoms from imidazole moieties have not been reported so far. Complexes of bis[(benz)imidazol-1-ylmethyl]benzenes are generally obtained by allowing the ligand and a suitable metal salt to crystallise during evaporation of the chosen solvent.^{35,62}

This approach, however, is unsuitable for Au^{I} as binary salts of weakly or non-coordinating anions are not available and, furthermore, exposure to the atmosphere during crystallisation may lead to decomposition of the complex. The latter concern proved to be insubstantial since it was found out later that Au^{I} complexes derived from bitmb are certainly amongst the most stable compounds reported in this dissertation and can be stored at room temperature without noticeable decomposition for years.

61 K. M. Lo, S. Selvaratnam, S. W. Ng, C. Wei and V. G. K. Das, *J. Organomet. Chem.* **1992**, 430, 149–166.

62 L. Dobrzańska, G. O. Lloyd, T. Jacobs, I. Rootman, C. L. Oliver, M. W. Bredenkamp and L. J. Barbour, *J. Mol. Struct.* **2006**, 796, 107–113.

Synthesis, therefore, started from (tht)AuCl with both the chloride and labile tht ligand to be substituted. Initially, a reaction was conducted by dissolving (tht)AuCl in ethanenitrile and adding 1.2 mole equivalents tht to stabilise the gold against loss of chloride. Subsequent addition of Ag[BF₄], filtration of precipitated AgCl and addition of a bitmb solution in MeCN afforded compound **2a** with the cation shown in Scheme 4.11. However, this procedure was found to be unsuitable and upon crystallisation, a crystal of a mixed [AgAu(μ-bitmb)₂]²⁺ species was isolated in place of the expected [Au₂(μ-bitmb)₂]²⁺ complex, a pure crystal was isolated only after an additional recrystallisation.



Scheme 4.11 Structure of the cation in compounds **2a** and **2b**.

To avoid further interference from Ag⁺, it was substituted by Na⁺ in a subsequent preparation using NaOTf that readily effected reaction in ethanenitrile. Owing to the negligible solubility of NaCl⁶³ – which precipitates and drives the reaction – in this solvent and the minimal affinity for Na⁺ towards the ligands employed, clean and high yield reactions were found. The same approach was subsequently used for all other reactions reported in the following chapters when chloride had to be exchanged under anhydrous conditions.

The products obtained by the two methods (with Ag⁺ or Na⁺ salts) both contained the cyclic cation shown in Scheme 4.11 but differ in the counter ions ([BF₄]⁻ in **2a** and CF₃SO₃⁻ in **2b**, respectively).

4.2.2.1 Spectroscopic characterisation.

The compounds *cyclo*-bis{[μ-1,3-bis(imidazol-1-ylmethyl)-2,4,6-trimethylbenzene]}-digold(2+) tetrafluoroborate, **2a**, and -triflate, **2b**, were characterised by ¹H and, for

63 T. Pavlopoulos and H. Strehlow, *Z. Phys. Chem.* **1954**, 202, 474–479.

2b, ^{13}C NMR spectroscopy as well as ESI-mass spectrometry. NMR data are given in Table 4.3. The solubility of the tetrafluoroborate salt was too low to allow recording of a ^{13}C NMR spectrum.

Table 4.3 NMR data of compounds **2a** and **2b** in CD_2Cl_2 solution.^a

Nucleus	Frequency	300 MHz		600 MHz (^1H) 151 MHz (^{13}C)	
^1H	H-2 imidazole (C11H)	7.80 (m, 4 H)		7.95 (m, 4 H)	
	H-4 imidazole (C12H)	7.36 (m, 4 H)		7.34 (m, 4 H)	
	H-5 imidazole (C13H)	7.18 (m, 6 H) ^b		7.16 (m, 4 H)	
	H-5 benzene (C34H)	7.18 (m, 6 H) ^b		7.14 (s, 2 H)	
	1/3- CH_2 (C14H ₂)	5.22 (s, 8 H)		5.19 (s, 8 H)	
	2- CH_3 (C33H ₃)	2.17 (s, 6 H)		2.14 (s, 6 H)	
	4/6- CH_3 (C43H ₃)	2.27 (s, 12 H)		2.27 (s, 12 H)	
	$^{13}\text{C}\{^1\text{H}\}$	C-2 imidazole (C11)			140.3 (s)
C-4 imidazole (C12)				121.0 (s)	
C-5 imidazole (C13)				130.0 (s)	
C-1/3 benzene (C31)				140.4 (s)	
C-2 benzene (C32)				138.4 (s)	
C-4/6 benzene (C35)				132.3 (s)	
C-5 benzene (C34)				127.6 (s)	
1/3- CH_2 (C14)				47.6 (s)	
2- CH_3 (C33)				15.6 (s)	
4/6- CH_3 (C34)				19.5 (s)	

^a The atom numbers in brackets correspond to the atom labels in Figures 4.5 and 4.7

^b The signals are not resolved at 300 MHz ^c The CF_3SO_3^- carbon was not observed due to low signal intensity and signal splitting. Aromatic carbon assignments are ambiguous

The mass spectroscopic data of **2a** and **2b**, summarised in Table 4.4, unambiguously confirmed the structures of the compounds as 2:2 complexes of the $[\text{Au}_2(\mu\text{-bitmb})_2]^{2+}$ type. These cations were observed as base peaks at a 15 V cone voltage. Especially the additional $[\text{Au}_2(\text{anion})(\mu\text{-bitmb})_2]^+$ signals are interesting as they already suggest cavities within the crystals wherein suitable guests can be accommodated. No evidence of mixed $[\text{AgAu}(\mu\text{-bitmb})_2]^{2+}$ -species was obtained from the mass spectrum of **2a**.

Table 4.4 ESI mass spectrometric data of **2a** and **2b**; L = bitmb.

Compound	2a	2b
Empirical formula	C ₃₄ H ₄₀ Au ₂ B ₂ F ₈ N ₈	C ₃₆ H ₄₀ Au ₂ F ₆ N ₈ O ₆ S ₂
Exact mass	1128.28 ^a	1252.17
<i>m/z</i> (Int.) [Au ₂ (μ ⁻² L) ₂] ²⁺ ^b	477 (100)	477 (100)
<i>m/z</i> (Int.) [Au ₂ (anion)(μ ⁻² L) ₂] ⁺	1041 (68)	1103 (20)
<i>m/z</i> (Int.) Others	715 (60) 685 (50)	281 (10) ^c

^a Calculated with ¹¹B isotope ^b Cation: [C₃₄H₄₀Au₂N₈]²⁺, exact mass 954.27 ^c [L + H]⁺

Attempts were made to utilise the two gold centres of **2a** in attracting another metal fragment towards the centre of the heterometallacyclic ring system. The distance between the gold atoms of *ca.* 2 × 3.5 Å should be suitable to accommodate metallophilic interactions. Furthermore, the flexible bis(imidazole)gold groups should be able to move closer to each other thus adjusting to the required distances for a particular situation. As a co-crystallising guest, chloro(2-isocyano-2-methylpropane)gold was selected. Crystallisation from ethanenitrile afforded only crystals having the same unit cell as the already known structure of **2a**·2MeCN.

Allowing for a too bulky dimethylethyl group, HgCl₂ was then utilised in another attempted co-crystallisation with compound **2b** from MeCN layered with Et₂O. Only an amorphous precipitate was obtained whereas **2b** always furnished crystals under these conditions.

4.2.2.2 Crystallographic characterisation of the complexes.

Bond lengths, angles and, for comparison, unit cell parameters of all structures obtained are summarised in Table 4.5. All products crystallise in the orthorhombic space group *Pnma* and exhibit a proper mirror plane that bisects the benzene rings and solvent molecules when contained in the cavity. Aurophilic interactions occur between the metal centres of different molecules.

Complex **2a** was crystallised from MeCN/Et₂O and colourless needles of **2a**·2CH₃CN were obtained. The [Au₂(μ-bitmb)₂]²⁺ cations form “boxes” (Figure 4.5) that accommodate the solvent guests ordered in an antiparallel manner as expected for the highly

Table 4.5 Bond lengths/Å, angles/° and unit cell parameters of structures of **2a** and **2b**

Compound	2a ·2CH ₃ CN	2a ·2CH ₂ Cl ₂	2b ·2CH ₂ Cl ₂	2b ·0.7CH ₂ Cl ₂
Au··Au'	3.5490(5)	3.3580(7)	3.2885(8) ^c	3.4444(5)
Au–N1	1.996(3)	2.013(7)	2.001(6)	1.987(4)
Au–N2	2.001(3)	2.000(7)	2.007(6)	2.002(4)
Box dimension ^a <i>x</i> /Å	7.060	7.107	6.806	6.719
Box dimension ^b <i>y</i> /Å	9.996	9.954	9.975	10.005
N1–Au–N2	176.9(2)	175.9(3)	175.4(2)	177.1(2)
Interplanar angle defined by the benzene rings of a box	19.4(3)	19.1(7)	22.8(6)	19.5(4)
Interplanar angle defined by Au(imidazole) ₂ fragments	88.31(7)	79.5(2)	43.0(2)	53.9(1)
<i>a</i> /Å	19.296(3)	19.691(3)	21.860(6)	21.076(3)
Unit cell axes <i>b</i> /Å	20.243(3)	19.921(3)	18.886(5)	19.034(3)
<i>c</i> /Å	11.081(2)	11.292(2)	11.726(3)	11.665(2)
Unit cell volume/Å ³	4328(1)	4429(2)	4841(2)	4680(2)

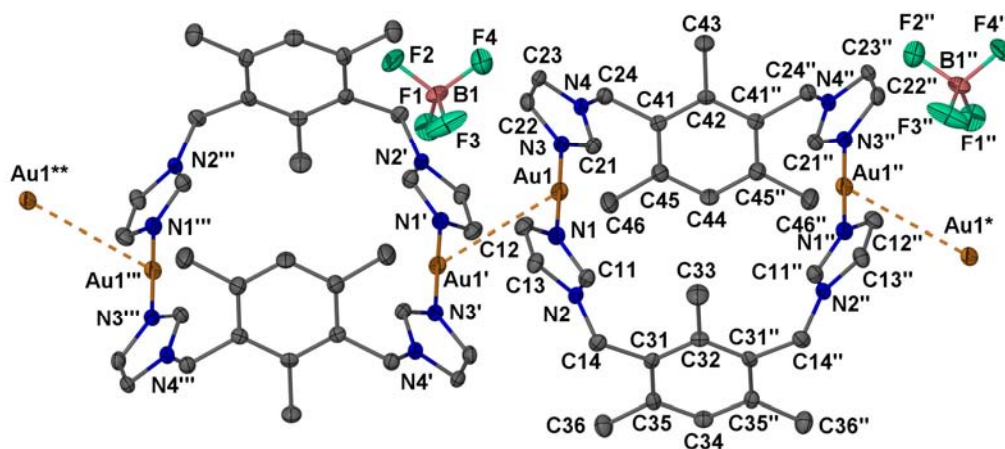
Symmetry code: ' $-x, 1 - y, -z$ ^a Intramolecular distance between Au atoms^b Intramolecular benzene ring centroid distance ^c Symmetry code $1 - x, -y, 1 - z$.

Figure 4.5 Two cationic metallacycles of **2a**·2CH₃CN linked by aurophilic interactions which are propagated along the *b* axis; the solvent molecules occupying the space within the cycles are not shown, only two representative [BF₄]⁻ anions are drawn and others are omitted for clarity; symmetry codes ' = $-x, 1 - y, 1 - z$; '' = $x, 3/2 - y, z$; ''' = $-x, y - 1/2, 1 - z$; * = $-x, 1/2 + y, 1 - z$ and ** = $x, 1/2 - y, z$; inversion centres are located halfway along aurophilic bonds and mirror planes bisect atoms C32, C33, C34, C42, C43 and C44.

dipolar ethanenitrile. Tetrafluoroborate counter ions are located outside the cation rings next to the gold centres, most likely attracted by Coulomb forces. The

heterometallacycles are themselves interlinked by relatively weak aurophilic interactions at 3.5490(5) Å. Owing to this attraction the N–Au–N angle [176.9(2)°] slightly deviates from the ideal linear geometry. The Au–N bond distances of 1.996(3) and 2.001(3) Å, respectively, are comparable to the only other report of a structure of a proper bis(imidazole- κN) coordination of Au^I, bis[4-(hydroxymethyl)-1,5-dimethylimidazole]gold(1+) chloride [2.011(5) and 2.000(5) Å].⁶⁴

The one objective of obtaining a porous structure was not realised. The individual boxes are oriented at *ca.* 90° towards each other in the *ac* plane and possible channels running in the *c* direction are partially obstructed by the trimethylbenzene rings.

Complex **2a** was therefore recrystallised from dichloromethane which yielded crystals of **2a**·2CH₂Cl₂ similar in appearance and unit cell dimensions to the previous crystal. A packing diagram of the crystal structure is shown in Figure 4.6. The aurophilic interactions linking the cations together along the *b* axis now occur at a much shorter distance [3.3580(7) Å] and are thus stronger than in the bis-ethanenitrile solvate. The Au–N bonds are not altered [2.000(7) and 2.013(7) Å] and are virtually the same as in bis[4-(hydroxymethyl)-1,5-dimethylimidazole]gold(1+) chloride.⁶⁴

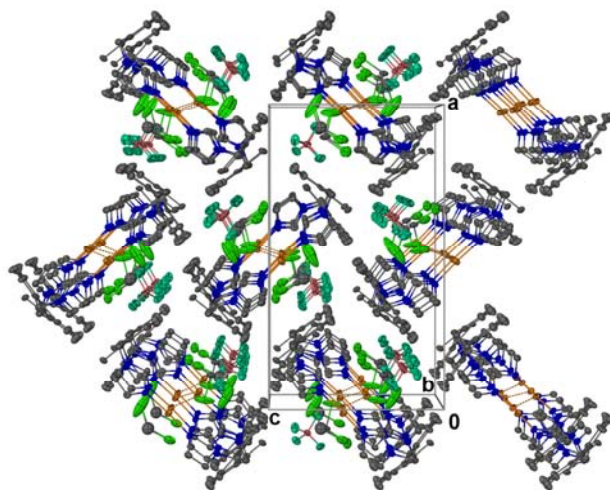


Figure 4.6 Packing of **2a**·2CH₂Cl₂ viewed along the *b* axis showing the orientation of the cations (linked by Au⁺–Au interactions parallel to the *b* axis) towards each other, in this arrangement trimethylbenzene rings obstruct possible movement of CH₂Cl₂ in the channels.

⁶⁴ C. J. L. Lock and Z. Wang, *Acta Crystallogr., Sect. C: Cryst. Struct. Commun.* **1993**, *49*, 1330–1333.

Compared to both solvates of **2a**, the interplanar angle of the two Au(imidazole)₂ fragments forming the “walls” of the box is smaller [43.0(2)° in **2b**·2CH₂Cl₂ compared to 79.5(2)° and 88.31(7)° for the structures of **2a**] leading to a smaller intramolecular separation of the Au centres. Accordingly, the *b* axis (along which the cations are arranged by aurophilic interactions) is significantly shorter in the crystal structure of **2b**·2CH₂Cl₂ compared to the solvates of **2a**.

One dichloromethane solvent molecule is heavily disordered and electron density belonging to it was removed using the Squeeze routine in the Platon set of programmes.⁵⁴ The other CH₂Cl₂ molecule, however, is firmly held in place by what could amount to agostic Au···H interactions (Au···H distance 2.77 Å, similar to those found for compound **8b** in Chapter 5 where the interaction is intramolecular and thus observable in the ¹H NMR spectrum) and the halogen may interact with the benzene rings (distance between Cl atoms and the benzene centroids 3.594 and 3.518 Å).

Although the metallacycles are again stacked at an angle against each other in the *ac* plane, pores are found to be running along the *c* axis that are not seriously obstructed by the benzene rings (Figure 4.8) and experiments exploring the porous character of the crystal were performed.

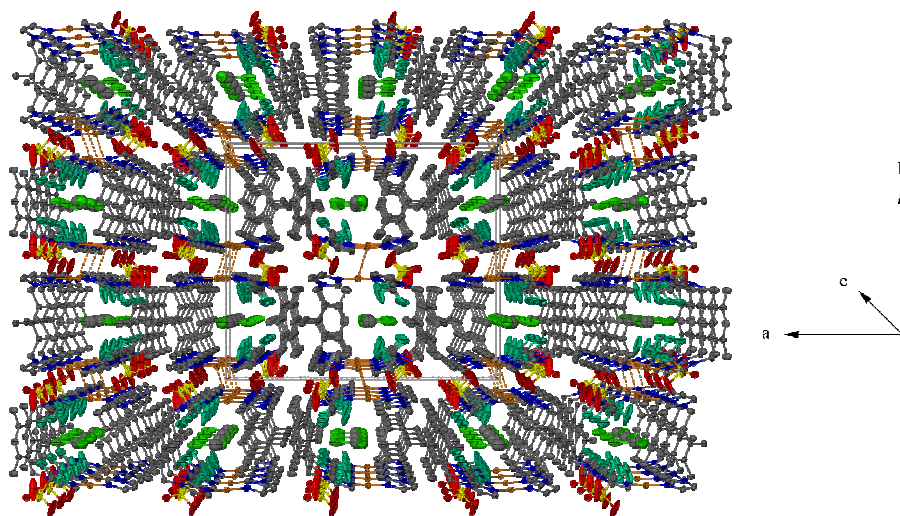


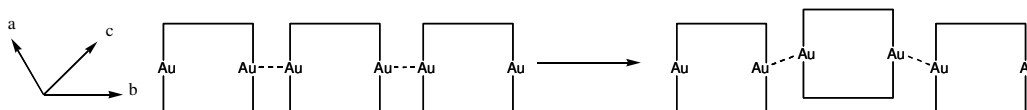
Figure 4.8 Packing diagram of **2b**·2CH₂Cl₂ seen along the *c* axis and showing the pores occupied by the dichloromethane solvent; only one CH₂Cl₂ is shown per asymmetric unit.

4.2.2.3 Removal of solvent from **2b**·2CH₂Cl₂.

Crystals of **2b**·2CH₂Cl₂ obtained from dichloromethane/pentane were heated under vacuum and the crystals then re-examined by X-ray diffraction. It was noted that evacuation causes the crystals to ‘crack’ and somewhat lose their shine. The diffraction pattern, however, clearly indicates preserved crystallinity in the material after removal of the solvent – the data quality obtained from the ‘cracked’ crystal was actually better than that of **2b**·2CH₂Cl₂.

After evacuation of **2b**·2CH₂Cl₂ for 45 min. at 72 °C the crystals were still found to contain 1.2 molecules of dichloromethane per [Au₂(μ-bitmb)₂]²⁺ unit. Subsequent heating at 90 °C for another hour under dynamic vacuum reduced the dichloromethane content to 0.7 per cation. Even prolonged heating and evacuation at this temperature for 12 hours did not lower the CH₂Cl₂ content any further, indicative of unusually strong host-guest interactions. It is not clear whether the Au[⋯]H interactions mentioned above play a role in this behaviour. Applying higher temperatures during evacuation was prohibitive due to the sensitivity of gold complexes. However, the possibility to remove 1.3 CH₂Cl₂ is proof that the pores in the crystal structure do allow migration of the solvent.

During removal of solvent the crystal structure underwent significant changes as is reflected in altered unit cell dimensions: the *a* and *c* axes are shortened by 0.78(1) Å and 0.061(5) Å, respectively, while the *b* axis increased by 0.15(1) Å resulting in a net decrease in unit cell volume of *ca.* 3%. The most notable difference in interaction is the much weaker aurophilic contact between the molecules, the Au[⋯]Au distance is lengthened from 3.2885(8) Å in **2b**·2CH₂Cl₂ to 3.4444(5) Å in **2b**·0.7CH₂Cl₂. The individual cations are also moved with respect to one another as is reflected in the N1–Au[⋯]Au' (' = -x, -y, -z) angle that changes from 83.0(2)° to 76.8(2)°, as schematically shown in Scheme 4.12. The Au–N bonds are unchanged on removal of the dichloromethane and the N–Au–N angle approaches 180° as a result of the weaker aurophilic interaction.

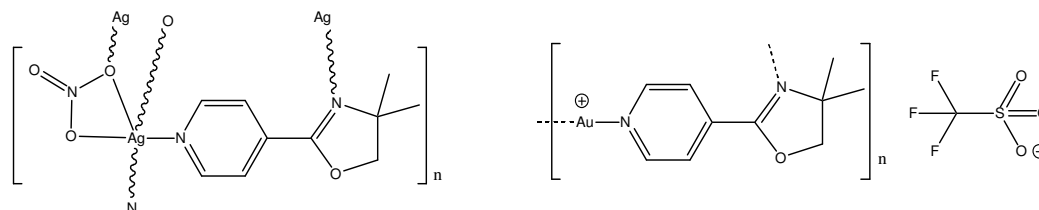


Scheme 4.12 Movement of cations perpendicular to the *b* axis upon removal of some co-crystallised CH_2Cl_2 (at 90°C , 12 h).

Summarising the results presented above, the cyclic cation **2** can be readily synthesised using the bidentate ligand bitmb and several crystal and molecular structures hosting MeCN and CH_2Cl_2 solvents were determined. The triflate salt **2b** crystallises in a porous lattice which accommodates two dichloromethane solvent molecules per heterometallacycle. Yet, only 1.3 molecules of CH_2Cl_2 can be removed by heating the crystals at 90°C (*cf.* b.p. of CH_2Cl_2 40°C) in a dynamic vacuum for 12 h showing unusually strong interaction of the heterometallacycle with CH_2Cl_2 . Removal of solvent is accompanied by changes in the arrangement of heterometallacycles in respect of each other as expressed by the significantly different unit cells.

4.2.3 Ag^{I} and Au^{I} complexes of 4,4-dimethyl-2-(pyridin-4-yl)-oxazoline, **3** and **4**

The scope of different oxazoline ligands to also form cyclic oligomers was probed by synthesising Ag^{I} and Au^{I} complexes of 4,4-dimethyl-2-(pyridin-4-yl)oxazoline (see Scheme 4.13), wherein the 2-thienyl group of the ligand used for complex **1** is replaced by a 4-pyridinyl group. The new ligand thus afforded cationic complexes *via* $N^{\wedge}N$ -coordination as opposed to 4,4-dimethyl-2-(thien-2-yl)oxazoline which afforded neutral compounds with an $N^{\wedge}C^{-}$ motif.



Scheme 4.13 Structures of compounds **3** and **4a**.

At first, a silver complex was prepared by reacting the bidentate ligand with one equivalent of AgNO_3 in MeCN to afford a precipitate of the silver complex, **3**, which

is fairly stable to ambient light in the solid state. The compound is only soluble in dmsO or water, hinting at a polymeric nature that was later verified by the determination of its crystal and molecular structure.

4.2.3.1 Spectroscopic characterisation.

NMR data of **3** is summarised in Table 4.6. The coordinated pyridine ring signals of the ligand are broadened compared to those in the free ligand which could be a sign of exchange in solution. The crystal and molecular structure of **3** (*vide infra*) revealed that the Ag^I bond to the pyridine is weaker than to the oxazoline and might be broken by dmsO or water in **3** or traces of tht for the Au–N bond in the analogous Au^I complex, **4**.

Table 4.6 NMR data of compounds **3** and **4a**.^a

Nucleus	Solvent Frequency	(CD ₃) ₂ SO	CDCl ₃
		300 MHz (¹ H) 75.4 MHz (¹³ C{ ¹ H})	600 MHz (¹ H) 151 MHz (¹³ C{ ¹ H})
¹ H	H-2/6 pyridine (C4H, C8H)	8.9 (vbr s, 2 H) ^b	8.9 (vbr s, 2 H) ^b
	H-3/6 pyridine (C5H, C7H)	7.90 (br s, 2 H)	7.94 (br s, 2 H)
	CH ₃ (C31H ₃ , C32H ₃)	1.30 (s, ¹ J _{CH} 127.5, 6 H)	1.37 (s, 6 H)
	CH ₂ (C2H ₂)	4.21 (s, ¹ J _{CH} 151.7, 2 H)	4.24 (s, 2 H)
¹³ C{ ¹ H}	C-2/6 pyridine (C4, C8)	150.9 (s)	150.5 (br s)
	C-3/5 pyridine (C5, C7)	122.5 (br s)	124.5 (br s)
	C-4 pyridine (C6)	135.0 (s)	137.7 (s)
	C-2 oxazoline (C1)	160.1 (s)	162.6 (s)
	C-4 oxazoline (C2)	67.9 (s)	69.0 (s)
	C-5 oxazoline (C3)	71.3 (s)	80.8 (s)
	CH ₃ (C31, C32)	27.9 (s)	28.2 (s)
	CF ₃ SO ₃ ⁻		121.8 (q, ¹ J _{FC} 319.7)

^a The numbering in brackets corresponds to the atom labels in Figure 4.9 (for **3**)

^b The presence of signals is supported by an integral curve with a maximum slope at 8.9 ppm.

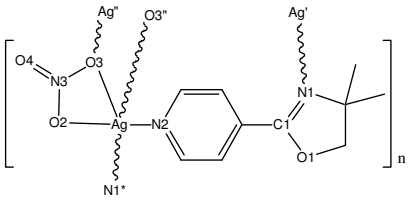
Mass spectrometric analysis of **3** using electrospray ionisation showed the protonated ligand (L) as a base peak (*m/z* 177), fragments containing silver were observed starting at *m/z* 324 (LAg⁺·MeCN; 100), other clusters containing various amounts of

Ag^+ and whose composition could not be elucidated, were observed at m/z 373 (Ag_3 , 60), 416 (Ag_2 , 40), 457 (Ag_2 , 30).

4.2.3.2 Crystallography.

Well defined polygons of **3** were obtained from a dmsO solution layered with MeCN. The molecular structure exhibits infinite chains, the silver centres are each coordinated by one pyridine and one oxazoline nitrogen atom as well as three oxygen atoms from two different nitrate anions (Figure 4.9). Bond lengths and angles are given in Table 4.7. This arrangement is in contrast to Pd^{II} complexes of a chiral 2-(pyridin-4-yl)oxazoline which forms monomeric *trans*- $[\text{PdCl}_2\text{L}_2]$ and tetrameric cyclic *all-trans*- $[(\text{PdCl}_2)_4(\mu\text{-}^2\text{L})_4]$ complexes wherein each palladium atom is exclusively coordinated by either pyridine- or oxazoline-nitrogen atoms and no head to tail arrangement is observed. In the monomeric Pd complex the pyridine nitrogen is also the preferred coordination site.⁶⁵ Examination of the relevant bond lengths reveals that the PdCl_2 fragment does not discriminate between the pyridine and oxazoline rings upon coordination. All Pd–N bonds in both complexes are in the range of 2.007(3)–2.029(4) Å while in **3** both Ag–N bonds [2.178(2) and 2.228(2) Å for oxazoline and

Table 4.7 Bond lengths/Å and angles/° of compound **3**.



N1–Ag' (oxazoline)	2.178(2)	N1*–Ag–N2	151.18(6)
N2–Ag (pyridine)	2.228(2)	N1*–Ag–O2	109.93(5)
Ag–O2	2.740(2)	N1*–Ag–O3	115.34(6)
Ag–O3	2.528(2)	N1*–Ag–O3''	109.09(5)
Ag–O3''	2.792(2)		
N3–O2	1.257(2)	N2–Ag–O2	88.35(5)
N3–O3	1.262(2)	N2–Ag–O3	93.48(6)
N3–O4	1.241(2)	N2–Ag–O3''	80.40(5)
O1–C1	1.342(2)	O2–Ag–O3	48.41(4)
N1–C1	1.271(2)	O2–Ag–O3''	115.96(4)
pyridine-oxazoline interplanar angle		26.54(9)	

Symmetry codes: ' 1 – x, ½ + y, ½ – z; '' 1 – x, 1 – y, 1 – z; * 1 – x, y – ½, ½ – z.

pyridine coordination, respectively] are longer and significantly different to each other indicating that in this instance, Ag^{I} not only discriminates between coordination by pyridine- and oxazoline nitrogen, but also probably prefers the latter yielding the shorter bond.

The nitrate counter ion engages in one strong $\text{Ag}-\text{O}3$ bond of $2.528(2)$ Å and further forms a $\text{Ag}\cdots\text{O}2$ contact of $2.740(2)$ Å to the same Ag centre with O2. The oxygen atom forming the shorter bond is further loosely bonded to a second silver centre [$\text{Ag}'\cdots\text{O}3$ $2.792(2)$ Å, $' = 1 - x, 2 - y, -z$] of a neighbouring chain and *vice versa*, effectively bridging two Ag atoms with two nitrate counterions and affording a $3 + 2$ coordination number at the metal (Figure 4.9). However, even the short $\text{Ag}-\text{O}2$ bond is not strong enough to effect a true trigonal-planar geometry thus the strongly bonding coordination environment around Ag resembles an intermediate situation between linear and trigonal planar coordination with an $\text{N}-\text{Ag}-\text{N}$ angle of $151.18(6)^\circ$.

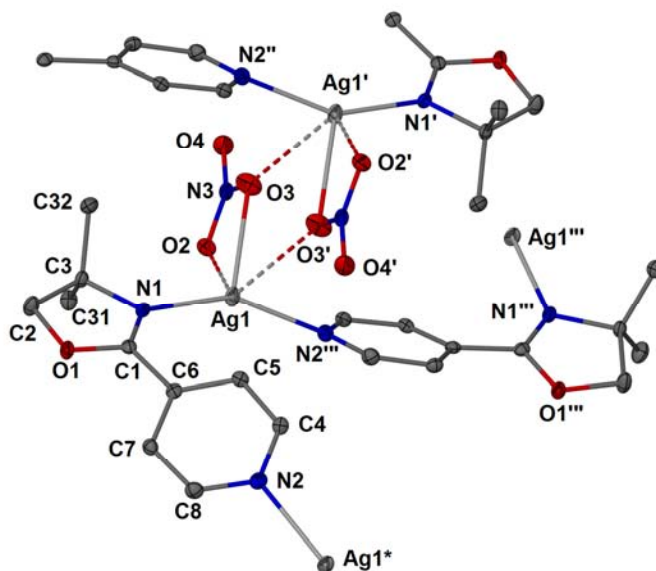


Figure 4.9 Section of a infinite $[\text{Ag}(\mu\text{-NO}_3)(\mu\text{-L})]_n$ chain of **3**, the nitrate counterions bridge two neighbouring chains; symmetry codes $' = 1 - x, 2 - y, -z$; $'' = x, \frac{3}{2} - y, x - \frac{1}{2}$; $''' = 1 - x, \frac{1}{2} + y, \frac{1}{2} - z$ and $* = 1 - x, y - \frac{1}{2}, \frac{1}{2} - z$.

The connectivity motif exhibited by **3** has been observed before for the related compound *catena*-(μ -nitrato)[μ -2-(pyridin-4-yl)pyridine]silver in which the $\text{Ag}-\text{N}(\text{py})$ bonds [$2.192(2)$ and $2.199(2)$ Å] are of intermediate length compared to the $\text{Ag}-\text{N}$

bonds found in **3**.⁶⁶ The chains in the bis(pyridine) complex furthermore show a helical arrangement while in **3** the chains are essentially flat (Figure 4.10).

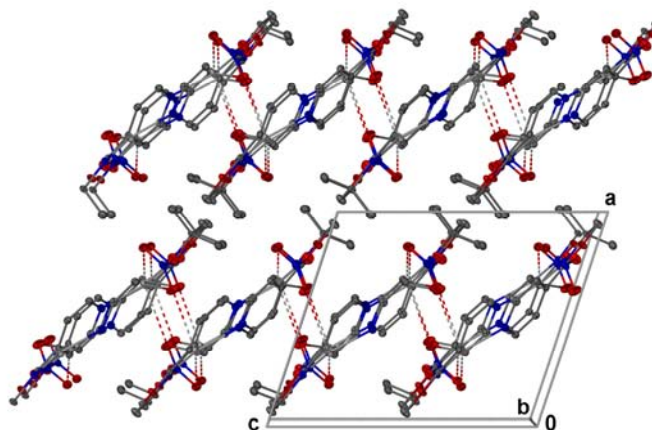


Figure 4.10 Packing diagram of **3** seen along the *b* axis showing layers of flat chains running parallel to the *b* axis that are bridged by nitrate anions along the *c* axis.

4.2.3.3 Au^I complexes of 4,4-dimethyl-2-(pyridin-4-yl)oxazoline, **4a** and **4b**.

The ligand 4,4-dimethyl-2-(thien-2-yl)oxazoline was also used in an attempt to prepare Au^I complexes by employing (tht)AuCl and NaOTf in MeCN to afford the gold complex [4,4-dimethyl-2-(pyridin-4-yl-κN)oxazoline-κN]gold(1+) triflate, **4a**. No crystals of this complex could be obtained and the reaction was repeated with Na[BF₄] to supply the counter ion [BF₄][−] yielding **4b** in an attempt to obtain a salt with a better ability to crystallise. Both compounds exhibit greatly enhanced solubility compared to the silver complex **3** which could be caused by the non-coordinating anions and the reluctance of Au^I to raise its coordination number beyond the common linear dicoordinate complexes. However, the better solubility also points to species of lower molecular weight that could mimic the palladium complexes discussed in Section 4.2.3.2 with **3**.⁶⁵

Unlike the silver complex, both products, **4a** and **4b**, are very unstable in solution and deposit metallic gold mirrors on the walls of crystallisation vessels after several days even at *ca.* −20 °C and a strong smell of tht is apparent. NMR chemical shifts of **4a** are reported in Table 4.6 (*vide supra*).

4.2.4 A novel tricyclic digold(I) complex: tris[μ -*N,N*-bis(1,3,2-dioxaphospholan-2-yl- κ P)methanamine]digold(2+) triflate, **5**

N,N-Bis(dichlorophosphanyl)methanamine was chosen as a starting material with low steric demand for the synthesis of a bidentate phosphite-type ligand with one bridging atom between the phosphorus donors, sterically similar to dmpm [bis(dimethylphosphanyl)methane]. At first, ethane-1,2-dithiol was utilised in the synthesis of a dithiophosphoramidite ligand aimed at complementing the investigation in Chapter 2. The ligand *N,N*-bis(1,3,2-dithiaphospholan-2-yl)methanamine, however, was too unstable in the presence of Au^I and a precipitate was observed soon after reacting the ligand with (tht)AuCl. The yellow colour of the precipitate indicated Au^I thiolate formation and showed that the P–S bonds were readily cleaved by gold.

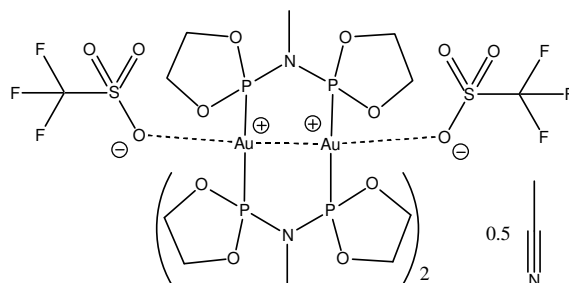
For the synthesis of a more stable ligand, ethane-1,2-diol was utilised to only offer one type of soft atom in the ligand while benefiting from stronger P–O bonds. *N,N*-bis(1,3,2-dioxaphospholan-2-yl)methanamine was obtained in the form of a colourless solid as opposed to a previous report⁶⁷ of a yellowish oil. Numerous crystal structures of phosphite ligands incorporating the P–N–P backbone have been reported, usually bridging two metal centres. However, only one crystal structure of a dioxaphospholane-type ligand, in which two *N*-ethyl homologues of the ligand used in this work bridge a hexacarbonyldicobalt fragment, is known.⁶⁸ A related bicyclic [(AuCl)₂(μ -²L)₂]²⁺-type complex of *N,N*-bis[bis(2,2,2-trifluoroethoxy)phosphanyl]-methanamine with Au^I has been reported only recently.⁶⁹

The synthesis of the gold complex tris[μ -*N,N*-bis(1,3,2-dioxaphospholan-2-yl- κ P)-methanamine]digold(2+) triflate, **5**, shown in Scheme 4.14, proceeded without precipitation, even though the reaction mixture became light yellow indicating slight decomposition of the ligand by gold. It was effected by the usual method of dissolving the ligand and CF₃SO₃Na in MeCN and adding (tht)AuCl.

67 S. Kim, M. P. Johnson and D. M. Roundhill, *Inorg. Chem.* **1990**, *29*, 3896–3898.

68 G. de Leeuw, J. S. Field and R. J. Haines, *J. Organomet. Chem.* **1989**, *359*, 245–254.

69 A. J. Esswein, J. L. Dempsey and D. G. Nocera, *Inorg. Chem.* **2007**, *46*, 2362–2364.



Scheme 4.14 Drawing of the structure of **5**·0.5CH₃CN.

4.2.4.1 Spectroscopic characterisation.

The NMR parameters of **5** are summarised in Table 4.8. Due to its symmetry, the cation in **5** only yields two signals in its ¹H and ¹³C NMR spectra. Compared to the free ligand, these signals are somewhat less shielded; the largest chemical shift difference $\Delta\delta$ expectedly being that of the ³¹P resonance with a $\Delta\delta$ of 8.3 which is a bit more than the chemical shift difference between (MeS)₃P and [Au{P(SMe)₃}₂]⁺ ($\Delta\delta$ 2.5; see Chapter 2).

Table 4.8 NMR data of compound **5** in CD₃CN.

Nucleus		
¹ H (400 MHz)	ring-CH ₂	4.40 (m, 24 H)
	bridge-NCH ₃	2.71 (s, 9 H)
¹³ C{ ¹ H} (101 MHz) ^a	ring-CH ₂	68.4 (s)
	bridge-NCH ₃	28.2 (br s)
³¹ P (162 MHz)	P	149.0 (br s)

^a a signal of the CF₃SO₃⁻ carbon was not observed due to low intensity and signal splitting

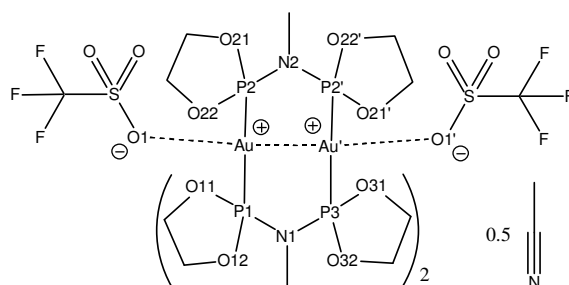
Mass spectrometry of **5** with electrospray ionisation shows different peaks to that of the ligand at low cone voltage (15V). At higher cone voltages the spectra of the free ligand and **5** are identical. However, the peaks cannot be interpreted.

4.2.4.2 Crystallography.

Crystallisation of **5** was difficult task and eventually only a few well defined, colourless crystals were fished from the amorphous precipitate obtained from an MeCN solution layered with Et₂O. The crystals obtained were very brittle indicating little cohesion of the lattice and contributing to a structure with inherent low precision. Bond lengths and angles are summarised in Table 4.9.

Complex **5**, shown in Figure 4.11, crystallises as a hemi-ethanenitrile solvate, only half of the [Au₂(μ⁻²L)₃]²⁺ core is asymmetric with a C₂ axis passing through one C–N vector of a methanamine group. A possible three-fold rotation axis, as was found in hexagonal [Au₂(μ-dppm)₃]²⁺,⁴² is not formed along the Au⋯Au' (' = -x, y, ½ - z) bond of 2.874(1) Å.

Table 4.9 Bond lengths/Å and angles/° of compound **5**·0.5CH₃CN.



Au–P1	2.337(3)	P1–N1	1.66(2)
Au–P2	2.337(4)	P2–N2	1.664(9)
Au–P3	2.318(3)	P3–N1'	1.70(2)
Au⋯Au'	2.874(1)	P2–O21	1.60(2)
Au⋯O1	3.10(2)	P2–O22	1.59(1)
P1–O11	1.606(9)	P3–O31	1.60(1)
P1–O12	1.606(9)	P3–O32	1.595(9)
Au–P1–N1	118.0(4)	O11–P1–O12	96.3(5)
Au–P2–N2	115.7(6)	O21–P2–O22	95.3(6)
Au–P3–N1'	114.4(4)	O31–P3–O32	97.4(5)
Au–P1–O11	115.3(4)	P1–N1–P3	123.9(7)
Au–P1–O12	115.5(4)	P2–N2–P2'	126(2)
Au–P2–O21	115.7(5)	Au–P1–O31	117.4(4)
Au–P2–O22	117.4(4)	Au–P1–O32	116.1(4)
P1–Au–P2	116.0(2)		
P2–Au–P3	122.2(2)		
P1–Au–P3	121.7(2)		

Symmetry code: ' -x, y, ½ - z

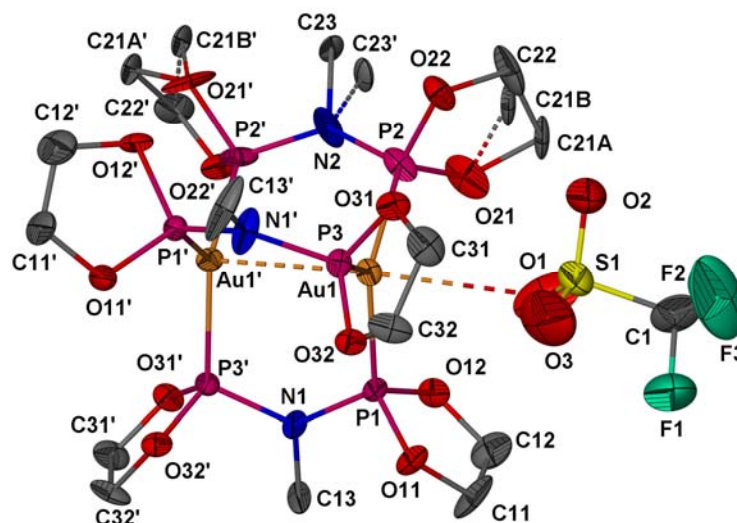


Figure 4.11 Molecular structure of $5 \cdot 0.5\text{CH}_3\text{CN}$, the solvent molecule and one triflate anion are omitted for clarity; primed atoms are related by a twofold rotation of symmetry code $-x, y, \frac{1}{2} - z$. C21 is disordered in a 3:2 (A:B) ratio by an envelope-flip of the dioxaphospholane ring; C23 equally occupies two orientations caused by non-planarity of N2 which lies on a two-fold rotation axis. The thermal ellipsoid of C13 (and thus also that of symmetry image C13') suggests a similar situation that is not resolved.

This distance is shorter than in both $[\text{Au}_2(\mu\text{-dmpm})_3]^{2+}$ and $[\text{Au}_2(\mu\text{-dppm})_3]^{2+}$ with separations of 3.040(1) and 3.050(1) Å³⁷ for the two asymmetric molecules in the former and 2.968(2) Å in the latter complex,⁴² but in the range of a multitude of other binuclear linear Au^{I} complexes where the gold atoms are bridged by ligands with one atom in between the donating atoms.⁷⁰

The triflate counter ions are located above and below each gold centre, also related by the C_2 axis, and engaging in weak $\text{Au} \cdots \text{O}$ contacts of 3.10(2) Å. The coordination geometry around the gold centres is ideally trigonal planar showing no significant influence of the triflate counter anions. In molecular structures that contain halide counter anions, severe distortion of the geometry towards tetrahedral coordination has been observed.^{48–50} The Au–P distances in $5 \cdot 0.5\text{CH}_3\text{CN}$ [2.337(3), 2.337(4) and 2.318(3) Å] are in good agreement with one another. Some other compounds with phosphane ligands show significantly longer distances.^{45,47}

⁷⁰ See for example: (a) J. Vicente, M.-T. Chicote, I. Saura-Llamas, P. G. Jones, K. Meyer-Bäse and C. F. Erdbrügger, *Organometallics* **1988**, *7*, 997–1006; (b) M. Bardají, N. G. Connelly, M. C. Gimeno, P. G. Jones, A. Laguna and M. Laguna, *J. Chem. Soc., Dalton Trans.* **1995**, 2245–2250; (c) R. J. Staples, J. P. Fackler, Jr. and Z. Assefa, *Z. Kristallogr.* **1995**, *210*, 379–380.

In such phosphane complexes distances range from 2.338(4) Å for the shortest Au–P bond in the {tris[μ -2,6-bis(diphenylphosphanyl)pyridine]}digold(2+) cation⁴⁴ to 2.400(2) Å in the Hg⁰ cryptate of the {tris[μ -1,10-bis(diphenylphosphanyl)phenanthroline]}digold(2+) cation.⁴⁶ However, in most of these structures there are significant differences amongst the lengths of crystallographically independent Au–P bonds, the longest Au–P distance in the former cation is 2.384(4) Å, almost 0.05 Å longer than the shortest bond. Most mononuclear trigonal planar tris(phosphane)-gold(1+) complexes also exhibit longer Au–P bonds at ca. 2.36 Å^{17,36} which can be attributed to steric demand as most ligands employed comprise the sterically bulky Ph₂P-group. Furthermore, phosphite Au–P bonds are usually shorter when compared to phosphane Au–P bonds (see also crystallography in Chapter 2).⁷¹

The ethanenitrile solvent molecule in **5**·0.5CH₃CN was found to be disordered, a C₂ axis passes through its methyl carbon atom and the geometry refined unsatisfactorily. The solvent was thus removed using the Squeeze routine in the Platon set of programmes.⁵⁴

The three bidentate ligands in **5**·0.5CH₃CN are all eclipsed in line with low twist ϕ and buckle δ angles as defined in the literature⁶⁸ [ϕ = Au–P–P–Au; δ is the interplanar angle between the Au–P–P–Au and the P–N–P planes; in **5**·0.5CH₃CN ϕ = 9° for Au–P1–P3'–Au' and 3° for Au–P2–P2'–Au', δ = 10(2)° and 1(1)°, respectively; ' = –x, y, ½ – z].

4.2.5 The attempted syntheses of other [Au₂(μ -²L)₃]²⁺ compounds

4.2.5.1 The attempted synthesis of [Au₂(μ -dppe)₃](CF₃SO₃)₂.

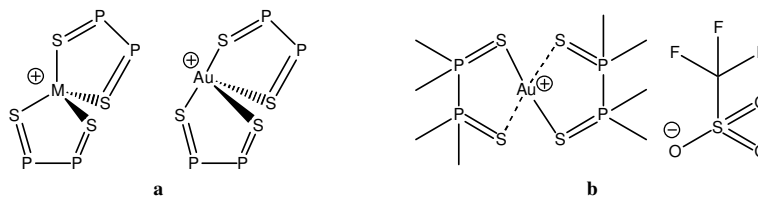
Other ligands principally capable of forming [Au₂(μ -²L)₃]²⁺ cations were considered as well, but no such structures could be obtained. Since such a complex with dppm has been isolated, the synthesis of the complex [Au₂(μ -dppe)₃](CF₃SO₃)₂ [dppe = 1,2-bis(diphenylphosphanyl)ethane] was attempted by a similar method as used in the preparation of **5**. The clear colourless solution in ethanenitrile was layered with Et₂O,

71 See for example the structures of Ph₃PAuCl and (PhO)₃PAuCl: (a) N. C. Baenziger, W. E. Bennett and D. M. Soboroff, *Acta Crystallogr., Sect. B: Struct. Crystallogr. Cryst. Chem.* **1976**, 32, 962–963; (b) P. B. Hitchcock and P. L. Pye, *J. Chem. Soc., Dalton Trans.* **1977**, 1457–1460.

however only crystals of the cyclic $[\text{Au}_2(\mu\text{-dppe})_2](\text{CF}_3\text{SO}_3)_2 \cdot 2\text{CH}_3\text{CN}$, the 2:2 adduct, **6**, were obtained. Examination of many other crystals gave the same unit cell which confirms that the structure obtained is the major product. It can therefore be concluded that even though $[\text{Au}_2(\mu\text{-dppe})_3]^{2+}$ may exist in the solid state,³⁸ isolation of crystals was not possible in the system selected. The molecular structure of the cyclic cation proved to be closely similar to the methanol solvate already reported⁷² and is unexceptional.

4.2.5.2 *The attempted synthesis of $[\text{Au}_2(\mu\text{-tmdpd})_3](\text{CF}_3\text{SO}_3)_2$ – crystal structure of $[\text{Au}(\text{tmdpd})_2]\text{CF}_3\text{SO}_3$, **7**.*

Another ligand suitable for the formation of a $[\text{Au}_2(\mu\text{-}^2\text{L})_3]^{2+}$ -type of complex of Au^{I} is tetramethyldiphosphane disulfide (tmdpd). Again, during the reaction of (tht)AuCl, tmdpd and NaOTf in ethanenitrile the formation of a yellow precipitate was observed indicative of ligand decomposition. Crystals were obtained but proved to be $[\text{Au}(\text{tmdpd})_2]\text{CF}_3\text{SO}_3$, **7** (shown in Scheme 4.15), a 2:1 rather than 3:2 coordination compound. Bond lengths and angles are given in Table 4.10.

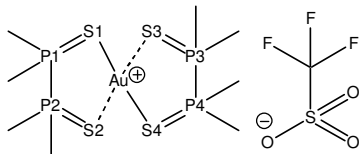


Scheme 4.15 (a) The different geometries of coinage metal tmdpd complexes ($\text{M} = \text{Cu}, \text{Ag}$); (b) connectivity of **7**.

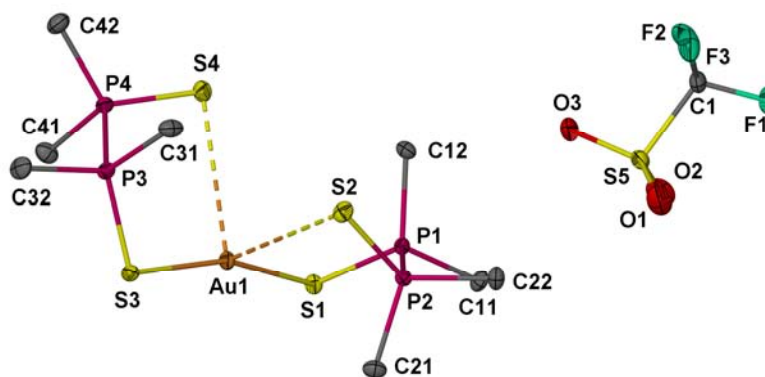
Tetraalkyldiphosphane disulfides are potentially ditopic ligands but enjoy only limited use in coordination chemistry. There are few crystal and molecular structures known, among them the Cu^{I} and Ag^{I} complexes with 2:1 stoichiometry.⁷³ These complexes are, in line with $[\text{ML}_4]^+$ species of the coinage metals, tetrahedral. However, the Au^{I} complex **7** shown in Figure 4.12 only exhibits distorted tetrahedral geometry where the gold atom has moved from the centre of the tetrahedron defined by the sulfur atoms of tmdpd to a position where it is nearly located in the middle between those

72 W. Schuh, H. Kopacka, K. Wurst and P. Peringer, *Chem. Commun.* **2001**, 2186–2187.

73 H. Liu, M. J. Calhorda, M. G. B. Drew and V. Félix, *Inorg. Chim. Acta* **2003**, 347, 175–180.

Table 4.10 Bond lengths/Å and angles/° of compound **7**.


Au–S1	2.3099(7)	Au–S1–P1	101.88(4)
Au–S3	2.3044(7)	Au–S3–P3	102.65(4)
Au⋯S2	3.3939(8)	Au⋯S2–P2	80.28(3)
Au⋯S4	3.2472(8)	Au⋯S4–P4	86.97(3)
P1–S1	2.009(1)	S1–Au–S3	161.49(3)
P2–S2	1.949(1)	S1–Au⋯S2	95.59(2)
P3–S3	2.011(1)	S1–Au⋯S4	99.84(2)
P4–S4	1.948(2)	S3–Au⋯S2	94.99(2)
P1–P2	2.229(1)	S3–Au⋯S4	95.71(2)
P3–P4	2.214(2)	S2⋯Au⋯S4	87.73(2)
S1–P1–P2–S2	81.71(5)	S3–P3–P4–S4	72.24(6)

**Figure 4.12** Molecular structure of **7**.

two sulfur atoms to which it forms true coordinative bonds. The other two phosphane sulfide groups only engage in close contacts of 3.3939(8) and 3.2472(8) Å with gold.

Compared to the Ag^{I} complex $[\text{Ag}(\eta^2\text{-tmdp})_2][\text{PF}_6]$ [$\text{Ag}-\text{S}$ 2.534(2) to 2.676(2) Å],⁷³ the different geometry in **7** causes a significant shortening of the Au–S bond lengths to 2.3099(7) (Au–S1) and 2.3044(7) Å (Au–S3) and the S1–Au–S3 angle of 161.49(3)° deviates sharply from the ideal 109.5° in a tetrahedron. In the Ag^{I} complex the S–Ag–S angles range from 99.03(5)° to 123.28(6)°. A comparison to other Au^{I} complexes where Au^{I} is coordinated to two phosphane sulfide ligands show that the additional Au⋯S contacts in **7** enlarge the Au–S bond lengths and at the same time

distort the ideal linear geometry at the gold centre. [1,1'-Bis(diphenylthiophosphoryl)-ferrocene]gold(1+) tetrachloroaurate(1-) exhibits Au-S bond lengths of 2.281(5) and 2.299(5) Å as well as a S-Au-S angle of 174.5(2)°;⁷⁴ and bis(triphenylphosphane sulfide)gold(1+) difluorophosphate shows geometric parameters of 2.277(2) Å for the single unique Au-S bond and 172.4(2)° for the S-Au-S angle,⁷⁵.

The structure of **7** also hints at the cause why no 3:2 complex was obtained even though the ligand has little steric demand: the phosphane sulfide is too weak a ligand to effect expansion of the usual linear dicoordinate geometry to form three proper coordinative bonds to the gold atom which would result in a trigonal planar centre.

When the structures of **5**, **6** and **7** are compared to other results,^{37,42} three conditions can be rationalised that should be fulfilled to obtain a $[\text{Au}_2(\mu\text{-}^2\text{L}_3)]^{2+}$ complex: (a) The ligand must not be sterically demanding, (b) the ligating atoms must be strong enough to effect expansion of the usual linear coordination around Au^{I} and (c) only one atom should bridge the ligating atoms. There are, however, exceptions to the last rule with more rigid ligands.^{44,45,47} While compound **5** fulfils all requirements, **6** fails on (c) and possibly (a), **7** fails on (b) and (c).

4.3 Conclusions

A trimeric thienyloxazoline heterometallacycle, **1**, was successfully prepared and characterised. The crystal and molecular structures of two solvates, one of which shows intermolecular aurophilic interactions, were also determined by X-ray diffraction. Due to the presence of gold-sulfur interactions in both solid-state structures of the cyclic trimers, accommodation of other Au^{I} or Ag^{I} centres within the cycle was not observed as the thiophene rings are held in place parallel to the plane. The necessary cavities to accommodate guests inside the macrocycle do not exist.

74 M. C. Gimeno, P. G. Jones, A. Laguna and C. Sarroca, *J. Organomet. Chem.* **2000**, 596, 10–15.

75 D. J. LeBlanc, J. F. Britten and C. J. L. Lock, *Acta Crystallogr., Sect. C: Cryst. Struct. Commun.* **1997**, 53, 1204–1206.

The first heterometallacyclic complexes with bis-imidazole $N^{\wedge}N$ -coordination of Au^I, **2a** and **2b**, were prepared and shown to be very stable. The cations host solvent inside a cavity created by the heterometallacyclus. While porosity is obstructed in the structures of **2a**, compound **2b** exhibits interconnected channels in its bis-dichloromethane solvate. Despite significant changes in the unit cell parameters upon partial removal of the crystal solvent, the triflate salt retains its general structural arrangement. This feature was for the first time demonstrated for a gold complex. The pores of the crystal, however, could not be emptied completely due to unusually strong interaction of the residual dichloromethane with the cyclic cation.

A related ligand, 4,4-dimethyl-2-(pyridin-4-yl)oxazoline formed an adduct with AgNO₃, **3**, that crystallised as a coordination polymer. Au^I complexes of this ligand gave no suitable crystals for an X-ray diffraction study. This failure of the ligand to form heterometallacycles could possibly be attributed to the absence sulfur donors that otherwise could encourage cyclisation.

Utilising a phosphite ligand for the first time, synthesis of a novel [Au₂(μ⁻²L)₃]²⁺ complex revealed stronger Au··Au interactions and shorter Au–P bonds than in related phosphane complexes and resemble the findings in the structure of the phosphite complex (MeO)₃PAuCl compared to phosphane analogues discussed in Chapter 2. Reactions with other ligands brought a better understanding as to which conditions must be met to obtain such compounds: Sufficiently strong donor atoms which are only bridged by one additional atom and little steric crowding. Tetramethyldiphosphane disulfide was shown to be too weak a ligand to effect coordination beyond the linear-dicoordinate geometry, bis(diphenylphosphanyl)ethane (dppe) is sterically unable to do so. The 2:1 complex of tetramethyldiphosphane disulfide with Au^I exhibits a geometry that is linear-dicoordinate, but somewhat distorted towards tetrahedral coordination (which is more generally observed for the Cu^I and Ag^I complexes) by two additional sub-van der Waals Au··S contacts.

4.4 Experimental

4.4.1 Crystallography

For details on collection and solution of the datasets see Chapter 2, p. 57.

Data and parameters associated with the structures reported in this Chapter are summarised in Tables 4.11 and 4.12. All gold complexes afforded colourless crystals. In the structures of **1**·2C₄H₈O, **2b**·2CH₂Cl₂ and **5**·0.5CH₃CN solvent molecules proved to be severely disordered (only one CH₂Cl₂ molecule in **2b**·2CH₂Cl₂) and could not be modeled satisfactorily, residual electron density belonging to these solvent molecules was thus removed using the Squeeze routine in the Platon set of programmes.⁵⁴ In **2a**·2CH₂Cl₂ and **2b**·2CH₂Cl₂ the Cl–C distances of the CH₂Cl₂ molecule(s) as well as the F–C and S–O distances of the triflate counter ion were restrained to be equal using a SADI command; in **1**·2C₄H₈O the C–C bonds of one thf molecule (one carbon disordered in an up/down envelope flip) were restrained to be equal by using the SADI command while those of the other thf molecule were constrained at a target value of 1.54 Å together with the O–C distances at 1.40 Å by DFIX instructions. In **5**·0.5CH₃CN one dioxaphospholan ring was also disordered by an up/down envelope flip of a carbon atom; the appropriate C–C bond distances were restrained to be equal with SADI.

4.4.2 Preparation of the compounds

For details on the instrumentation used see Chapter 2, p. 59.

Chemicals were obtained from the following suppliers and used without further purification if not stated otherwise: Butyllithium solution in hexanes, 2-isocyano-2-methylpropane, phosphorus trichloride, pyridine and thiophene-2-carbonyl chloride were obtained from Aldrich Chemical Co. Mercury and silver nitrate were obtained from Merck KG. 1,2-Bis(diphenylphosphanyl)ethane, Celite (diatomaceous earth), methylammonium chloride, pyridine-4-carboxylic acid, sodium tetrafluoroborate and sodium trifluoromethanesulfonate were obtained from Fluka AG.

Table 4.11 Crystallographic parameters of the solvates of **1** and **2a** as well as **2b**·2CH₂Cl₂

Compound	1·0.75C ₄ H ₈ O	1·2C ₄ H ₈ O	2a·2CH ₃ CN	2a·2CH ₂ Cl ₂	2b·2CH ₂ Cl ₂
Empirical formula	C ₂₇ H ₃₀ Au ₃ N ₃ O ₃ S ₃ ·0.75C ₄ H ₈ O	C ₂₇ H ₃₀ Au ₃ N ₃ O ₃ S ₃ ·2C ₄ H ₈ O	C ₃₄ H ₄₀ Au ₂ B ₂ F ₈ N ₈ ·2C ₂ H ₃ N	C ₃₄ H ₄₀ Au ₂ B ₂ F ₈ N ₈ ·2CH ₂ Cl ₂	C ₃₆ H ₄₀ Au ₂ F ₆ N ₈ O ₆ S ₂ ·2CH ₂ Cl ₂
<i>M_r</i>	1185.7	1275.8	1210.4	1298.2	1337.7
Crystal habit	Polygon	Plate	Needle	Needle	Needle
Crystal dimensions/mm	0.15 × 0.12 × 0.11	0.21 × 0.20 × 0.09	0.28 × 0.07 × 0.06	0.26 × 0.03 × 0.03	0.24 × 0.07 × 0.05
Crystal system	Monoclinic	Triclinic	Orthorhombic	Orthorhombic	Orthorhombic
Space group	<i>C2/c</i> (No. 15)	<i>P</i> $\bar{1}$ (No. 2)	<i>Pnma</i> (No. 62)	<i>Pnma</i> (No. 62)	<i>Pnma</i> (No. 62)
<i>a</i> /Å	28.72(2)	10.901(2)	19.296(3)	19.691(3)	21.860(6)
<i>b</i> /Å	10.001(7)	13.921(3)	20.243(3)	19.921(3)	18.886(5)
<i>c</i> /Å	26.06(2)	14.061(3)	11.081(2)	11.292(2)	11.726(3)
α /°	90	90.951(3)	90	90	90
β /°	110.98(1)	103.407(3)	90	90	90
γ /°	90	110.896(3)	90	90	90
<i>V</i> /Å ³	6990(8)	1927.5(6)	4328(1)	4429(2)	4841(2)
<i>Z</i> , <i>D_c</i> /Mg m ⁻³	8, 2.253 ^b	2, 2.198	4, 1.857	4, 1.947	4, 1.952 ^b
μ (MoK α)/mm ⁻¹	12.771 ^b	11.595	6.847	6.930	6.437 ^b
No. of reflections, unique	19877, 7075	20635, 7866	24538, 4553	24514, 4676	27684, 5161
<i>R</i> _{int}	0.0298	0.0329	0.0376	0.0737	0.0542
<i>hkl</i> index range	-35 to 22, -11 to 12, -30 to 32	± 13, ± 17, ± 17	-23 to 24, ± 25, -13 to 9	-24 to 13, -22 to 24, ± 14	-21 to 27, ± 23, -14 to 13
θ range/°	1.67–26.38	1.58–26.41	2.01–26.38	2.04–26.45	1.86–26.56
Data, restraints, parameters	6504, 0, 358	7188, 11, 453	3747, 0, 295	3024, 6, 297	4122, 7, 302
<i>F</i> (000)	4416 ^b	1204	2336	2496	2752 ^b
<i>R</i> ₁ , <i>wR</i> ₂ [<i>I</i> > 2 σ (<i>I</i>)] ^a	0.0251, 0.0567	0.0323, 0.0823	0.263, 0.579	0.0467, 0.0985	0.0447, 0.1132
<i>R</i> ₁ , <i>wR</i> ₂ (all data) ^a	0.0285, 0.0578	0.0360, 0.0843	0.357, 0.617	0.0875, 0.1187	0.0580, 0.1205
Goodness-of-fit	1.089	1.054	1.044	1.032	1.042
Max. and min. transmission	0.244, 0.114	0.425, 0.194	0.668, 0.496	0.810, 0.386	0.726, 0.494
Largest differential peak and hole/eÅ ⁻³	1.549, -0.906	3.961, -0.999	1.228, -0.402	4.399, -3.876	2.174, -2.647

^a $w = 1/[\sigma^2(F_o^2) + (aP)^2 + bP]$ where $P = (F_o^2 + 2F_c^2)/3$ ^b Including crystal solvent removed by the Squeeze routine.

Table 4.12 Crystallographic parameters of **2b**·0.7CH₂Cl₂, **3**, **5**·0.5CH₃CN, **6**·2CH₃CN and **7**.

Compound	2b ·0.7CH ₂ Cl ₂	3	5 ·0.5CH ₃ CN	6 ·2CH ₃ CN	7
Empirical formula	C ₃₆ H ₄₀ Au ₂ F ₆ N ₈ O ₆ S ₂ ·0.7CH ₂ Cl ₂	C ₁₀ H ₁₂ AgN ₃ O ₄	C ₁₇ H ₃₃ Au ₂ F ₆ N ₃ O ₁₈ P ₆ S ₂ ·0.5C ₂ H ₃ N	C ₅₄ H ₄₈ Au ₂ F ₆ O ₆ P ₄ S ₂ ·2C ₂ H ₃ N	C ₉ H ₂₄ AuF ₃ O ₃ P ₄ S ₅
<i>M_r</i>	1312.3	346.10	1345.7	1571.0	718.43
Crystal habit	Needle	Prism	Block	Block	Plate
Crystal dimensions/mm	0.43 × 0.07 × 0.05	0.25 × 0.20 × 0.20	0.16 × 0.08 × 0.04	0.21 × 0.15 × 0.07	0.22 × 0.17 × 0.108
Crystal system	Orthorhombic	Monoclinic	Monoclinic	Monoclinic	Monoclinic
Space group	<i>Pnma</i> (No. 62)	<i>P2₁/c</i> (No. 14)	<i>C2/c</i> (No. 15)	<i>P2₁/c</i> (No. 14)	<i>P2₁/c</i> (No. 14)
<i>a</i> /Å	21.076(3)	9.4727(8)	23.006(3)	11.7942(9)	13.012(1)
<i>b</i> /Å	19.034(3)	11.4339(9)	13.102(2)	37.016(3)	12.680(1)
<i>c</i> /Å	11.665(2)	11.3210(9)	17.256(3)	14.384(2)	14.289(2)
<i>α</i> /°	90	90	90	90	90
<i>β</i> /°	90	108.250(1)	130.924(2)	113.011(1)	90.800(1)
<i>γ</i> /°	90	90	90	90	90
<i>V</i> /Å ³	4680(2)	1164.5(2)	3930(1)	5779.7(8)	2357.2(3)
<i>Z</i> , <i>D_c</i> /Mg m ⁻³	4, 1.863 ^b	4, 1.974	4, 2.275 ^b	4, 1.805	4, 2.024
<i>μ</i> (MoKα)/mm ⁻¹	6.507 ^b	1.742	7.910 ^b	5.325	6.986
No. of reflections, unique	25769, 4956	6525, 2369	11141, 4037	33365, 11786	13530, 4790
<i>R</i> _{int}	0.0494	0.0147	0.0432	0.0469	0.0251
<i>hkl</i> index range	-26 to 12, ± 23, ± 14	-11 to 10, -14 to 7, ± 14	-14 to 28, ± 16, -21 to 20	± 14, -46 to 36, -18 to 17	-15 to 16, ± 15, -16 to 17
<i>θ</i> range/°	1.93–26.43	2.26–26.37	1.95–26.42	1.63–26.41	2.15–26.42
Data, restraints, parameters	3665, 0, 284	2281, 0, 165	3194, 2, 253	9710, 0, 723	4513, 0, 234
<i>F</i> (000)	2534 ^b	688	2580 ^b	3072	1392
<i>R</i> ₁ , <i>wR</i> ₂ [<i>I</i> > 2σ(<i>I</i>)] ^a	0.0363, 0.0841	0.0194, 0.0469	0.0748, 0.1636	0.0398, 0.0846	0.0210, 0.0509
<i>R</i> ₁ , <i>wR</i> ₂ (all data) ^a	0.0556, 0.0901	0.0204, 0.0475	0.0960, 0.1723	0.0526, 0.0898	0.0229, 0.0517
Goodness-of-fit	1.003	1.070	1.174	1.028	1.047
Max. and min. transmission	0.726, 0.400	0.705, 0.614	0.778, 0.328	0.692, 0.506	0.499, 0.305
Largest differential peak and hole/eÅ ⁻³	2.196, -0.876	0.476, -0.282	3.755, -4.091	2.059, -0.708	1.100, -0.627

^a $w = 1/[\sigma^2(F_o^2) + (aP)^2 + bP]$ where $P = (F_o^2 + 2F_c^2)/3$ ^b Including crystal solvent removed by the Squeeze routine.

2-Amino-2-methylpropan-1-ol and thionyl chloride were obtained from Riedel-de Haën. Anhydrous sodium sulfate was obtained from Saarchem, mercury(II) chloride from ACE c.c., tetrahydrothiophene from ACROS and tetramethyldiphosphane disulfide from Strem. Thin layer chromatography plates were supplied by Macherey-Nagel GmbH & Co. KG.

Chloro(tetrahydrothiophene)gold,⁷⁶ *N,N*-Bis(dichlorophosphanyl)methanamine,⁷⁷ *N,N*-bis(1,3,2-dithiaphospholan-2-yl)-methanamine,⁶⁷ 4,4-dimethyl-2-(thien-2-yl)oxazoline,⁵² *cyclo*-tris{[μ -4,4-dimethyl-2-(thien-2-yl- κ C⁵)oxazoline- κ N]gold},¹⁰ **1**, and 4,4-dimethyl-2-(pyridin-4-yl)oxazoline,⁷⁸ were prepared according to literature.

A gift of bitmb by *Dr. Liliana Dobrzańska* is greatly acknowledged.

4.4.2.1 Attempted reaction of **1** with silver nitrate.

In a Schlenk tube **1** (73 mg, 65 μ mol) was dissolved in 15 ml thf and AgNO₃ (18 mg, 0.11 mmol, 1.6 eq.) was added. The reaction mixture was protected from light and stirred for 3 days at room temperature. The suspension was filtered under inert conditions and the filtrate evaporated to dryness yielding 69 mg of a colourless solid. It was crystallised from thf layered with pentane, but only crystals of **1**·2C₄H₈O could be isolated.

4.4.2.2 Attempted co-crystallisation of **1** with Me₃CNCAuCl.

In a Schlenk tube **1** (40 mg, 35 μ mol) and chloro(2-isocyano-2-methylpropane)gold (11 mg, 35 μ mol, 1 eq.) were dissolved in 15 ml thf and stirred for 2 h. The solution was brought to dryness, the grey solid dissolved in 4 ml thf and layered with 25 ml pentane. Crystals of **1**·2C₄H₈O could later be isolated, no other crystal species was found.

M.p. of **1**·2C₄H₈O: 175°C (dec. without melting)

76 (a) A. Haas, J. Helmbrecht and U. Niemann, in *Handbuch der Präparativen Anorganischen Chemie*, ed. G. Brauer, Enke, Stuttgart, **1978**, p. 1014;

(b) R. Uson, A. Laguna and M. Laguna, *Inorg. Synth.* **1989**, 26, 85–91.

77 J. F. Nixon, *J. Chem. Soc. A* **1968**, 2689–2692.

78 A. I. Meyers and R. A. Gabel, *J. Org. Chem.* **1982**, 47, 2633–2637.

4.4.2.3 *Cyclo-bis{μ-1,3-bis[(imidazol-1-yl-κN)methyl]-2,4,6-trimethylbenzene}-digold(2+) tetrafluoroborate, 2a.*

Method A:

In a Schlenk tube (tht)AuCl (212 mg, 0.66 mmol) was dissolved in 30 ml MeCN, 0.07 ml tht and Ag[BF₄] (129 mg, 0.66 mmol, 1 eq.) were added subsequently. After stirring for 1 h the resulting AgCl precipitate was filtered off. In a separate Schlenk tube, bitmb (189 mg, 0.67 mmol, 1.0 eq.) was dissolved in 20 ml MeCN and the solution transferred to the gold(I) solution *via* a Teflon cannula. The clear solution was stirred for 1 h and then evaporated to dryness yielding a colourless solid. To remove last traces of AgCl it was re-dissolved in MeCN (*ca.* 50 ml) and inversely filtered under inert conditions affording 267 mg (71.3%) of a colourless solid. Crystals were grown from both ethanenitrile layered with Et₂O and CH₂Cl₂ layered with Et₂O. In the former case, a crystal of bad quality was obtained initially in which some Au was substituted for Ag. After recrystallising a small quantity in the same solvent system, a crystal of **2a**·2CH₃CN that gave a satisfactory crystal structure was obtained. Found: C, 32.3; H, 4.0; N, 8.9. C₃₄H₄₀Au₂B₂F₈N₈·2.6CH₂Cl₂ requires C, 32.6; H, 3.4; N, 8.3%.

M.p. 188 °C (dec. without melting)

The compound is soluble in MeCN and CH₂Cl₂ but is insoluble in Et₂O and alkanes. The solubility of **2a** is generally noticeably lower than that of **2b**.

4.4.2.4 *Cyclo-bis{μ-1,3-bis[(imidazol-1-yl-κN)methyl]-2,4,6-trimethylbenzene}-digold(2+) trifluoromethanesulfonate, 2b.*

Method B:

In a Schlenk tube were placed bitmb (114 mg, 0.41 mmol, 1.2 eq.), NaOTf (58 mg, 0.34 mmol, 1 eq.) and the solids were dissolved in 20 ml MeCN. A small quantity of NaCl crystals to seed precipitation of NaCl during the reaction was added as well. A solution of (tht)AuCl (110 mg, 0.34 mmol, 1 eq.) in 20 ml thf was subsequently added to the ligand solution *via* Teflon cannula upon which the reaction mixture gradually became hazy. After stirring for 2 h, the suspension was filtered through Celite, the filter pad washed with a little MeCN and all volatiles were removed *in vacuo*. The obtained crude product was thoroughly digested with Et₂O (*ca.* 50 ml) to remove

excess ligand. Found: C, 32.3; H, 3.3; N, 7.7. $C_{36}H_{40}Au_2F_6N_8O_6S_2 \cdot 2CH_2Cl_2$ requires C, 32.1; H, 3.1; N, 7.9%.

M.p. 185 °C (dec. without melting)

The compound is soluble in MeCN and CH_2Cl_2 , soluble with difficulty in trichloromethane and propanone but insoluble in Et_2O and alkanes.

4.4.2.5 *Catena-[\mu-4,4-dimethyl-2-(pyridin-4-yl-κN)oxazoline-κN]-*

[\mu-nitrato-κ³O(Ag):O(Ag):O(Ag)]silver, 3.

In a Schlenk tube 4,4-dimethyl-2-(pyridin-4-yl)oxazoline (328 mg, 1.86 mmol, 1 eq) was dissolved in 30 ml MeCN, the vessel covered with aluminium foil and $AgNO_3$ (312 mg, 1.84 mmol, 0.99 eq.) was added as a solid. A colourless precipitate formed immediately and the suspension was stirred for 30 min whereupon the solvent was removed *in vacuo*. The compound was obtained in quantitative yield. Two crystallisations were set up from water layered with methanol and dmsolayered with MeCN. Faceted crystals suitable for X-ray diffraction were obtained from the latter vessel, while no crystals grew in the former. Found C, 34.3; H, 4.1; N, 11.9. $C_{10}H_{12}AgN_3O_4$ requires C, 34.7; H, 3.5; N, 12.1%.

M.p.: Irreversible decomposition with discolouring to yellow at 184 °C, to orange at 210 °C and black at 240 °C without melting or losing crystalline luster.

The compound exhibits mediocre solubility in water and dmsolayered with MeCN, methanol, ethanol, propanone, thf, Et_2O or CH_2Cl_2 . It is fairly stable against sunlight for limited periods of time and stable indefinitely when protected from light.

4.4.2.6 *[4,4-dimethyl-2-(pyridin-4-yl-κN)oxazoline-κN]gold(I+)*

trifluoromethanesulfonate, 4a.

A Schlenk tube was charged with 4,4-dimethyl-2-(pyridin-4-yl)oxazoline (80 mg, 0.45 mmol), NaOTf (78 mg, 0.45 mmol, 1 eq.) and some NaCl crystals. The reagents were dissolved in 40 ml MeCN and (tht)AuCl (146 mg, 0.46 mmol, 1 eq.) was added as a solid. The clear solution was stirred for 1 h and all volatiles were removed *in vacuo* yielding a colourless solid which was subsequently re-dissolved in 30 ml MeCN and inversely filtered under inert conditions. The compound did not give a satisfactory elemental analysis.

M.p. 75 °C

The compound is soluble in MeCN and CH₂Cl₂ but insoluble in Et₂O and alkanes. It is stable as a solid at low temperatures, however in solution it decomposes readily within days even at low temperature.

4.4.2.7 *[4,4-dimethyl-2-(pyridin-4-yl-κN)oxazoline-κN]gold(1+)*
tetrafluoroborate, 4b.

The compound was prepared in the same way as **4a** using 4,4-dimethyl-2-(pyridin-4-yl)oxazoline (100 mg, 0.57 mmol), Na[BF₄] (62 mg, 0.57 mmol, 1 eq.) and (tht)AuCl (182 mg, 0.57 mmol, 1 eq.).

M.p. 86 °C

The compound shows similar solubility and stability properties as the triflate salt.

4.4.2.8 *N,N-Bis(1,3,2-dioxaphospholan-2-yl)methanamine.*

The compound was prepared in a modified literature procedure.⁶⁷ A Schlenk flask equipped with a dropping funnel was charged with *N,N*-bis(dichlorophosphanyl)methanamine (1.145 g, 4.92 mmol) and the compound was dissolved in CH₂Cl₂ (80 ml). NEt₃ (2.9 ml, 21 mmol, 4.2 eq.) was subsequently added to the solution *via* syringe and a solution of 0.55 ml absolute 1,2-ethanediol in 50 ml thf/CH₂Cl₂ 3:2 was placed into the dropping funnel. The contents of the Schlenk flask were cooled to 0°C and the 1,2-ethanediol solution was slowly added with stirring. After 1 h all volatiles were removed *in vacuo*, the remaining colourless solid was extracted with 70 ml methylbenzene and inversely filtered under inert conditions. After bringing the methylbenzene solution to dryness *in vacuo*, 0.83 g of a colourless solid (the literature⁶⁷ reports a yellowish oil) was obtained. ³¹P NMR showed a purity of 85%, the yield was thus 68%. As the literature states the compound is very sensitive, no attempt was made to further purify it.

4.4.2.9 *Tris[μ-N,N-bis(1,3,2-dioxaphospholan-2-yl-κP)methanamine]digold(2+)*
trifluoromethanesulfonate, 5.

In a Schlenk tube *N,N*-bis(1,3,2-dioxaphospholan-2-yl)methanamine (264 mg, 1.1 mmol, 1.6 eq. based on 85% purity) was dissolved in MeCN (70 ml), subsequently

(tht)AuCl (216 mg, 0.67 mmol, 1 eq.) and NaOTf (116 mg, 0.67 mmol, 1 eq.) were added. The solution turned yellow immediately and a slight haze was observed. Some NaCl crystals were added to seed NaCl precipitation. After stirring for 1 h the solution was filtered under inert conditions and the obtained apricot yellow filtrate was brought to dryness *in vacuo* affording 0.54 g of crude product still containing MeCN. A crystal suitable for X-ray diffraction was obtained from an MeCN solution layered with Et₂O. Found: C, 13.5; H, 4.4; N, 3.3. C₁₇H₃₃Au₂F₆N₃O₁₈P₆S₂ requires C, 15.4; H, 2.5; N, 3.2%. MS (ESI): *m/z* 353 (18), 454 (15), 469 (60), 515 (100), 544 (35), 590 (85), 619 (58), 665 (25), 711 (8).

M.p. 90 °C.

The solid is soluble in MeCN but insoluble in Et₂O and alkanes.

4.4.2.10 Synthesis of [Au₂(μ-dppe)₂](CF₃SO₃)₂·2CH₃CN, **6**.

A Schlenk vessel was charged with dppe (184 mg, 0.46 mmol, 1 eq.), NaOTf (53 mg, 0.31 mmol, 1 eq.) and 20 ml ethanenitrile. The suspension was stirred briefly and solid (tht)AuCl (99 mg, 0.31 mmol, 1 eq.) and several NaCl crystals were added. After 1 h the suspension was brought to dryness, the solid was re-dissolved in 20 ml ethanenitrile, filtered and reduced to *ca.* 7 ml *in vacuo*. Layering with Et₂O and storing in a freezer furnished crystals of the title compound.

M.p. 255 °C

The compound is soluble in ethanenitrile but insoluble in Et₂O.

4.4.2.11 Synthesis of [Au(tmdp)₂]CF₃SO₃, **7**.

Synthesis was performed as described in 4.4.2.10 with tetramethyldiphosphane disulfide (129 mg, 0.69 mmol), NaOTf (86 mg, 0.50 mmol) and (tht)AuCl (150 mg, 0.47 mmol). Isolated crystals were washed with methylbenzene to remove precipitated yellow amorphous solids prior to X-ray diffraction measurement.

M.p. 185 °C (dec.)

The compound is soluble in ethanenitrile but insoluble in Et₂O and methylbenzene.

5 Carbene and Carbyne Complexes with Unconventional *N*-heterocyclic Side Chains: Interaction with Gold(I) Fragments

5.0 Abstract

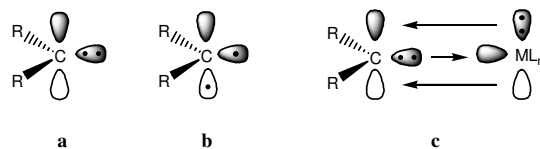
The chemistry of tungsten carbene and carbyne complexes that contain heterocyclic substituents as well as their interactions with chosen Au^I compounds, were investigated. It was found that tungsten carbyne complexes with 2-thiazolyl substituents are unstable and cannot be prepared in pure form. Related carbene and carbyne complexes were subsequently isolated using 1-(thiazol-2-yl)piperidine, **1a**, and 2-phenylthiazole, **1b**, which can be lithiated in the 5-position of the thiazole ring. Utilising both ligands, a variety of complexes were characterised, among them the tetramethylammonium pentacarbonyl(thiazol-5-ylcarbonyl)tungstate(1⁻) salts, **5a** and **5b**; Fischer carbene complexes pentacarbonyl[methoxy(thiazol-5-yl)methylidene]-tungsten, **6a** and **6b**, and the *N*-donor stabilised carbyne complexes *cis*-dicarbonyl-chloro-*cis*-bis-(pyridine)(thiazol-5-ylmethylidyne)tungsten, **7a** and **7b**. The carbene ligand in **6b** could be transferred to AuCl yielding **8b**, the first Fischer-type carbene complex of gold that exhibits aurophilic interactions. Reaction of the carbenate complexes **4a** (Li⁺-analogue of **5a**) and **5b** with Ph₃PAuCl afforded a unique CO-expulsion in **4a** to give a novel 5-aurated *pseudo-abnormal* carbene complex, **9a**, with the W(CO)₅ fragment from the starting material retained and coordinated to an imine nitrogen of a thiazolyl group. In the case of **5b**, a previously postulated product in related anionic carbene transfer reactions from tungsten to gold with the W(CO)₅ fragment coordinated to the carbene oxygen, **10b**, could be isolated for the first time. Reaction of **7a** with (tht)AuCl (tht = tetrahydrothiophene) yielded an addition product, **11a**, wherein the AuCl moiety coordinates to the W–C triple bond; reaction of (tht)AuC₆F₅ with **7b** is not straightforward and ligand scrambling made identification of reaction products difficult.

To further investigate carbene transfer reactions to Au^I, remote *N*-heterocyclic carbene (*r*NHC) complexes of chromium and tungsten, pentacarbonyl(1,2-dimethyl-5-phenyl-1*H*-pyridin-4-ylidene)chromium, **12Cr**, and -tungsten, **12W**, prepared by cyclisation methods, were reacted with a variety of gold compounds affording the first examples of *r*NHC gold complexes with the fragments AuCl, **13**, and AuPPh₃⁺, **14**. Reaction of pentacarbonyl(1-methyl-1*H*-pyridin-4-ylidene)chromium, **15**, with (tht)AuCl yielded the *r*NHC complex **16** by ligand transfer. From NMR investigations it was concluded that in these novel, stable complexes the charge-separated pyridinium rather than 1*H*-pyridin-4-ylidene resonance structure clearly is the more important contributing structure.

5.1 Introduction

5.1.1 Carbenes

Carbenes are a molecular species that contain a divalent carbon atom, usually assumed to be *sp*²-hybridised with two electrons in a free *sp*²-orbital (singlet state). This orbital is available for coordination to a suitable metal centre, the bond is further strengthened by the carbon's vacant *p*-orbital which acts as an acceptor of electron density from the metal (Scheme 5.1).¹ Some carbenes, like dichlorocarbene, CCl₂, exist in a triplet state where both *sp*² and *p* orbitals are occupied by a single electron; triplet carbenes are a highly reactive and thus elusive species.² A detailed study on the electronic structure of some transition metal (including Au) carbene complexes has been published by *Frenking*.¹

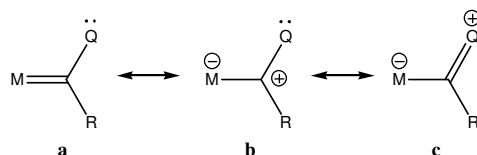


Scheme 5.1 (a) Electronic structure of a singlet- and (b) triplet-carbene; and (c) the idealised bonding situation in a metal–singlet carbene bond.

1 G. Frenking, M. Solà and S. F. Vyboishchikov, *J. Organomet. Chem.* **2005**, 690, 6178–6204.

2 W. Kirmse, *Angew. Chem., Int. Ed. Engl.* **2003**, 42, 2117–2119 (*Angew. Chem.* **2003**, 115, 2165–2167).

Carbenes, while acting as ligands in organometallic complexes, can be divided into two large classes, the Schrock-type and the Fischer-type. The former class comprise ‘divalent’ carbon atoms that are bonded to other carbon or hydrogen atoms with the first example synthesised by *Schrock*³ in 1975 by deprotonating the bis(cyclopentadienyl)dimethyltantalum(1+) cation with a base yielding bis(cyclopentadienyl)methyl(methylene)tantalum. The second class incorporates a heteroatom adjacent to the carbene carbon and was discovered by *E. O. Fischer*⁴ in 1964 by reaction of hexacarbonyltungsten with phenyllithium and subsequent alkylation of the resulting benzoyl(pentacarbonyl)tungstate(1–) anion with sulfuric acid and diazomethane. The latter steps are now usually replaced by reaction with Meerwein salts such as $[\text{Me}_3\text{O}][\text{BF}_4]$ allowing convenient and safe handling. The heteroatom in the carbene complex is able to donate electron density from its free electron pair(s) giving rise to mesomeric structures representing the so-called carbene and zwitterionic/cationic contributions. *Fürstner* and *Morency* supplied evidence⁵ suggesting the canonic form (a) in Scheme 5.2 has little weight in Au^{I} carbene complexes which is better represented by (b) and (c) (see also Chapter 1, p. 25). Although this conclusion was drawn in conjunction with Schrock-type carbene complexes, it can be inferred that in heteroatom-stabilised Fischer-type carbenes it will have at least some validity.⁶



Scheme 5.2 Canonic contributions to a Fischer-type carbene complex; Q represents a heteroatom with a free electron pair, R is an organic residue.

Carbenes form a very important ligand class found in numerous organometallic complexes. They appear as intermediates in catalytic processes (see Chapter 1, p. 24) as well as in organic synthesis where carbenes are very powerful reagents that allow

3 R. R. Schrock, *J. Am. Chem. Soc.* **1975**, *97*, 6577–6578.

4 E. O. Fischer and A. Maasböl, *Angew. Chem., Int. Ed. Engl.* **1964**, *3*, 580–581 (*Angew. Chem.* **1964**, *76*, 645).

5 A. Fürstner and L. Morency, *Angew. Chem., Int. Ed. Engl.* **2008**, *47*, 5030–5033 (*Angew. Chem.* **2008**, *120*, 5108–5111).

6 A. S. K. Hashmi, *Angew. Chem., Int. Ed. Engl.* **2008**, *47*, 6754–6756 (*Angew. Chem.* **2008**, *120*, 6856–6858).

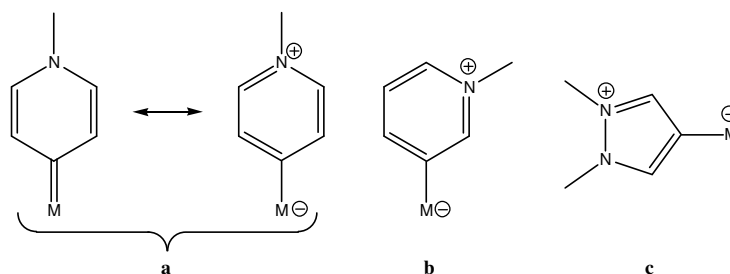
access to a vast variety of cycloadditions,⁷ heterocycles⁸ and enable alkene meta-thesis.⁹

A third class of carbene ligands that are related to the Fischer-type are *N*-heterocyclic carbenes (NHCs). They comprise a heterocycle containing at least one nitrogen adjacent to the carbene carbon. Imidazol-2-ylidenes are most common but other 5-membered heterocycles such as pyrazole, 1,2,4-triazole and thiazole are now also employed.¹⁰ The discovery of this ligand class has been made independently by Öfele¹¹ and Wanzlick.¹²

Recently, a review on the antimicrobial activity of silver NHC complexes has been published.¹³ Despite having comparable donor properties to phosphanes,^{9a,14} carbenes are usually not stable on their own; the discovery of *Arduengo*¹⁵ that imidazol-2-ylidenes are indeed stable compounds came as a surprise. This greatly facilitated certain organometallic syntheses because carbenes were now available as free ligands, as opposed to having to assemble the carbene step by step at the metal centre – a synthetic approach that is still without alternative in the case of group 6 Fischer carbene complexes.

-
- 7 (a) L. S. Hegedus, *Tetrahedron* **1997**, 53, 4105–4128; (b) A. de Meijere, H. Schirmer and M. Duetsch, *Angew. Chem., Int. Ed. Engl.* **2000**, 39, 3964–4002 (*Angew. Chem.* **2000**, 112, 4124–4162); (c) Y.-T. Wu, T. Kurahashi and A. de Meijere, *J. Organomet. Chem.* **2005**, 690, 5900–5911.
- 8 (a) R. Aumann and P. Hinterding, *Chem. Ber.* **1992**, 125, 2765–2772; (b) J. Barluenga, J. Santamaría and M. Tomás, *Chem. Rev.* **2004**, 104, 2259–2283.
- 9 (a) W. A. Herrmann, *Angew. Chem., Int. Ed. Engl.* **2002**, 41, 1290–1309 (*Angew. Chem.* **2002**, 114, 1342–1363); (b) C. M. Crudden and D. P. Allen, *Coord. Chem. Rev.* **2004**, 248, 2247–2273; (c) T. J. Katz, *Angew. Chem., Int. Ed. Engl.* **2005**, 44, 3010–3019 (*Angew. Chem.* **2005**, 117, 4630–4633); (d) R. R. Schrock and C. Czekelius, *Adv. Synth. Catal.* **2007**, 349, 55–77.
- 10 See for example: H. Braband, T. I. Kückmann and U. Abram, *J. Organomet. Chem.* **2005**, 690, 5421–5429.
- 11 K. Öfele, *J. Organomet. Chem.* **1968**, 12, P42–P43.
- 12 H.-W. Wanzlick and H.-J. Schönherr, *Angew. Chem., Int. Ed. Engl.* **1968**, 7, 141–142 (*Angew. Chem.* **1968**, 80, 154).
- 13 A. Kascatan-Nebioglu, M. J. Panzner, C. A. Tessier, C. L. Cannon and W. J. Youngs, *Coord. Chem. Rev.* **2007**, 251, 884–895.
- 14 R. H. Crabtree, *J. Organomet. Chem.* **2005**, 690, 5451–5457.
- 15 A. J. Arduengo III, R. L. Harlow and M. Kline, *J. Am. Chem. Soc.* **1991**, 113, 361–363.

Recently much attention was paid to *remote*-NHC (*r*NHC) complexes in this laboratory and by various collaborators.¹⁶ These carbenes are different from the classic Fischer-carbene and NHCs in that the single nitrogen heteroatom is not located α to the carbene carbon but generally occurs in the β - or γ - position of a 5- or 6-membered ring. (Scheme 5.3) While for the one-N, 6-membered carbenes with the metal bonded in the γ - position, both classic carbene and 6π -aromatic pyridinium structures can be drawn in what effectively amounts to a vinylogous Fischer-type carbene, the β -bonded carbenes afford an “unusual” or “abnormal” carbene complex as it is impossible to draw a classic carbene complex resonance structure with a M–C double bond for this species without undue charge separation. The same holds true for the illustrated 5-membered example coordinated in the β -position.



Scheme 5.3 Examples of *r*NHC ligands where a nitrogen atom is located at the β - or γ - position: (a) can exist in either the classic “carbene” or the charge-separated “pyridinium” structure while for (b) and (c) charge separation is necessary and the former structure cannot be drawn.

It was later shown that such *r*NHCs with one nitrogen atom induce a higher *trans*-effect at the metal centre and are better σ -donors as well as π -acceptors compared to their classic *normal*-NHC-counterparts owing to a HOMO at higher energy enhancing σ -donation and a HOMO–1 of *p*-character that is less centered on the carbene carbon, thus facilitating π -back donation by the metal.^{16c} These effects give rise to a

16 (a) H. G. Raubenheimer, M. Desmet, P. Olivier and G. J. Kruger, *J. Chem. Soc., Dalton Trans.* **1996**, 4431–4438; (b) W. H. Meyer, M. Deetlefs, M. Pohlmann, R. Scholz, M. W. Esterhuysen, G. R. Julius and H. G. Raubenheimer, *Dalton Trans.* **2004**, 413–420; (c) S. K. Schneider, P. Roembke, G. R. Julius, C. Loschen, H. G. Raubenheimer, G. Frenking and W. A. Herrmann, *Eur. J. Inorg. Chem.* **2005**, 2973–2977; (d) S. K. Schneider, G. R. Julius, C. Loschen, H. G. Raubenheimer, G. Frenking and W. A. Herrmann, *Dalton Trans.* **2006**, 1226–1233; (e) S. K. Schneider, P. Roembke, G. R. Julius, H. G. Raubenheimer and W. A. Herrmann, *Adv. Synth. Catal.* **2006**, 348, 1862–1873; (f) O. Schuster and H. G. Raubenheimer, *Inorg. Chem.* **2006**, 45, 7997–7999; (g) S. K. Schneider, C. F. Rentzsch, A. Krüger, H. G. Raubenheimer and W. A. Herrmann, *J. Mol. Catal. A: Chem.* **2007**, 265, 50–58.

significant strengthening of the metal–carbene bond by *ca.* 84 kJ mol⁻¹ leading to superior activities in the case of palladium-catalysed cross-coupling reactions.¹⁷

Today *r*NHC complexes are known – to name the most important examples – with [M(CO)₅] (M = Cr, W)^{8a} and [MX(PR₃)₂] (M = Ni, Pd, Pt)¹⁶ fragments. An unusual example is the coordination of a *N*-alkylated 2-(thien-2-yl)-4,4-dimethyl-oxazoline to [FeCp(CO)₂] at the C-5 carbon atom of the thiophene ring^{16a} that can be rationalised as an oxazolinylidene-NHC with a thiophene ring inserted as a spacer between the metal and the carbene functionality.

5.1.2 Carbynes

Carbyne complexes contain formal metal–carbon triple bonds. Such complexes can be rationalised as alkynes wherein one carbon atom has been replaced by an isolobal organometallic fragment, the carbon atom is *sp* hybridised and its geometry thus linear. The oxidation state of the metal is somewhat hard to define; while Fischer carbene ligands are thought to be neutral in respect of oxidation state of the metal, carbyne ligands are counted as if they carry a triple negative charge. These formalisms, however, do not represent the real situation in these complexes.¹⁸

The first carbyne complex was discovered in 1973 in the group of *E. O. Fischer*¹⁹ when the then well-known group 6 Fischer carbene complexes were treated with boron trihalides in an attempt to synthesise the analogous halocarbene complexes. Instead, formal abstraction rather than substitution of methoxide afforded a metal–carbon triple bond. In the course of this reaction, the initially generated (alkyldiyne)-pentacarbonylmetal complex cation subsequently loses the *trans*-CO ligand which is substituted by a halide affording a neutral complex.

17 H. G. Raubenheimer and S. Cronje, *Dalton Trans.* **2008**, 1265–1272.

18 J. P. Collman, L. S. Hegedus, J. R. Norton and R. G. Finke, in *Principles and Applications of Organotransition Metal Chemistry*, University Science Books, Mill Valley CA, **1987**, pp. 22–30.

19 E. O. Fischer, G. Kreis, C. G. Kreiter, J. Müller, G. Huttner and H. Lorenz, *Angew. Chem., Int. Ed. Engl.* **1973**, *12*, 564–565 (*Angew. Chem.* **1973**, *85*, 618–620).

Later the synthetic pathway was simplified by *Mayr* and coworkers²⁰ when a formal oxide dianion was directly abstracted from anionic (acyl)pentacarbonylmetallates(1–) using COCl_2 , ClC(O)OCCl_3 or $(\text{COX})_2$ ($\text{X} = \text{Cl}, \text{Br}$) thus obliterating the alkylation step. The group 6 *trans*- $[\text{M}(\equiv\text{CR})\text{X}(\text{CO})_4]$ species that form are not very stable compared to their carbene precursors and decomposition is already noticeable at temperatures below room temperature. However, two adjacent carbonyl ligands and the halide are relatively labile and susceptible to substitution with other donors such as amines,²⁰ tertiary phosphanes, imines,²¹ phosphites,^{21a} cyclopentadienide²² or tris(pyrazolyl)borate^{21b,23}, the resulting products exhibit largely improved stabilities.

Complexes prepared *via* this route are called Fischer-carbynes by inference of their origin, even though there is no heteroatom bonded to the carbyne carbon. However, it is possible to synthesise heteroatom-containing species following the same methodology by simply replacing the lithium alkyl reagent by an alkyl amide to finally afford an aminoalkylidyne ligand.²⁴

Schrock has described carbyne ligands derived from his type of carbene complexes in 1978 after deprotonating a cationic tantalum carbene complex with a base.²⁵ A most remarkable example of synthetic determination was the isolation and structural characterisation of $[\text{W}\{\text{C}(\text{CMe}_3)\}\{\text{CH}(\text{CMe}_3)\}\{\text{CH}_2(\text{CMe}_3)\}(\text{dmpe})]$ [dmpe = 1,2-bis(dimethylphosphanyl)ethane], a compound that contains an alkyl, an alkylidene and an alkylidyne substituent. A comparative study of bonding parameters for alkyl, carbene and carbyne substituents simultaneously without the interference that would be introduced by the synthesis of three different complexes, is thus

20 A. Mayr, G. A. McDermott and A. M. Dorries, *Organometallics* **1985**, *4*, 608–610.

21 (a) E. O. Fischer, A. Ruhs and F. R. Kreißl, *Chem. Ber.* **1977**, *110*, 805–815;

(b) G. A. McDermott, A. M. Dorries and A. Mayr, *Organometallics* **1987**, *6*, 50–55.

22 E. O. Fischer, T. L. Lindner and F. R. Kreißl, *J. Organomet. Chem.* **1976**, *112*, C27–C30.

23 (a) T. Desmond, F. J. Lalor, G. Ferguson and M. Parvez, *J. Chem. Soc., Chem. Commun.* **1984**, 75–77; (b) D. C. Brower, M. Stoll and J. L. Templeton, *Organometallics* **1989**, *8*, 2786–2792.

24 E. O. Fischer, G. Kreis, F. R. Kreißl, W. Kalbfus and E. Winkler, *J. Organomet. Chem.* **1974**, *65*, C53–C56.

25 S. J. McLain, C. D. Wood, L. W. Messerle, R. R. Schrock, F. J. Hollander, W. J. Youngs and M. R. Churchill, *J. Am. Chem. Soc.* **1978**, *100*, 5962–5964.

possible.²⁶ The chemistry of Schrock carbynes has been the subject of a number of review articles.^{9d,27}

Only a few examples of Fischer carbyne complexes that contain heterocyclic substituents bonded to the carbyne carbon have been reported. Amongst the compounds described are complexes incorporating heterocyclic 2-furyl²⁸ and thien-2-yl^{28,29} substituents as well as the organometallic residues ferrocenyl,³⁰ ruthenocenyl,^{30d} (phenyl- η^6)tricarbonylchromium³¹ as well as cymantrenyl {cymantrene = [MnCp(CO)₃]}.^{29c,32} The halide and/or CO ligands are sometimes substituted by hydridotris(pyrazolyl)borate,^{28a} 1,1'-bis(diphenylphosphanyl)ferrocene^{28b} or hydrido-tris(2-thionoimidazol-1-yl)borate.^{29c}

5.1.3 Carbene and carbyne transfer to gold fragments

Carbene ligands can be transferred from one metal centre to another, thus enabling the synthesis of complexes that would otherwise not have been accessible. For the instance of gold, two methodologies are of interest, namely the transfer of Fischer-type carbenes³³ which cannot readily be synthesised starting with metal centres other than Cr, Mo or W; and NHCs which can be synthesised directly but are more easily accessible by preparing the appropriate silver NHC complex *in situ* before reacting it with a gold compound. This latter methodology is applicable for the synthesis of Au^I, Pd^{II}, Pt^{II}, Rh^I, Ru^{II}, Ru^{III}, Ir^I and Cu^I carbene complexes.³⁴

26 M. R. Churchill and W. J. Youngs, *Inorg. Chem.* **1979**, *18*, 2454–2458.

27 R. R. Schrock, *Acc. Chem. Res.* **1986**, *19*, 342–348.

28 (a) J. H. Davis, Jr., C. M. Lukehart and L. Sacksteder, *Organometallics* **1987**, *6*, 50–55;

(b) M. Sekino, M. Sato, A. Nagasawa and K. Kikuchi, *Organometallics* **1994**, *13*, 1451–1455.

29 (a) E. O. Fischer and T. Selmayr, *Z. Naturforsch., B: Anorg. Chem. Org. Chem.* **1977**, *32*, 105–107;

(b) S. Anderson, D. J. Cook and A. F. Hill, *J. Organomet. Chem.* **1993**, *463*, C3–C4;

(c) M. R. St.-J. Foreman, A. F. Hill, A. J. P. White and D. J. Williams, *Organometallics* **2003**, *22*, 3831–3840.

30 (a) E. O. Fischer, M. Schluge and J. O. Besenhard, *Angew. Chem., Int. Ed. Engl.* **1976**, *15*, 683–684

(*Angew. Chem.* **1976**, *88*, 719–720); (b) E. O. Fischer, T. L. Lindner, G. Huttner, P. Friedrich,

F. R. Kreißl and J. O. Besenhard, *Chem. Ber.* **1977**, *110*, 3397–3404; (c) E. O. Fischer, M. Schluge,

J. O. Besenhard, P. Friedrich, G. Huttner and F. R. Kreißl, *Chem. Ber.* **1978**, *111*, 3530–3541;

(d) E. O. Fischer, F. J. Gammel, J. O. Besenhard, A. Frank and D. Neugebauer,

J. Organomet. Chem. **1980**, *191*, 261–282.

31 E. O. Fischer, F. J. Gammel and D. Neugebauer, *Chem. Ber.* **1980**, *113*, 1010–1019.

32 E. O. Fischer, V. N. Postnov and F. R. Kreißl, *J. Organomet. Chem.* **1977**, *127*, C19–C21.

33 S.-T. Liu and K. R. Reddy, *Chem. Soc. Rev.* **1999**, *28*, 315–322.

34 I. J. B. Lin and C. S. Vasam, *Comment. Inorg. Chem.* **2004**, *25*, 75–129.

The transfer of a Fischer-type carbene group to a gold metal centre has been effected by reacting a suitable starting compound of Cr, Mo or W with either $\text{H}[\text{AuCl}_4]$,³⁵ Ph_3PAuCl ³⁶ or $(\text{R}_2\text{S})\text{AuCl}$.³⁷ The pathway when using tetrachloroauric acid is thought to proceed *via* the oxidation of the pentacarbonyltungsten moiety to ultimately yield *cis*- $[\text{WCl}_2(\text{CO})_4]$ and the Au^{I} carbene complex; although Au^{III} species have also been observed as products. To date, only a few reports of Fischer-type carbenes of gold were published and as a consequence the knowledge in this field remains limited.

Transfer reactions employing *r*NHCs have not attracted the attention of the scientific community yet. In our group, an *r*NHC complex of chromium prepared by the method of Aumann^{8a} was employed recently for the first time as a source of a carbene ligand when transferred to $[\text{Rh}_2(\mu\text{-Cl})_2(\text{CO})_4]$ to afford a novel *r*NHC Rh^{I} complex.³⁸

Carbyne transfer reactions from one metal centre to another, however, are rare which may be attributed to the strong metal–ligand bond in this case. A single example, involving a Fischer-type carbyne complex, involves reaction between *trans*- $[\text{Cr}(\equiv\text{CR})\text{Br}(\text{CO})_4]$ and $[\text{Co}_2(\text{CO})_8]$ furnishing $[\text{Co}_3(\mu_3\text{-RC})(\text{CO})_9]$.³⁹ However, alkylidyne ligands participate in alkyne metathesis^{27,40} and thus cannot be considered inert.

-
- 35 (a) R. Aumann and E. O. Fischer, *Chem. Ber.* **1981**, *114*, 1853–1857; (b) E. O. Fischer, M. Böck and R. Aumann, *Chem. Ber.* **1983**, *116*, 3618–3623; (c) E. O. Fischer and M. Böck, *Monatsh. Chem.* **1984**, *115*, 1159–1164; (d) E. O. Fischer and M. Böck, *J. Organomet. Chem.* **1985**, *287*, 279–285; (e) R.-Z. Ku, J.-C. Huang, J.-Y. Cho, F.-M. Kiang, K. R. Reddy, Y.-C. Chen, K.-J. Lee, J.-H. Lee, G.-H. Lee, S.-M. Peng and S.-T. Liu, *Organometallics* **1999**, *18*, 2145–2154.
- 36 (a) H. G. Raubenheimer, M. W. Esterhuysen, A. Timoshkin, Y. Chen and G. Frenking, *Organometallics* **2002**, *21*, 3173–3181; (b) H. G. Raubenheimer, M. W. Esterhuysen, G. Frenking, A. Y. Timoshkin, C. Esterhuysen and U. E. I. Horvath, *Dalton Trans.* **2006**, 4580–4589.
- 37 F. Kessler, N. Szesni, C. Maaß, C. Hohberger, B. Weibert and H. Fischer, *J. Organomet. Chem.* **2007**, *692*, 3005–3018.
- 38 E. Stander-Grobler, *Ph.D. thesis*, Stellenbosch University, **2008**.
- 39 (a) E. O. Fischer and A. Däweritz, *Angew. Chem., Int. Ed. Engl.* **1975**, *14*, 346–347 (*Angew. Chem.* **1975**, *87*, 360–361); (b) E. O. Fischer and A. Däweritz, *Chem. Ber.* **1978**, *111*, 3525–3529.
- 40 For a review on recent advances in alkyne metathesis see: W. Zhang and J. S. Moore, *Adv. Synth. Catal.* **2007**, *349*, 93–120.

5.1.4 Aims of this study

The aims of the investigation described in this Chapter were to synthesise and fully characterise tungsten carbyne complexes that bear thiazole groups at the carbyne carbon atom and to explore their properties and inclination towards interaction with chosen Au^I compounds.

The synthesis of these novel carbyne complexes necessarily involves the formation of pentacarbonyl(thiazolylcarbonyl)tungstates(1–) which are suitable as precursors for the synthesis of a wide variety of other compounds such as the corresponding carbene complexes and also transfer products from their reaction with gold electrophiles. It was foreseen that characterisation of the former products complements earlier reports of Fischer-type carbene complexes in our laboratory⁴¹ that have been utilised in the ‘complex-of-complexes’ concept.⁴² In the latter case the question arose whether during ligand transfer the displaced W(CO)₅ group would remain attached to the formed Au^I complex given that the thiazole ring present would offer *N*- or possibly *S*-coordination.

A final goal was to broaden the scope of group 6 metal to gold carbene transfer reactions to also include *r*NHC ligands, such complexes have not been described for gold. Apart from their usual characterisation, further insight into the bonding situation in the Au^I–carbene bond [see Scheme 5.3 (a)] was expected from these complexes.

5.2 Results and discussion

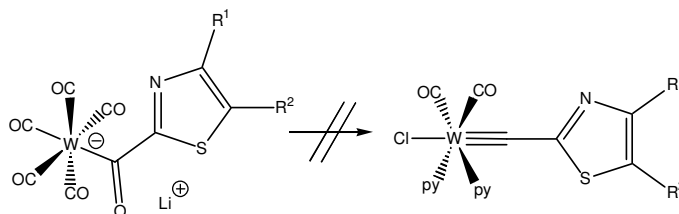
5.2.1 The attempted synthesis of 2-thiazolyl carbyne complexes

Initially attention was directed towards the preparation of 2-thiazolyl carbyne complexes and as starting material tetramethylammonium (benzothiazol-2-ylcarbonyl)-pentacarbonyltungstate(1–), **2**, was prepared.⁴¹ Following a modified procedure of

41 H. G. Raubenheimer, Y. Stander, E. K. Marais, C. Thompson, G. J. Kruger, S. Cronje and M. Deetlefs, *J. Organomet. Chem.* **1999**, 590, 158–168.

42 H. G. Raubenheimer, A. du Toit, M. du Toit, J. An, L. van Niekerk, S. Cronje, C. Esterhuysen and A. M. Crouch, *Dalton Trans.* **2004**, 1173–1180.

Mayr²⁰ and for the first time employing the self-purifying (all products from hydrolysis are gaseous) bis(trichloromethyl)carbonate (“triphosgene”) as a convenient solid reagent (Scheme 5.4) rather than gaseous COCl₂ (whose handling is dangerous and cumbersome) or (trichloromethyl)chlorocarbonate (which can be contaminated with HCl). Subsequently the product of a possible carbyne formation was stabilised by the addition of pyridine affording the *cis*-bis(pyridine) derivatives because *trans*-[M(≡CR)X(CO)₄] complexes are relatively labile compounds (their stability increases in the series M = Mo < Cr < W and X = Cl < Br < I).



Scheme 5.4 R¹ = Me and R² = H or R¹R² = -(CH)₄- Reaction conditions: (CCl₃O)₂CO, -78 °C to 0 °C, pyridine, r.t., CH₂Cl₂.

During this unsuccessful probing of the viability of the reaction procedure and reagents it became evident that the starting material had indeed been consumed but only a black solid could be isolated that yielded virtually no neutral products when subjected to chromatography under inert conditions at -30 °C employing silica gel as a stationary phase and CH₂Cl₂/thf mixtures of increasing thf content as eluents.

The fact that attempts to prepare 2-thiazolyl carbyne complexes were unsuccessful, could probably be attributed to the heterocycle’s strong electron-withdrawing effect on the carbyne ligand, hence destabilising the complex.

Subsequently, synthesis of *cis*-dicarbonylchloro[(4-methylphenyl)methylidyne]-*cis*-bis(pyridine)tungsten, **3**, was achieved under the chosen conditions to test their viability. Two crystal and molecular structures were determined for **3**, a solvent-free structure and a thf solvate obtained from a failed reaction.

5.2.2 Syntheses of 5-thiazolyl carbyne and carbene complexes

Other possibilities to prepare thiazolyl carbyne complexes were envisaged considering the results above. For such complexes to be stable, the heterocycle bound to the carbyne carbon atom should not exert a too strong electron-withdrawing effect. Two straightforward options allow for the electronic tuning of a thiazole ring: firstly, introduction of electron-donating substituents at appropriate positions and, secondly, performing the lithiation at a less electron-withdrawing position. Such a site can simply be identified by comparison of the ^1H NMR chemical shifts of the three thiazole protons; for the 2-, 4- and 5-positions the respective chemical shifts are 8.88, 7.98 and 7.41 ppm.⁴³ Thiazoles can easily be lithiated in the 5-position, provided the more acidic 2-position is blocked by appropriate substituents (a methyl group was found unsuitable);⁴⁴ the 2-position, furthermore, lends itself to facile incorporation of substituents with free electron pairs, in turn alleviating electron demand within the heterocycle.

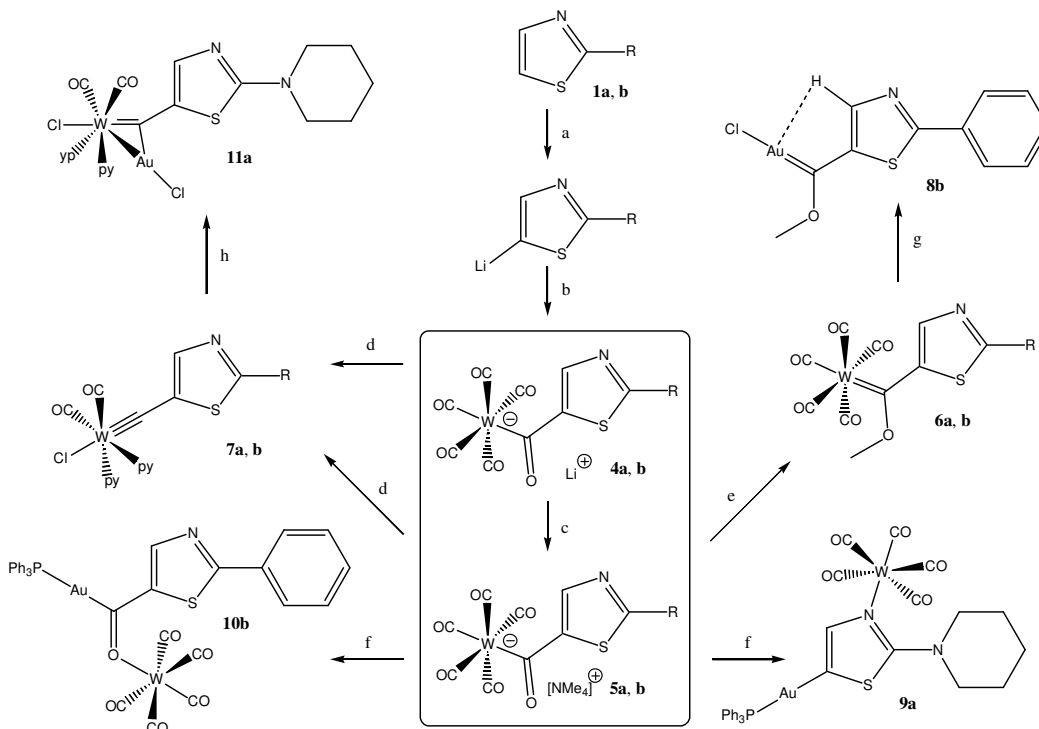
1-(Thiazol-2-yl)piperidine, **1a**, was selected as a ligand incorporating both “improvements” of the initial concept. The compound is readily accessible by reacting 2-bromothiazole with piperidine.⁴⁵ In addition, 2-phenylthiazole, **1b**, was chosen as a ligand without additional electron push into the ring; again lithiation proceeds readily at the 5-position. It was prepared by a modified literature synthesis from benzene thiocarboxamide and 2-bromo-1,1-diethoxyethane.⁴⁶ Scheme 5.5 summarises the synthetic pathways and conditions employed in the synthesis of the new heterocyclic carbenes and carbynes.

43 E. Pretsch, P. Bühlmann, C. Affolter and M. Badertscher, in *Spektroskopische Daten zur Strukturaufklärung Organischer Verbindungen*, 4th edn., Springer, Berlin, **2001**, p. 104.

44 M. Schlosser, in *Organometallics in Synthesis. A Manual*, ed. M. Schlosser, Wiley, Chichester, **2002**, p. 244.

45 T. E. Young and E. D. Anstutz, *J. Am. Chem. Soc.* **1951**, *73*, 4773–4775.

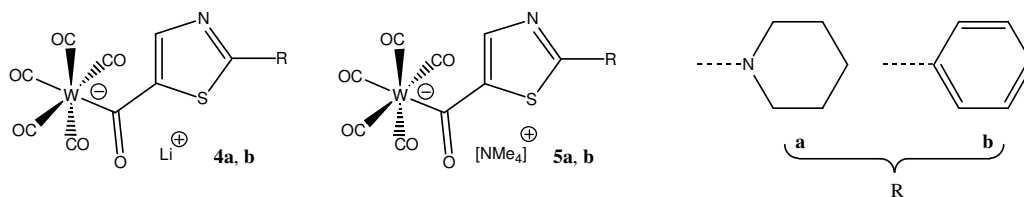
46 G. J. Durant, C. R. Ganellin, D. W. Hills, P. D. Miles, M. E. Parsons, E. S. Pepper and G. R. White, *J. Med. Chem.* **1985**, *28*, 1414–1422.



Scheme 5.5 Synthetic pathways leading to the carbene and carbyne complexes **4** to **11**; R = 1-piperidynyl (**a**) and phenyl (**b**); reaction conditions: (a) BuLi, $-78\text{ }^{\circ}\text{C}$, thf; (b) $\text{W}(\text{CO})_6$, $-78\text{ }^{\circ}\text{C}$ to r.t., thf; (c) aqueous $[\text{NMe}_4]\text{Cl}$; (d) $(\text{Cl}_3\text{CO})_2\text{CO}$, $-78\text{ }^{\circ}\text{C}$ to r.t., pyridine, CH_2Cl_2 ; (e) $[\text{Me}_3\text{O}][\text{BF}_4]$, $0\text{ }^{\circ}\text{C}$, $\text{CH}_2\text{Cl}_2/\text{MeCN}$; (f) Ph_3PAuCl , $-78\text{ }^{\circ}\text{C}$ to r.t., thf; (g) $(\text{tht})\text{AuCl}$, $-5\text{ }^{\circ}\text{C}$, thf; (h) $(\text{tht})\text{AuCl}$, $-10\text{ }^{\circ}\text{C}$ to r.t., thf.

5.2.2.1 Syntheses of (acyl)pentacarbonyltungstates(1 $-$) **4a**, **4b** and **5a**, **5b**.

Lithiation of the ligand precursors and reaction with $\text{W}(\text{CO})_6$ afforded the orange or red lithium salts of the (acyl)pentacarbonyltungstates(1 $-$), **4a** and **4b**, which could be converted to the tetramethylammonium salts, **5a** and **5b**, by aqueous $[\text{NMe}_4]\text{Cl}$. Structures of the compounds are shown in Scheme 5.6.



Scheme 5.6 Structures of compounds **4a**, **4b** and **5a**, **5b**.

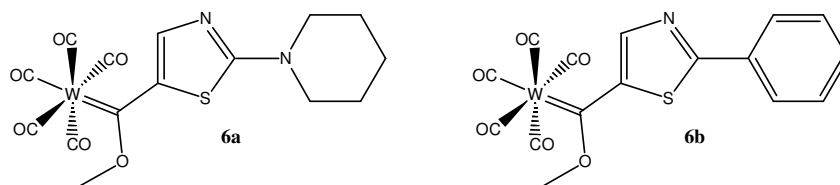
An interesting property of **5a** is its low solubility in dichloromethane and tendency to initially form a black supersaturated solution when it is extracted from the aqueous phase with small amounts of solvent. It thus readily precipitates during evaporation of

the solvent forming an ochre solid. Extraction from the aqueous solution must be performed with 20% ethanenitrile in CH_2Cl_2 to dissolve the residual precipitate which yields a crystalline orange product of analytical purity. Products prepared from **4a**, **5a** and **5b** were all purified by inert column chromatography, and **4a** could be utilised without any further purification in most reactions. On the other hand, the more stable compound **5b** dissolves freely in dichloromethane affording blood-red crystals upon removal of the solvent. This is a general finding for the colours of complexes derived from **1a** and **1b**, the former are generally of a translucent orange and the latter are of a much darker red colour, presumably caused by the different thiazole substituents.

The tetramethylammonium carbeniate salts, **5a** and **5b**, are fairly stable to air as solids and can be exposed to the atmosphere for short periods of time. This behaviour is in stark contrast to the 2-thiazolyl carbeniate complexes which, as solids, decompose rapidly upon contact with air and virtually immediately in solution. The use of lithium and tetramethylammonium salts for synthesis in one instance resulted in markedly different products (*vide infra*).

5.2.2.2 Syntheses of Fischer-type methoxy carbene complexes **6a** and **6b**.

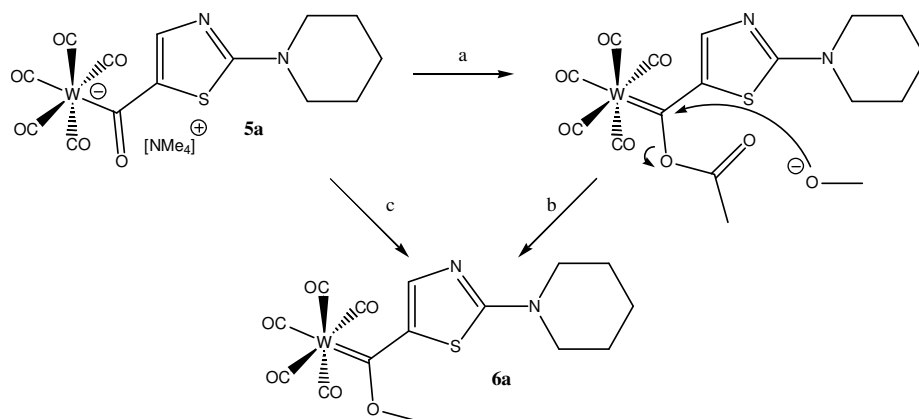
Due to the novelty of substitution at the 5-position of the thiazole rings in this group of complexes, the corresponding Fischer-type carbene compounds, **6a** and **6b**, were also prepared (Scheme 5.7).



Scheme 5.7 Compounds **6a** and **6b**.

To exclude the possibility of competing *N*-alkylation of the respective carbeniate salt, preparation of **6a** was first attempted by acylating the lithium carbeniate salt **4a** with ethanoyl chloride and then methanolysing the intermediary (ethanoyloxy)carbene complex. While this method has its merits especially with the introduction of substituents unsuitable as direct alkylating reagents or to protect other sensitive groups in

the complex from attack by the Meerwein salt,⁴⁷ the cumbersome chromatographic separation of **6a** from the (ethanoyloxy)carbene, results in a yield of **6a** that was not significantly higher than that obtained by alkylation of **4a** which is a much simpler process (Scheme 5.8).



Scheme 5.8 Synthetic pathways for **6a** – the analogue, **6b**, was only prepared *via* (c); (a) MeCOCl , NEt_3 , -40°C MeCN ; (b) MeOH , NEt_3 , -40°C to r.t., MeCN ; (c) $[\text{Me}_3\text{O}][\text{BF}_4]$, 0°C , $\text{CH}_2\text{Cl}_2/\text{MeCN}$.

Both carbene complexes were isolated from the product mixtures by flash chromatography under inert conditions at -20°C on a silica gel column in poor to modest yield (**6a** 7.4%, **6b** 35%). Serious competition from *N*-alkylation could be responsible, especially during the formation of **6a**. Stability of the compounds at room temperature and upon exposure to air for short periods is fair; decomposition occurs slowly and is indicated by the characteristic odour of the respective ligand precursors. Again, an observation already made for carbeniate complexes **5a** and **5b** is the much deeper colour of **6b** (purplish-black as a solid and purplish-red in solution) compared to the colour of orange **6a**. Yet, single crystals of **6b** appear dark orange when separated from the bulk product material.

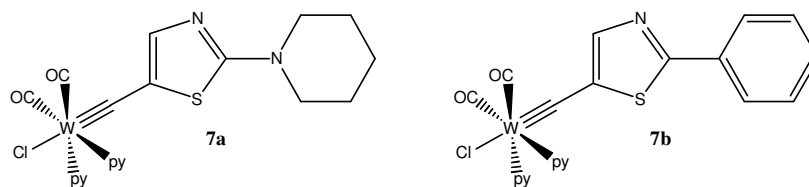
5.2.2.3 Syntheses of the carbyne complexes **7a** and **7b**.

The carbyne complex **7a** was obtained by first acylating the lithium carbeniate salt **4a** with $(\text{Cl}_3\text{CO})_2\text{CO}$ furnishing a dark-red solution. Upon warming to 0°C the (chloro-carbonyloxy)carbene complex believed to have formed²⁰ collapsed liberating CO_2 and the *trans*-CO ligand of the pentacarbonyl group. Addition of excess pyridine and

47 J. W. Herndon and J. J. Matasi, *J. Org. Chem.* **1990**, *55*, 786–788.

warming to room temperature afforded **7a** by substitution of a set of *cis*-CO ligands. The product was obtained as a brownish-orange solid in *ca.* 49% yield but was still contaminated with highly coloured trace impurities even after purification by flash chromatography on Florisil under inert conditions at $-30\text{ }^{\circ}\text{C}$. Single crystals appeared orange and are much lighter in colour than the bulk powder.

Carbyne complex **7b** was prepared from the $[\text{NMe}_4]^+$ -carbeniate salt **5b** and isolated as a pure amorphous red paste in 54% yield after column chromatography under inert conditions. The compound can be obtained as a foam by trituration with Et_2O and quick evacuation of the solvent but crystallises only in the presence of dichloromethane to form red needles of **7b** $\cdot\text{CH}_2\text{Cl}_2$. The carbyne complexes shown in Scheme 5.9 are reasonably stable at room temperature, albeit decomposition is observed after several days. In solution the compounds are markedly less stable; even at low temperature decomposition ensues over a period of weeks. The carbynes do not display similar R_f values on thin layer chromatographic plates than on low temperature inert silica gel columns. Much more polar solvent mixtures are needed to elute the compounds preparatively from the latter than would appear necessary by preliminary tlc testing.

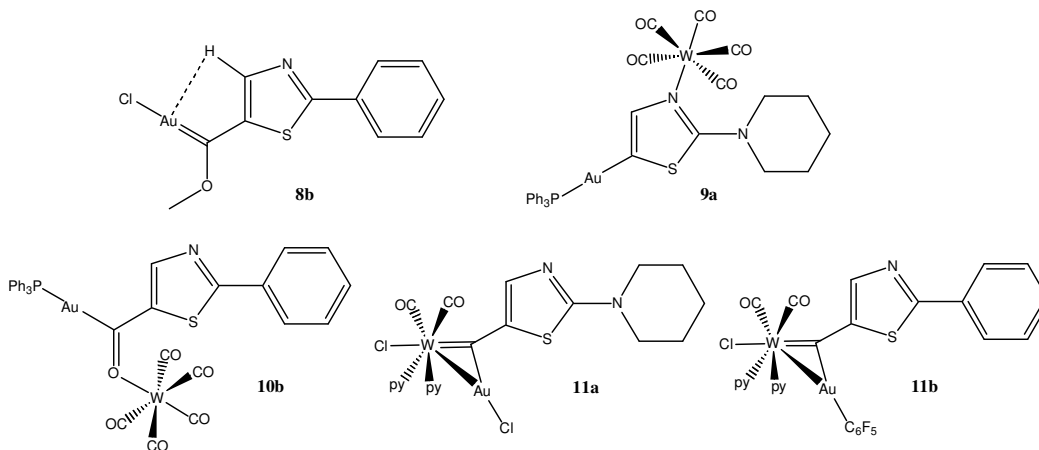


Scheme 5.9 Structures of compounds **7a** and **7b**.

5.2.3 Transfer to gold(I) centres

5.2.3.1 Transfer of heterocyclic carbene ligands to the gold fragments *AuCl* and Ph_3PAu^+ – isolation of **8b**, **9a**, and **10b**.

Compounds formed by transfer of carbene ligands to Au^{I} centres or coordination of Au^{I} fragments to carbyne complexes are summarised in Scheme 5.10.



Scheme 5.10 Structures of compounds **8b–11b**.

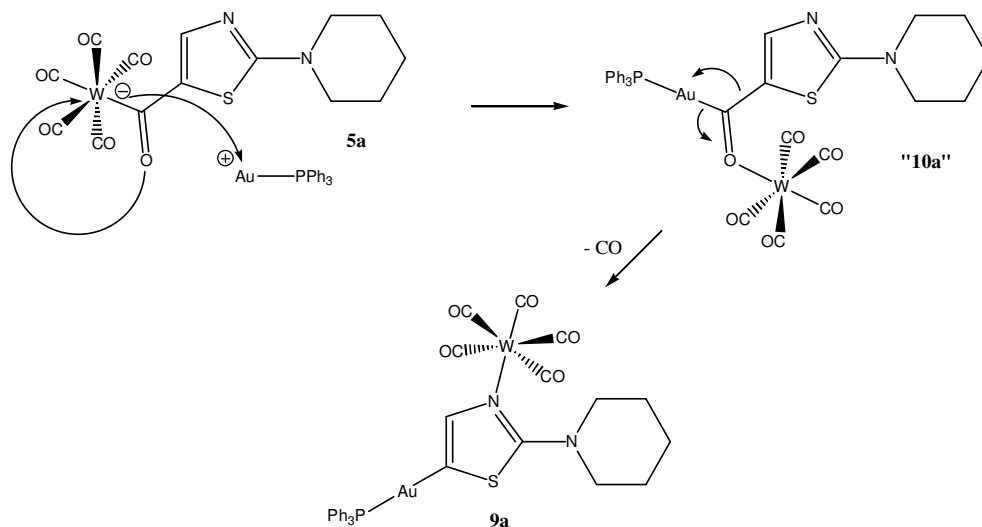
The Fischer-type carbene complex **6b** was selected to probe the feasibility of transferring the new type of carbene ligand from W⁰ to Au¹. When equimolar amounts of (tht)AuCl and **6b** were dissolved in thf at $-5\text{ }^{\circ}\text{C}$, a black precipitate formed after several hours. Monitoring of the reaction progress by tlc was made impossible by the sensitivity of both (tht)AuCl and especially chloro[methoxy(2-phenylthiazol-5-yl)methylidene]gold, **8b**; the former decomposes rapidly, the latter instantly when spotted onto a tlc plate. Crystallisation of the crude product afforded a modest yield (62%) of beautifully faceted orange-red crystals.

In the solid state the molecules of **8b** associate *via* aurophilic interactions (*vide infra*) rendering the compound only slightly soluble in dichloromethane or thf, whereas the crude product could be dissolved quite readily. In addition, both ¹H and ¹³C NMR spectra as well as X-ray crystallography supplied evidence for Au[⋯]H agostic interactions involving H-4 of the thiazole group. Complex **8b** is therefore not only a rare example of a compound exhibiting agostic Au[⋯]H interactions but also the only Fischer-type carbene complex of gold known to undergo aurophilic interactions in the solid state.

Encouraged by these results, the reactions of the carbeniates **4a** and **5b** with another gold complex, Ph₃PAuCl, were examined (Scheme 5.5). Addition of the lithium carbeniate salt **4a** to a solution of Ph₃PAuCl in thf at $-78\text{ }^{\circ}\text{C}$ and allowing the reaction vessel to reach room temperature, gave rise to several products as evidenced by tlc. In stark contrast to the gold carbene complex **8b**, these products were extremely stable

and could easily be separated by column chromatography under inert conditions on Florisil at $-30\text{ }^{\circ}\text{C}$, a rare phenomenon among compounds of gold. Two fractions were obtained, the less polar one yielded crystals of the aurated thiazole complex, **9a**, (now suitable for X-ray crystallography) in poor yield (16%). The identity of the more polar fraction could not be determined.

Yellow crystals of **9a** are fairly stable but decompose when exposed to the atmosphere for longer periods of time. The detailed mechanism for the formation of **9a** is not known. Scheme 5.11 shows a working mechanism for the process: nucleophilic attack on Ph_3PAu^+ could initially [by $\text{W}(\text{CO})_5$ -migration] lead to “**10a**”, a structure similar to **10b** which has been fully characterised (*vide infra*). When CO is expelled, the more nucleophilic thiazole nitrogen scavenges the $\text{W}(\text{CO})_5$ group. The formation of this compound is the first example of a Au^{I} acyl complex that undergoes a decarbonylation reaction. Furthermore, **8b** is a *pseudo-abnormal* carbene complex since the $\text{W}(\text{CO})_5$ fragment is isolobal to H^+ .



Scheme 5.11 Possible mechanism for the formation of **9a** via an intermediate similar to **10b**.

CO Insertion into a Au–C bond has been shown to occur when forced by pressure and heat in one example by *Cinellu et al.*, but no reaction is observed under standard conditions.⁴⁸ *Komiya et al.* have reported the reversible carbonylation of a Au^{III} complex, iodo-*cis*-dimethyl(triphenylphosphane)gold. This compound then affords

48 M. A. Cinellu, A. Zucca, S. Stoccoro, G. Minghetti, M. Manassero and M. Sansoni, *J. Chem. Soc., Dalton Trans.* **1995**, 2865–2872.

(methoxycarbonyl)-*cis*-dimethyl(triphenylphosphane)gold upon reaction with NaOMe and CO; the product could be decarbonylated again by reaction with acids.⁴⁹ Ph₃PAuCl was also reported to undergo methoxycarbonylation in methanol to afford (methoxycarbonyl)(triphenylphosphane)gold.^{49b} Proof of the reactivity of Au^I complexes towards CO is also provided by the catalysis of the formylation of amines by [Au(PPh₃)₂]⁺ and other related compounds.⁵⁰

The propensity of the [NMe₄] tungsten carbenate salt, **5b**, to also expel CO upon transfer to Ph₃PAu⁺ was subsequently investigated. To facilitate progress of the reaction, Na[BF₄] was added as scavenger of free chloride; in this reaction no Li⁺ was present that could, otherwise, have served this purpose. Two reaction products were identified by tlc and could in part be separated by column chromatography under inert conditions on Florisil at –30 °C.

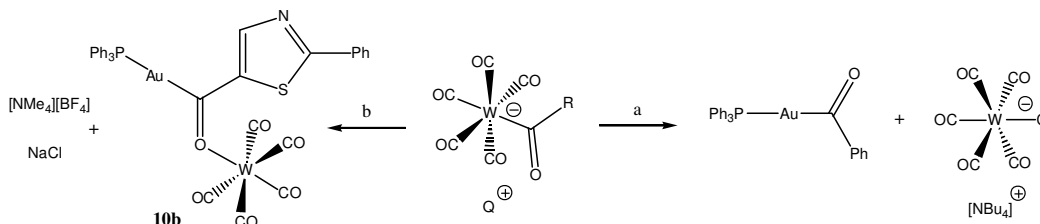
A first, apolar fraction consisted of two compounds in an approximate 3:1 ratio, identified by their respective ¹³C NMR carbene carbon signals at δ 252.3 (d, J_{PC} 134 Hz, 3 C) and 251.5 (d, J_{PC} 136 Hz, 1 C), and by the characteristic coupling indicative of Ph₃PAu⁺ groups coordinated to this carbene complex. However in the ¹H NMR spectrum, the ratio of phenyl *o*-CH groups belonging to the heterocyclic ligand to PPh₃ was exactly 1:2 hence pointing towards the presence of more than one Ph₃PAu⁺ unit per carbenate molecule in at least one of the two species detected. A necessary charge for a species comprising more than one Ph₃PAu⁺ fragment per carbenate contradicts the very apolar behaviour during chromatography. The presence of unconsumed Ph₃PAuCl cannot be excluded, but would be unlikely given that no crystals could be obtained from this fraction; Ph₃PAuCl is known to crystallise most readily. Given these facts and the presence of two products in the mixture no structure can be rationalised without reasonable doubt.

The second fraction contained the main product of the reaction, **10b**. The carbenate ligand was transferred to a Ph₃PAu⁺ fragment while the W(CO)₅ group migrated to the carbenate oxygen atom (*cf.* “**10a**” in Scheme 5.11). The resulting complex

49 (a) S. Komiya, M. Ishikawa and S. Ozaki, *Organometallics* **1988**, 7, 2238–2239; (b) S. Komiya, T. Sone, S. Ozaki, M. Ishikawa and N. Kasuga, *J. Organomet. Chem.* **1992**, 428, 303–313.
50 F. Shi, Y. Deng, H. Yang and T. SiMa [*sic*], *Chem. Commun.* **2001**, 345–346.

exhibits surprising stability given that *O*-bonded $W(CO)_5$ arrangements are normally prone to decomposition. This compound structurally represents the proposed product previously assumed to initially form in the synthesis of $Ph_3PAu-C(O)Ph$ in which the $W(CO)_5$ group is later scavenged by $[NBu_4]Cl$ by forming $[NBu_4][WCl(CO)_5]$ which precipitates from the ethereal reaction solution.⁵¹ Related isostructural products have been characterised for carbene-imidate complexes in the same report. This proposed mechanism has now been largely substantiated for O-containing carbeniates as well.

The isolation of this complex is very surprising given that oxygen is not an ideal ligating atom for the $W(CO)_5$ fragment; however, migration of this group to the thiazole imine nitrogen atom was not observed. It is not clear why the $W(CO)_5$ group is not lost in the preparation of **10b**. One cause may be the addition of $Na[BF_4]$ intended to promote chloride abstraction from Ph_3PAuCl which could ultimately precipitate $NaCl$ and $[NMe_4][BF_4]$, as side products and not $[NMe_4][WCl(CO)_5]$ (Scheme 5.12). Solvent and substituent effects (the piperidinyl group is replaced by a phenyl group).



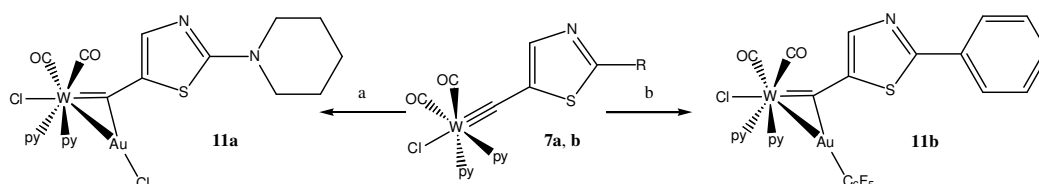
Scheme 5.12 Formation of acylgold complexes: (a) $R = Ph$, $Q^+ = [NBu_4]^+$, conditions: Ph_3PAuCl , Et_2O , $-78\text{ }^\circ C$; (b) $R = 2\text{-phenylthiazol-5-yl}$, $Q^+ = [NMe_4]^+$, conditions: Ph_3PAuCl , $Na[BF_4]$, thf , $-78\text{ }^\circ C$.

Further, loss of CO did not occur which may have electronic grounds related to the replacement of the piperidinyl with the phenyl group in the ligand. Utilisation of **5b** instead of **4b**, furthermore, did not introduce Li^+ into the reaction mixture; this cation might have assisted in the decarbonylation reaction.

51 (a) M. W. Esterhuysen, *Ph.D. thesis*, Stellenbosch University, **2003**; (b) H. G. Raubenheimer, M. W. Esterhuysen and C. Esterhuysen, *Inorg. Chim. Acta* **2005**, 358, 4217–4228.

5.2.3.2 Interaction of carbyne complexes **7a** and **7b** with gold centres.

Interaction of the carbyne complexes **7a** and **7b** with gold centres (Scheme 5.13) was also studied to elucidate which of the two donor positions (formal W–C triple bond or imine nitrogen) that presented themselves would be preferred. The first reaction of **7a** with (tbt)AuCl proceeded readily and an orange-brown adduct, **11a**, could be isolated. The reaction involved coordination of the AuCl fragment to the formal metallalkyne. However, the tungsten centre did not separate from the alkyne carbon and no transfer was effected – owing to the somewhat longer W–C bond in heterocyclic carbynes, it was considered that gold fragments could be successful in replacing the tungsten carbonyl on the ligand.



Scheme 5.13 Interaction of gold fragments with carbynes **7a** and **7b**: (a) **7a**, (tbt)AuCl, $-10\text{ }^{\circ}\text{C}$, thf; (b) **7b**, (tbt)AuC₆F₅, $-60\text{ }^{\circ}\text{C}$, thf; R = piperidin-1-yl for (a) and phenyl for (b).

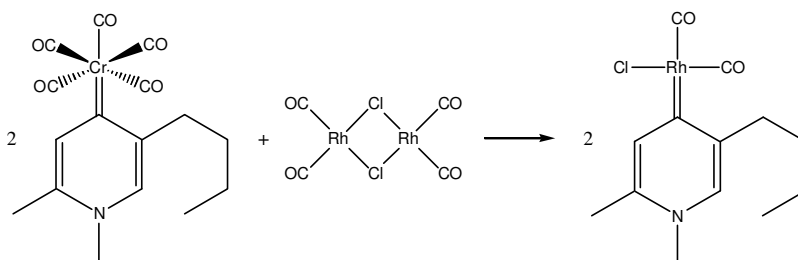
Carbyne complex **7b** was then reacted with (tbt)AuC₆F₅ in thf at $-60\text{ }^{\circ}\text{C}$. Two products containing gold were identified by tlc (silica gel plate, CH₂Cl₂ as mobile phase; R_f 0.72 and R_f 0). Their stability was sufficient for column chromatography under inert conditions and they were separated on a Florisil column at $-30\text{ }^{\circ}\text{C}$. Two fractions were obtained corresponding to the tlc analysis, again highlighting the difference in behaviour of these substances on a column compared to tlc plates; in this case the product with R_f 0 on the silica tlc plate could be eluted at low temperature. However, the crystals obtained from the less polar fraction were **7b**·CH₂Cl₂. In the ¹³C NMR spectrum of the first fraction two signals for carbene carbons at δ 243.0 and 240.7 were observed corroborating existence of **7b** (δ 240.8) as well as indicating the presence of another gold complex as the signal at δ 243, possibly attributable to **11b**. The CO signals for the products were observed at δ 220.0 (**7b**: 220.1) and 212.9. The isolation of crystals of free **7b** may result from a homoleptic rearrangement of **11b** as

such rearrangements have frequently been observed for the AuC_6F_5 fragment.⁵² The resulting cation $[\text{Au}(\mathbf{7b})_2]^+$ may have undergone solvolysis, which was reported for similar complexes,⁵³ liberating $\mathbf{7b}$ that crystallised under these conditions.

The second fraction failed to yield any crystals and only NMR evidence supported the formation of a complex similar to that in the first fraction. ^{13}C NMR signals for carbyne and CO species are similar to those in the first fraction to within ± 0.1 ppm.

5.2.3.3 Transfer of *r*NHC ligands to Au^I.

Carbene transfer from chromium and tungsten is well documented in the literature^{35–37} and given the successful synthesis of $\mathbf{8b}$, $\mathbf{9a}$ and $\mathbf{10b}$ above, the transfer of *r*NHC ligands to gold was also attempted after it was recently found in a preliminary investigation that transfer of a *r*NHC occurs from a *r*NHC chromium complex to $[\text{Rh}_2(\mu\text{-Cl})_2(\text{CO})_4]$ as shown in Scheme 5.14.³⁸



Scheme 5.14 Product obtained by transfer of a *r*NHC ligand to Rh^I.

Utilising the same chromium complex and $(\text{tht})\text{AuC}_6\text{F}_5$ as a substrate, a crystalline product was obtained but the fine colourless needles were too small for X-ray crystallography. Proof of transfer could therefore only be obtained by FAB mass spectrometry showing signals at m/z 360 $[\text{AuL}]^+$, 523 $[\text{AuL}_2]^+$, 887 $[\text{AuL}_2\cdot\text{AuC}_6\text{F}_5]^+$ and 1054 $[\text{AuL}_2\cdot\text{Au}(\text{C}_6\text{F}_5)_2]^+$ ($\text{L} = 5\text{-butyl-1,2-dimethyl-1H-pyridin-4-ylidene}$), the only question that remains unanswered is whether the product exists as neutral LAuC_6F_5 or in the form of the homoleptically rearranged salt $[\text{AuL}_2][\text{Au}(\text{C}_6\text{F}_5)_2]$. The rearranged fragment ions observed might have formed during the ionisation process. Owing to

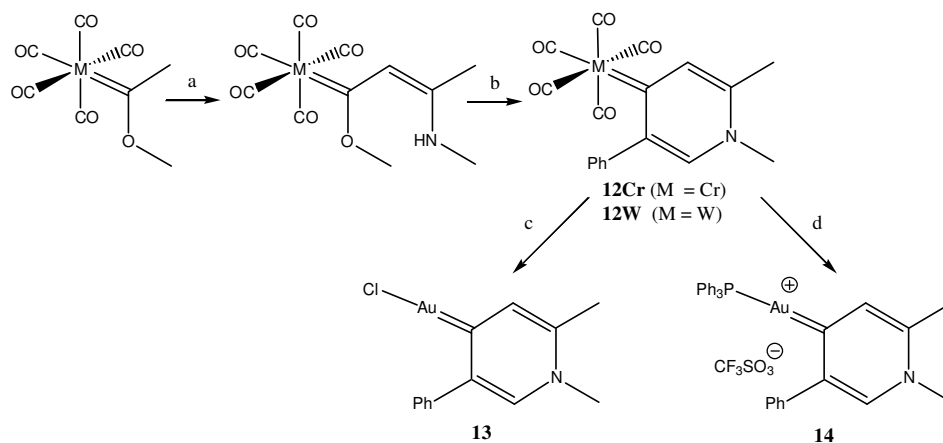
52 (a) K. Coetzee, *M.Sc. thesis*, Stellenbosch University, **2005**;

(b) W. F. Gabrielli, *Ph.D. thesis*, Stellenbosch University, **2006**, pp. 106 and 163;

(c) L. de Jongh, *M.Sc. thesis*, Stellenbosch University, **2008**.

53 G. A. Carriedo, V. Riera, G. Sánchez, X. Solans and M. Labrador, *J. Organomet. Chem.* **1990**, *391*, 431–437.

the thermal movement of the butyl group it is unlikely that compounds containing this *r*NHC ligand would crystallise readily. To overcome this possible limitation, two new pentacarbonyl *r*NHC chromium, **12Cr**, and *r*NHC tungsten, **12W**, complexes were prepared (Scheme 5.15).



Scheme 5.15 Synthetic pathway to substituted group 6 *r*NHC complexes **12–14** starting from pentacarbonyl(1-methoxyethylidene)chromium and -tungsten complexes as well as the gold complexes obtained after ligand transfer; conditions: (a) BuLi, [MeCNMe][BF₄], –78 °C, thf; (b) PhC≡CH, 70 °C, thf, 12 h; (c) (tht)AuCl, –35 °C to r.t., CH₂Cl₂; (d) Ph₃PAuCl, NaOTf, –45 °C to r.t., MeCN.

Following the protocol established in the synthesis of **8b**, the *r*NHC gold chloride complex **13** was synthesised from **12W** and (tht)AuCl at –35 °C by mixing homogeneous CH₂Cl₂ solutions of the reagents. The product was obtained by simple workup due to its lower solubility compared to the pentacarbonylmetal side product.

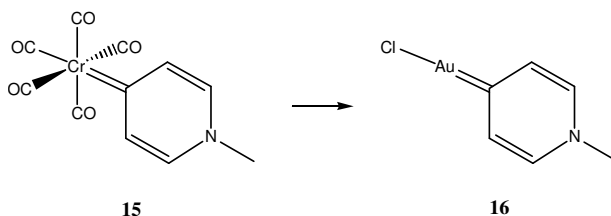
Likewise, **12Cr** was reacted with Ph₃PAuCl and NaOTf in ethanenitrile affording a cationic *r*NHC gold complex, **14**, in 78% yield. Intriguingly, workup in the usual manner (precipitation of product with Et₂O or pentane) was not possible as this compound is more soluble than its neutral counterparts and tends to form supersaturated solutions. Crystallisation from CH₂Cl₂/pentane yielded the pure complex in the form of long colourless needles.

Both **12Cr** and **12W** are thus suitable carbene sources for the transfer reactions, although the employment of chromium compounds is preferred. The reaction of the precursor of **12W** with ethynylbenzene does not go to completion and

chromatographic separation is exceedingly difficult given the minute difference in R_f values of product and starting material. Transfer itself, however, proceeds similarly with both reagents.

Following *Stone*,⁵⁴ the simplest member of remote pyridinylidene carbene complex family, pentacarbonyl(1-methyl-1*H*-pyridin-4-ylidene)chromium, **15**, was synthesised according to a method never again utilised since 1974 despite its inherent simplicity. After $\text{Cr}(\text{CO})_6$ had been conveniently reduced to $\text{Na}_2[\text{Cr}(\text{CO})_5]$ by sodium naphthalenide, addition of 4-chloro-1-methylpyridinium triflate yielded **15** in a one-pot reaction. Purification by flash chromatography under inert conditions followed. Although the product was obtained in poor yield (11%), this procedure is much more convenient than the method of *Aumann*^{8a} which, starting with $\text{M}(\text{CO})_6$, requires 4 reaction steps and at least two chromatographic purifications. However, the former protocol requires access to the selected pyridinium salt.

When the novel *r*NHC complex **15** and (tht)AuCl were dissolved together in CH_2Cl_2 , immediate surfacial decomposition of the solid gold compound was observed; nonetheless **16** could be isolated in 20% yield (Scheme 5.16).



Scheme 5.16 Synthesis of **16** from **15**; conditions: (tht)AuCl, r.t., CH_2Cl_2 .

5.3 Spectroscopic characterisation

The compounds were characterised by a number of techniques, most notably multinuclear NMR spectroscopy and single crystal X-ray diffraction. Infrared spectroscopy yielded unrivaled information about the electronic environment of the

⁵⁴ P. J. Fraser, W. R. Roper and F. G. A. Stone, *J. Chem. Soc., Dalton Trans.* **1974**, 760–764.

carbonyl ligands and mass spectrometry gave valuable information on the stability of the compounds, especially towards decarbonylation.

5.3.1 Infrared spectroscopy

From the location, intensity and number of the vibration bands of the CO ligands, information on the local geometry can be obtained. For the compounds reported here, this involves the $M(\text{CO})_5$ and *cis*- $M(\text{CO})_2$ fragments. For pentacarbonylchromium and pentacarbonyltungsten complexes, theory predicts three IR-active bands of symmetry $A_1^{(1)}$, $A_1^{(2)}$ and E, while for *cis*-dicarbonyltungsten complexes two bands of A_1 and B_1 symmetry should be observed.⁵⁵

Table 5.1 contains the wavenumbers of the new carbonyl complexes. In the actual solid-state spectra the $A_1^{(1)}$ bands could be assigned unambiguously and the (IR-inactive but often observed) B_1 band with relative safety, the assignment of the E and $A_1^{(2)}$ bands was not always without ambiguity, as more than two bands were often observed. In certain cases where two molecules were found in the asymmetric unit (**5b** and **6a**) additional bands may in fact be caused by the different environment experienced by the CO ligands of each unique molecule. Solution spectra in dichloromethane only furnished $A_1^{(1)}$ and E bands.

For carbene complexes it is obvious that the piperidine substituent at the thiazole ring influences the carbonyl frequencies to an appreciable extent compared to the phenyl analogues. The $A_1^{(1)}$ band is always found at lower frequencies for the piperidinylthiazole-derived compounds **5a** and **6a** compared to phenylthiazole-derived compounds **5b** and **6b**. Both heterocyclic ligands cause a shift of the $A_1^{(1)}$ band to lower frequencies compared to the $A_1^{(1)}$ band in $\text{Ph}(\text{MeO})\text{C}=\text{W}(\text{CO})_5$,⁵⁶ although for **6b** this difference is only 3 cm^{-1} .

In the instance of the carbynes, the A_1 band is shifted to somewhat lower wavenumbers compared to the 4-methylphenyl carbyne complex **3**. The piperidine substituent of **7a** again donates electron density to the tungsten centre causing a shift

⁵⁵ M. Bigorgne, *J. Organomet. Chem.* **1975**, *94*, 161–180.

⁵⁶ R. M. Dahlgren and J. I. Zink, *J. Am. Chem. Soc.* **1979**, *101*, 1448–1454.

Table 5.1 IR band wavenumbers ν/cm^{-1} of carbonyl compounds **3–15**^a

Band	A ₁ ⁽¹⁾	B ₁	E	A ₁ ⁽²⁾
5a (solid)	2044 (s)	1949 (m)	1881, 1859 (vs)	1840 (vs)
6a (solid)	2058 (s)	1969, 1952 (m)	1891 (vs)	1884 (vs)
6a (solution)	2062 (s)		1929 (vs)	
9a (solid)	2065 (w)	1903 (br)		
5b (solid)	2046 (s)	1941, 1919 (m)	1870 (vs)	1835 (vs)
5b (solution)	2050 (s)		1907 (vs)	
6b (solid)	2070 (s)	1969, 1948 (s)	1880 (vs)	^b
6b (solution)	2068 (vs)		1942 (vs)	
10b (solid)	2067 (w)	1923		
Ph(MeO)C=W(CO) ₅ ⁵⁶	2073		1944	1961
15 (solid)	2043 (s)	1962 (s)	1909 (vs)	1857 (vs)
15 (solution)	2044 (s)		1917 (vs)	
12Cr (solid)	2037 (s)	1958 (w)	1931 (m)	1883 (vs)
12Cr (solution)	2041 (s)		1917 (vs)	
12W (solid)	2049 (s)	1963 (s)		1875 (vs)
12W (solution)	2052 (s)		1929 (vs)	
3 (solid)	1978 (vs) ^c	1876 (vs)		
7a (solid)	1965 (vs) ^c	1877 (vs)		
7b (solid)	1972 (vs) ^c	1886 (vs)		

^a All solid spectra are recorded on a ZnSe ATR accessory, all liquid spectra were recorded as CH₂Cl₂ solutions in NaCl cells. Assignments: (vs) very strong, (s) strong, (m) medium, (w) weak; ^b Obscured by broad E band; ^c A₁ band.

to even lower frequency. The B₁ band of **7a** and **7b** follows this trend of a lower wavenumber for the piperidine-substituted complex. In **3**, the B₁ band is of comparable energy to that in **7b**. Therefore, the heterocyclic substituent additionally effects a smaller $\Delta\nu$ between the A₁ and B₁ vibrations.

5.3.2 Mass spectrometry

The ionisation method found to be most suitable for mass spectrometric assay of the compounds discussed above, was Fast Atom Bombardment (FAB). Matrix Assisted Laser Desorption Ionisation (MALDI) was also used but gave no interpretable results.

Using FAB ionisation, the molecular ions of most complexes as well as the associated fragmentation patterns could be identified. The successive loss of up to 4 CO groups is common for carbonyl complexes. Peaks and intensities are shown in Table 5.2. Negative mode FAB for the carbenate salts **5a** and **5b** was not recorded and

Table 5.2 FAB mass spectra of compounds **5a–14**. All m/z are based on ^{184}W and ^{35}Cl isotopes, intensities in parentheses. Base peak at m/z 154 [(3-nitrophenyl)methanol + H] $^+$ if no other fragment at 100% intensity.

Compound	5a	5b	6a	6b	7a	7b	8b	9a	10b	11a	12Cr	12W	13	14	15	16
Empirical formula	$\text{C}_{18}\text{H}_{23}\text{N}_3\text{O}_6\text{SW}$	$\text{C}_{19}\text{H}_{18}\text{N}_2\text{O}_6\text{SW}$	$\text{C}_{15}\text{H}_{14}\text{N}_2\text{O}_6\text{SW}$	$\text{C}_{16}\text{H}_9\text{N}\text{O}_6\text{SW}$	$\text{C}_2\text{H}_2\text{Cl}\text{N}_4\text{O}_2\text{SW}$	$\text{C}_2\text{H}_2\text{Cl}\text{N}_3\text{O}_2\text{SW}$	$\text{C}_{11}\text{H}_9\text{Au}\text{Cl}\text{N}\text{O}$	$\text{C}_3\text{H}_2\text{Au}\text{N}_2\text{O}_5\text{PSW}$	$\text{C}_3\text{H}_2\text{Au}\text{N}\text{O}_6\text{PSW}$	$\text{C}_{21}\text{H}_{21}\text{Au}\text{Cl}_2\text{N}_4\text{O}_2\text{SW}$	$\text{C}_{13}\text{H}_{13}\text{Cr}\text{N}\text{O}_5$	$\text{C}_{18}\text{H}_{13}\text{N}\text{O}_5\text{W}$	$\text{C}_{13}\text{H}_{13}\text{Au}\text{Cl}\text{N}$	$\text{C}_{31}\text{H}_{28}\text{Au}\text{N}\text{P}^f$	$\text{C}_{11}\text{H}_7\text{Cr}\text{N}\text{O}_5$	$\text{C}_6\text{H}_7\text{Au}\text{Cl}\text{N}$
Exact mass	593.08	586.04	534.01	526.96	612.06	605.02	434.98	950.05	971.00	843.99	375.02	507.03	415.04	642.12 ^l	284.97	324.99
(M + H) $^+$	520 (12) ^{a,b}		535 (3) ^a	528 (10) ^a	613 (0.5) ^a	606 (2) ^a				845 (0.3) ^a						
M $^+$	519 (5) ^{a,b}	512 (2) ^{a,b}	534 (3) ^a	527 (8) ^a	612 (1) ^a	605 (3) ^a				844 (0.9) ^a	375 (10)	507 (5)		642 (100) ^l	285 (100)	
(M – CO + H) $^+$	492 (7) ^a	485 (1) ^a														
(M – CO) $^+$	491 (7) ^a	484 (1) ^a	506 (3)	499 (16)	584 (3)	577 (16)				816 (1)	347 (16)	479 (7)			257 (52)	
(M – 2CO + H) $^+$	464 (17) ^a	457 (1) ^a		472 (7) ^a												
(M – 2CO) $^+$	463 (2) ^a	456 (2) ^a	478 (8)	471 (11) ^a			549 (15)									
(M – 3CO + H) $^+$	436 (7) ^a															
(M – 3CO) $^+$	435 (7) ^a			443 (12)					887 (1)			423 (14)				
(M – 4CO + H) $^+$	408 (8) ^a															
(M – 4CO) $^+$	407 (10) ^a												263 (23)			
(M – Cl) $^+$					577 (2)	570 (7)				809 (0.5)			380 (100)			290 (100)
(M – py + H) $^+$						527 (3) ^a										
(M – py) $^+$						526 (1) ^a										
(M – py – CO) $^+$					505 (3)	498 (5)										
(M – py – 2CO + H) $^+$						471 (2) ^a				710 (0.5) ^a						
(M – py – 2CO) $^+$					477 (3)	470 (4) ^a				709 (1.5) ^a						
Ph_3PAu^+								459 (21)	459 (100)					459 (17)		
$[\text{Au}(\text{PPh}_3)_2]^+$								721 (13)	721 (22)							
$[\text{M} - \text{W}(\text{CO})_5 + \text{H}]^+$								627 (1)	648 (25)							
Others	667 (12) ^c	660 (8) ^c 301 (26)	450 (1) ^{a,d} 449 (1) ^{a,d} 422 (3) ^e				367 (18) ^f	386 (4) ^g 377 (3) 358 (3) ^h 341 (3)	1409 (2)	1078 (4) ⁱ	630 (0.8) ^{a,j} 629 (1.2) ^{a,j}	235 (19) ^k		380 (47) ^m		615 (11) ⁿ

^a Approximate ratio calculated from the overlapping pattern of the R $^+$ and [R + H] $^+$ peaks; ^b M $^+$ refers to mass of the anion after loss of two electrons

^c [M + NMe $_4$] $^+$ ^d [M – C $_5$ H $_{11}$ N] $^+$ and H $^+$ adduct ^e [M – CO – C $_5$ H $_{11}$ N] $^+$ ^f [Cl(CO) $_2$ (py)W \equiv CH] $^+$ ^g [M – Cl – CH $_3$ + H] $^+$ ^h [M – Cl – CH $_3$ – CO + H] $^+$

ⁱ [M – W(CO) $_5$ + Ph $_3$ PAu – CO] $^+$ ^j [M – 2CO – 2py] $^+$ and H $^+$ adduct ^k [M – 5CO] $^+$ ^l Cation only ^m [M – PPh $_3$] $^+$ ⁿ [2M – Cl] $^+$

unexpectedly was not even necessary to observe a molecular ion. Intriguingly, clusters of the type $[2\text{NMe}_4\cdot\text{anion}]^+$ (m/z 667 for **5a**, 660 for **5b**) comprising three ions in total, were found in the positive ion spectrum.

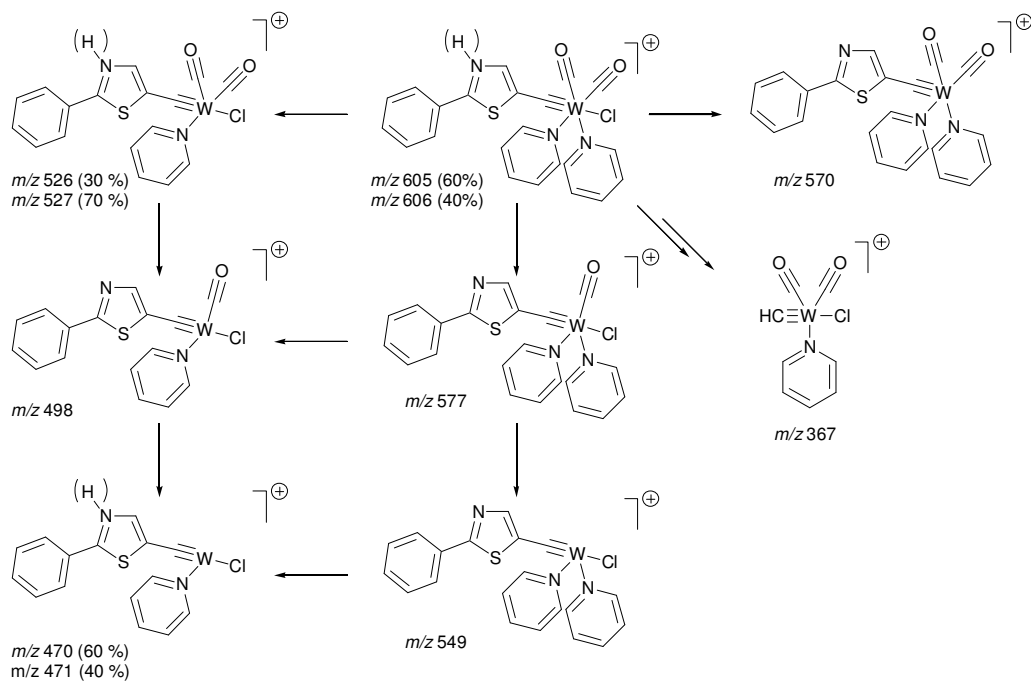
Since thiazoles can be protonated at the imine nitrogen (for complexes of ligand **1a** possibly also at the piperidinyl group) a multitude of peaks show a pattern resembling an overlay of the radical cation and the protonated species and an approximate ratio could be deduced from the intensities (I) of the two peaks at lowest m/z of each cluster according to Equation (5.1):

$$I(m) = (M^+, {}^{182}\text{W}); I(m+1) = [(M+H)^+, {}^{182}\text{W} + M^+, {}^{183}\text{W}] \quad (5.1)$$

With $I(M^+, {}^{182}\text{W})$ and therefore $I(M^+, {}^{183}\text{W})$ known, $I[(M+H)^+, {}^{182}\text{W}]$ could be calculated assuming negligible interference from ${}^{180}\text{W}$ (0.12% abundance) species and noise. Unexpectedly, complexes derived from phenylthiazole, **1b**, showed protonation to the same extent as the piperidinylthiazole compounds. However, the order of basicity of simple compounds was shown to follow entirely different rules when going from solution to the gas phase, *e.g.* $\text{H}_2\text{O}_{(\text{g})}$ is a weaker base than $\text{H}_2\text{S}_{(\text{g})}$.⁵⁷ Therefore, higher gas-phase basicity of compounds derived from piperidinylthiazole **1a** cannot be accepted and the extent of protonation of the complexes cannot be predicted.

The carbyne complexes **7a** and **7b** either lose pyridine *or* chloride yielding two fragmentation pathways by successively losing CO ligands; pyridine *and* chloride loss was never observed (Scheme 5.17). Pyridine loss affords radical cations (unless protonated) while chloride loss yields an even-electron species. The Fischer-type carbene complex **6a** and the AuCl-coordinated carbyne complex **11a** also fragment by expelling piperidine, which is not observed with any other complex derived from **1a**, though carbyne complex **7b** gave a peak at m/z 367 indicative of cleavage of the carbyne carbon–thiazole bond.

⁵⁷ E. P. L. Hunter and S. G. Lias, *J. Phys. Chem. Ref. Data* **1998**, 27, 413–656.



Scheme 5.17 Proposed fragmentation pathways of carbyne complex **7b**; compound **7a** exhibits similar patterns, but not all the corresponding species are observed.

The Fischer-type gold carbene complex **8b** yielded neither a molecular ion peak nor an $[M - Cl]^+$ peak which is usually observed with $LAuCl$ compounds. Fragmentation quickly proceeded beyond this probably very unstable intermediate to also expel a methyl group giving the hydroxycarbene (or *N*-protonated carbeniate) at m/z 386 which then further loses the CO group yielding protonated (2-phenylthiazol-5-yl)gold(1+) (m/z 358).

In the gold carbene transfer products **9a** and **10b** the $W(CO)_5$ unit is lost during fragmentation (m/z 627 and 648, respectively). Compound **10b** also exhibits a fragment resulting from a triple CO loss from the *O*-coordinated $W(CO)_5$ group (m/z 887); the $O-W(CO)_2$ bond seems to be sufficiently strong to allow this fragmentation. Furthermore, **10b** yields a synthetically not accessible CO-expulsion (m/z 1078) from the carbeniate complex forming a complex similar to **9a**, but lacking the $W(CO)_5$ group in favour of a second Ph_3PAu^+ fragment.

The *r*NHC gold complexes yield an $[M - Cl]^+$ base peak (m/z 380 for **13** and 290 for **16**) while **16** also affords a chloride-bridged $[(AuL)_2(\mu-Cl)]^+$ fragment (m/z 615).

Ionic **14** naturally yields the cation as the base peak (m/z 642) accompanied by $[\text{AuPPh}_3]^+$ (m/z 459) and $[\text{AuL}]^+$ (m/z 380) in a ratio of 1:3.

5.3.3 NMR spectroscopy

The nuclear magnetic resonance data of the compounds reported are summarised in Tables 5.3 (complexes obtained from **1a**), 5.4 (**1b**) and 5.5 (*r*NHC complexes).

From the measured ^1H and ^{13}C NMR spectra it can be concluded that the electronic distribution within the heterocycle in the Cr and W *r*NHC complexes has a higher contribution of the canonic pyridinylidene form than the Au *r*NHC complexes which more resemble metalated pyridinium salts.

5.3.3.1 ^1H NMR spectroscopy.

With the only probe near the metal centre being the H-4 proton of the thiazole ring, the proton magnetic resonance spectra of the compounds **5a–10b** are of limited use in estimating their electronic properties. The chemical shift of this proton in the carbene and carbyne complexes, except for carbyne complex **7b**, is observed at a somewhat lower field compared to the free ligand. This effect is most pronounced in the Fischer-type gold carbene complex **8b** ($\Delta\delta$ 1.34)⁵⁸ and carbyne complex **7a** ($\Delta\delta$ 1.52). Usually it was possible to extract a $^1J_{\text{CH}}$ coupling constant from the ^{13}C -satellite signals of the sharp thiazolyl proton resonance.

The H-4 proton of **8b**, however, shows a very broad signal at room temperature which is unusual for thiazole protons and prompted an investigation into its shape as a function of temperature (Figure 5.1). A significant decrease of the signal half-width from 10.5 Hz at 10 °C (283 K) to 0.93 Hz at –55 °C (218 K) is observed while the shapes of other peaks are not affected, except for a loss of resolution at lower temperatures likely due to precipitation from the saturated solution. The chemical shifts of all proton resonances vary slightly with temperature assuming that the reference signal of CH_2Cl_2 is constant. Again the thiazole proton shows odd

⁵⁸ Chemical shift differences are quoted as absolute values to avoid confusion. The actual sign must be obtained from context.

Table 5.3 NMR data of compounds **5a–9a**. Coupling constants are given in Hz.

Compound					
Nucleus	Solvent	CD ₃ OD	CDCl ₃	CDCl ₃	CDCl ₃
¹ H (400 MHz)	CH thiazole	7.80 (s, 1 H)	8.50 (s, ¹ J _{CH} 184.0, 1 H)	8.69 (br s, 1 H) ^a	7.54 (m, 16 H) ^{a,d}
	4- and 3/5-CH ₂ piperidine	1.66 (m, 6 H)	1.73 (m, 6 H)	1.68 (m, 6 H) ^a	1.83 (m, 4 H, 3/5-pip); ^a 1.62 (m, 2 H, 4-pip) ^a 3.01 (m, 4 H) ^a
¹³ C{ ¹ H} (101 MHz)	2/6-CH ₂ piperidine	3.48 (m, 4 H)	3.67 (m, 4 H)	3.52 (m, 4 H) ^a	3.01 (m, 4 H) ^a
	NMe ₄ ⁺ / OMe	3.18 (t, ² J _{NH} 0.59, 12 H, NMe ₄ ⁺)	4.49 (s, ¹ J _{CH} 146.7, 3 H, OMe)		
	<i>o</i> -CH PPh ₃ /pyridine			9.08 (m, 4 H, py) ^a	7.54 (m, 16 H, <i>o</i> -Ph) ^{a,d}
	<i>m</i> -CH PPh ₃ /pyridine			7.33 (m, 4 H, py) ^a	7.54 (m, 16 H, <i>m</i> -Ph) ^{a,e}
	<i>p</i> -CH PPh ₃ /pyridine			7.81 (tt, ³ J _{HH} 7.65, ⁴ J _{HH} 1.67, 2 H, py) ^a	7.54 (m, 16 H, <i>p</i> -Ph) ^{a,d}
	Carbene / Carbyne	271.8 (s, ¹ J _{183WC} 85.8)	274.3 (s, ¹ J _{183WC} 97.4)	245.1 (s) ^{b,c}	203.5 (s, ¹ J _{183WC} 151.1) ^b
	<i>trans</i> -CO	206.8 (s, ¹ J _{183WC} 133.1)	202.1 (s, ¹ J _{183WC} 124.2)		199.4 (s, ¹ J _{183WC} 131.1) ^b
	<i>cis</i> -CO	203.1 (s, ¹ J _{183WC} 127.3)	198.1 (s, ¹ J _{183WC} 126.7)	220.9 (s, ¹ J _{183WC} 170.7) ^b	199.4 (s, ¹ J _{183WC} 131.1) ^b
	C-2 thiazole	174.7 (s)	176.6 (s)	169.7 (s) ^b	182.1 (d, ⁴ J _{PC} 3.9) ^b
	C-4 thiazole	148.8 (s)	163.5 (br s)	149.6 (br s) ^b	150.2 (d, ³ J _{PC} 3.4) ^b
	C-5 thiazole	150.8 (s, ¹ J _{183WC} 21.2)	140.2 (s)	142.2 (s) ^b	156.0 (d, ² J _{PC} 125.2) ^b
	<i>i</i> -CH phenyl				130.1 (<i>i</i> -C ₆ H ₅) ^{b,e}
<i>o</i> -CH phenyl/pyridine			152.8 (s, py) ^b	134.3 (d, ² J _{PC} 13.7, PPh ₃) ^b	
<i>m</i> -CH phenyl/pyridine			125.0 (s, py) ^b	129.3 (d, ³ J _{PC} 11.3, PPh ₃) ^b	
<i>p</i> -CH phenyl/pyridine			138.1 (s, py) ^b	131.7 (d, ⁴ J _{PC} 2.0, PPh ₃) ^b	
³¹ P{ ¹ H} (121 MHz)	4-CH ₂ piperidine	50.3 (s)	49.9 (s)	49.5 (s) ^b	55.3 (s) ^b
	3/5-CH ₂ piperidine	26.2 (s)	25.3 (s)	25.1 (s) ^b	24.8 (s) ^b
	2/6-CH ₂ piperidine	25.0 (s)	23.8 (s)	24.0 (s) ^b	23.7 (s) ^b
	NMe ₄ ⁺ / OMe	55.9 (t, ¹ J _{14NC} 4, NMe ₄ ⁺)	67.2 (s, OMe)		
	PPh ₃				43.2 (s)

^a at 300 MHz ^b at 75.4 MHz ^c ¹⁸³W satellites not observed due to low intensity ^d multiplet at 7.54 ppm contains both PPh₃ and H-4 thiazole signals ^e presumably the low-field part of the expected doublet, the high-field part is obscured by the *m*-C₆H₅ signal

Table 5.4 NMR data of compounds **5b–10b**. Coupling constants are given in Hz.

Compound	Nucleus	Solvent	CD ₂ Cl ₂		CDCl ₃		CDCl ₃		CD ₂ Cl ₂		CDCl ₃	
	¹ H (400 MHz)	CH thiazole	8.38 (s, ¹ J _{CH} 187.3, 1 H)	8.83 (s, ¹ J _{CH} 187.0, 1 H)	7.79 (s, 1 H)	9.21 (br s, ¹ J _{CH} 192) ^c	8.62 (s, ¹ J _{CH} 184.4, 1 H)					
	<i>o</i> -Ph	7.98 (m, 2 H)	8.07 (m, 2 H)	7.91 (m, 2 H)	8.14 (m, 2 H)	8.01 (m, 2 H)						
	<i>m</i> -Ph and <i>p</i> -Ph	7.42 (m, 3 H)	7.51 (m, 3 H)	7.44 (m, 3 H)	7.64 (m, 1 H, <i>p</i> -C ₆ H ₅); 7.54 (m, 2 H, <i>m</i> -C ₆ H ₅)	7.52 (m, 18 H) ^b						
	NMe ₄ ⁺ / OMe	3.35 (m, 12 H, NMe ₄ ⁺)	4.70 (s, ¹ J _{CH} 147.8, OMe)		4.84 (s, ¹ J _{CH} 150.4, OMe)							
	<i>o</i> -CH PPh ₃ /pyridine			9.09 (m, 4 H, py)		7.52 (m, 18 H, PPh ₃) ^b						
	<i>m</i> -CH PPh ₃ /pyridine			7.36 (m, 4 H, py)		7.52 (m, 18 H, PPh ₃) ^b						
	<i>p</i> -CH PPh ₃ /pyridine			7.83 (tt, ³ J _{HH} 7.65, ⁴ J _{HH} 1.71, py)		7.52 (m, 18 H, PPh ₃) ^b						
	¹³ C{ ¹ H} (101 MHz)	Carbene / Carbyne	268.2 (s) ^a	291.6 (s, ¹ J _{183WC} 103.8)	240.8 (s, ¹ J _{183WC} 205.7)	248.6 (s)	252.3 (d, ² J _{PC} 133.7)					
	<i>trans</i> -CO	207.2 (s, ¹ J _{183WC} 134)	202.1 (s, ¹ J _{183WC} 117.2)			202.6 (s) ^a						
	<i>cis</i> -CO	203.1 (s, ¹ J _{183WC} 127.4)	197.1 (s, ¹ J _{183WC} 127.4)	220.1 (s, ¹ J _{183WC} 168.8)		198.7 (s, ¹ J _{183WC} 131.2)						
	C-2 thiazole	168.7 (s)	174.8 (s)	165.7 (s)	183.1 (s)	171.6 (s)						
	C-4 thiazole	160.9 (s)	156.7 (s)	143.9 (s)	168.9 (br s)	150.1 (s)						
	C-5 thiazole	147.7 (s)	152.7 (s)	148.0 (s)	144.4 (br s)	143.6 (s)						
	NMe ₄ ⁺ / OMe	56.9 (t, ¹ J _{14NC} 3.8, NMe ₄ ⁺)	68.7 (s, OMe)		71.7 (s, OMe)							
	<i>i</i> -CH phenyl	135.1 (s)	132.8 (s)	133.4 (s)	134.1 (s)	133.8 (s)						
	<i>o</i> -CH phenyl	127.0 (s)	131.9 (s)	130.2 (s)	132.7 (s)	128.9 (s)						
	<i>m</i> -CH phenyl	129.4 (s)	129.2 (s)	129.0 (s)	130.1 (s)	126.9 (s)						
	<i>p</i> -CH phenyl	130.6 (s)	127.1 (s)	126.4 (s)	128.6 (s)	130.7 (s)						
	<i>i</i> -CH PPh ₃					129.8 (d, ¹ J _{PC} 50.3, PPh ₃)						
	<i>o</i> -CH PPh ₃ /pyridine			152.7 (s, py)		134.2 (d, ² J _{PC} 13.4, PPh ₃)						
	<i>m</i> -CH PPh ₃ /pyridine			125.2 (s, py)		129.2 (d, ³ J _{PC} 10.8, PPh ₃)						
	<i>p</i> -CH PPh ₃ /pyridine			138.4 (s, py)		131.5 (d, ⁴ J _{PC} 1.3, PPh ₃)						
	³¹ P{ ¹ H} (162 MHz)	PPh ₃					38.8 (s)					

^a ¹⁸³W Satellites not observed due to low intensity ^b Multiplet with *m/p*-phenyl and PPh₃ proton resonances ^c Coupling constant obtained from ¹H NMR spectrum at -55 °C

Table 5.5 NMR data of compounds **12–16**. Coupling constants are given in Hz.

Compound							
		12Cr	12W	13	14	15	16
Nucleus	Solvent	CDCl ₃	CDCl ₃ / CD ₂ Cl ₂	(CD ₃) ₂ CO	CD ₂ Cl ₂	CDCl ₃	(CD ₃) ₂ CO
¹ H (400 MHz)	H-2/6 pyridinylidene	8.74 (s, 1 H)	8.74 (s, 1 H)	7.99 (s, 1 H)	8.40 (s, ¹ J _{CH} 183.8, 1 H)	8.47 (d, ³ J _{HH} 4.9, 2 H)	8.32 (d, ³ J _{HH} 6.5, 2 H)
	H-3/5 pyridinylidene	7.38 (s, 1 H)	7.36 (s, 1 H)	7.96 (s, 1 H)	8.06 (s, ¹ J _{CH} 167.9, 1 H)	7.07 (d, ³ J _{HH} 4.9, 2 H)	7.92 (d, ³ J _{HH} 6.5, 2 H)
	<i>o</i> -CH phenyl	7.50 (m, 5 H)	7.45 (m, 5 H)	7.82 (m, 2 H)	7.81 (m, 2 H)		
	<i>m/p</i> -CH phenyl			7.48 (m, 3 H)	7.44 (m, 15 H)		
	NCH ₃	3.96 (s, 3 H)	3.86 (s, 3 H)	3.98 (s, 3 H)	4.20 (s, ¹ J _{CH} 144, 3 H)	3.93 (s, 3 H)	4.30 (s, ¹ J _{CH} 144, 3 H)
	CCH ₃	2.67 (s, 3 H)	2.56 (s, 3 H)	2.55 (s, 3 H)	2.73 (s, ¹ J _{CH} 130.5, 3 H)		
¹³ C{ ¹ H} (101 MHz)	Carbene	238.0 (br s)	218.9 (s) ^a	186.5 (s)	199.5 (br s)	241.2 (s)	185.3 (s)
	<i>trans</i> -CO	225.7 (s)	206.3 (s, ¹ J _{WC} 127.3)			226.1 (s)	
	<i>cis</i> -CO / CF ₃ SO ₃ ⁻	219.9 (s)	201.5 (s, ¹ J _{WC} 127.3)		121.5 (q, ¹ J _{FC} 321, CF ₃ SO ₃ ⁻)	220.0 (s)	
	C-2 pyridinylidene	155.1 (s)	155.6 (s)	149.0 (s)	149.4 (s)	144.2 (s)	140.1 (s)
	C-3 pyridinylidene	130.9 (s)	133.3 (s)	141.2 (s)	140.2 (s)		
	C-5 pyridinylidene	143.3 (s)	145.0 (s)	146.1 (s)	147.7 (s)	128.5 (s)	139.7 (s)
	C-6 pyridinylidene	147.0 (s)	149.6 (s)	141.8 (s)	140.4 (s)	144.2 (s)	140.1 (s)
	<i>i</i> -CH phenyl	134.7 (s)	138.6 (s)	138.7 (s)	141.1 (s)		
	<i>o</i> -CH phenyl	129.9 (s)	130.7 (s)	129.5 (s)	129.7 (s)		
	<i>m</i> -CH phenyl	128.2 (s)	129.1 (s)	129.0 (s)	129.3 (s)		
	<i>p</i> -CH phenyl	127.9 (s)	128.9 (s)	128.9 (s)	129.0 (s)		
	NCH ₃	42.7 (s)	43.9 (s)	45.0 (s)	45.7 (s)	45.4 (s)	47.2 (s)
	CCH ₃	18.8 (s)	19.7 (s)	19.9 (s)	20.1 (s)		
	<i>i</i> -CH PPh ₃				130.3 ^b		
	<i>o</i> -CH PPh ₃				134.4 (d, ² J _{PC} 14.0)		
<i>m</i> -CH PPh ₃				129.7 (d, ³ J _{PC} 11.5)			
<i>p</i> -CH PPh ₃				132.3 (d, ⁴ J _{PC} 1.9)			
³¹ P{ ¹ H} (121 MHz)	P(C ₆ H ₅) ₃				41.8 (s)		

^a ¹⁸³W Satellites not observed due to low intensity ^b Presumably the low-field part of the expected doublet, the high-field part is obscured by the *m*-PPh₃ signal

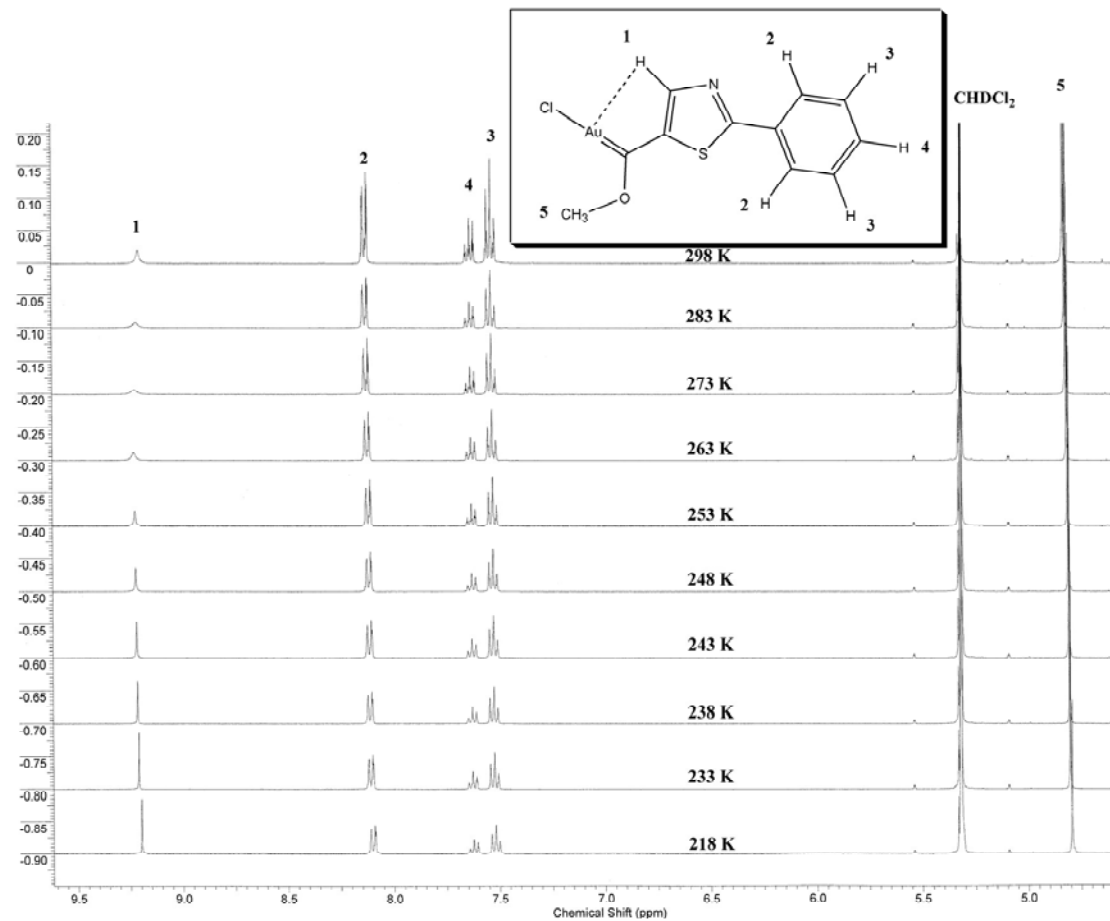


Figure 5.1 ^1H NMR spectrum of **8b** (400 MHz) in the region between 4.5 and 9.5 ppm at different temperatures; the spectrum at 298 K has been collected with an independent sample and is not included in the discussion. The y axis shows arbitrary units of intensity.

behaviour in that the signal appears at the lowest field at $-10\text{ }^{\circ}\text{C}$ (263 K) and slightly moves to higher field on both cooling and warming ($d\delta/dT \approx 7 \cdot 10^{-4}$ and $-6 \cdot 10^{-4} \delta \text{K}^{-1}$ on warming to and from $-10\text{ }^{\circ}\text{C}$, respectively). The other signals also experience slight and sometimes insignificant variations in chemical shift with temperature, however, their trend is always monotonic (*cf.* $d\delta/dT$ values for: OMe $5 \cdot 10^{-4} \delta \text{K}^{-1}$; *ortho*-Ph $5 \cdot 10^{-4} \delta \text{K}^{-1}$; *meta*-Ph $3 \cdot 10^{-4} \delta \text{K}^{-1}$ and *para*-Ph: $2 \cdot 10^{-4} \delta \text{K}^{-1}$).

It was suspected that in **8b** an agostic interaction of H-4 with the gold centre was responsible for this anomaly, this phenomenon could then be verified by determining the molecular structure in the solid state (*vide infra*). As there is no coupling partner for this proton, no analysis of the line shapes of multiplets or determination of coalescence temperature is possible. Agostic Au \cdots H interactions have received little attention in literature and only *Baukova et al.* have reported low-temperature NMR spectroscopic experiments.⁵⁹

In the *r*NHC complexes **12** to **16** proton magnetic resonance spectroscopy is more useful. The chemical shift difference of H-2/6 vs. H-3/5 of the organic pyridine ring, which are separated by *ca.* $\Delta\delta 1.4$ in the group 6 metal complexes, decreases in the Au complexes resulting in an average separation of only $\Delta\delta 0.4$ in **16** and **14** and just $\Delta\delta 0.03$ in **13**. The phenyl- and *N*-methyl group resonances experience a small shift to lower field indicating a stronger electronic pull by the heterocycle in the gold complexes.

5.3.3.2 $^{13}\text{C}\{^1\text{H}\}$ NMR spectroscopy.

A naturally more useful tool for elucidating the electronic and bonding situation in the complexes reported are proton-decoupled carbon-13 NMR spectra. In the tungsten compounds, ^{183}W satellites (natural abundance 26.4%, $I = 1/2$) and associated J_{WC} coupling constants allow further insight into the metal–carbene, metal–carbyne and metal–CO bonding. The carbeniate carbons of **5a** and **5b** and carbene carbon of **6a** resonate around $\delta 270$. The carbene signal of **6b** appears at lower field ($\delta 291.6$) with

⁵⁹ (a) T. V. Baukova, L. G. Kuz'mina, N. A. Oleinikova and D. A. Lemenovskii, *Izv. Akad. Nauk., Ser. Khim.* **1995**, 2032–2034; (b) T. V. Baukova, L. G. Kuz'mina, N. A. Oleinikova, D. A. Lemenovskii and A. L. Blumenfel'd, *J. Organomet. Chem.* **1997**, 530, 27–38.

J_{WC} coupling constants of 85–100 Hz. In the related complex $\text{Ph}(\text{MeO})\text{C}=\text{W}(\text{CO})_5$ the carbene carbon is observed at $\delta 321.9^{60}$ thus showing the marked shielding effect of the thiazolyl group ($\Delta\delta$ ca. 30 to 48) compared to the phenyl group.

The resonances of the carbyne carbons are observed at $\delta 245.1$ and 240.8 for **7a** and **7b**, respectively. The analogous phenyl carbyne signal is observed at higher field ($\delta 263$) again showing the shielding effect ($\Delta\delta$ 18 to 23) of the thiazolyl group at the carbene carbon, albeit less pronounced than in the carbene complexes. Carbyne **7b** shows a $^1J_{WC}$ of 207 Hz in line with the larger *s* character of the C(carbyne) hybridisation. The signals for the *cis*- and *trans*-CO groups in Fischer-type carbeniates **5a** and **5b** as well as carbenes **6a** and **6b** are commonly observed at ca. $\delta 200$ and 204 , respectively, with typical $^1J_{WC}$ coupling constants of 130 Hz. Carbyne complexes **7a** and **7b** exhibit signals for the *cis*-CO ligands at $\delta 220$ with a larger coupling constant $^1J_{WC}$ of 170 Hz.

The spectrum of the CO-loss product **9a** does not exhibit a signal in the carbene region but the signals of the thiazole ring are split by J_{PC} coupling ($^2J_{PC}$ 125 Hz) with the triphenylphosphane ligand which is higher than in Ph_3PAuBu ($^2J_{PC}$ 95.4 Hz)^{36b} indicating more *s*-character in the overlapping orbitals of the heterocyclic carbene complex. Another feature of **9a** is the resonance of C-2/6 in the piperidine ring that resonates at lower field ($\delta 55.3$) compared to all other compounds derived from **1a** (δ ca. 50).

The gold carbene signals of the carbene transfer products **8b** and **10b** at ($\delta 248.6$ and 252.3 , respectively) are observed at higher field strength than in their group 6 analogue **6b** ($\delta 291.6$). In addition, **8b** exhibits the most deshielded signals for C-2 and C-4 ($\delta 183.1$ and 168.9 , respectively) in the thiazole ring of the phenylthiazole complexes. The C-4 signal of **8b** is also broadened to an appreciable extent at room temperature – at -25 °C the peak shape is visibly sharper – but a good signal to noise ratio could not be obtained due to the low solubility of the compound at this temperature; a value for the line width is therefore not available.

60 J. A. Connor, E. M. Jones, E. W. Randall and E. Rosenberg, *J. Chem. Soc., Dalton Trans.* **1972**, 2419–2424.

The carbene carbon atoms in the *r*NHC ligands 1,2-dimethyl-5-phenyl-1*H*-pyridin-4-ylidene and 1-methyl-1*H*-pyridin-4-ylidene in **12–16** appear at significantly higher field strength (δ 238.0, 218.9, 186.5, 198.5, 241.2 and 185.3 for **12Cr**, **12W** and **13–16**, respectively) than the Fischer-type carbene signals with heterocyclic side chains in **6a**, **6b**, **8b** and **10b** (at *ca.* δ 250–290), caused by the absence of an α -hetero atom and the concomitant contribution of the pyridinium resonance structure. Again, transfer of the ligands to gold causes a greater shielding of the carbon in **13**, **14**, and **16**, the difference being most extensive between **15** and **16**, showing a $\Delta\delta$ of 56 towards higher field strength. This evidence is most reliable in determining the contributions of the respective canonical forms for the 1*H*-pyridin-4-ylidene ligand; compared to the group 6 *r*NHC complexes, the *r*NHC gold complexes thus show a higher contribution of the charge-separated 6π -aromatic pyridinium form.

As reflected in the ^1H NMR spectra, the ^{13}C NMR chemical shift difference for the signals between C-2/6 and C-3/5 of the pyridinylidene group becomes smaller upon transfer of the ligand from Cr or W to Au: $\Delta\delta$ 15.7 in **15** compared to 0.4 in **16**. The chemical shifts for the carbene carbon and the shift differences of the 2/6- and 3/5-pyridinylidene carbons of the *r*NHC gold complexes are also reflected in the corresponding resonances for *trans*-chloro(1-methyl-1*H*-pyridin-4-ylidene)bis(triphenylphosphane)nickel(1+).^{16d} This chemical shift difference could be attributed to a higher contribution of the charge-separated pyridinium form for **13**, **14** and **16** compared to their group 6 metal analogues.

5.3.3.3 $^{31}\text{P}\{^1\text{H}\}$ NMR spectroscopy.

Compounds **9a**, **10b** and **14** all incorporate a triphenylphosphane ligand and were also examined by $^{31}\text{P}\{^1\text{H}\}$ NMR spectroscopy. The data are reported in Tables 5.3–5.5. All compounds show one singlet resonance of the phosphorus atom, the signals are all observed at a lower field compared to Ph_3PAuCl (δ 33.0).⁶¹ The cationic *r*NHC complex **14** shows the most deshielded phosphorus (δ 41.8) and Fischer-type gold carbene **10b** exhibits a resonance (δ 38.8) upfield of the CO-loss product **9a** (δ 43.2).

61 G. H. Woehrle, L. O. Brown and J. E. Hutchison, *J. Am. Chem. Soc.* **2005**, *127*, 2172–2183.

5.3.3.4 Solid-state CPMAS ^{13}C NMR spectroscopy.

The carbenate complex **5b** crystallised with two unique molecules in the asymmetric unit (*vide infra*) and the question then arose whether the environment around them was different enough for split signals to be observed in the solid state. Therefore, a sample was measured with the Cross-Polarisation Magic Angle Spinning (CPMAS) technique utilising spinning frequencies of 5 to 11 kHz for identification of the usually observed, strong spinning side bands. Data are summarised in Table 5.6. Figure 5.2 shows an array of the measured spectra.

The signals for the thiazole carbons are well resolved while the resonances for the phenyl carbon signals, however, do not allow identification of each unique carbon atom except for the *ipso*-peaks, as the signals overlap due to small shift differences. Two signals were observed for the $[\text{NMe}_4]^+$ counter ions, which are thought to rather stem from different carbons in each unique cation than represent each unique cation. In the molecular structure determined by single crystal X-ray diffraction, both $[\text{NMe}_4]^+$ ions are aligned so that the carbenate oxygen is equally surrounded by 3 methyl groups. These methyl groups and the lone CH_3 at the “apex” of the $[\text{NMe}_4]^+$ -tetrahedron might give rise to different resonances.

Table 5.6 Solid-state ^{13}C NMR data (δ in ppm) at 126 MHz of compound **5b**.
 $\Delta\delta$ values (in ppm and Hz) in brackets.

	CP-MAS solid-state NMR spectrum	Liquid NMR in CD_2Cl_2^c
<i>cis</i> -CO	202.8 ^b	203.1
C-2 thiazole (C2) ^a	171.0, 168.1 (2.92, 367)	168.7
C-4 thiazole (C3) ^a	160.7, 160.0 (0.65, 82)	160.9
C-5 thiazole (C4) ^a	148.3, 147.7 (0.65, 82)	147.9
<i>i</i> -phenyl	134.7, 132.5 (2.26, 284)	135.1
<i>o,m,p</i> -phenyl peak group	130.2, 129.2, 128.6, 127.3, 125.7, 124.4	130.6, 129.4, 127.0
$[\text{NMe}_4]^+$	56.1, 54.4 (1.62, 204)	56.9

^a See Figure 5.2 for numbering in brackets

^b Observed only without cross-polarisation ^c see also Table 5.4

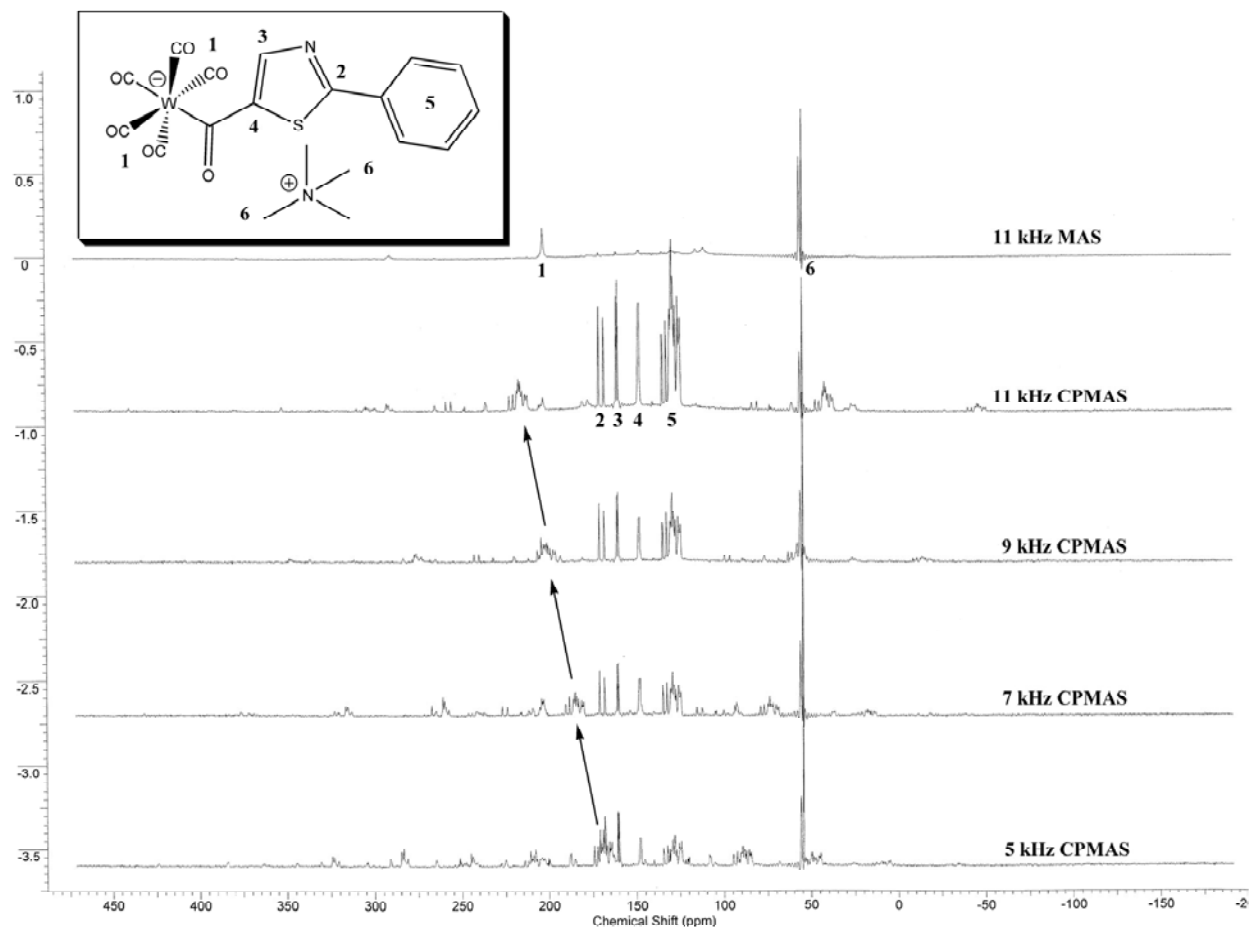


Figure 5.2 Solid-state ¹³C CPMAS NMR spectrum of **5b** at different spinning frequencies and conditions, the y axis shows arbitrary units of intensity. Arrows indicate movement of a spinning side band as the frequency is increased.

Signals for the pentacarbonyl group could not be identified in the CP experiments due to interfering spinning side bands, but in an experimental run without cross-polarisation, the *cis*-CO carbons appear as a broad peak at δ 202.8 while the intensities of the thiazolyl and phenyl signals are much weaker. The carbeniate carbon and *trans*-CO, however, could not be observed in any of the spectra.

5.4 Single crystal X-ray diffraction

Most complexes and atom connectivities therein were characterised by single-crystal X-ray diffraction. Some complexes represent the first examples of their kind while for others only few related structures have been reported. Bond lengths and angles for compounds **5a–9a** are reported in Table 5.7, of compounds **5b–10b** in Table 5.8 and of *r*NHC complexes **12–16** in Table 5.9.

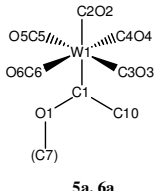
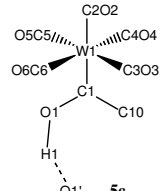
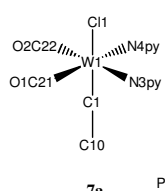
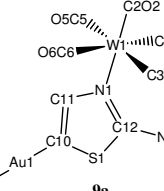
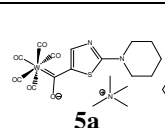
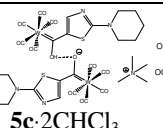
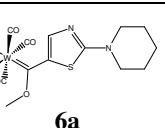
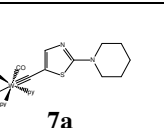
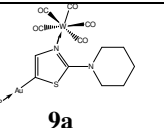
5.4.1 Molecular structure of the carbeniate complexes **5a** and **5b**

Molecular structures of unassociated tungsten carbeniate complexes have not been reported before. The only example in the Cambridge Crystallographic Database is a report of a hydrogen-bonded dimer of benzoylpentacarbonyltungstate(1–) and the related hydroxycarbene $\text{H}[\text{WBz}(\text{CO})_5]_2^-$ as a lithium salt.⁶² Therefore, the crystal and molecular structures of **5a** (shown in Figure 5.3) and **5b** (Figure 5.4) cannot be compared to existing data.

The W–C(carbeniate) bonds with values of 2.251(5) Å in **5a** and 2.251(3) and 2.248(3) Å in **5b** fall at the longer end of the range for Fischer W–C(carbene) bonds (see Section 5.4.3 for an evaluation of the W–C bond lengths of Fischer-type pentacarbonyltungsten alkoxy-carbenes), although the bonding situation in **5a** and **5b** may also be considered that of an anionic acyl complex. The W–C bonds of the *trans*-CO ligands [1.994(5) Å in **5a** and 1.994(4) and 2.019(4) Å in **5b**] are shortened

62 M. W. Esterhuysen and H. G. Raubenheimer, *Eur. J. Inorg. Chem.* **2003**, 3861–3869.

Table 5.7 Bond lengths/Å and angles/° of compounds **5a–9a**.

Compound					
					
M1–C1 ^a	2.251(5)	2.246(7)	2.231(8), 2.240(9)	1.841(4)	2.042(8), 2.046(8) ^f
W1–C2 ^b	1.994(5)	2.012(7)	2.02(1), 2.02(1)		1.95(1), 1.953(9)
W1–C3	2.040(6)	2.022(9)	2.06(1), 2.06(1)	1.996(4) ^c	2.068(9), 2.08(1)
W1–C4	2.031(5)	2.012(8)	2.04(1), 2.048(9)	1.990(4) ^d	2.03(1), 2.051(8)
W1–C5	2.042(6)	2.033(8)	2.053(9), 2.03(1)		2.042(9), 2.040(9)
W1–C6	2.027(5)	2.028(8)	2.04(1), 2.04(2)		2.03(1), 2.060(9)
C1–O1	1.248(5)	1.284(8)	1.37(1), 1.34(2)		
C1–C10	1.467(6)	1.437(9)	1.41(2), 1.40(2)	1.411(5)	
N1–C11	1.371(5)	1.362(9)	1.33(2), 1.33(2)	1.359(5)	1.37(1), 1.41(1)
N1–C12	1.320(6)	1.335(9)	1.36(2), 1.34(2)	1.325(5)	1.33(1), 1.29(2)
N2–C12	1.358(5)	1.332(9)	1.33(2), 1.33(2)	1.337(5)	1.39(1), 1.37(1)
S1–C10	1.756(4)	1.756(7)	1.759(9), 1.764(8)	1.760(4)	1.725(8), 1.718(8)
S1–C12	1.743(4)	1.733(7)	1.734(9), 1.75(1)	1.762(4)	1.726(9), 1.759(9)
C10–C11	1.367(6)	1.35(1)	1.40(2), 1.38(2)	1.367(6)	
N2– ϵ , $\epsilon \equiv$ C12C13C17	0.185(5)	0.146(8)	0.06(2), 0.06(2)	0.074(5)	0.413(9), 0.38(1)
Other bond lengths and angles		2.418(9) (O1–O1')		2.523(2) (W1–C11)	2.265(7), 2.271(7) (W1–N1)
		3.09(1) (C7–N1)		2.276(3) (W1–N3)	2.283(2), 2.298(2) (Au1–P1)
				2.269(3) (W1–N4)	3.2117(5) (Au1...Au2)
					3.267(2), 3.285(2) (Au1A/B...S1A/B) ^g
					3.392(2), 3.315(2) (Au1A/B...S1B/A) ^h
					177.7(2), 177.9(2) (P–Au–C)
C1–W1–C2	173.6(2)	178.9(3)	179.1(4), 178.1(4)	176.7(2) ^e	173.8(3), 176.4(3) ⁱ
W1–C1–C10	125.0(3)	124.4(5)	125.2(6), 125.5(6)	175.1(3)	
W1–C1–O1	121.9(3)	125.2(5)	127.5(6), 127.0(7)		

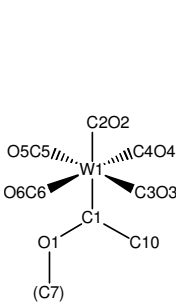
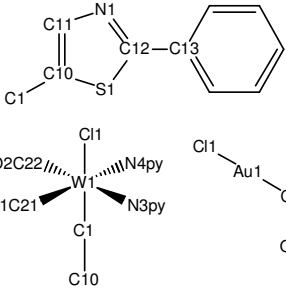
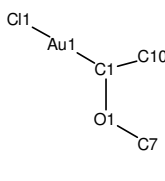
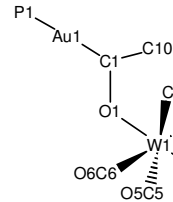
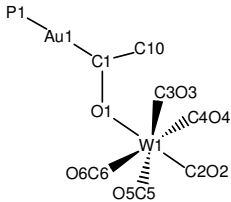
Symmetry code: ' 1 – x, y, ³/₂ – z (related by C₂-axis)

^a M = W for **5a–7a** and Au for **9a** ^b trans-CO of the pentacarbonyltungsten group

^c W1–C21 ^d W1–C22 ^e C11–W1–C1 ^f Au1–C10

^g Intramolecular contact ^h Intermolecular contact ⁱ N1–W1–C2

Table 5.8 Bond lengths/Å and angles/° of compounds **5b–8b**.

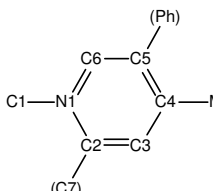
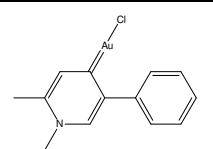
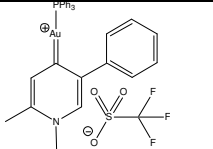
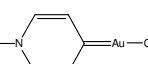
Compound					
	5b	6b	7b·CH₂Cl₂	8b	10b·C₅H₁₂
M1–C1 ^a	2.251(3), 2.248(3)	2.195(5)	1.822(3)	1.976(4), 1.959(4)	2.053(7)
W1–C2 ^b	1.994(4), 2.019(4)	2.029(5)			1.953(7)
W1–C3	2.040(3), 2.039(4)	2.037(5)	2.001(3) ^c		2.015(8)
W1–C4	2.025(4), 2.032(4)	2.041(5)	1.993(3) ^d		2.027(8)
W1–C5	2.037(4), 2.029(4)	2.053(5)			2.045(8)
W1–C6	2.040(4), 2.039(4)	2.055(5)			2.045(8)
C1–O1	1.245(4), 1.246(4)	1.330(5)		1.296(5), 1.302(5)	1.247(8)
C1–C10	1.495(5), 1.507(4)	1.447(7)	1.418(5)	1.430(6), 1.433(6)	1.460(9)
N1–C11	1.363(4), 1.375(4)	1.356(6)	1.364(4)	1.343(6), 1.350(5)	1.351(9)
N1–C12	1.316(4), 1.311(4)	1.323(6)	1.308(4)	1.323(5), 1.316(5)	1.314(9)
S1–C10	1.730(3), 1.735(3)	1.746(5)	1.735(3)	1.734(4), 1.730(4)	1.729(7)
S1–C12	1.731(3), 1.735(3)	1.733(5)	1.729(3)	1.730(4), 1.738(4)	1.740(7)
C10–C11	1.360(5), 1.353(4)	1.370(7)	1.374(5)	1.374(6), 1.383(6)	1.365(9)
C12–C13	1.468(5), 1.470(4)	1.455(7)	1.468(4)	1.468(6), 1.469(6)	1.453(9)
Other bond lengths and angles			2.5107(8) (W1–Cl1)	2.289(1), 2.279(2) (Au1–Cl1)	2.205(5) (W1–O1)
			2.246(3) (W1–N3)	3.3866(3) (Au1A···Au1B),	2.301(2) (Au1–P1)
			2.254(3) (W1–N4)	3.4871(4) (Au1B···Au1B')	173.1(2) (P1–Au1–C1)
				2.87, 2.97 (Au1···H11)	127.1(5) (O1–C1–Au1)
C1–W1–C2	177.7(2), 174.4(2)	175.2(2)	170.9(1) ^e	174.8(2), 177.5(2) ^f	175.0(2) ^g
W1–C1–C10	123.7(2), 123.1(2)	124.6(3)	169.4(3)		
W1–C1–O1	122.6(2), 123.9(2)	129.4(3)			132.1(4) ^h
C ₆ H ₅ –C ₃ HNS interpl. angle	5.2(2), 16.3(2)	8.2(2)	21.9(2)	1.9(3), 13.8(3)	5.2(4)

Symmetry code: ' 2 – x, 1 – y, –z (related by centre of inversion)

^a M = W for **5b–7b** and Au for **8b** and **10b** ^b *trans*-CO of the pentacarbonyltungsten group

^c W1–C21 ^d W1–C22 ^e Cl1–W1–C1 ^f Cl1–Au1–C1 ^g O1–W1–C2 ^h W1–O1–C1

Table 5.9 Bond lengths/Å and angles/° of compounds **12W–16**.

Compound				
	12W	13	14	16
Au–P			2.2888(8)	
Au–Cl		2.304(2)		2.314(2)
M–C4 ^a	2.271(4)	1.991(7)	2.049(3)	1.979(6)
W–C21 ^b	2.003(4)			
W–C22	2.031(4)			
W–C23	2.032(4)			
W–C24	2.036(4)			
W–C25	2.038(4)			
N1–C2	1.357(5)	1.36(2)	1.359(4)	1.354(8)
N1–C6	1.355(5)	1.35(2)	1.346(4)	1.361(8)
C2–C3	1.378(5)	1.38(2)	1.389(4)	1.362(9)
C3–C4	1.416(5)	1.42(1)	1.395(4)	1.414(9)
C4–C5	1.414(5)	1.41(2)	1.408(4)	1.422(8)
C5–C6	1.377(5)	1.38(2)	1.381(4)	1.371(9)
N1–C1	1.475(5)	1.48(1)	1.476(4)	1.472(8)
C2–C7	1.492(5)	1.50(2)	1.486(4)	
C4–Au1–Cl1		178.7(2)	176.92(9)	179.1(2)
C4–W1–C21	176.1(2)			
C3–C4–C5	113.0(3)	115.2(7)	116.6(3)	114.2(6)
C2–N1–C6	119.5(3)	120.1(7)	121.1(3)	118.8(6)
C ₆ H ₅ –C ₅ H ₂ N interplanar angle	68.8(2)	43.3(3)	48.9(2)	

^a M = Au or W ^b *trans*-CO of the pentacarbonyltungsten group

compared to the analogous *cis*-CO bond lengths (this is not significant in the latter unique molecule of **5b**) owing to the internal electron-donating properties of the carbenate and is in good agreement with the values in H[WBz(CO)₅]₂[−] [1.996(6) Å].

Another effect seen in the molecular structures of **5b** is the significant elongation of the C1–C10 bond [1.495(5) and 1.507(4) Å in **5b**, *cf.* 1.467(6) Å in **5a**] compared to the other carbene complexes derived from ligand **1b** with the notable exception of the distance in **10b**·C₅H₁₀ [1.460(9) Å].

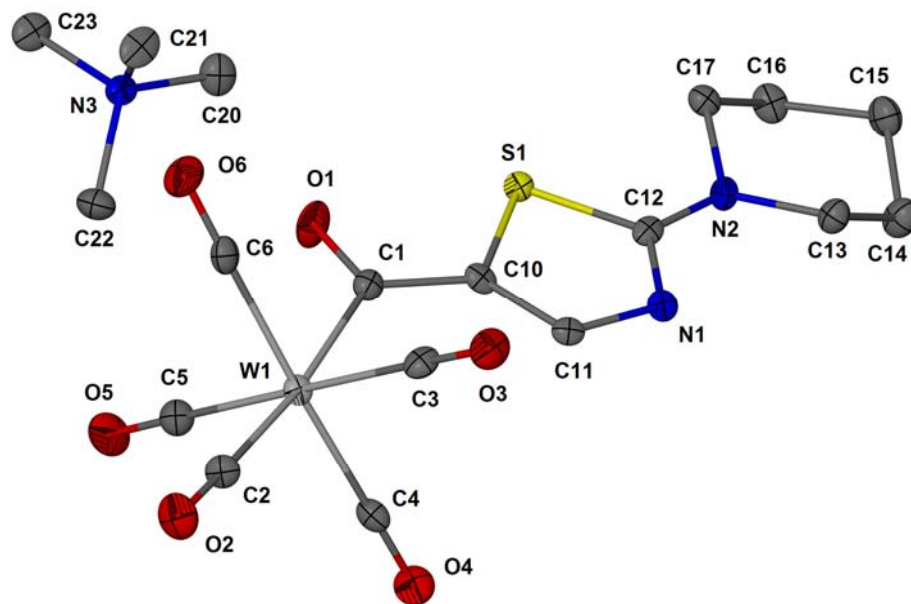


Figure 5.3 Molecular structure of **5a**.

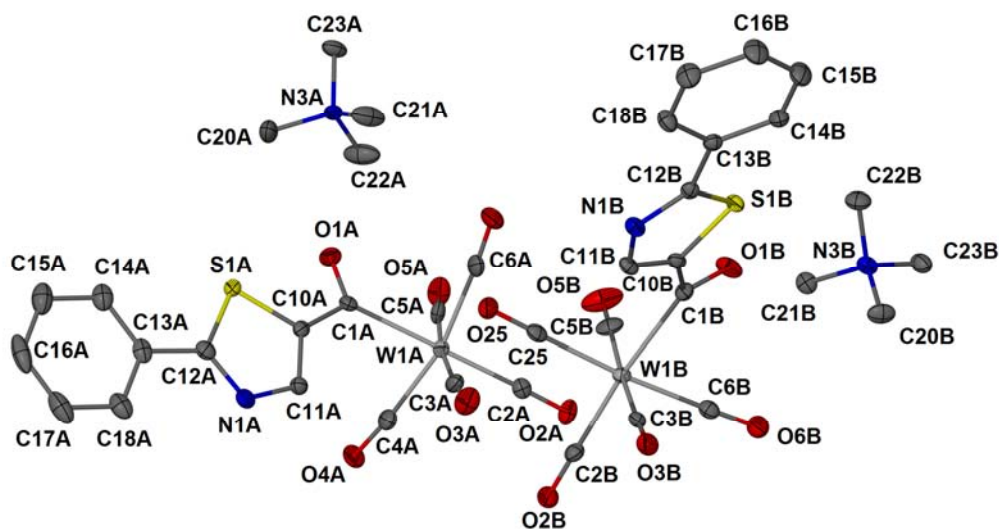


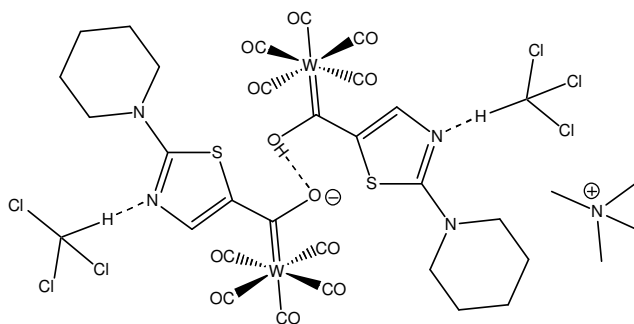
Figure 5.4 Molecular structure of the two asymmetric molecules of **5b**.

For all complexes in which the piperidine nitrogen lone pair participates in electron delocalisation across the complex molecule, **5a** has the largest distance of the piperidine nitrogen to the plane generated by its three bonded carbon atoms [0.185(5) Å]. The angles C12–N2–C13 [118.6(4)°] and C12–N2–C17 [120.0(3)°] are smaller than in **7a** [121.1(3)° and 122.7(3)°, respectively]. The nitrogen thus exhibits sp^2 hybridisation that has a low, but significant, sp^3 contribution. The thiazolyl group can still be

regarded as an equatorial substituent of the piperidine ring which is arranged in the chair conformation. In all other complexes except **9a**·0.5CH₂Cl₂ (where the piperidine ring is forced out of plane) discrimination between equatorial and axial substitution is lost due to an essentially planar nitrogen centre. Electron density supplied by the piperidine nitrogen should also be reflected in the bond lengths within the thiazole ring which show appropriate trends, yet the differences are always comparable to the uncertainties; the angles of N2 with its bonded carbon atoms are also not a sharp measure compared to the associated s.u.s. This leaves the distance of N2 to the plane of its bonded carbon atoms as a measure of lone pair delocalisation that can be estimated with greater confidence.

5.4.2 Molecular structure of H⁺-bridged carbeniate **5c**·2CHCl₃

In an attempt to crystallise the Fischer carbene complex **6a** from the crude product obtained by method A (see Section 5.6.3.3, p. 231), crystals of a proton-bridged bis-carbeniate, **5c**·2CHCl₃ shown in Scheme 5.18 and Figure 5.5, were isolated in the crystallisation vessel.



Scheme 5.18 Schematic representation of **5c**·2CHCl₃.

The formation of **5c**·2CHCl₃ is ascribed to the initial method used in the synthesis. With traces of ethanoic acid present, the partial protonation of the carbeniate group can be explained. The basicity of **5a** may also be large enough to deprotonate [HNEt₃]⁺ formed in the course of the synthesis. A similar complex – and the only one reported thus far, but with a phenyl group bonded to the carbene carbon – was isolated after column chromatography on silica gel where OH groups present on the adsorbent are thought to have protonated the carbeniate.⁶²

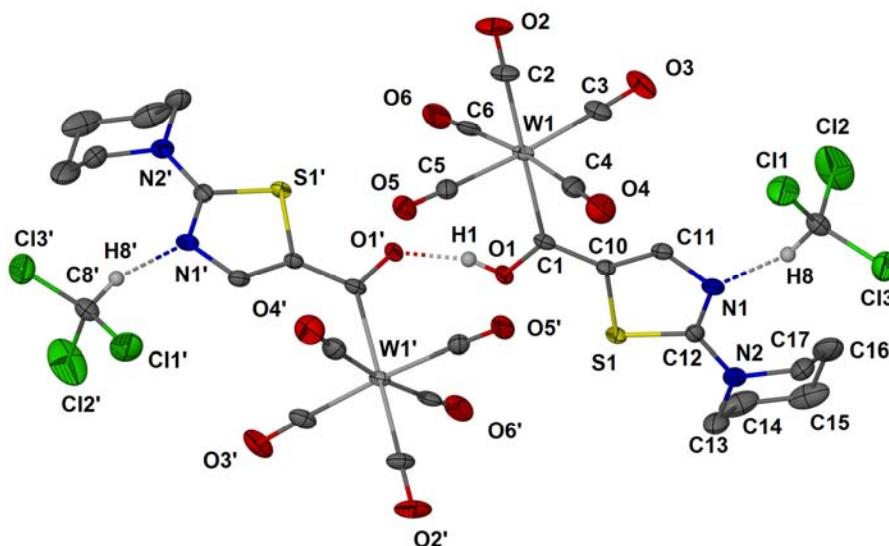


Figure 5.5 An asymmetric and symmetry generated molecule constituting **5c**·2CHCl₃; primed atoms are related by a two-fold rotation of symmetry code $1 - x, y, \frac{3}{2} - z$; H1 has been arbitrarily located at the right-hand molecule, the disordered [NMe₄]⁺ cation has been omitted for clarity.

Complex **5c**·2CHCl₃ crystallises in the monoclinic space group *C2/c* with one molecule in the asymmetric unit. By applying a two-fold rotation the other molecule involved in the hydrogen bond is generated with the *C*₂ axis located between the oxygen atoms forming the hydrogen bond. This also strictly means that the symmetry of the crystal is higher than that of the molecule and the proton must therefore randomly be located on either of the oxygen atoms leading to space group symmetry in the overall crystal structure.

One N–C bond of the cation lies on a *C*₂ axis which induces a higher symmetry than [NMe₄]⁺ possesses in this orientation, leading to disorder of the other three methyl groups equally over two sites. The imine nitrogen within the thiazolyl group is engaged in an interaction with a hydrogen atom of a trichloromethane solvent molecule.

Given the overall half-protonated state of the carbeniate, the C–O bond distance of the heterocyclic ligand [1.284(8) Å] is a roughly intermediate between an effective double bond as in the carbeniate complexes [1.248(5) Å in **5a**; 1.245(4) and 1.246(4) Å in **5b**] and more of a single bond as in the carbene complexes [1.37(1) and 1.34(2) Å in

6a and 1.330(5) Å in **6b**]. There is no evidence that different discrete locations (and hence differing C–O bond lengths) of the oxygen atom exist for the hydroxycarbene and carbeniate of the dimer.

The W–C bond of the *trans*-CO ligand [2.012(7) Å] has a comparable bond length to the W–C bond of the *cis*-CO ligands [averaged 2.02(1) Å] which is in contrast to the structures of the carbeniates **5a** and **5b** as well as of $\text{H}[\text{WBz}(\text{CO})_5]_2^{-62}$ where the *trans*- and *cis*-CO W–C bonds are of different length, but in agreement with the carbene complexes **6a** and **6b** which also show no difference between these bond lengths in the *cis*- and *trans*-CO ligands. In line with a structure intermediate between a carbeniate and carbene complex, the distance of the piperidine nitrogen to the plane of its three bonded carbons in **5c**·2CHCl₃ [0.148(8) Å] is comparable to **5a** and **5b** [0.185(5) Å] and shorter than in **9a**·0.5CH₂Cl₂ [0.413(9) and 0.38(1) Å, however, the piperidine rings are turned out of plane in this complex], but higher than in all other complexes.

5.4.3 Crystal and molecular structures of the Fischer-type methoxy-carbene complexes **6a** and **6b**

The tendency of **6a** and **6b** to crystallise varies widely. While long needles of **6b** can be obtained easily by the usual layering technique, this approach failed for **6a** due to its high solubility and a crystal was only found when a side fraction of the chromatographic purification that only contained a few mg of an oil, was left for several weeks at room temperature. The dataset of the crystal, although of low quality, nonetheless gave valuable insight into the bonding situation. The two asymmetric molecules of **6a** shown in Figure 5.6 are related by a *pseudo*-centre of symmetry that is not reflected in the space group symmetry while **6b** crystallises with one molecule per asymmetric unit (Figure 5.7). The W–C(carbene) bonds [2.231(8) and 2.240(9) Å in **6a** and 2.195(5) Å in **6b**] fall within the typical range observed for Fischer-type pentacarbonyltungsten alkoxy-carbene complexes [average bond length 2.20(4) Å for 99 compounds in the Cambridge Crystallographic Database]. One bond length in **6a** is significantly elongated compared to that in **6b** in what may reflect the influence of the piperidine nitrogen atom.

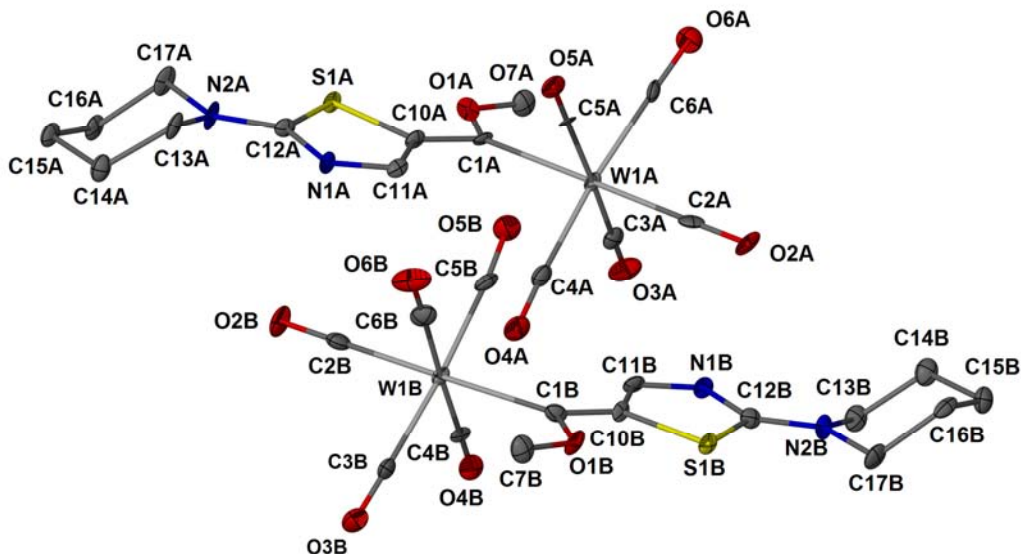


Figure 5.6 Molecular structure of **6a**.

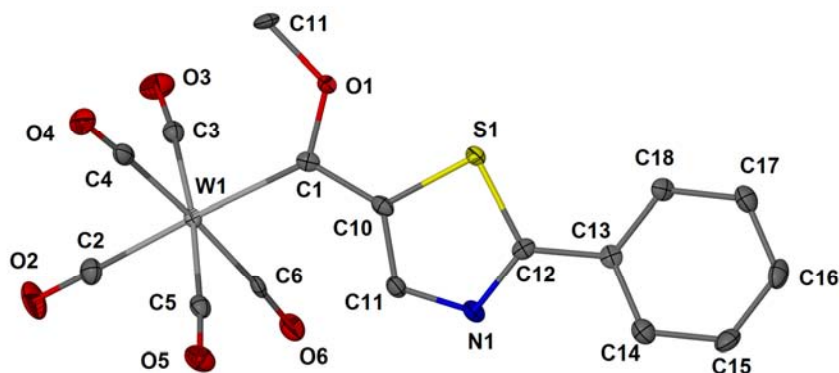
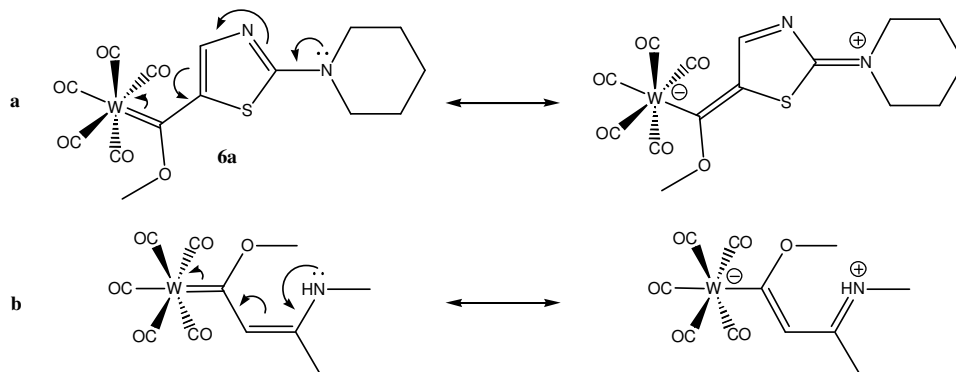


Figure 5.7 Molecular structure of **6b**.

A similar effect is observed in the molecular structure of the synthetic intermediate pentacarbonyl[(*Z*)-1-methoxy-3-(methylamino)but-2-en-1-ylidene]tungsten, used in preparing the *r*NHC complex **12W**, in which the W–C bond [2.255(3) Å] is also at the longer end of the range found as a result of the lone pair on the methylamino group supplying additional electron density. In this complex the formal C–C double bond [1.416(4) Å] is longer than the formal C–N single bond [1.319(4) Å] to the methylamino group (Scheme 5.19).⁶³

63 E. Stander, S. Cronje and H. G. Raubenheimer, *Dalton Trans.* **2007**, 424–429.



Scheme 5.19 (a) Resonance structures for compound **6a** and (b) a related tungsten carbene complex; the structures to the right cause elongation of the W–C(carbene) bond.

In the molecular structure of **6a** and **6b**, the W–C bonds of the *trans*-CO ligands are similar [2.02(1) Å each; average for *cis*-CO 2.05(2) Å in **6a** as well as 2.029(5) Å for *trans*-CO and 2.047(9) for the average *cis*-CO in **6b**, respectively]. The C–O bond in the carbene ligand is further lengthened [1.37(1) and 1.34(2) Å for **6a** and 1.330(5) Å for **6b**] when compared to **5a** and **5b** [average 1.246(5) Å] showing the lower bond order, though still being shorter than a regular C–O single bond.⁶⁴

The distances of N2A and N2B to the plane of their bonded atoms in **6a** are 0.06(2) Å each, these atoms thus essentially exhibit trigonal planar geometry in contrast to **5a** or **5c**·2CHCl₃, where N2 is still somewhat pyramidal [analogous distances 0.185(5) and 0.146(8) Å].

The packing of **6b** is shown in Figure 5.8. The domains of pentacarbonyl- and phenylthiazole groups ordered by π -stacking of the thiazole rings (distance of the ring centroids 3.715 Å) each run along the *c*-axis.

Comparison with the molecular structure of **6b** with that of Ph(EtO)C=W(CO)₅⁶⁵ reveals the same W–C bond length [2.20(2) Å] as in **6b**. The carbene–phenyl bond [1.59 Å] is elongated by > 0.1 Å compared to **6a** [1.41(2) and 1.40(2) Å] and **6b** [1.447(7) Å] showing lacking electronic participation of the phenyl group. However, as only atom positions but, strangely, neither bond lengths (which were calculated

⁶⁴ F. H. Allen, O. Kennard, D. G. Watson, L. Brammer, A. G. Orpen and R. Taylor, *J. Chem. Soc., Perkin Trans. 2* **1987**, S1–S19.

⁶⁵ R. J. Staples, D. M. Potts and J. C. Yoder, *Z. Kristallogr.* **1995**, *210*, 381–382.

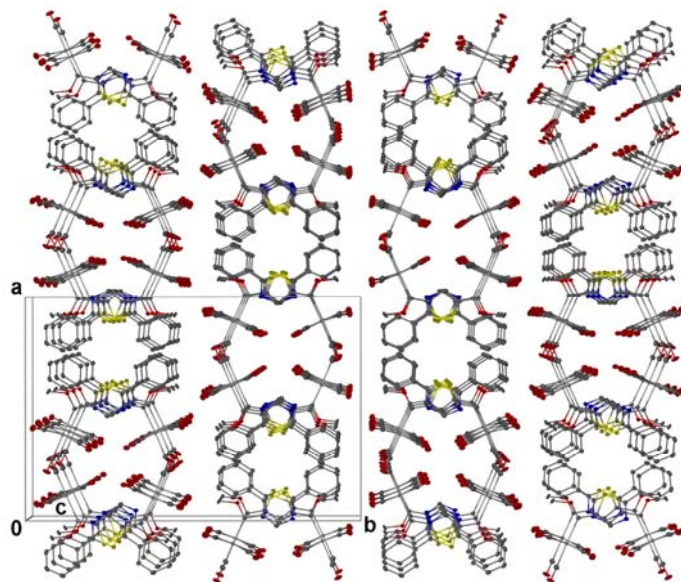


Figure 5.8 Packing diagram of **6b** viewed along the *c*-axis showing alignment of the molecules to form carbonyl and (hetero)aromatic domains.

from the positions in this discussion) or associated s.u.s were given for these bonds, the uncertainty associated with them cannot be estimated but it is believed that the difference is significant as bond length s.u.s for the elements involved in contemporary determinations are in the range of 0.03 Å.⁶⁶

The ethoxy(phenyl)methylidene ligand also exerts little effect on the *trans*-CO, the W–CO bond length is similar to the *cis*-CO ligands. The situation in $\text{Fc}(\text{MeO})\text{C}=\text{W}(\text{CO})_5$ ⁶⁷ is more like that in the heterocyclic carbenes with W–C [2.215(4) Å], C–O [1.315(5) Å] and C(carbene)–C(Fc) bond [1.465(6) Å] bond lengths similar to those of **6a** and **6b**. The latter bond length suggests electronic participation of the ferrocene sandwich in contrast to that in the phenyl(ethoxy)carbene discussed above. Again, the *trans*-W–CO bond [2.018(5) Å] is not significantly different than those for the *cis*-CO ligands [average 2.04(1) Å].

66 (a) G. J. Kruger, P. J. Olivier and H. G. Raubenheimer, *Acta Crystallogr., Sect. C: Cryst. Struct. Commun.* **1996**, 52, 624–626; (b) G. J. Kruger, P. J. Olivier, R. Otte and H. G. Raubenheimer, *Acta Crystallogr., Sect. C: Cryst. Struct. Commun.* **1996**, 52, 1159–1161.

67 J. G. López-Cortés, L. F. Contreras de la Cruz, M. C. Ortega-Alfaro, R. A. Toscano, C. Alvarez-Toledano and H. Rudler, *J. Organomet. Chem.* **2005**, 690, 2229–2237.

5.4.4 Molecular structures of the carbyne complexes **7a** and **7b**

Carbyne complexes **7a** and **7b** were characterised by X-ray diffraction. Both compounds crystallise in the triclinic space group $P\bar{1}$ with one molecule in the asymmetric unit. In contrast to **6a** and **6b**, **7a** (shown in Figure 5.9) crystallises more readily. Complex **7b** (Figure 5.10) was originally isolated as an oil but crystallised from a failed reaction (the attempted synthesis of AuC₆F₅-adduct of **7b**; *vide supra*) as the dichloromethane solvate forming red needles of **7b**·CH₂Cl₂. The W–C(carbyne) bond of **7a** [1.841(4) Å] is comparable to that in **7b** [1.822(3) Å], Δ 5 s.u.

Overall, the metal–carbyne carbon bonds of both the new complexes are comparable other carbyne complexes. [W(≡CPh-4-I)Cl(CO)₂{tris(pyridin-2-yl)phosphane-κ²N:N'}] is the only determined molecular structure for a tungsten carbyne with *cis*-pyridine substituents, the W–C bond length is 1.806(6) Å.⁶⁸ For the two crystal structures determined of the (4-methylphenyl)carbyne complex **3**, the solvent-free molecular structure has a W–C(carbyne) bond of 1.806(9) Å while in the thf solvate it is 1.83(2) Å similar to **7a** and **7b**. Related bond lengths in two crystallographically independent molecules of [W(≡CPh-4-I)Cl(CO)₂(tmeda)] (tmeda = *N,N,N',N'*-tetramethylethan-1,2-diamine), 1.807(8) and 1.818(8) Å,⁶⁹ are comparable to that in **7b**·CH₂Cl₂, but this observation might be affected by the absence π-acceptor ligands on the metal.

The *cis*-CO groups in **7a** and **7b** are not affected by the nature of the carbyne ligand. Their average W–CO bond length of 1.995(5) Å is in line with other pyridine- and tmeda-chelated carbyne complexes^{68,69} suggesting the presence (but not the nature) of a *trans*-nitrogen donor as the only significant influence on the CO ligands. The better electron-donating ability of **1a** owing to the exocyclic piperidinyl nitrogen atom is only observed in the W–Cl bond distance which is significantly longer in **7a** [W–Cl 2.523(2) Å] when compared to **7b**·CH₂Cl₂ [2.5107(8) Å]. Both W–Cl distances in **7a** and **7b** are nonetheless sometimes significantly shorter than in other reported tungsten carbyne complexes such as the above mentioned complexes where bond lengths of

68 F.-W. Lee, M. C.-W. Chan, K.-K. Cheung and C.-M. Che, *J. Organomet. Chem.* **1998**, 563, 191–200.

69 M. P. Y. Yu, K.-K. Cheung and A. Mayr, *J. Chem. Soc., Dalton Trans.* **1998**, 2373–2378.

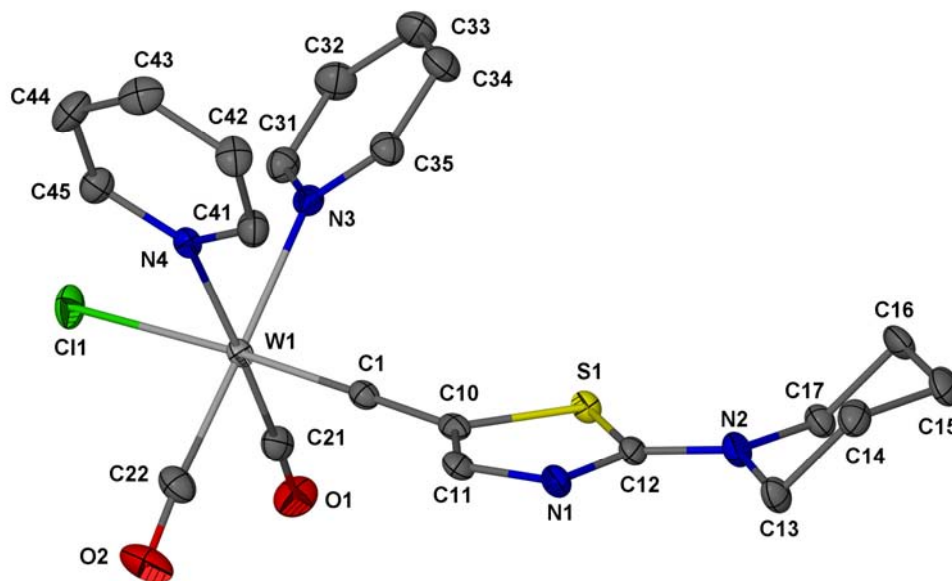


Figure 5.9 Molecular structure of **7a**.

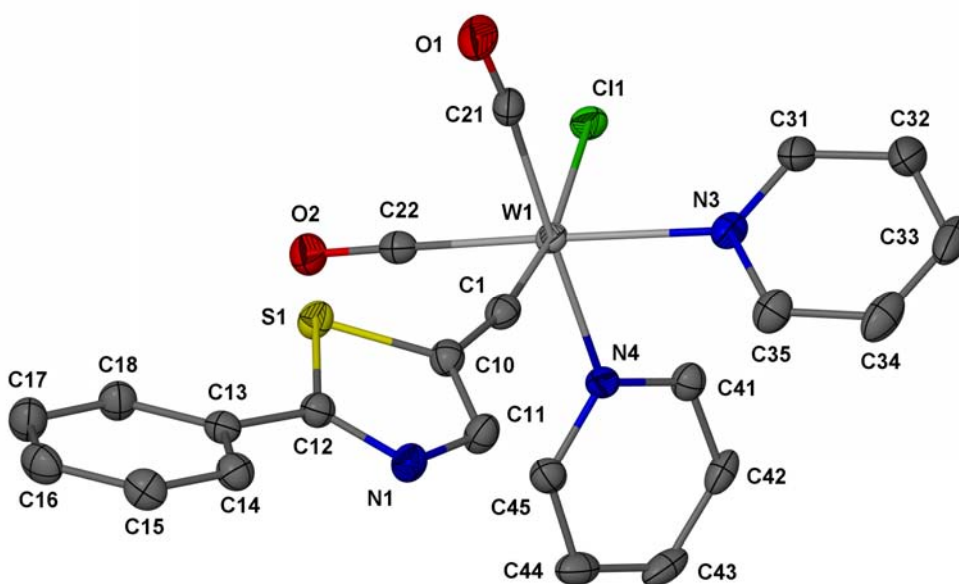


Figure 5.10 Molecular structure of **7b**-CH₂Cl₂; the solvent molecule is omitted for clarity.

2.542(2), 2.536(2) and 2.534(2) Å are found for the tris(pyridin-2-yl)phosphane- and the two unique molecules of the tmeda-chelated complexes. The former complex is the only one suitable for comparison of the W–N distances, 2.254(5) and 2.255(5) Å, which are comparable with the values in **7a** [2.276(3) and 2.269(3) Å] and **7b** [2.246(3) and 2.254(3) Å]. The structures of the 4-methylphenyl carbyne complex, **3**, also contain W–N bonds of similar length, on average 2.26(1) Å.

The angle at the carbyne carbon deviates from the expected linearity in **7a** [175.1(3)°] and **7b**·CH₂Cl₂ [169.4(3)°], this might be attributed to packing forces and thus a hybridisation deviating from the ideal *sp*-model. Compound **7b** exhibits the largest interplanar angle between the thiazolyl and phenyl groups [21.9(2)°] in all complexes derived from ligand **1b**, albeit still less pronounced than in phenylpyrazolinyldiene Fischer-type carbenes of gold (*vide infra*).³⁷

The distance of N2 to the plane of its bonded carbon atoms in **7a** is 0.074(5) Å and thus comparable to the situation found in **6a** [0.06(2) Å], but different to **5a** [0.185(5) Å] and **5c**·2CHCl₃ [0.146(8) Å].

5.4.5 Crystal and molecular structure of a gold Fischer-type carbene complex, **8b**

Complex **8b** crystallises with two unique molecules in the asymmetric unit, that are linked by aurophilic interactions [Au1A···Au1B 3.3866(3) Å]. This dimer is further linked to its symmetry-generated image (related to the former by a centre of inversion located between Au1B and Au1B', Figure 5.11), *via* an aurophilic bond [Au1B···Au1B' 3.4871(4) Å, ' = 2 - x, 1 - y, z]. The molecules of **8b** thus form an ABB'A' pattern of four gold atoms in a chain. In this manner Au1A experiences only a single crossed-sword type aurophilic bond while Au1B bridges both Au1A by a shorter as well as symmetry generated Au1B' by a longer Au···Au interaction of

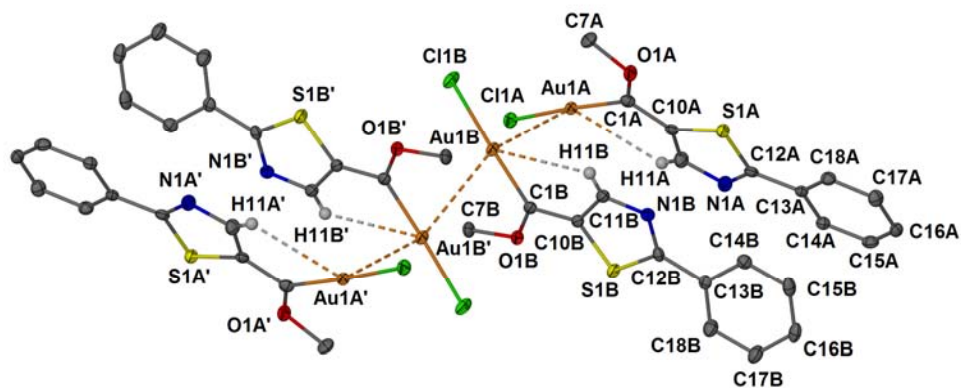
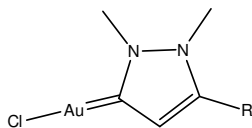


Figure 5.11 Complex **8b** forming a tetrameric zigzag chain in the solid state, two molecules are asymmetric; primed atoms are related by an inversion centre located between Au1B and Au1B' (symmetry code 2 - x, 1 - y, -z).

crossed-sword [Cl1A–Au1A··Au1B–Cl1B 88.20(4)°] and (necessitated by the centre of inversion) antiparallel [Cl1B–Au1B··Au1B'–Cl1B' 180°] orientations, respectively. Compound **8b** is the only neutral Fischer-type carbene complex of gold known to undergo aurophilic interactions in the solid state.

The determination of the bonding parameters in the molecular structures of **6b** and **8b** allow comparison of the different ways in which the units W(CO)₅ and AuCl influence the carbene ligand. Only a few reports have dealt with molecular structures of related gold carbene complexes. The complex Ph(Me₂N)C=AuCl⁷⁰ and a series of pyrazolin-3-ylidene complexes³⁷ (Scheme 5.20) have been reported. The various Au–C distances in these compounds [2.02(3) for the former and 1.981(6) and 1.991(5) Å for the latter complexes] are comparable to those in **8b** [1.976(4) and 1.959(4) Å]. Comparison of **8b** to Ph(Me₂N)C=AuCl is hampered by the large s.u. and the better electron-donating property of the NMe₂ group compared to the OMe group.



Scheme 5.20 Pyrazolin-3-ylidene gold(I) complexes synthesised by *Kessler et al.*³⁷ R = phenyl or 4-(dimethylamino)phenyl.

The Au–Cl bond of the unique molecule engaging in two aurophilic interactions [Au1B–Cl1B 2.279(2) Å] is shorter than in the pyrazolylidene complexes mentioned above [Au–Cl 2.307(2) and 2.299(2) Å], in the instance of Ph(Me₂N)C=AuCl [Au–Cl 2.30(1) Å] comparison is again hampered by the same shortcomings mentioned above. This is in contrast to findings for the polymorphs of chloro[tris(4-methylthiazol-2-yl)phosphane]gold (see Chapter 3, p. 87) where aurophilic interactions cause lengthening of the Au–Cl bond distances.

Another feature that discriminates between **8b** and the pyrazolinylidene complexes, is the torsion angle between the heterocycle and the phenyl group. For **8b**, as in most other complexes derived from ligand **1b**, the angles are 1.9(3)° and 13.8(3)° but for the pyrazolinylidene compounds they range between 45.9° and 47.7°.

Already observed in the ^1H NMR spectrum of **8b**, the agostic $\text{Au}\cdots\text{H}$ interaction of the thiazole hydrogen atom with the gold centre [$\text{Au}\cdots\text{H}$ distances 2.87 and 2.97 Å] was verified in the molecular structure of the compound. This additional stabilising effect could be larger than that of a $\text{Au}\cdots\text{S}$ interaction which, in principle, would be possible if the thiazole ring was flipped by 180° and which is usually observed in gold complexes containing thiazole rings, *e.g.* **9a** $\cdot 0.5\text{CH}_2\text{Cl}_2$ (*vide infra*) and all but one of the tris(thiazol-2-yl)phosphane gold complexes in Chapter 3. The crystal structures of bis-aurated diphenylmethane and 1,2-diphenylethane, which were examined by low-temperature NMR, show $\text{Au}\cdots\text{H}$ distances of 2.6 to 3.0 Å.⁵⁹ Additionally, Friedrichs and Jones published a comprehensive study of hydrogen interactions in the crystal structures of bis(thione)gold(1+) complexes with different anions,⁷¹ the authors found $\text{Au}\cdots\text{H}$ contacts of similar length (2.80–3.07 Å) as in **8b**. In a more recent study, agostic $\text{Au}\cdots\text{H}$ interactions (distances 2.83–2.88 Å), that also compare favourably with **8b**, were found in the crystal structures of Au^{I} pyridinethiolate complexes.⁷² The experimental results in the latter publication were also accompanied by theoretical calculations.

The C–O bond distances of the carbene ligands in **8b** [1.296(5) and 1.302(5) Å] may be shorter compared to the tungsten carbene complex **6b** [1.330(5) Å] (the former difference is just significant, the latter just not). Whether this is caused by the lower ability of Au^{I} to effect π -back donation^{5,6,73} cannot be answered based on this data alone but probably requires theoretical calculations.

5.4.6 Molecular structure of the decarbonylated gold complex **9a** $\cdot 0.5\text{CH}_2\text{Cl}_2$

The crystallised product of an unprecedented CO-elimination (*cf.* Scheme 5.11) from a gold acyl complex that occurred on transfer of the carbene ligand from $\text{W}(\text{CO})_5$ to Ph_3PAu^+ , **9a** $\cdot 0.5\text{CH}_2\text{Cl}_2$, is shown in Figure 5.12. The structure also

71 (a) S. Friedrichs and P. G. Jones, *Z. Naturforsch. B: Chem. Sci.* **2004**, *59*, 49–57;

(b) S. Friedrichs and P. G. Jones, *Z. Naturforsch. B: Chem. Sci.* **2004**, *59*, 793–801;

(c) S. Friedrichs and P. G. Jones, *Z. Naturforsch. B: Chem. Sci.* **2004**, *59*, 1429–1437.

72 M. T. Räisänen, N. Runeberg, M. Klinga, M. Nieger, M. Bolte, P. Pyykkö, M. Leskelä and T. Repo, *Inorg. Chem.* **2007**, *46*, 9954–9960.

73 P. K. Hurlburt, J. J. Rack, J. S. Luck, S. F. Dec, J. D. Webb, O. P. Anderson and S. H. Strauss, *J. Am. Chem. Soc.* **1994**, *116*, 10003–10014, and references cited therein.

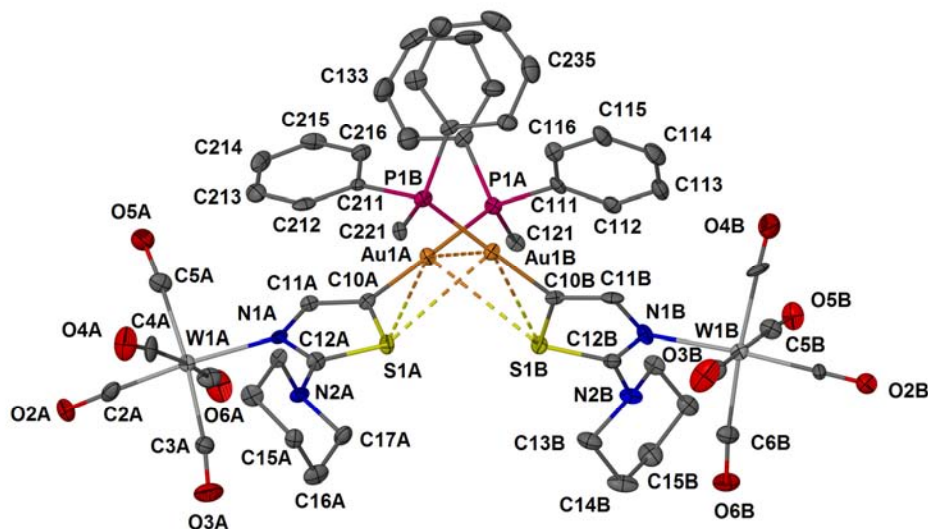


Figure 5.12 Molecular structure of **9a**·0.5CH₂Cl₂; a *pseudo*-C₂ axis passes between the Au and S atoms; for clarity, one phenyl ring each of the triphenylphosphane ligands is only represented as the *ipso* carbon atom and the CH₂Cl₂ solvent molecule has been omitted.

incorporates a nitrogen atom of a C-5-aurated thiazole ring coordinating to a W(CO)₅ fragment. Despite readily accessible 5-lithiothiazoles,⁴⁴ no complexes of this kind have been reported, only carbenes and carbeniates of gold comprising 2-thiazolyl ligands are known.^{66,74} The Au–C bond lengths for the two unique molecules of **9a** are 2.042(8) and 2.046(8) Å; Au–C distances of known 2-thiazolylidene complexes vary from 1.92(2) Å in the cationic complex bis(4-methyl-3*H*-thiazol-2-ylidene)gold(1+) tetrachlorozincate(2–)^{66b} to 2.05(1) Å in bis(3,4-dimethyl-3*H*-thiazol-2-ylidene)-gold(1+) triflate,^{66a} averaging 2.00 Å.

The neutral complex **9a**·0.5CH₂Cl₂ crystallises in the chiral orthorhombic space group *P*2₁2₁2₁ despite being achiral itself, two molecules are crystallographically independent. They are, however, approximately related by a *pseudo*-C₂ axis of rotation. An aurophilic bond of 3.2117(5) Å links the two asymmetric molecules which is astoundingly short given the steric demand of the ligands – the less crowded Ph₃PAuCl crystallises without any aurophilic interaction.⁷⁵ Such associations of bulky

74 (a) H. G. Raubenheimer, F. Scott, M. Roos and R. Otte, *J. Chem. Soc., Chem Commun.* **1990**, 1722–1723; (b) H. G. Raubenheimer, F. Scott, G. J. Kruger, J. G. Toerien, R. Otte, W. van Zyl, I. Taljaard, P. Olivier and L. Linford, *J. Chem. Soc., Dalton Trans.* **1994**, 2091–2097.

75 N. C. Baenziger, W. E. Bennett and D. M. Soboroff, *Acta Crystallogr., Sect. B: Struct. Crystallogr. Cryst. Chem.* **1976**, 32, 962–963.

molecules have been observed before. An example is $\text{Ph}_3\text{PAuS}[\text{Cr}(\text{CO})_5]\text{Ph}$, where a benzenethiolate bridges $\text{Cr}(\text{CO})_5$ and Ph_3PAu^+ fragments, two molecules are themselves linked by an aurophilic bond of $3.1869(4) \text{ \AA}$.^{36b}

Due to steric restraints ensuing from the tight association of dimers of $\mathbf{9a} \cdot 0.5\text{CH}_2\text{Cl}_2$, the piperidine rings are twisted out of plane relative to the thiazole ring, thus hampering the delocalisation of the nitrogen lone pair as is reflected in the large distances of N2A and N2B to the plane of their bonded carbon atoms. The C–N2–C angles are in the range of $110.3(6)^\circ$ to $115.5(7)^\circ$ which is closest to sp^3 -hybridisation for all complexes derived from $\mathbf{1a}$, as well as N2–C12 bond distances [$1.39(1)$ and $1.37(1) \text{ \AA}$] that are close to the value of a C–N single bond.⁶⁴ The concomitant shortening of the N1–C12 bonds [$1.33(1)$ and $1.29(2) \text{ \AA}$] that should be observed in this case is – as was mentioned with compounds $\mathbf{5a}$ and $\mathbf{5b}$ – small compared to the s.u.s involved. The same drawback holds true for the N1–C11 bonds [$1.37(1)$ and $1.41(1) \text{ \AA}$] in the thiazole ring, which should be longer owing to greater localisation of the formal double bonds (C10–C11 and N1–C12).

The pentacarbonyltungsten fragment is coordinated to the imine nitrogen atom of the thiazole ring and is consequently not lost during carbene transfer like in the Fischer-type gold carbene $\mathbf{8b}$. Crystal and molecular structures incorporating $\text{W}(\text{CO})_5$ groups coordinated to a thiazole nitrogen atom have not been published, but *de Jongh* has prepared a series of N-3-coordinated 2-aminoazole pentacarbonylchromium and tungsten complexes for the first time and also reported their crystal- and molecular structures.^{52a} The W–N bond lengths in $\mathbf{9a} \cdot 0.5\text{CH}_2\text{Cl}_2$ [$2.265(7)$ and $2.271(7) \text{ \AA}$] are comparable to the similar bond in (2-aminobenzothiazole- κN^3)pentacarbonyltungsten, $2.274(4) \text{ \AA}$. The *trans*-CO ligand forms a very short W–C bond in $\mathbf{9a} \cdot 0.5\text{CH}_2\text{Cl}_2$ [$1.95(1)$ and $1.953(9) \text{ \AA}$] compared to the analogous distances for the *cis*-CO ligands [$2.03(1)$ to $2.08(1) \text{ \AA}$] which is corroborated in the results for the 2-aminobenzothiazole complex mentioned above [$1.960(5) \text{ \AA}$ and $2.026(5)$ – $2.054(5) \text{ \AA}$ for *cis*- and *trans*-W–CO bonds, respectively].

As has been documented in the chapters preceding this one (see Chapters 3 and 4, pp. 88 and 124), the structure of $\mathbf{9a} \cdot 0.5\text{CH}_2\text{Cl}_2$ is no exception when it comes to $\text{Au} \cdots \text{S}$

interactions with a thiazole or thiophene sulfur atom. The Au and S atoms are located at the corners of a distorted tetrahedron involving Au1A, Au1B, S1A and S1B in which the intramolecular Au \cdots S contacts [3.267(2), 3.285(2) Å] are shorter than the intermolecular associations [3.392(2) and 3.315(2) Å]; nevertheless, all are below the sum of the van der Waals radii of the concerned atoms. The distance between the sulfur atoms in the dimer is 3.943 Å and therefore longer than the sum of the van der Waals radii, it was not refined. Despite being very poor donors for the formation of coordinative bonds (no S-coordination of thiophenes or any thia-azoles to gold has been reported), the thiazole sulfur atoms apparently assist in stabilising the dimer and in overcoming steric repulsion.

5.4.7 Molecular structure of the carbene transfer product **10b**·C₅H₁₂

Compound **10b** was isolated as crystals of a red pentane solvate. The Ph₃PAu⁺ group coordinates to what essentially amounts to be an acyl carbon while the displaced W(CO)₅ fragment becomes uniquely attached to the acyl oxygen atom. A reaction process wherein Ph₃PAu⁺ first attacks the W–C(carbene) bond and W(CO)₅ subsequently migrates to the oxygen atom affording a C(Au)/O(W) product has been postulated after this reaction was first explored by *Esterhuysen*.^{51a} However, conclusive proof in support of this mechanism was not available and the products isolated could not be unequivocally characterised. N-coordination of W(CO)₅ was observed in the related carbene-imidate complexes.

Compound **10b**·C₅H₁₂ shown in Figure 5.13 therefore confirms the existence of the proposed intermediate product on the way to W(CO)₅-free gold acyls. This result is even more surprising when the presence of a free imine-nitrogen in **10b**, that is unable to keep the W(CO)₅ fragment away from the carbeniate oxygen, is taken into account. Such an association probably occurred in the related process when the *pseudo-abnormal* carbene complex **9a** was formed. Complex **10b** may also be seen as a *pseudo*-carbene complex since W(CO)₅ is isolobal to H⁺.

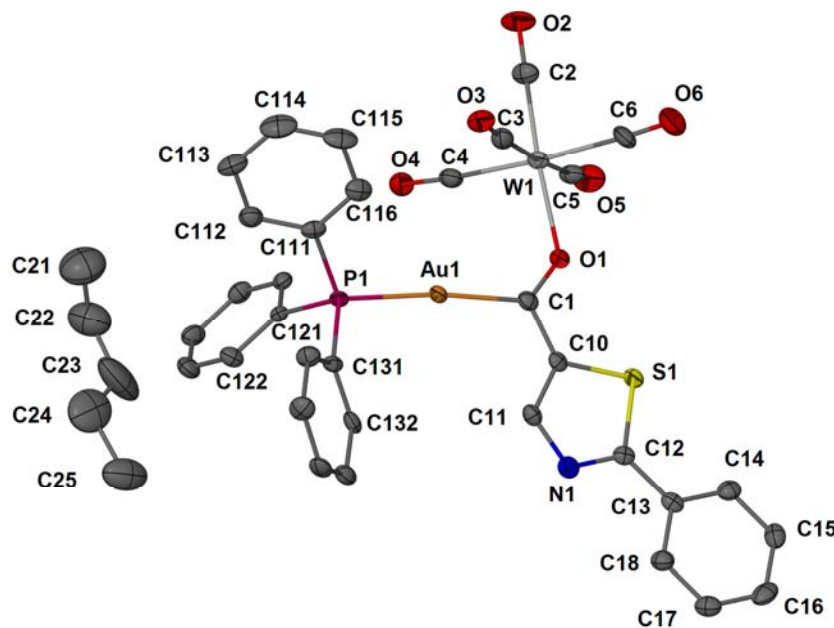
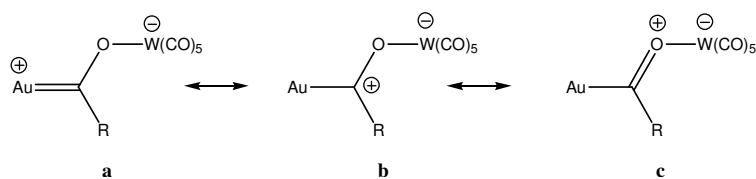


Figure 5.13 Molecular structure of **10b**·C₅H₁₂.

The Au–C bond length in **10b**·C₅H₁₂ [2.053(7) Å] is comparable to the uncoordinated complex Ph₃PAu–C(O)Ph [2.085(5) Å],^{51b} the W(CO)₅ fragment is therefore not as effective as an alkyl cation in discouraging the acyl structure (*c*) in Scheme 5.21 and does not enhance the contribution of the carbene structure (*a*). The Au–C distance is therefore longer than the same distances in the proper Fischer-type carbene complex **8b** [1.976(4) and 1.959(4) Å].



Scheme 5.21 Contributing resonance structures in **10b**.

The Au–P bond in **10b**·C₅H₁₂ is somewhat shorter [2.301(2) Å] than that found in the free benzoyl complex Ph₃PAu–C(O)Ph [2.313(1) Å] while the C–O bond in **10b**·C₅H₁₂ [1.247(8) Å] is just longer compared to Ph₃PAu–C(O)Ph [1.200(7) Å].^{51b} This effect may be caused by both the influence of the coordinated W(CO)₅ group as well as the heteroaromatic substituent.

Another report of a structurally related, *O*-metal coordinated gold carbene complex is that of a (pentanoyl)(triphenylphosphane)gold moiety *O*-coordinating to one rhenium

atom of the heptacarbonylbis(μ -diphenylphosphanido)dirhenium fragment.⁷⁶ The dimensions at the gold centre [Au–C 2.05(2) Å, Au–P 2.301(3) Å] and the Re–O–C angle [131.1(7)°] are virtually identical to related bonds and angles in **10b**·C₅H₁₂ [W–O–C 132.1(4)°]; the C–O [1.23(2) Å] bond in the pentanoylgold complex is comparable to that in **10b**·C₅H₁₂ [C–O 1.247(8) Å].

Oxygen, classified as a hard donor atom, is usually not suitable for coordination to a W(CO)₅ fragment and only a few structure determinations have been reported, often with the statement that the complex was only of limited stability or had to be handled in a CO atmosphere. Ph₃PO–W(CO)₅ is the only neutral structurally characterised complex known.⁷⁷ The W–O distance in this complex is longer [2.244(3) Å], but the W–O–P angle of 134.3(2)° is comparable to the situation in **10b**·C₅H₁₂. The anion [W(OPh)(CO)₅][–] in its [Et₄N]⁺-salt, on the other hand, exhibits W–O bond distances of 2.18(2) Å and 2.20(2) Å from two asymmetric molecules and W–O–C angles of 131(2)° and 134(2)°⁷⁸ that are similar to the situation in **10b**·C₅H₁₂. A comparable W–O distance of 2.168(9) Å but somewhat more acute W–O–C angle [128.4(7)°] than in **10b**·C₅H₁₂ is found in the sterically crowded [Et₄N]⁺-salt of pentacarbonyl-(2,6-diphenylphenoxy)tungstate(1–).⁷⁹

The W–C bond length of the *trans*-CO group in **10b**·C₅H₁₂ is shortened considerably [1.953(7) Å] compared to the analogous *cis*-CO bond lengths in the compound [2.015(8)–2.045(8) Å], it is of the same length as the analogous bonds in **9a**·0.5CH₂Cl₂ [1.95(1) and 1.953(9) Å], Ph₃PO–W(CO)₅ and [W(phenolate)(CO)₅][–] compounds.

In **10b**·C₅H₁₂ the thiazole group is oriented the same way as in **8b**, *i.e.* their alignment enables a possible Au···H (distance 2.84 Å) rather than a Au···S contact which would be in line with the distances observed in other crystal structures.⁷¹ The ¹H NMR spectrum at room temperature, however, yields a sharp signal for the proton involved.

76 H.-J. Haupt, D. Petters and U. Flörke, *J. Organomet. Chem.* **1998**, 553, 497–501.

77 J. B. Cook, B. K. Nicholson and D. W. Smith, *J. Organomet. Chem.* **2004**, 689, 860–869.

78 D. J. Darensbourg, K. M. Sanchez, J. H. Reibenspies and A. L. Rheingold, *J. Am. Chem. Soc.* **1989**, 111, 7094–7103.

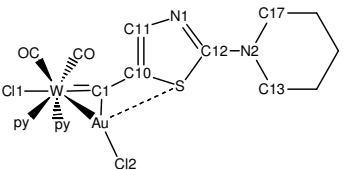
79 D. J. Darensbourg, B. L. Mueller, C. J. Bischoff, S. S. Chojnacki and J. H. Reibenspies, *Inorg. Chem.* **1991**, 30, 2418–2424.

5.4.8 Molecular structure of **11a**·0.5C₄H₈O

Various complexes wherein a Au^I centre coordinates to a tungsten carbyne have been reported. The product **11a**·0.5C₄H₈O, however, is the first AuCl adduct to be crystallographically characterised. Selected bond lengths and angles are reported in Table 5.10. Given the low quality of the diffraction dataset, comparison of the structure must be limited to the distances of the heavier atoms.

The structure shown in Figure 5.14 contains a W–Au–C metallacycle with the W–C1–C10 angle now bent and C1, concomitantly, re-hybridised to allow efficient coordination to the AuCl moiety. The gold atom forms bonds to both tungsten and carbon atoms [Au–W 2.7826(7), Au–C 2.03(1)] and is also stabilised by a, now familiar, Au··S interaction [Au··S 3.361(3) Å] with the thiazole ring. The bond lengths in the triangle are almost identical to those in [μ-(4-MePh)C][AuC₆F₅]-[WBr(bipy)(CO)₂],⁸⁰ [Au–W 2.7829(1), Au–C 2.080(3) Å]

Table 5.10 Bond lengths/Å and angles/° of compound **11a**·0.5C₄H₈O.



W–Au	2.7826(7)	S–C10	1.75(2)
W–C1	1.89(2)	S–C12	1.75(2)
W–Cl1	2.451(3)	C1–C10	1.45(2)
Au–C1	2.03(1)	C10–C11	1.37(2)
Au–C12	2.281(3)	N1–C11	1.36(2)
Au··S	3.361(3)	N1–C12	1.31(2)
W–N3	2.269(9)	C12–N2	1.33(2)
W–N4	2.246(9)	Au–W–C1	42.9(4)
W–C21 (CO)	1.97(1)	Au–C1–C10	117.1(8)
W–C22 (CO)	1.98(2)	Cl1–W–C1	152.3(3)
W–Au–C12	146.01(9)	C1–Au–W	42.8(4)
W–C1–Au1	90.4(5)	C1–Au–C12	171.2(4)
W–C1–C10	152.4(8)	N2–ε	0.17(2)
C11–W–Au	160.85(8)	ε ≡ C12 C13 C17	

⁸⁰ G. A. Carriedo, V. Riera, G. Sánchez and X. Solans, *J. Chem. Soc., Dalton Trans.* **1988**, 1957–1962.

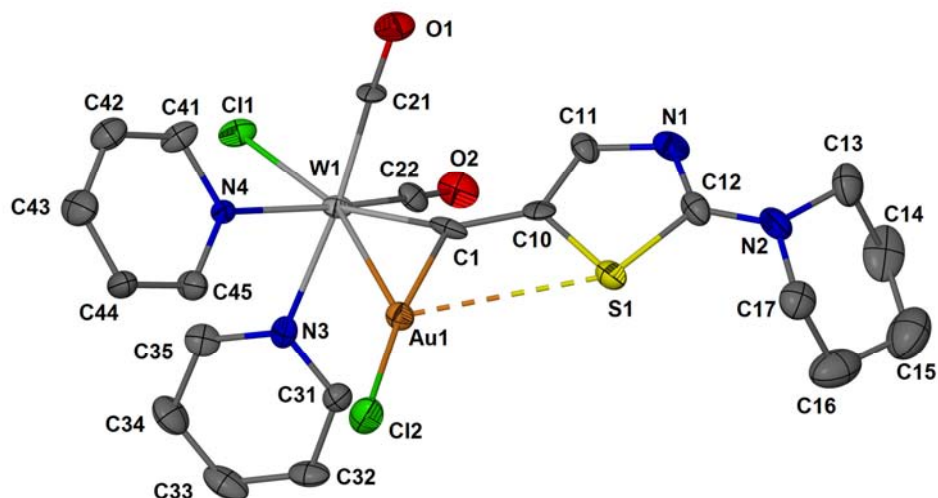


Figure 5.14 Molecular structure of **11a**·0.5C₄H₈O, the thf molecule has been omitted for clarity.

suggesting little influence of the carbyne ligand. Indeed, the distance of N2 to the plane defined by its three bonded carbon atoms [0.17(2) Å] is comparable to the tungsten carbenate **5a** [0.185(5) Å].

Compared to the free carbyne complex, **7a** [W–Cl 2.523(2) Å], the W–Cl bond in **11a**·0.5C₄H₈O [2.451(3) Å] is shortened considerably upon coordination of AuCl. The other bond lengths at the tungsten centre are fairly similar to those in **7a**, and the Au–Cl [2.281(3) Å] bond is of similar length to the ones found in **8b** [2.289(1) and 2.279(2) Å].

5.4.9 Molecular structures of *r*NHC complexes **12W**, **13** and **14**

As mentioned previously no gold complexes of *r*NHCs are known the first X-ray crystal and molecular structures of such compounds were determined in this study. In the molecular structure of **13**, which is a substituted *r*NHC complex (shown in Figure 5.15), the Au–C bond distance [1.991(7) Å] is comparable to and the Au–Cl bond [2.304(2) Å] insignificantly shorter (5 s.u.) than in the simple unsubstituted example **16** (*vide infra*).

The Au–C bond of cationic **14** (Figure 5.16), is significantly longer [2.049(3) Å] than in the neutral *r*NHC gold chloride compounds **13** [1.991(7) Å] and **16** [1.979(6) Å] and comparable to those found in the two asymmetric molecules of the cationic NHC

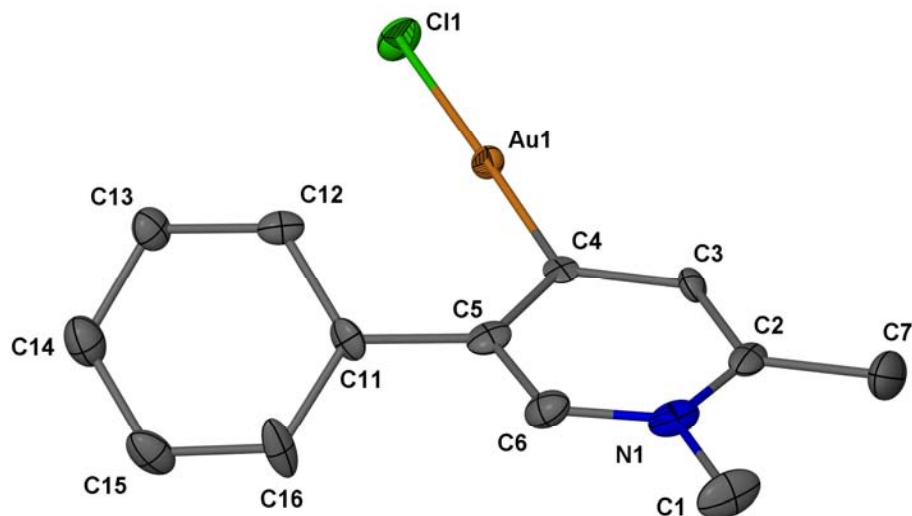


Figure 5.15 Molecular structure of 13.

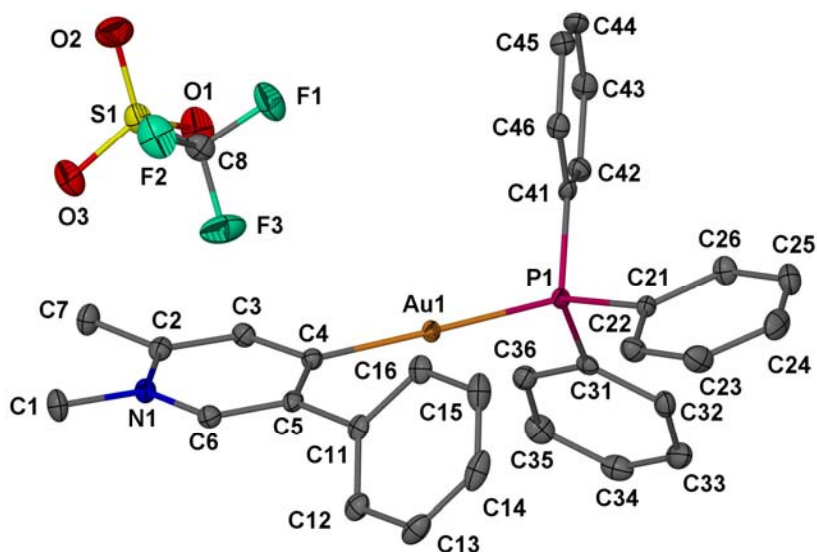


Figure 5.16 Molecular structure of 14.

complex [1,3-bis(1,1-dimethylethyl)imidazol-2-ylidene](triphenylphosphane)gold(1+) hexafluorophosphate [2.044(4) and 2.034(4) Å], also showing the *trans* influence of a phosphane ligand.⁸¹ The Au–P distance in **14** [2.2888(8) Å] is significantly longer than the same distances in the latter NHC compound [2.275(1) and 2.274(1) Å] highlighting the greater *trans*-influence of the one-N, six-membered *r*NHC ligand.

⁸¹ M. V. Baker, P. J. Barnard, S. J. Berners-Price, S. K. Brayshaw, J. L. Hickey, B. W. Skelton and A. H. White, *J. Organomet. Chem.* **2005**, 690, 5625–5635.

Though first synthesised in 1992 by *Aumann*,^{8a} structures of *r*NHC–W(CO)₅ adducts have not yet been reported. In order to establish the first such molecular structure and to examine the influence the *r*NHC ligand exerts on the W(CO)₅ fragment, the molecular structure of **12W**, wherein the AuCl or AuPPh₃⁺ fragments are replaced by isolobal W(CO)₅, has been determined. Furthermore, the structural elucidation of this complex would possibly enable the observation of differences in the ligand geometry when coordinated to different metals and aid in the assignment of the main contributing canonic structure. It has been mentioned above that the gold complexes show smaller chemical shift differences between the 2/6- and 3/5-CH resonances in their ¹H and ¹³C NMR spectra when compared to their W(CO)₅ analogues. The carbene ¹³C NMR resonances also appear at higher field strength in the *r*NHC gold complexes.

The impact of the transition metal fragment on the bond lengths in the pyridinylidene backbone was of particular interest, especially as reflected in the C–N bond lengths of the six-membered heterocycle that should decrease owing to the higher bond order if the charge-separated pyridinium resonance becomes more important compared to the classic neutral carbene contributing structure in one of the two complex families. However, only insignificant positive and negative differences within the molecular structures of the *r*NHC complexes can be observed when the individual structures are compared. X-ray crystallographic analysis, therefore, does not seem an effective method for determining the main contributing structures in *r*NHC complexes or for discrimination between different contributions in a series of compounds.^{16f} Differences highlighted by NMR measurements are thus not coherently substantiated by bond distance variations from X-ray studies.

Complex **12W** shown in Figure 5.17 exhibits the expected octahedral geometry around the tungsten centre, the largest deviation from linearity for a given set of mutually *trans*-located ligands is between two CO ligands [C22–W–C24 170.7(2)°]. This deviation can be explained by steric influence of the nearby phenyl- and pyridinylidene groups as the other related angle, where the CO groups are further away from the *r*NHC ligand, is close to the ideal value [C23–W–C25 178.0(2)°] The pyridinylidene ring forms an angle of 26.5(2)° with the C21–C22–C24–W (*i.e.* the carbon atoms of the CO ligands whose C–W–C angle deviates most from linearity and

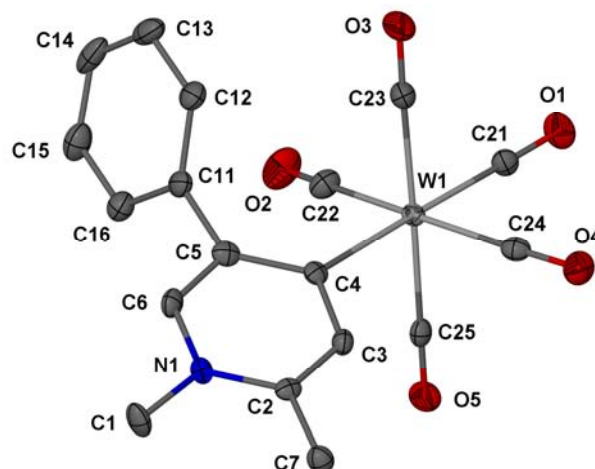


Figure 5.17 Molecular structure of **12W**.

the carbon atom of the *trans*-CO ligand) plane, thus resembling an intermediate between staggered and eclipsed conformation.

The effect of the *r*NHC ligand on the *trans*-CO W–C distance [2.003(4) Å] in **12W** is comparable to the related one-N six-membered *normal*-NHC complexes of tungsten where the distance was found to be 2.014 and 2.007 Å for two asymmetric molecules in one complex⁸² and 1.993 Å in another.⁸³ The W–C(carbene) distances of the latter complexes, 2.287 and 2.285 Å as well as 2.277(5) Å, are also comparable to the same distance in **12W** [2.271(4) Å].

The interplanar angle of the phenyl group with the pyridinylidene ring is larger in **12W** [68.8(2)°] than in the *r*NHC gold complexes [43.3(3)° in **13** and 48.9(2)° in **14**] reflecting the higher steric demand of the W(CO)₅ fragment.

5.4.10 Molecular structure of *r*NHC complex **16**

It came as somewhat of a surprise that the molecular structure of **16**, shown in Figure 5.18, consists of discrete molecules, devoid of any close, sub-van der Waals interactions. Given the low steric demand of the 1-methyl-1*H*-pyridin-4-ylidene ligand, this complex seemed a natural and almost certain candidate for Au⁺–Au interactions (or possibly Au⁺–Cl contacts as in the molecular structure of **2b(iii)** in Chapter 3).

82 R. Aumann, M. Kößmeier, K. Roths and R. Fröhlich, *Synlett* **1994**, 1041–1044.

83 R. Aumann, K. Roths and M. Grehl, *Synlett* **1993**, 669–671.

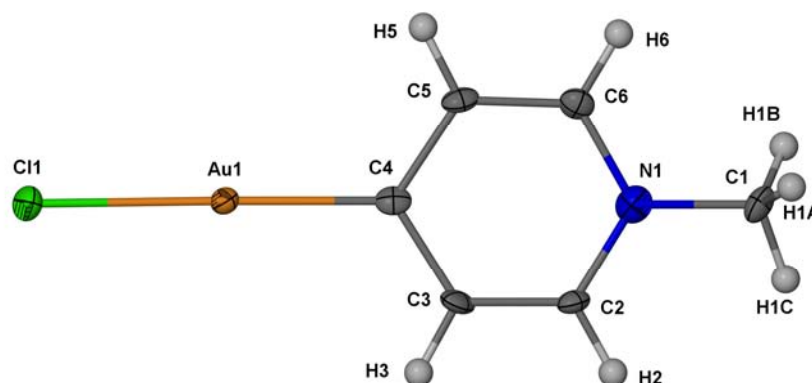


Figure 5.18 Molecular structure of **16**.

Indeed, as no such interactions were found in any of the *r*NHC gold complexes reported here, further examples are needed to determine whether this is an intrinsic feature of these complexes or an incidental result. The Au–C bond length in **16** [1.979(6) Å] is comparable to the NHC complex bis(1*H*-pyridin-2-ylidene)gold(1+) chloride [2.03(2) and 2.02(2) Å],⁸⁴ and is also similar to the same bond in **8b** [1.976(4) and 1.959(4) Å]. However, the Au–Cl bond in **16** [2.314(2) Å] is clearly longer than in **8b** [2.289(1) and 2.279(2) Å] and Ph₃PAuCl⁷³ [2.279(3) Å] but roughly comparable to the same separation in gold pyrazolin-3-ylidene complexes [2.307(2) and 2.299(2) Å],³⁷ indicating the superior *trans*-influence of the *r*NHC ligand compared to the heterocyclic carbene in compound **8b**.

5.5 Conclusions

It was demonstrated for the first time that relatively stable heterocyclic carbene and carbyne complexes can be synthesised by reacting 5-thiazolylithium reagents with W(CO)₆ and then subjecting the obtained carbenate to either alkylation or formal oxide abstraction. The metal–carbon triple bond of the obtained carbyne complexes acts as a ligand towards various Au^I centres, it was shown to be a better coordination site for AuCl than the imine nitrogen of the 2(1-piperidinyl)thiazole group. However, complications from homoleptic rearrangement arise when (tht)AuC₆F₅ is used.

⁸⁴ H. G. Raubenheimer, J. G. Toerien, G. J. Kruger, R. Otte, W. van Zyl and P. Olivier, *J. Organomet. Chem.* **1994**, 466, 291–295.

Neutral and anionic heterocyclic Fischer-type carbene complexes derived from such thiazoles deprotonated in an unusual position were also prepared, although the necessary final alkylation step afforded only poor yields which might be a result of competing *N*-alkylation. The carbene ligands in these complexes were readily transferred to gold(I) electrophiles in some unexpected pathways: the thiazolyl substituent, for example, is effective in stabilising the first characterised product of an acyl transfer to gold in which a W(CO)₅-fragment becomes attached to an oxygen atom of the carbene group. This molecular structure is unprecedented. Additionally, with a different ligand a unique CO-expulsion reaction occurred during carbene transfer to Au^I. This result complements rare synthetic CO-insertion reactions found by *Cinellu et al.* and *Komiya et al.* and the discovery could provide a further incentive to rationalise and develop this neglected area in gold chemistry. Furthermore, the new tungsten and gold carbene complexes with heterocyclic side chains supplement the limited data available for this class of compounds, or, as for the carbeniate salts and the *pseudo-carbene* complexes **9a** and **10b**, are the first ones structurally characterised.

Finally, carbene transfer reactions could be successfully expanded to include the unusual *remote N*-heterocyclic carbenes (*r*NHCs) to afford the first examples of *r*NHC gold complexes. The compounds are very stable and could find further application in homogeneous catalysis as has been already shown for *r*NHC-complexes of group 10 metals. Based on observations in the NMR spectra it was concluded that relative to the group 6 metal *r*NHC complexes, a higher contribution of the metalated pyridinium structure with a formal Au–C single bond is found in the gold *r*NHC complexes. As other techniques are not able to discriminate between the pyridinium- and classic carbene structures of the ligand, theoretical calculations could shed more light on the bonding situation in this compound class. All transfer products as well as a tungsten *r*NHC complex have been structurally characterised and constitute the first molecular structures of *r*NHC complexes determined for these metals, again expanding the data available on this topic.

5.6 Experimental

5.6.1 Crystal structure determinations

For measurement and data processing conditions refer to Chapter 2, p. 57. Data and parameters of the crystal structure determinations are summarised in Tables 5.11 to 5.13.

In the structure of **3**·C₄H₈O, the thf molecule could not be modeled due to extensive disorder. The thf molecule in **11a**·0.5C₄H₈O was disordered across an inversion centre, and the geometry did not refine satisfactorily. Both solvent molecules were removed using the Squeeze routine in the Platon set of programmes.⁸⁵

In the structure of **5c**·2CHCl₃ the bridging H1 was refined with an occupancy factor of 0.5 resembling the bulk average. The N–C bond distances of the tetramethylammonium cation were restrained by a SADI instruction to have the same length in the case of the disordered carbon atoms.

The pentane in **10b**·C₅H₁₂ did not exhibit satisfactory bond lengths and the pairs of CH₃–CH₂ and CH₂–CH₂ bonds were hence each restrained by a SADI instruction to have the same length. Slight disorder of the solvent molecule was not resolved and only the main site was refined.

In the crystal structure of **13**, the carbene carbon became non-positive definite upon anisotropic refinement, it was restrained to approximate isotropic behaviour by an ISOR instruction. The identity of the atom to be indeed carbon can be secured by the synthetic pathway and the structure of **12W**, to which it is directly related, as well as NMR and MS measurements.

⁸⁵ A. L. Spek, *J. Appl. Crystallogr.* **2003**, *36*, 7–13.

Table 5.11 Crystallographic parameters of **3–7a**.

Compound	3	3·C₄H₈O	5a	5c·2CHCl₃	6a	7a
Empirical formula	C ₂₀ H ₁₇ ClN ₂ O ₂ W	C ₂₀ H ₁₇ ClN ₂ O ₂ W·C ₄ H ₈ O	C ₁₈ H ₂₃ N ₃ O ₆ SW	C ₁₈ H ₂₄ N ₃ O ₆ SW·C ₁₄ H ₁₁ – N ₂ O ₆ SW·2CHCl ₃	C ₁₅ H ₁₄ N ₂ O ₆ SW	C ₂₁ H ₂₁ ClN ₄ O ₂ SW
<i>M_r</i>	536.66	608.76	593.30	1352.2	534.19	612.78
Crystal habit	Needle	Needle	Prism	Needle	Block	Prism
Crystal colour	Orange	Orange	Orange	Orange	Orange	Orange
Crystal dimensions/mm	0.32 × 0.09 × 0.04	0.43 × 0.10 × 0.07	0.19 × 0.15 × 0.13	0.10 × 0.03 × 0.01	0.44 × 0.34 × 0.06	0.18 × 0.10 × 0.03
Crystal system	Monoclinic	Monoclinic	Monoclinic	Monoclinic	Monoclinic	Triclinic
Space group	<i>C</i> 2/ <i>c</i> (No. 15)	<i>P</i> 2 ₁ / <i>c</i> (No. 14)	<i>C</i> 2/ <i>c</i> (No. 15)	<i>C</i> 2/ <i>c</i> (No. 15)	<i>P</i> 2 ₁ / <i>n</i> (No. 14)	<i>P</i> $\bar{1}$ (No. 2)
<i>a</i> /Å	26.655(4)	7.1554(7)	22.688(4)	26.273(7)	7.363(2)	8.657(2)
<i>b</i> /Å	7.127(2)	12.665(2)	9.098(2)	11.491(3)	19.382(4)	8.917(2)
<i>c</i> /Å	23.559(4)	25.983(3)	21.294(3)	16.925(5)	24.478(6)	16.718(4)
α°	90	90	90	90	90	98.687(4)
β°	121.419(2)	95.697(2)	92.674(2)	111.940(4)	90.636(3)	96.490(4)
γ°	90	90	90	90	90	118.054(3)
<i>V</i> /Å ³	3819(1)	2343.0(4)	4391(2)	4740(2)	3493(2)	1100.5(4)
<i>Z</i> , <i>D_c</i> /Mg m ⁻³	8, 1.867	4, 1.726	8, 1.795	4, 1.895	8, 2.032	2, 1.849
μ (MoK α)/mm ⁻¹	6.205	5.072	5.395	5.336	6.767	5.490
No. of reflections, unique	10600, 3889	12751, 4730	12017, 4456	13592, 5220	18558, 6943	11537, 4490
<i>R</i> _{int}	0.0431	0.0343	0.0351	0.0507	0.0428	0.0289
<i>hkl</i> index range	–33 to 23, \pm 8, –20 to 29	\pm 8, –11 to 15, \pm 32	\pm 28, –8 to 11, –24 to 26	–33 to 27, –14 to 12, \pm 21	–9 to 8, –17 to 24, \pm 30	\pm 10, \pm 11, –20 to 21
θ range/ $^\circ$	1.79–26.40	1.79–26.38	1.80–26.42	1.67–27.18	1.66–26.43	2.52–26.62
Data, restraints, parameters	3340, 0, 236	4387, 0, 237	4102, 0, 266	4051, 6, 290	6190, 0, 451	4202, 0, 271
<i>F</i> (000)	2064	1192	2320	2616	2048	596
<i>R</i> ₁ , <i>wR</i> ₂ [<i>I</i> > 2 σ (<i>I</i>)] ^a	0.0500, 0.1295	0.0658, 0.1414	0.0387, 0.0974	0.0525, 0.1153	0.0589, 0.1613	0.0268, 0.0661
<i>R</i> ₁ , <i>wR</i> ₂ (all data) ^a	0.0586, 0.1349	0.0704, 0.1429	0.0415, 0.1000	0.0731, 0.1245	0.0642, 0.1660	0.0293, 0.0671
Goodness-of-fit	1.064	1.392	1.080	1.025	1.079	1.082
Max. and min. transmission	0.789, 0.514	0.718, 0.560	0.497, 0.314	0.949, 0.576	0.679, 0.278	0.852, 0.627
Largest differential peak and hole/eÅ ⁻³	4.715, –2.208	2.242, –2.587	3.448, –3.509	3.446, –1.245	3.998, –4.155	2.535, –0.883

^a $w = 1/[\sigma^2(F_o^2) + (aP)^2 + bP]$ where $P = (F_o^2 + 2F_c^2)/3$

Table 5.12 Crystallographic parameters of **5b–10b**·C₅H₁₂

Compound	5b	6b	7b ·CH ₂ Cl ₂	8b	9a ·0.5CH ₂ Cl ₂ ^b	10b ·C ₅ H ₁₂
Empirical formula	C ₁₉ H ₁₈ N ₂ O ₆ SW	C ₁₆ H ₉ NO ₆ SW	C ₂₂ H ₁₆ ClN ₃ O ₂ SW·CH ₂ Cl ₂	C ₁₁ H ₉ AuClNOS	C ₃₁ H ₂₆ AuN ₂ O ₅ PSW ·0.5CH ₂ Cl ₂	C ₃₃ H ₂₁ AuNO ₆ PSW·C ₅ H ₁₂
<i>M_r</i>	586.26	527.15	690.66	435.67	992.85	1043.5
Crystal habit	Needle	Needle	Needle	Prism	Prism	Prism
Crystal colour	Orange	Dark orange	Red	Orange	Yellow	Orange
Crystal dimensions/mm	0.48 × 0.12 × 0.03	0.56 × 0.05 × 0.03	0.57 × 0.08 × 0.07	0.21 × 0.13 × 0.10	0.29 × 0.11 × 0.04	0.13 × 0.09 × 0.07
Crystal system	Orthorhombic	Orthorhombic	Triclinic	Monoclinic	Orthorhombic	Triclinic
Space group	<i>Pbca</i> (No. 61)	<i>Pccn</i> (No. 56)	<i>P</i> $\bar{1}$ (No. 2)	<i>P2₁/c</i> (No. 14)	<i>P2₁2₁</i> (No. 19)	<i>P</i> $\bar{1}$ (No. 2)
<i>a</i> /Å	12.602(1)	17.336(2)	9.1923(7)	14.223(2)	10.952(2)	11.5111(7)
<i>b</i> /Å	19.302(2)	26.055(3)	9.2850(8)	11.5834(9)	21.853(2)	12.0437(8)
<i>c</i> /Å	34.983(3)	7.4114(9)	15.704(2)	14.811(2)	26.999(3)	13.8342(9)
α°	90	90	101.302(1)	90	90	100.005(1)
β°	90	90	92.103(1)	106.345(1)	90	102.850(1)
γ°	90	90	105.720(1)	90	90	94.026(1)
<i>V</i> /Å ³	8510(2)	3347.5(7)	1259.4(2)	2341.5(3)	6462(2)	1829.6(2)
<i>Z</i> , <i>D_c</i> /Mg m ⁻³	16, 1.830	8, 2.092	2, 1.821	8, 2.472	8, 2.041	2, 1.894
μ (MoK α)/mm ⁻¹	5.565	7.059	5.013	12.947	8.332	7.293
No. of reflections, unique	47050, 8711	17901, 3425	13500, 5154	13330, 4783	36568, 13206	19796, 7474
<i>R</i> _{int}	0.0383	0.0406	0.0237	0.0287	0.0435	0.0346
<i>hkl</i> index range	-8 to 15, -23 to 24, \pm 43	\pm 21, -28 to 32, -9 to 8	\pm 11, \pm 11, \pm 19	\pm 17, -9 to 14, \pm 18	-12 to 13, -26 to 27, -25 to 33	\pm 14, \pm 15, \pm 17
θ range/ $^\circ$	1.99–26.40	2.35–26.39	2.31–26.45	2.27–26.39	1.51–26.43	1.73–26.42
Data, restraints, parameters	7556, 0, 531	3009, 0, 226	4908, 0, 298	4444, 0, 291	12003, 0, 784	6485, 2, 444
<i>F</i> (000)	4544	2000	668	1616	3768	1000
<i>R</i> ₁ , <i>wR</i> ₂ [<i>I</i> > 2 σ (<i>I</i>)] ^a	0.0241, 0.0547	0.0312, 0.0697	0.0241, 0.0572	0.0234, 0.0548	0.0365, 0.0815	0.0397, 0.0870
<i>R</i> ₁ , <i>wR</i> ₂ (all data) ^a	0.0309, 0.0572	0.0366, 0.0719	0.0257, 0.0579	0.0260, 0.0560	0.0427, 0.0837	0.0473, 0.0898
Goodness-of-fit	1.049	1.102	1.081	1.040	1.022	1.075
Max. and min. transmission	0.855, 0.548	0.806, 0.468	0.703, 0.469	0.273, 0.190	0.715, 0.406	0.598, 0.462
Largest differential peak and hole/eÅ ⁻³	1.606, -0.409	2.371, -1.309	1.616, -0.541	1.211, -0.625	3.471, -1.147	3.713, -1.101

^a $w = 1/[\sigma^2(F_o^2) + (aP)^2 + bP]$ where $P = (F_o^2 + 2F_c^2)/3$; ^b Flack *x* parameter -0.005(7)

Table 5.13 Crystallographic parameters of **11a**·0.5C₄H₈O–**16**.

Compound	11a·0.5C ₄ H ₈ O	12W	13	14	16
Empirical formula	C ₂₁ H ₂₁ AuCl ₂ N ₄ O ₂ SW·0.5C ₄ H ₈ O	C ₁₈ H ₁₃ NO ₅ W	C ₁₃ H ₁₃ AuCIN	C ₃₂ H ₂₈ AuF ₃ NO ₃ PS	C ₆ H ₇ AuCIN
<i>M_r</i>	881.25	507.14	415.66	791.55	325.54
Crystal habit	Plate	Prism	Needle	Needle	Prism
Crystal colour	Orange	Yellow	Colourless	Colourless	Colourless
Crystal dimensions/mm	0.10 × 0.09 × 0.04	0.10 × 0.06 × 0.06	0.28 × 0.09 × 0.03	0.51 × 0.08 × 0.07	0.06 × 0.04 × 0.02
Crystal system	Triclinic	Monoclinic	Monoclinic	Monoclinic	Triclinic
Space group	<i>P</i> $\bar{1}$ (No. 2)	<i>P</i> 2 ₁ / <i>c</i> (No. 14)	<i>P</i> 2 ₁ / <i>n</i> (No. 14)	<i>P</i> 2 ₁ / <i>c</i> (No. 14)	<i>P</i> $\bar{1}$ (No. 2)
<i>a</i> /Å	10.603(2)	12.5486(8)	10.412(2)	8.4149(4)	5.7342(7)
<i>b</i> /Å	11.881(2)	10.1357(6)	7.227(1)	16.9169(9)	7.3911(8)
<i>c</i> /Å	11.932(2)	14.7976(9)	17.365(2)	21.224(2)	9.257(2)
α°	70.039(2)	90	90	90	109.679(2)
β°	83.042(2)	112.760(1)	104.892(2)	97.182(1)	101.668(2)
γ°	69.143(3)	90	90	90	92.292(2)
<i>V</i> /Å ³	1320.2(3)	1735.54(18)	1262.8(3)	2997.6(3)	359.27(7)
<i>Z</i> , <i>D_c</i> /Mg m ⁻³	2, 2.126	4, 1.941	4, 2.186	4, 1.754	2, 3.009
μ (MoK α)/mm ⁻¹	10.208	6.683	11.832	5.084	20.748
No. of reflections, unique	14111, 5400	18120, 3557	6755, 2567	17310, 6109	3852, 1462
<i>R</i> _{int}	0.0489	0.0367	0.0338	0.0258	0.0284
<i>hkl</i> index range	± 13, ± 14, ± 14	± 15, ± 12, ± 18	-12 to 13, -7 to 9, -17 to 21	± 10, -20 to 21, -23 to 26	± 7, ± 9, ± 11
θ range/°	1.82–26.48	1.76–26.40	2.08–26.43	1.93–26.40	2.40–26.35
Data, restraints, parameters	4425, 6, 289	3175, 0, 228	2377, 6, 147	5499, 0, 381	1386, 0, 83
<i>F</i> (000)	828	968	776	1552	292
<i>R</i> ₁ , <i>wR</i> ₂ [<i>I</i> > 2 σ (<i>I</i>)] ^a	0.623, 0.1199	0.0255, 0.0551	0.0388, 0.0814	0.0235, 0.0553	0.0254, 0.0530
<i>R</i> ₁ , <i>wR</i> ₂ (all data) ^a	0.806, 0.1259	0.0306, 0.0570	0.0435, 0.0832	0.0276, 0.0568	0.0279, 0.0540
Goodness-of-fit	1.218	1.089	1.149	1.055	1.080
Max. and min. transmission	0.666, 0.489	0.669, 0.569	0.704, 0.128	0.700, 0.471	0.662, 0.469
Largest differential peak and hole/eÅ ⁻³	2.242, -2.976	1.352, -0.544	3.038, -2.448	1.315, -0.389	1.274, -0.784

^a $w = 1/[\sigma^2(F_o^2) + (aP)^2 + bP]$ where $P = (F_o^2 + 2F_c^2)/3$;

5.6.2 General procedures and reagents

For a summary of used instrumentation refer to Chapter 2, p. 59.

Water was deoxygenised by boiling it for a short time and then bubbling nitrogen through the hot liquid for 15 min. Excess 1-bromo-2,2-diethoxyethane was destroyed in an ammonia/propan-1-ol solution, excess methyl triflate was destroyed with a propan-1-ol/potassium 1-propoxide solution.

Chromatography under inert conditions was conducted in jacketed columns with propan-1-ol circulating at the appropriate temperature. The adsorbent was flushed with dry Et₂O, dried overnight *in vacuo* and all apparatus was kept under an argon atmosphere during the separation. The dimensions of the columns refer to adsorbent height × column diameter.

Chemicals were obtained from the following suppliers and used without further purification if not stated otherwise: Aluminium oxide for chromatography (150 mesh Brockmann grade I), butyllithium solution in hexanes, 1-iodo-4-methylbenzene, methylolithium solution in Et₂O, Florisil (synthetic magnesium silicate adsorbent) 100–200 mesh, hexacarbonyltungsten, 4-methylbenzenesulfonic acid monohydrate and benzene thiocarboxamide were obtained from Aldrich Chemical Co. 1-Bromo-2,2-diethoxyethane, ethanoyl chloride, silica gel 60 for column chromatography and tetramethylammonium chloride were obtained from Merck KG. Trimethyloxonium tetrafluoroborate, (2,5-dimethoxyphenyl)methanol, sodium tetrafluoroborate and sodium trifluoromethanesulfonate were obtained from Fluka AG. Anhydrous sodium sulfate and anhydrous magnesium sulfate were obtained by Saarchem. Thin layer chromatography plates on polyethylene or aluminium support were obtained by Macherey-Nagel GmbH & Co. KG.

The gifts of 4-chloro-1-methylpyridinium triflate and (5-butyl-1,2-dimethylpyridin-4-ylidene)pentacarbonylchromium by *Dr. Elzet Stander-Grobler* and chloro(dimethylsulfane)gold by *Dr. Ulrike E. I. Horvath* are greatly acknowledged.

5.6.3 Syntheses of the compounds

cis-Dicarbonylchloro[(4-methylphenyl)methylidene]-*cis*-bis(pyridine)tungsten, **3**,⁸⁶ 4-methylphenyllithium,⁸⁷ pentacarbonyl(1-methoxyethylidene)chromium,⁸⁸ *N*-methylethanenitrilium tetrafluoroborate,⁸⁹ pentacarbonyl(1-methoxyethylidene)tungsten,⁸⁸ pentacarbonyl[(*Z*)-1-methoxy-3-(methylamino)but-2-en-1-ylidene]chromium,⁶³ pentacarbonyl[(*Z*)-1-methoxy-3-(methylamino)but-2-en-1-ylidene]tungsten,⁶³ 1-(thiazol-2-yl)piperidine,⁴⁵ chloro(tetrahydrothiophene)gold⁹⁰ and (pentafluorophenyl)(tetrahydrothiophene)gold^{90b} were prepared according to the literature procedures.

5.6.3.1 Lithium pentacarbonyl{[2-(1-piperidinyl)thiazol-5-yl]carbonyl}-tungstate(1-), **4a**.

The compound was prepared separately following the procedure for **5a** (*vide infra*) employing 1-(thiazol-2-yl)piperidine (872 mg, 5.18 mmol), butyllithium (3.40 ml of a 1.54 M solution in hexanes; 5.24 mmol, 1.01 eq.) and W(CO)₆ (1.86 g, 5.29 mmol, 1.02 eq.) in 30 ml thf. The golden-red foam obtained after evaporation of the solvent *in vacuo* was washed with 50 ml pentane. The yield was not determined as the solid still contained unknown amounts of thf, due to this no further analyses were performed.

The compound is nearly insoluble in dichloromethane once aged (colour changes from orange-red to ochre).

5.6.3.2 Tetramethylammonium pentacarbonyl{[2-(1-piperidinyl)thiazol-5-yl]-carbonyl}tungstate(1-), **5a**.

In a Schlenk tube 1-(thiazol-2-yl)piperidine (1.068 g, 6.35 mmol) was dissolved in 30 ml thf and cooled to -78 °C. Butyllithium (6.1 ml, 1.05 M in hexanes, 6.41 mmol, 1.0 eq.) was added dropwise *via* syringe and after stirring for 1 h solid W(CO)₆ (2.172 g, 6.17 mmol, 0.97 eq.) was added, whereupon the light yellow solution slowly

86 G. A. McDermott, A. M. Dorries and A. Mayr, *Organometallics* **1987**, *6*, 925–931.

87 M. P. R. Spee, J. Boersma, M. D. Meijer, M. Q. Slagt, G. van Koten and J. W. Geus, *J. Org. Chem.* **2001**, *66*, 1647–1656.

88 T. Ito, in *Synthesis of Organometallic Compounds: A Practical Guide*, ed. S. Komiya, Wiley, Chichester, **1997**.

89 S. C. Eyley, R. G. Giles and H. Heaney, *Tetrahedron Lett.* **1985**, *26*, 4649–4652.

90 (a) A. Haas, J. Helmbrecht and U. Niemann, in *Handbuch der Präparativen Anorganischen Chemie*, ed. G. Brauer, Enke, Stuttgart, **1978**, p. 1014;

(b) R. Uson, A. Laguna and M. Laguna, *Inorg. Synth.* **1989**, *26*, 85–91.

turned brownish-red. After 2.5 h the temperature had risen to $-25\text{ }^{\circ}\text{C}$ and the cooling bath was removed. The suspension was stirred for another 1.5 h at r.t., whereupon the solvents were removed *in vacuo*. A golden-red foam of the lithium salt of the title compound was obtained which was washed with 60 ml pentane to remove excess $\text{W}(\text{CO})_6$. In an extraction funnel under inert atmosphere, $[\text{NMe}_4]\text{Cl}$ (819 mg, 7.47 mmol, 1.2 eq.) was dissolved in 20 ml deoxygenised water and 100 ml CH_2Cl_2 was added. The lithium salt of the title compound was dissolved in 50 ml deoxygenised water affording a blood-red solution which was filtered through a pad of Celite into the extraction funnel. A first black-red organic phase was separated, some yellow precipitate of the title compound remained in the extraction funnel. Another extraction with CH_2Cl_2 /ethanenitrile 4:1 yielded a red organic phase. Both fractions were evaporated to dryness, the CH_2Cl_2 extract formed an ochre precipitate while the $\text{MeCN}/\text{CH}_2\text{Cl}_2$ fraction yielded an orange crystalline solid. Total yield 2.0 g (55%). Crystals suitable for X-ray diffraction were grown from the $\text{MeCN}/\text{CH}_2\text{Cl}_2$ fraction in ethanenitrile layered with Et_2O . Found: C, 36.4; H, 4.0; N, 7.1. $\text{C}_{18}\text{H}_{23}\text{N}_3\text{O}_6\text{SW}$ requires C, 36.4; H, 3.9; N, 7.1%.

M.p. $145\text{ }^{\circ}\text{C}$ (dec.)

The compound is soluble in ethanenitrile and methanol, sparingly soluble in CH_2Cl_2 and thf but insoluble in Et_2O or alkanes.

5.6.3.3 *Pentacarbonyl{methoxy[2-(1-piperidinyl)thiazol-5-yl]methylidene}-tungsten, 6a.*

Method A:

A Schlenk tube was charged with **5a** (1.016 g, 1.71 mmol), the solid dissolved in 40 ml ethanenitrile and the solution cooled to $-40\text{ }^{\circ}\text{C}$. NEt_3 (0.25 ml, 1.73 mmol, 1 eq.) and freshly distilled MeCOCl (0.15 ml, 2.1 mmol, 1.2 eq.) were added in quick succession, the ethanoyl chloride caused the solution to become purple instantly. Stirring was continued for 1 h after which 1 ml methanol was added and the solution warmed to r.t. The reaction mixture was allowed to stir for another 30 min., after which reaction progress was checked by tlc (silica adsorbent, Et_2O as eluent). A yellow (R_f 0.63) and a purple (R_f 0.41) product was observed, attributed to the title compound and unreacted (ethanoyloxy)carbene, respectively. Stirring was continued for 2.5 h with another quantity of MeOH (*ca.* 5 ml), after which all volatiles were

removed *in vacuo* with help of methylbenzene to azeotropically remove any ethanoic acid present. Most of the crude product was purified by chromatography under inert conditions on silica gel (25 × 5 cm) at –30 °C, the column was first eluted with Et₂O and then CH₂Cl₂. Only very little pure product could be obtained, a mixed fraction contained both products. After evaporating all fractions to dryness, the mixed fraction was dissolved in methanol and stored in the freezer overnight which yielded more product. Total yield 150 mg (16%). A crystal suitable for X-ray diffraction was obtained by storing a side fraction from the chromatographic purification at r.t. which caused the oily residue to yield few orange needles. Recrystallisation of the crude product from trichloromethane layered with hexane afforded only few crystals of **5c**·2CHCl₃.

Method B:

In a Schlenk flask **5a** (927 mg, 1.56 mmol) was suspended in 20 ml CH₂Cl₂ and the suspension was cooled in an ice bath. A solution of [Me₃O][BF₄] (250 mg, 1.69 mmol, 1.08 eq.) in 40 ml ethanenitrile was slowly added via a dropping funnel. The first drops added caused dissolution of **5a**. After 3 hours all solvents were removed *in vacuo*. The crude product was subjected to chromatography under inert conditions on a silica gel column (9 × 5 cm) at –20 °C eluting with 150 ml CH₂Cl₂/pentane 1:1 and 150 ml CH₂Cl₂/Et₂O 1:1. Two fractions were collected, a first light yellow fraction contained mainly W(CO)₆ and an orange second fraction the desired product. After evaporation to dryness 62 mg (7.4%) of **6a** was isolated. Found: C, 33.8; H, 3.2; N, 5.5. C₁₅H₁₄N₂O₆SW requires C, 33.7; H, 2.6; N, 5.2%.

M.p. 106 °C (dec.)

The substance is soluble in CH₂Cl₂, Et₂O, methylbenzene and methanol but sparingly soluble in alkanes.

5.6.3.4 *cis*-Dicarbonylchloro{[2-(1-piperidinyl)thiazol-5-yl]methyldiyne}-*cis*-bis(pyridine)tungsten, **7a**.

Two Schlenk tubes were prepared and charged with **4a** (499 mg, ≤ 0.95 mmol) and (Cl₃CO)₂CO (104 mg, 0.35 mmol, ≥ 1.1 eq.), respectively. The lithium salt was suspended in 30 ml CH₂Cl₂ and the triphosgene dissolved in 10 ml CH₂Cl₂. After

cooling the orange suspension and clear solution, respectively, to $-78\text{ }^{\circ}\text{C}$ the triphosgene solution was transferred to the lithium acyl suspension *via* a Teflon cannula. The colour of the suspension immediately changed to dark red. Stirring was continued for 1.5 h, after which the Schlenk tube was immersed in an ice bath for 30 min. Freshly distilled pyridine (3 ml; the pyridine must be handled excluding contact to metal) was added, the solution warmed to r.t. and stirred for another 2.3 h. All volatiles were removed *in vacuo*, facile removal of pyridine by azeotrope formation was effected by adding methylbenzene; excessive triphosgene was quenched with 5 drops of MeOH. The orange-brown solid obtained was subjected to flash chromatography under inert conditions on silica gel ($7 \times 5\text{ cm}$) at $-30\text{ }^{\circ}\text{C}$. $\text{W}(\text{CO})_6$ and other apolar impurities were eluted with 100 ml CH_2Cl_2 , the eluent was subsequently changed to CH_2Cl_2 /methanol 19:1 (50 ml) and CH_2Cl_2 /methanol 16:1 (80 ml). Removal of all solvents of the product fraction yielded 285 mg (49% calculated with starting material free of thf, the actual yield is lower) of an orange-brown solid. Crystals suitable for X-ray diffraction were grown by layering a CH_2Cl_2 solution with hexanes. Found: C, 41.3; H, 3.4; N, 9.2. $\text{C}_{21}\text{H}_{21}\text{ClN}_4\text{O}_2\text{SW}$ requires C, 41.2; H, 3.45; N, 9.1%.

M.p. $73\text{ }^{\circ}\text{C}$ (dec. with evolution of gas)

The compound is soluble in CH_2Cl_2 and thf, sparingly soluble in Et_2O and methylbenzene but insoluble in alkanes.

5.6.3.5 *Pentacarbonyl-2 κ^5 C-[\mu-2-(1-piperidinyl)thiazol-5-yl-1 κ^5 :2 κ^3]-triphenylphosphane-1 κ^P]goldtungsten, 9a.*

In a Schlenk tube Ph_3PAuCl was synthesised *in situ* by reacting $(\text{tht})\text{AuCl}$ (154 mg, 0.48 mmol) with PPh_3 (124 mg, 0.47 mmol, 0.99 eq.) in 20 ml thf, all volatiles were removed *in vacuo* after 10 min. The product was re-dissolved in 40 ml thf, cooled to $-78\text{ }^{\circ}\text{C}$ and solid **4a** (300 mg, $\leq 0.57\text{ mmol}$, $\leq 1.2\text{ eq.}$) was added. The orange suspension was stirred for 1 h while the mixture became homogeneous and paler in colour. Warming to r.t. caused the colour to darken again and the Schlenk tube was protected from light while the solution stirred for another hour. Evaporation of the solvent yielded a honey-brown oil, tlc was performed to check for Au-containing species (CH_2Cl_2 , silica adsorbent), a yellow product at R_f 0.9 was identified. The crude product was purified on a Florisil column ($6 \times 5\text{ cm}$) under inert conditions,

eluting with CH₂Cl₂/hexanes 2:1 (70 ml), CH₂Cl₂ (50 ml) and finally CH₂Cl₂/thf 2:1. Two yellow fractions and an orange fraction were collected. The first yellow fraction contained 197 mg, the second 16 mg and the third orange fraction 194 mg product; the major fractions were crystallised from CH₂Cl₂ layered with hexanes, only the first yielded crystals (74 mg, 16 %) of the title compound. Found: C, 41.0; H, 3.8; N, 3.4. C₃₁H₂₆AuN₂O₅PSW·0.5C₆H₁₄ requires C, 41.1; H, 3.4; N, 2.8%.

M.p. 104 °C (dec. with evolution of gas)

The yellow prisms are soluble in CH₂Cl₂, thf and trichloromethane, but insoluble in alkanes.

5.6.3.6 *cis*-Dicarbonyl-2- κ^2 C-dichloro-1- κ ;2- κ -{ μ -[2-(1-piperidinyl)thiazol-5-yl]-methylidyne-1- κ C^l:2- κ C^l}-*cis*-bis(pyridine-2- κ N)goldtungsten(Au–W), **11a**.

A solution of **7a** (52 mg, 85 μ mol) in 10 ml thf was cooled to –10 °C and solid (tht)AuCl (27 mg, 84 μ mol) was added. After stirring for 1 h the cooling bath was removed and after another hour the reaction mixture was brought to dryness. The product was crystallised from CH₂Cl₂ layered with hexane. The compound did not give a satisfactory elemental analysis.

M.p. 105 °C (dec. without melting)

The substance is soluble in CH₂Cl₂ and thf, it is insoluble in Et₂O or alkanes.

5.6.3.7 – 2-Phenylthiazole, **1b**.

A procedure described in literature⁴⁶ was modified. In a round-bottom flask equipped with a reflux condenser were placed benzene thiocarboxamide (4.33 g, 31.6 mmol) and 30 ml propanone yielding a canary yellow solution. 1-Bromo-2,2-diethoxyethane (5.0 ml, 32 mmol, 1.0 eq.) was added *via* syringe followed by 2 ml water and a catalytic quantity (< 5 mg) of 4-methylbenzenesulfonic acid monohydrate. The homogeneous solution was heated to reflux for 5 hours and progress was checked by tlc (silica adsorbent with Et₂O as eluent). Product (R_f 0.67) had formed and only little benzene thiocarboxamide (R_f 0.50) remained. All volatiles were thus removed *in vacuo*, 40 ml CH₂Cl₂ was added and the resulting suspension was transferred into an extraction funnel charged with 18 ml 2 M aqueous NaOH solution and 50 ml water. Extraction was repeated twice with 20 ml CH₂Cl₂ aliquots. The combined organic

phases were reduced *in vacuo* and the crude product was distilled in an oil pump vacuum. The fraction distilling at 96.5 to 98.5 °C was collected, 3.82 g (75.1%) of the title compound was obtained as a slightly yellowish oil.

5.6.3.8 *Tetramethylammonium pentacarbonyl[(2-phenylthiazol-5-yl)carbonyl]-tungstate(1-), 5b.*

The title compound was obtained following the same procedure as described for **5a** employing 2-phenylthiazole (1.681 g, 10.4 mmol), 7.0 ml butyllithium in hexanes (1.4 M, 9.8 mmol, 0.94 eq.) and $W(CO)_6$ (3.71 g, 10.5 mmol, 1.01 eq.). The product was extracted with $CH_2Cl_2/MeCN$ 4:1 yielding a blood-red solution. Upon removal of the solvents, the blood-red (purple when wet with solvent) crystals were washed with methylbenzene to remove residual $W(CO)_6$ and free 2-phenylthiazole. Yield 5.78 g (*ca.* 75%), still containing *ca.* 20% $W(CO)_6$ (as judged by ^{13}C NMR). Crystals suitable for X-ray diffraction were grown from CH_2Cl_2 layered with hexanes. Found: C, 38.6; H, 3.5; N, 4.5. $C_{19}H_{18}N_2O_6SW$ requires C, 38.9; H, 3.1; N, 4.8%.

M.p.: Onset of decomposition from 80 °C, fast decomposition with evolution of gas at 124 °C.

The compound is soluble in CH_2Cl_2 and ethanenitrile, to a lesser extent in trichloromethane. It is insoluble in Et_2O , methylbenzene and alkanes.

5.6.3.9 *Pentacarbonyl[methoxy(2-phenylthiazol-5-yl)methylidene]tungsten, 6b.*

The compound was prepared following method B (described in 5.6.3.3) using **5b** (1.140 g, 1.94 mmol) and $[Me_3O][BF_4]$ (293 mg, 1.98 mmol, 1.02 eq.). Column chromatography under inert conditions on silica gel (11 × 5 cm) at -20 °C was performed with 150 ml CH_2Cl_2 /hexanes 1:1 initially and 200 ml CH_2Cl_2 /hexanes/ Et_2O 2:1:1 subsequently. A first light yellow fraction of 150 ml contained mainly $W(CO)_6$ and was discarded, a second dark purple fraction of 150 ml contained the desired product. Yield 356 mg (34.7%) of a purplish-black microcrystalline solid. Crystals suitable for X-ray diffraction were grown from CH_2Cl_2 layered with hexanes and individually are of a dark orange colour. Found C, 33.7; H, 2.3; N, 3.7. $C_{16}H_9NO_6SW$ requires C, 36.5; H, 1.7; N, 2.7%.

M.p. 147 °C

The compound is freely soluble in CH₂Cl₂, trichloromethane, Et₂O and thf; alkanes still dissolve it to an appreciable extent.

5.6.3.10 *cis*-Dicarbonylchloro[(2-phenylthiazol-5-yl)methylidyne]-*cis*-bis(pyridine)tungsten, **7b**.

The compound was prepared following the procedure described for **7a** (5.6.3.4), employing **5b** (1.015 g, 1.73 mmol) and (Cl₃CO)₂CO (208 mg, 0.70 mmol, 1.2 eq.). When the Schlenk tube was warmed to r.t., a freshly distilled mixture of pyridine and 2-methyl-2-propanol (ca. 2:1; the pyridine must not come into contact with metal) was added to quench excessive triphosgene and effect substitution of two carbonyl groups simultaneously. After removing all volatiles *in vacuo* a red oil was obtained. The crude product was purified by flash chromatography under inert conditions on Florisil (5 × 5 cm) at –30 °C eluting with 80 ml CH₂Cl₂, 100 ml CH₂Cl₂/MeCN 19:1 and 100 ml CH₂Cl₂/MeCN 9:1. A yellowish side fraction (120 ml) was collected first, followed by an orange-red fraction of the product (ca. 100 ml). Evaporation to dryness afforded 562 mg (54%) of a red oil. Triturating with Et₂O (ca. 20 ml) and drying in high vacuum furnished an orange foam. A crystal of the dichloromethane solvate suitable for X-ray diffraction was obtained from the crystallisation of fraction 1 of **11b**. Found: C, 43.6; H, 2.7; N, 6.9. C₂₂H₁₆ClN₃O₂SW requires C, 43.2; H, 2.8; N, 8.0%.

M.p. of **7b**·CH₂Cl₂: 84 °C (dec. with evolution of gas)

The compound is soluble in CH₂Cl₂, ethanenitrile and methylbenzene, sparingly soluble in Et₂O but insoluble in alkanes.

5.6.3.11 Chloro[methoxy(2-phenylthiazol-5-yl)methylidene]gold, **8b**.

Compound **6b** (145 mg, 0.28 mmol) was dissolved in 10 ml thf in a Schlenk tube. The blood-red solution was cooled to –5 °C and solid (tht)AuCl (89 mg, 0.28 mmol, 1 eq.) was added. The reaction mixture was stirred for 1 h finally reaching 5 °C and all volatiles were subsequently removed *in vacuo*. The resulting solid was re-dissolved in 30 ml CH₂Cl₂ and inversely filtered under inert conditions. tlc Analysis was rendered impossible by the highly sensitive compound which yielded a purple spot indicative of Au precipitate immediately upon spotting onto the tlc plate. The CH₂Cl₂ solution

was layered with 60 ml hexanes and stored in a freezer. Well-defined red, faceted crystals (75 mg, 62%) could be isolated which were suitable for X-ray diffraction. No further crop could be obtained. Found: C, 29.9; H, 2.1; N, 4.0. C₁₁H₉AuClNOS requires C, 30.3; H, 2.1; N, 3.2%.

M.p. 75 °C (dec.)

The substance was initially well soluble in thf and CH₂Cl₂ possibly owing to impurities inhibiting crystallisation, once the crystals were isolated, they dissolve only in dichloromethane with difficulty and are insoluble in thf, propanone, ethanenitrile, trichloromethane and methanol.

5.6.3.12 *Pentacarbonyl-2κ⁵C-[μ-(2-phenylthiazol-5-yl)carbonyl-1κC:2κO]-*
(triphenylphosphane-1κP)goldtungsten, 10b.

In a Schlenk tube Ph₃PAuCl was prepared *in situ* from PPh₃ (202 mg, 0.77 mmol) and (Me₂S)AuCl (227 mg, 0.77 mmol, 1 eq.) as described for **9a**. The solution of Ph₃PAuCl was cooled to -50 °C and **5b** (568 mg, 0.78 mmol based on 80 % purity) was added as a solid, after 2 h the mixture reached 10 °C and Na[BF₄] (88 mg, 0.80 mmol, 1.04 eq.) was added to aid the abstraction of chloride from Ph₃PAuCl. The slightly turbid orange solution was stirred for another hour at r.t., tlc analysis (silica plate with CH₂Cl₂ as eluent) of the reaction mixture revealed two products containing Au at R_f 0.69 (main product) and R_f 0.81 (side product). The solvent was removed *in vacuo* affording an orange-brown oil which was subjected to column chromatography under inert conditions on Florisil (15 × 5 cm) at -30 °C eluting with CH₂Cl₂ (200 ml), CH₂Cl₂/thf 19:1 (100 ml) and CH₂Cl₂/thf 12:1. Two product fractions were obtained, the first one contained a mixture of two products, the second contained 414 mg (57 %) of the title compound. Crystals suitable for X-ray diffraction were obtained from a thf solution layered with pentane. Found: C, 40.8; H, 2.3; N, 1.2. C₃₃H₂₁AuNO₆PSW requires C, 40.8; H, 2.2; N, 1.4%.

M.p. 90 °C (dec. with evolution of gas)

The orange-red compound is soluble in CH₂Cl₂ and thf, sparingly soluble in Et₂O but insoluble in alkanes.

5.6.3.13 Reaction of 7b with (tht)AuC₆F₅ – attempted synthesis of 11b.

Compound **7b** (155 mg, 0.26 mmol) was dissolved in 10 ml thf and cooled to –60 °C whereupon solid (tht)AuC₆F₅ (114 mg, 0.25 mmol, 0.98 eq.) was added resulting in a deep orange-red solution. The cooling bath temperature reached 0 °C after 3 h and the reaction mixture was stirred for another 30 min. at room temperature. Methylbenzene (ca. 10 ml) was added to allow efficient removal of tht and the solution was brought to dryness. The solid was re-dissolved in 40 ml Et₂O, inversely filtered under inert conditions and brought to dryness affording an orange foam. The crude product was purified by chromatography under inert conditions on Florisil at –30 °C eluting with CH₂Cl₂ (150 ml) and CH₂Cl₂/thf 4:1 (150 ml). Two fractions containing gold were obtained, the first yielded 74 mg of an orange product while the second afforded 100 mg of a yellow solid. A crystal obtained from the first fraction proved to be **7a**·CH₂Cl₂.

5.6.3.14 Pentacarbonyl(1,2-dimethyl-5-phenyl-1H-pyridin-4-ylidene)chromium, 12Cr.

The compound was prepared according to literature procedures.^{8a,63,88} Care must be taken as the R_f values of the title compound and its precursor pentacarbonyl[(Z)-3-(methylamino)-1-methoxybut-2-en-1-ylidene]chromium are virtually identical. Yield (based on last alkyne addition step) 32%. Found: C, 55.4; H, 3.8; N, 3.3. C₁₈H₁₃CrNO₅ requires C, 57.6; H, 3.5; N, 3.7%.

M.p. 130 °C (dec. without melting)

The compound is soluble in most organic solvents except alkanes where it is only sparingly soluble.

5.6.3.15 Pentacarbonyl(1,2-dimethyl-5-phenyl-1H-pyridin-4-ylidene)tungsten, 12W.

The compound was prepared according to literature procedures.^{8a,63,88} The same remarks as for **12Cr** (5.6.3.14) apply. Yield (based on last alkyne addition step) 20 %. Found: C, 40.1; H, 3.1; N, 2.5. C₁₈H₁₃NO₅W requires C, 42.6; H, 2.6; N, 2.8%.

M.p. 178 °C (dec. with evolution of gas)

5.6.3.16 Chloro(1,2-dimethyl-5-phenyl-1H-pyridin-4-ylidene)gold, 13.

Two Schlenk tubes were charged with (tht)AuCl (93 mg, 0.29 mmol) and **12W** (150 mg, 0.29 mmol, 1 eq.), respectively. Both compounds were dissolved in 10 ml CH₂Cl₂ each and the solutions were cooled to –35 °C. The (tht)AuCl solution was transferred to the carbene complex solution *via* a Teflon cannula. After the cooling bath had reached 0 °C (2 h), it was removed and the solution stirred at r.t. for another 1.5 h. Completion of the reaction was indicated by tlc (silica adsorbent, CH₂Cl₂/Et₂O 1:1 as mobile phase) when starting material was not detected any more and instead a spot at R_f 0.83 was attributed to [W(CO)₅(tht)], R_f(**13**) 0. All volatiles were removed *in vacuo*, the residue re-dissolved in 30 ml CH₂Cl₂, inversely filtered under inert conditions and concentrated to about 7 ml. Layering the solution with pentane yielded 85 mg (71%) of a cream-coloured microcrystalline solid. A crystal suitable for X-ray diffraction was obtained by recrystallising a small quantity from thf layered with pentane. Found: C, 37.5; H, 3.3; N, 3.1. C₁₃H₁₃AuCIN requires C, 37.6; H, 3.2; N, 3.4%.

M.p. 154 °C (dec.)

The compound is moderately soluble in CH₂Cl₂ and thf but is insoluble in Et₂O and alkanes.

5.6.3.17 (1,2-Dimethyl-5-phenyl-1H-pyridin-4-ylidene)(triphenylphosphane)-gold(1+) trifluoromethanesulfonate, 14.

The complex Ph₃PAuCl was prepared *in situ* from (Me₂S)AuCl (58 mg, 0.20 mmol) and PPh₃ (52 mg, 0.20 mmol, 1 eq.) in 10 ml ethanenitrile and the suspension was stirred at r.t. for 45 min. Separately, a solution of **12Cr** in 20 ml ethanenitrile was prepared. Both Schlenk tubes were cooled to –45 °C. To the solution of Ph₃PAuCl, solid NaOTf (34 mg, 0.20 mmol, 1 eq.) was added. After 10 min. the solution of **12Cr** was transferred to the Schlenk tube containing Ph₃PAuCl *via* a Teflon cannula. Stirring continued for 4 h whereupon the cooling bath reached room temperature and the colour of the solution lightened to lemon yellow. tlc Analysis (silica gel adsorbent, Et₂O as eluent) showed that almost all chromium carbene had reacted and an apolar yellow side product, assumed to be [Cr(CO)₅(Me₂S)], had formed. All volatiles were removed *in vacuo* and the resultant solid was re-dissolved in CH₂Cl₂. Inverse filtration

under inert conditions and evaporation to dryness afforded a yellow residue which was extracted with methylbenzene to remove most of the side product. Crystallisation from a CH_2Cl_2 solution layered with pentane gave 0.12 g (78 %) colourless needles suitable for X-ray diffraction. Found: C, 49.0; H, 3.5; N, 1.6. $\text{C}_{32}\text{H}_{28}\text{AuF}_3\text{NO}_3\text{PS}$ requires C, 48.6; H, 3.6; N, 1.8%.

M.p. 225 °C (dec.), slight onset of decomposition noticeable from 205 °C.

The compound is soluble in CH_2Cl_2 , ethanenitrile and thf but insoluble in Et_2O , methylbenzene or alkanes. Precipitation from solutions by adding alkanes or Et_2O is, however, slow due to supersaturation and not suitable for fast purification.

5.6.3.18 Pentacarbonyl(1-methyl-1H-pyridin-4-ylidene)chromium, 15.

A 0.2 M solution of sodium naphthalenide was prepared by adding an appropriate amount of finely diced sodium metal to a solution of naphthalene in thf (100 ml in total) and stirring overnight. In a Schlenk tube, $\text{Cr}(\text{CO})_6$ (730 mg, 3.32 mmol) was suspended in 20 ml thf and cooled to -50 °C. Sodium naphthalenide solution (33 ml, 6.6 mmol, 1 eq.) was added dropwise *via* syringe and the naphthalenide radical anion was consumed quickly indicated by the colour changing from green to brown. After 1 h the temperature had reached -30 °C and solid 4-chloro-1-methylpyridinium triflate (782 mg, 2.8 mmol, 0.85 eq.) was added and stirring was continued for another 2 h at r.t. furnishing a black suspension. To separate any insoluble and explosive disodium ethynediolate ($\text{Na}_2\text{C}_2\text{O}_2$), the suspension was filtered under inert conditions before evaporating to dryness. The black oil obtained was purified by inert column chromatography on Florisil (12×5 cm) eluting with CH_2Cl_2 /pentane 1:1 (200 ml), CH_2Cl_2 /pentane/ Et_2O 3:2:1 (100 ml), CH_2Cl_2 / Et_2O 1:1 (100 ml), and CH_2Cl_2 / Et_2O 4:3 (100 ml). The yellow product fraction was collected and upon evaporation gave 101 mg (11%) of a yellow crystalline solid. Found: C, 43.9 H, 2.9; N, 4.3. $\text{C}_{11}\text{H}_7\text{CrNO}_5$ requires C, 46.3; H, 2.5; N, 4.9%.

M.p. 143 °C (dec.)

The compound is soluble in CH_2Cl_2 , trichloromethane, thf and Et_2O , it is slightly soluble in alkanes.

5.6.3.19 Chloro(1-methyl-1H-pyridin-4-ylidene)gold, 16.

A Schlenk tube was charged with **15** (45 mg, 0.15 mmol), (tht)AuCl (51 mg, 0.16 mmol, 1.0 eq.) and 5 ml CH₂Cl₂ was added. Partial decomposition of (tht)AuCl was immediately observed by the characteristic purple gold precipitate, the suspension was stirred for 2 h at r.t. Inverse filtration under inert conditions, evaporation of all volatiles *in vacuo* and extraction of side products with Et₂O (*ca.* 20 ml) afforded 14 mg (27 %) of a colourless microcrystalline solid. Crystals just big enough for X-ray diffraction were obtained from a thf solution layered with pentane. Found: C, 22.0; H, 2.3; N, 4.2. C₆H₇AuClN requires C, 22.1; H, 2.2; N, 4.3%.

M.p. 140 °C (dec.)

The compound is soluble in propanone, only sparingly soluble in CH₂Cl₂ and thf but insoluble in Et₂O and alkanes.